# Identification of ATRX as a Restriction Factor during Herpes Simplex Virus Latent Infection and Characterization of Phase I of Reactivation

Abigail Leslie Whitford
Dayton, OH

Bachelor of Science in Biochemistry and Molecular Biology,
Centre College, Danville, KY, 2020

A Dissertation presented to the Graduate Faculty of the
University of Virginia in Candidacy for the Degree of
Doctor of Philosophy

Department of Microbiology, Immunology, and Cancer Biology

University of Virginia
May 2025

# Abstract

Herpes simplex virus-1 (HSV-1) establishes a lifelong latent infection in neurons and reactivation from this latent state is the cause of recurrent oral and ocular infections, herpes simplex keratitis, and encephalitis. Neuronal conditions during initial HSV-1 infection have a long-term impact on latency, modulating how responsive latent genomes are to reactivation and, therefore, their ability to cause disease. We find that type I interferon (IFNα) exposure during initial infection results in a more restrictive form of HSV-1 latency and the deposition of a repressive heterochromatin mark, H3K9me3, and its reader, ATRX (alpha-thalassemia/ mental retardation, X-linked). ATRX is highly abundant in neurons and is essential for maintaining cellular heterochromatin during neuronal stress. We find that ATRX restricts *de novo* lytic gene expression, promotes latency establishment, and inhibits reactivation. This work highlights how neuronal-specific factors limit HSV-1 infection to promote latency and restrict reactivation.

In addition to understanding what factors limit neuronal HSV-1 infection, we also investigated the neuronal pathways HSV-1 commandeers to reactivate. Using novel systems to study HSV-1 latency, we find that reactivation in both an *ex vivo* murine system and an *in vitro* human system can be triggered with physiologically relevant triggers. In an *ex vivo* system we confirm that reactivation is biphasic and dependent on the neuronal stress kinases dual leucine zipper kinase (DLK) and c-Jun N-terminal kinase (JNK). This work aids in the development of potential therapeutic interventions by identifying neuron-specific factors involved in HSV-1 latency and reactivation.

# Acknowledgements

This dissertation is the culmination of five years of work, growth, patience, and resilience. Having started this journey during the pandemic, a time that was isolating for everyone, I am incredibly grateful for the communities I had that supported me through this process.

My first acknowledgement goes to my mentor, Dr. Anna Cliffe. Anna is an incredibly creative and passionate scientist. I am so grateful to Anna for having shared this passion with me during graduate school. Thinking about science with her has been eye opening, exciting, and so much fun. I am also in dept to Anna for the numerous opportunities she has given me. She has gone above and beyond what is expected of a mentor, and I feel as though every achievement I have is a direct result of her.

I would also like to thank the Cliffe Lab. I am grateful to all the previous members of the lab who served as my mentors and taught me techniques, gave me advise, and created a fun working environment. I am especially grateful to Sean and Matthew, who grew to be close friends. I also need to acknowledge the current members of the lab: Matt, Patryk, James, Shrisha, Wyate, Christian, and Dilruba. I am so grateful to my current lab mates for being kind, easy to work with, and great people. Having a collaborative environment makes lab such a fun place to work and that is all thanks to them.

So many faculty members at UVA have had a hand in helping me through graduate school. I owe so much thanks to Dr. Dan Engel, Dr. Dean Kedes, Dr. Mariano Garcia Blanco, Dr. Clint Miller, and Dr. Tajie Harris for serving as my

committee members, helping to guide my science, and writing me letters of reference. I also need to thank Dr. Barry Condron for serving as a teaching mentor to me and encouraging me to explore opportunities I had not thought possible. Finally, I would like to thank Dr. Sarah Dremel who helped me learn sequencing analysis. I am so indebted to her for being an incredibly patient and kind teacher.

Next, I would like to thank my friends. Thank you to Meredith, Jenny, and Emma who have been my best friends for almost 20 years. I am so grateful to have people who know and accept everything about me and have been with me through so many major life events. Thank you to Marina and Mary Carter who became my best friends the first week of college and stuck by my side through the highs and lows of one of the most transformative times of my life. And finally, thank you Audrey, Shelby, Sarah, Kathy, Isaiah, and Cami who have been such genuine and kind friends in graduate school. Thank you for your unwavering support, for validating my feelings, and being incredible listeners.

I am also so grateful to my fiancé, Tim. Tim makes every day so much more joyful, calm, and fun. He has perfectly mastered the art of cheering me up and making me feel celebrated. I am always in awe of his empathy for others and thoughtfulness, both of which have made me a kinder and more patient person in graduate school. Thank you for the countless meals, walks, facetimes, and laughs. In addition, I would also like to thank Tim's family for their kindness and for always making me feel welcome.

Lastly, I would like to thank my family who have loved me whole-heartedly for my entire life. In particular, I would like to thank my parents who given me so many incredible opportunities. Thank you for always prioritizing my education and happiness. I am so grateful to know that you are proud of me, it has made all the difference.

# Table of Contents

# Herpes Simplex Virus Infection and the Role of Interferons in HSV-1 Latency

*Parts of this chapter have been adapted from:*

Whitford, A. L., & Cliffe, A. R. (2022). Key questions on the epigenetics of herpes simplex virus latency. *PLoS Pathog*, *18*(6), e1010587. https://doi.org/10.1371/journal.ppat.1010587

## HSV-1

Herpes simplex virus one (HSV-1) is of the order *Herpesvirales* and family *Herpesviridae.* The *Herpesviridae* family infects birds, reptiles, and mammals and is sorted into *Alphaherpesvirinae*, *Betaherpesvirinae* and *Gammaherpesvirinae* subfamilies (Davison et al., 2009). Herpesviruses are generally specific to their host species with only nine identified as infecting humans. The human *Alphaherpesvirinae* subfamily includes HSV-1, HSV-2, and varicella zoster virus (VZV). These viruses infect epithelia and establish a latent infection in neurons. The *Betaherpesvirinae* have a lymphocyte tropism and include the human pathogen human cytomegalovirus (HCMV), and human herpes viruses 6 and 7 (HHV6A, HHV6B, and HHV7). Finally, viruses of the *Gammaherpesvirinae* establish latency in lymphoid cells and monocytic cells and include Epstein-Barr virus (EBV) and Kaposi's Sarcoma Virus (KSHV) (Knipe & Howley, 2013).

HSV-1 is a large (152 kB) dsDNA virus. The DNA of HSV-1 consists of two covalently bound unique segments that are referred to as $U_L$ (unique long) and $U_S$ (unique short). Both sequences are flanked by a series of inverted repeats. The presence of the inverted repeats allows for the inversion of the $U_L$ and $U_S$ segments which can result in four distinct combinations of the viral DNA. Within the inverted repeat section of DNA lies coding regions for viral proteins (e.g. ICP0 and ICP4) and the lncRNA latency associated transcript (LAT) (Whitley & Roizman, 2001).

In the virion, viral DNA is packaged into an icosahedral (T=16) capsid that is surrounded by tegument (Davison et al., 2009). The viral tegument is composed of over 20 viral proteins (Table 1) (Kelly et al., 2009). Finally, the viral capsid and tegument are contained within the viral envelope, made of a lipid bilayer derived from the host cell and viral glycoproteins. The HSV-1 virion has a diameter of ~210 nm (Brown & Newcomb, 2011).

| **Protein** | **Function** |
|---|---|
| pUL7 | Mitochondrial regulation |
| pUL11 | Secondary envelope |
| pUL13 | Protein kinase, inhibits interferon response and regulates apoptosis, tegument dissociation |
| pUL14 | Involved in nuclear import, apoptosis inhibition, and capsid targeting to the nucleus |
| pUL16 | Secondary envelope |
| pUL21 | Secondary envelope, regulates microtubule assembly |
| pUL23 | Thymidine kinase, involved in viral DNA regulation |
| pUL36 (VP1/2) | Secondary envelope, involved in capsid transport, release of viral DNA, and deubiquitination. |
| pUL37 | Secondary envelope, regulates viral transcription |
| pUL41 | Regulates viral transcription, host transcription, and the immune response |
| pUL46 (VP11/12) | Secondary envelope, regulates transcription by pUL48 |
| pUL47 (VP13/14) | Secondary envelope, regulates transcription by pUL48 |
| pUL48 (VP16, VMW65, αTIF) | Secondary envelope, regulates viral transcription |
| pUL49 (VP22) | Secondary envelope, regulates microtubule assembly |
| pUL50 | dUTPase, involved in viral DNA replication |
| pUL51 | Unknown |
| pUL55 | Unknown |
| pUS2 | Unknown |
| pUS3 | Protein Kinase, involved in de-envelopment, tegument dissociation, and actin assembly |
| pUS10 | Unknown |
| pUS11 | Regulates host translation, involved in capsid transport |
| ICP34.5 | Regulates host translation, viral DNA replication, and the immune response |

| | |
|---|---|
| ICP0 | Regulates viral transcription and anti-viral host factors |
| ICP4 | Regulates viral transcription via transcription factor assembly |

**Table 1.1: List of HSV-1 Tegument Proteins.** Adapted from Kelly et al., (2009). ICP34.5, ICP0, and ICP4 have distinct nomenclature because they are not encoded by US or UL genes.

## HSV-1 Epidemiology, Pathology, and Treatment

Over 66% of Americans aged 0-49 are infected with HSV-1, with rates increasing with age (James et al., 2020). HSV-1 transmission occurs when people encounter the lesions, mucosal surface, or genital or oral secretions of an infected individual. Transmission by viral shedding can occur even when clinical symptoms are not apparent. HSV-1 disproportionally affects women and non-black Hispanic persons (McQuillan et al., 2018). HSV-1 is associated with painful oral lesions (cold sores) but, more recently there has been a reported rise in genital HSV-1 cases. Genital HSV-1 infection can produce painful genital ulcer disease and is particularly concerning as neonates can be infected by their mother during birth. Neonates can also be infected from caregivers orally after birth which can cause encephalitis and is highly fatal (James et al., 2020). HSV-1 is responsible for severe disease in adults as well. Keratitis caused by HSV-1 is the leading cause of infectious corneal blindness in the United States (Tullo, 2003). HSV-1 has also been implicated in the progression of late-onset Alzheimer's disease (AD) (discussed further below) (Itzhaki et al., 1997; Lovheim et al., 2019). Currently, there is no vaccine against HSV-1 and infection is treated with acyclovir (ACV), valaciclovir, famciclovir, and penciclovir (Whitley & Roizman, 2001). When phosphorylated by the host, these nucleoside analogues

compete with host nucleotide dGTP and inhibit viral DNA polymerase (Bacon et al., 2003).

## HSV-1 Lytic Replication

### Viral Entry

Initial infection of the host by HSV-1 occurs at the epithelia at the body's surface in cells such as keratinocytes. Infection begins when glycoproteins B and/or C (gB, gC) on the viral envelope bind to heparan sulfate (HS). Once initial attachment occurs, glycoprotein D (gD) can associate with one of the three described host receptors: Nectin-1 (epithelial and neuronal cells), the herpesvirus entry mediator (HVEM) (epithelial cells, fibroblasts, T lymphocytes, and neurons), or 3-O sulfated HS (present in the brain) (Knipe & Howley, 2013). This association initiates changes in gH and gL, activation of gB, and fusion of the viral envelope with the plasma membrane. Infection proceeds via endocytosis, direct membrane fusion, or a phagocytosis-like pathway. The pathway of entry seems to be dependent on cell type and the cell receptors present (Knipe & Howley, 2013).

Fusion of the virus with the plasma membrane results in the release of the capsid and tegument proteins from the envelope. The capsid is then transported along microtubules by dynein to the nuclear pore. Evidence suggests that DNA within the capsid is released via a port in the capsid into the nucleus (Knipe &

Howley, 2013). The tegument proteins are released into the cytoplasm and migrate to their destinations independently of the capsid (Knipe & Howley, 2013).

## Lytic Gene Expression

The HSV-1 genome is epigenetically naïve in the capsid (Oh & Fraser, 2008). Upon entry into the nucleus, viral DNA is circularized and associates with host chromatin rapidly. The epigenetic changes made to the viral genome during lytic infection impact viral gene expression and DNA replication. Viral DNA has been found to associate with histones as early as one-hour post-infection, with association peaking at 3 hours post-infection (Cliffe & Knipe, 2008; Oh & Fraser, 2008). Histones are enriched on viral promoters (Oh & Fraser, 2008) and are post-translationally modified. For example, acetylation on histone H3 is detected as early as one-hour post-infection (Kent et al., 2004). Histone association then decreases at later time points in a DNA polymerase-independent and transcription-independent manner (Cliffe & Knipe, 2008). Histones are actively removed from viral DNA during lytic replication by viral protein ICP0 (Cliffe & Knipe, 2008). Although the HSV-1 genome associates with histones during lytic infection, the nucleosomes occupancy is not like that of cellular chromatin and is not evenly spaced, suggesting the viral genome has a highly dynamic chromatin structure (Kent et al., 2004; Lacasse & Schang, 2010; Leinbach & Summers, 1980; Muggeridge & Fraser, 1986).

VP16, a viral tegument protein, is required for maximum viral gene expression during lytic infection. VP16 promotes chromatin modification as early as 2 hours

post-infection by recruiting histone writers to immediate early (IE) protein promoters (Herrera & Triezenberg, 2004). Immediate early (IE) genes (α genes) are the first HSV-1 gene class expressed during lytic infection and their expression is independent of viral protein synthesis. Instead VP16 recruits HCF, a cell cycle regulatory protein, and Oct1, a host transcription factor. VP16, HCF, and Oct1 form the VP16 induced complex (VIC) that binds to distinct DNA elements on the promoters of IE genes. This complex then recruits additional transcription factors and promotes the expression of the five viral IE genes, initiating entry into the lytic cycle (Knipe & Howley, 2013).

| **IE Protein** | **Function** |
|---|---|
| ICP0 (RL2) | Regulates viral transcription and anti-viral host factors. Not required but enhances viral infection. |
| ICP4 (RS1) | Regulates viral transcription via transcription factor assembly. Interacts with TFIIB, TATA-binding protein, and TFIID. Essential for viral infection. Required for E and L gene expression. |
| UL54 (ICP27) | Inhibits pre-mRNA splicing and host protein synthesis. Required for Early gene expression, DNA replication, and late gene expression. ICP27 promotes transcription by recruiting host RNA polymerase II to the viral genome. Found in both the nucleus and cytoplasm and promotes export of viral mRNA into the cytoplasm. Regulates translation by binding RNA and interacting with multiple viral and cellular proteins. Essential for viral infection. |
| Us1 (ICP22) | Enhances late gene expression via modulation of topoisomerase and RNA polymerase II. Not required but enhances viral infection. |
| Us1.5 | Not required but enhances viral infection. |
| Us12 (ICP47) | Blocks antigen presentation by inhibiting TAP1/TAP2. Not required but enhances viral infection. |

**Table 1.2: List of HSV-1 Immediate Early Proteins** (Knipe & Howley, 2013).

IE proteins (including ICP4, ICP0 and ICP27) promote the expression of the subsequent gene class of HSV-1 lytic infection: Early (E) genes (β genes). Many E genes are essential for DNA replication. After E gene expression, IE and E proteins and the viral DNA form replication compartments, displacing cellular chromatin. How viral DNA replication occurs is somewhat debated. An older model proposes viral DNA undergoes theta replication. In this model, ICP8 (viral ssDNA binding protein) and UL9 (origin binding protein) bind to the circularized HSV-1 DNA episome and form the initiation site. UL9 in this model could bind to either *ori*S or *ori*L. ICP8 unwinds the viral DNA so that the two DNA strands separate. Viral replication then occurs in opposing directions along the DNA circle. The bubble of ssDNA at one end of the circular episome makes the process look like the Greek letter “θ”. It was then thought that replication switched to rolling circle replication, where replication occurs on a single strand in one direction on a circular template (Knipe & Howley, 2013).

There is evidence (genomic inversions, head-to-tail concatemers) that HSV-1 replication does not follow a simple rolling circle mechanism and instead occurs through recombination mechanisms. If DNA replication were to occur through a nick or gap or if HSV-1 replication occurred on a linear rather than circular molecule, double stranded breaks (DSBs) would likely occur on viral DNA. Recombination is known to initiate at DSBs and at ssDNA gaps. Both replicating and encapsidated viral genomes contain nicks and gaps that are randomly located and present on both strands (Weller & Sawitzke, 2014), suggesting HSV-1 linked replication and recombination. Furthermore, during the encapsidation

phase, it is expected that the viral terminase complex will cleave concatemeric DNA, packaging a viral genome on one side of the packaging sequence and leaving a DSB on the other. HSV-1 also encodes a viral primase that is inefficient at low concentrations, providing a possible mechanism for the formation of nicks and gaps. Thus, HSV-1 DNA replication is likely to produce DSBs and DNA molecules with gaps, conditions that would be expected to stimulate recombination events (Weller & Sawitzke, 2014).

HSV-1 may have evolved to utilize the two-component recombinase UL12/ICP8 to promote recombination-dependent replication by single strand annealing (SSA) because this pathway is conducive to the production of concatemeric DNA, which can be packaged into an infectious virus. HSV-1 proteins UL12 (5’ to 3’ exonuclease) and ICP8 (a single-strand annealing protein [SSAP]) make up a two-component recombinase. They can function alone or with host machinery. Although DNA synthesis occurs in the absence of UL12, the production of aberrant genomes suggests that alternate pathways may be deleterious to produce an infectious virus (Weller & Sawitzke, 2014).

Replicated concatemerized viral DNA is cleaved during virion assembly and then packaged into pre-formed capsids. Although histones can be detected on viral DNA after replication, this association decreases (Cliffe & Knipe, 2008) and no histones are found in the capsid. Therefore, there must be a mechanism of de-chromatinization of the viral genome. Capsid formation and DNA organization is facilitated by many late proteins (Knipe & Howley, 2013).

| E Protein | Function |
|---|---|
| UL5, UL8, UL52 | Helicase-primase complex components. |
| UL5 & UL52 | This complex has ATPase, GTPase, DNA primase, and DNA helicase activities. |
| UL9 | Viral origin binding protein. Acts as an ATPase and helicase at the origin of viral DNA synthesis. Required for the initiation of synthesis. |
| UL12 | Alkaline exonuclease that allows for recombination and viral DNA replication. |
| UL29 (ICP8) | A single stranded DNA binding protein that allows for the unwinding of DNA. It also acts as a scaffold protein to allow for the organization of the replication complex. It is associated with recombinase activity. |
| UL30, UL42 | Viral DNA polymerase: catalytic subunit (UL30), DNA polymerase processivity factor that increases processivity by binding dsDNA and tethering it to the DNA polymerase (UL42), |

**Table 1.3: List of HSV-1 Early Proteins Required for DNA Replication**(Knipe & Howley, 2013).

The final class of genes expressed during HSV-1 lytic infection are the late (L) genes. Although the last group of genes to be initiated, late gene expression is initiated as early as three hours post-infection (Dremel & DeLuca, 2019). L gene expression is dependent on viral DNA replication. There are two categories of late genes: the leaky late genes (γ1), which can be expressed without DNA synthesis although their expression is enhanced by it, and the true late genes (γ2), which are dependent on viral DNA synthesis for expression. It is not entirely clear how DNA replication allows for the expression of L genes, but it is hypothesized that it may be due to the augmentation of RNA polymerase II (RNA Pol II) machinery by viral early gene products. After DNA replication, RNA Pol II,

TATA-binding protein (TBP), and transcription initiation factor TFIID subunit 1 (TAF1) occupancy at L gene promoters is increased. DNA replication, in *cis*, alters the accessibility of L gene promoters to transcriptional machinery, making newly synthesized genomes more accessible for active transcription. Original genomes then initiate the assembly and packaging process (Dremel & DeLuca, 2019). Late proteins are required for vDNA packaging, virus assembly, and egress.

| **L Protein(s)** | **Function** |
|---|---|
| UL1 (gL), UL22 (gH), UL27 (gB), UL49.5 (gN), Us6 (gD) | Envelope glycoproteins. |
| UL6, UL15, UL28, UL33 | The virion portal protein found on the HSV capsid (UL6), the terminase complex (UL15&UL28), and other proteins required for DNA cleavage and packaging. |
| UL16 | Tegument protein (see Table 1) |
| UL18 (VP23), UL19 (VP5), UL25, UL38 (VP19C) | Capsid proteins |
| UL26<br>UL26.5 | A protease and scaffolding protein important for capsid assembly. |
| UL31, UL33 | Promotes nuclear lamina disruption (UL31) and the formation of the envelop at the nuclear membrane (UL31&UL33). |
| UL32 | A zinc binding protein that cleaves viral DNA concatemers and helps package DNA into capsids. |
| UL36 (VP1-2) | Tegument protein (see Table 1) |
| UL37 | Tegument protein (see Table 1) |
| UL48 (VP16) | Tegument protein (see Table 1) |

**Table 1.4: List of Essential HSV-1 Late Proteins** (Knipe & Howley, 2013).

### Viral Egress

Upon the expression of L genes, capsid subunits localize to the nucleus, and the capsid assembles. There are three subtypes of capsid (A, B, and C) that can be assembled. Although they all are the same diameter, only C capsids have viral DNA insertion and mature into infectious virus. HSV-1 concatemeric DNA is fed, via a portal, into the capsids in an ATP-dependent manner. The DNA concatemers are cleaved into monomers during the encapsidation process (Knipe & Howley, 2013).

Once the nucleocapsid is formed, the capsid must move to the cell membrane to be released from the cell. Viral egress is proposed to function in one of three ways: envelopment—de-envelopment—re-envelopment, the luminal pathway, or the nuclear pore egress pathway. The envelopment—de-envelopment—re-envelopment pathway is the most widely accepted. In all models, the virus uses host membranes (from the nucleus or cytoplasm) as its envelope (Knipe & Howley, 2013).

## HSV-1 Latency

HSV-1 has established a successful mechanism to persist long-term in its host by maintaining a latent infection in neurons. Following initial infection of non-neuronal cells at the body's surface, *de novo* virus reaches the innervating axons of peripheral neurons. The cell bodies of these innervating nerves make up peripheral ganglia including trigeminal, superior cervical, and dorsal root ganglia.

Upon entering the neuron, the viral capsid is transported in a retrograde fashion to the nucleus where the viral genome can enter and establish a latent infection.

Latent infection is defined as long-term carriage of the viral genome but lack of detectable infectious virus and the ability to reactivate following a specific stimulus. During HSV-1 latency, the viral genome is transcriptionally restricted and the 80 genes that are expressed during the lytic cycle are not transcribed. The latency-associated transcript (LAT) is a lncRNA that is produced during latency. It is made from an 8.3 kb primary RNA processed into two major LATS (1.5/2 Kb) and several microRNAs. LAT expression favors survival in neurons and promotes reactivation (Knipe & Howley, 2013).

During latency, the HSV-1 genome exists as a nuclear, unintegrated episome. Although multiple factors regulate entry into latent infection, the epigenetic structure of the latent HSV-1 genome in neurons differs from the configuration of the viral genome during lytic infection of non-neuronal cells and therefore may play an important role in regulating viral gene transcription. Since the initial discoveries of chromatinization of the HSV-1 genome during latency (Deshmane & Fraser, 1989), multiple new discoveries have been made in understanding the nature of epigenetic silencing on the latent viral genome (Whitford & Cliffe, 2022). However, no studies so far have addressed the direct contribution of the viral epigenetic structure to the establishment and maintenance of HSV latency.

*The epigenetic environment of the latent HSV genome.*

Alterations in gene expression that are not encoded by the DNA sequence are known as epigenetic modifications. Gene silencing of cellular, non-viral DNA can be mediated by DNA methylation. Thus far there is limited evidence of canonical CpG methylation on the HSV-1 genome (Kubat et al., 2004). This is based on a lack of canonical CpG methylation on regions of the viral genome containing high levels of CpG such as the latency associated transcript (LAT) region and the viral lytic gene, ICP4 (Kubat et al., 2004).

Cellular DNA is further condensed when wrapped around an octamer of histone proteins H2A, H2B, H3, and H4, to form a nucleosome. Micrococcal nuclease digestion of viral DNA from the brainstem of mice indicates a nucleosomal structure is present on the viral genome (Deshmane & Fraser, 1989). Histone H3 is associated with the HSV genome during latency and its N-terminus can be subject to post-translational modifications (PTMs) that affect gene transcription. During HSV latency, marks associated with repressive heterochromatin, including histone di- and tri-methyl lysine 9 (H3K9me2/3) and histone trimethyl lysine 27 (H3K27me3), are abundant on transcriptionally inactive areas, such as lytic promoters (Cliffe et al., 2009; Kwiatkowski et al., 2009; Nicoll et al., 2016; Wang et al., 2005). In contrast, a region of the viral genome containing the promoter and enhancer LAT, which undergoes robust transcription during latency, is enriched for euchromatin marks including H3K4me3 as well as acetylation on histone H3 (Cliffe et al., 2009; Kubat et al.,

2004). It is unknown what factors are involved in the writing, reading, and erasing of these marks during HSV-1 latency and reactivation.

Although histone PTMs can directly regulate gene expression, the major epigenetic consequences result from binding of histone reader proteins. Methylated H3K9 on cellular chromatin can be read by many proteins including heterochromatin proteins 1 (HP1) and ATRX (Valenzuela et al., 2021). Yet, it is unknown if these proteins act as readers on viral DNA. H3K27me3 is read by Polycomb group repressive complexes (PRC). The complex that adds the H3K27me3 mark, and also has H3K27me3 reading function (PRC2), is known to associate with the HSV genome following the resolution of acute infection in mice (Cliffe et al., 2013). A second complex, known as PRC1, exists in multiple forms and can bind H3K27me3 to mediate gene silencing via genome compaction, three-dimensional interactions, and/or formation of phase separated domains (Dochnal et al., 2021). A component of PRC1, Bmi1, has only limited association with the latent HSV genome (Cliffe et al., 2013; Kwiatkowski et al., 2009). Therefore, it is likely that PRC1 has either limited association or different forms of PRC1 lacking Bmi1 associate with the latent viral genome. The viral genome is thus epigenetically regulated, but there are still uncertainties as to what other histones, histone modifications, and histone readers are enriched on the viral genome, as well as whether different histone PTMs are located on the same or distinct populations of HSV genomes.

*Neuronal epigenetics contribute to the initiation and maintenance of HSV gene silencing.*

HSV only establishes a latent infection in post mitotic neurons. Thus, understanding what makes neurons epigenetically unique to other cell types could have significant implications to our understanding of latency. Although it is unclear why certain histone PTMs become enriched during latency and how these changes contribute to the onset and maintenance of latent infection, one possibility is that certain forms of epigenetic silencing occur secondarily to a reduction in lytic gene transcription. For example, the timing of H3K27me3 formation on the latent genome suggests this modification is more important in maintenance, but potentially not the initiation, of gene silencing (Cliffe et al., 2013). The complex responsible for formation of H3K27me3 can be targeted indiscriminatingly to regions of chromatin but can only methylate H3K27 in the absence of active transcription and euchromatic modifications (Blackledge & Klose, 2021). Neuronal specific microRNAs miR-138 and miR-9 have been shown to limit the levels of transcription factors ONECUT Family, Oct1, or FOXC1 that promote HSV lytic gene transcription and limit heterochromatin formation (Deng et al., 2024; Sun et al., 2021). In particular, Oct1 forms a complex with the viral trans activator VP16 and HCF1, both of which display distinct localization patterns in neurons. HCF1 displays a cytoplasmic localization in sensory neurons (Kolb & Kristie, 2008) and VP16 trafficking along axons is slower than nucleocapsid trafficking, resulting in a reduced ability to transactivate lytic genes following neuronal axon-specific infections (Antinone & Smith, 2010;

Hafezi et al., 2012). As a result, due to a lack of transcription factors, some forms of epigenetic modification could be secondary to reduced transcription in neurons.

Neurons are a specialized, terminally differentiated, post-mitotic cell type with unique patterns of gene expression and response to stimuli. Therefore, it is plausible that the unique chromatin environment and resulting differential expression or function of host proteins or RNA in neurons contributes to epigenetic silencing in HSV latency. The composition of the Polycomb Group complexes changes following neuronal differentiation and during maturation. This includes a switch in the predominant H3K27 methyltransferase as EZH1 replaces EZH2 as the major species present in mature neurons (von Schimmelmann et al., 2016). In addition, the relative levels of PRC1 proteins also changes with neuronal maturation (Duan et al., 2018). Given the immense diversity in protein composition of the Polycomb group complexes (Dochnal et al., 2021), it is probable that are multiple unexplored differences in the epigenetic environment of neurons compared to non-neuronal cells, and likely also between different neuronal subtypes, which could influence epigenetics on the HSV genome. In addition, expression of distinct non-coding RNAs in neurons could modulate recruitment or activity Polycomb group proteins on viral genomes. There is evidence for of neuronal specific long non-coding RNAs that can interact with Polycomb proteins and regulate gene expression important in neuronal identify, function and plasticity (Xu et al., 2020). The neuronal-specific HSV LAT also regulates the association of heterochromatin on the HSV genome in latency and

there is evidence that the LAT alters the levels of H3K27me3 on the latent genome (Cliffe et al., 2009; Kwiatkowski et al., 2009). The mechanisms by which the LAT regulates the HSV epigenome remains to be determined, especially as it does not appear to function in direct recruitment of the PRC2 complex (Cliffe et al., 2013). Finally, the HSV genome may have a distinct higher order chromatin structure in neurons which could regulate heterochromatin deposition. The chromatin insulator protein, CTCF, stabilizes three-dimensional DNA interactions to form domains containing genes in similar transcriptional states (Amelio et al., 2006; Xiang & Corces, 2021). CTCF binding sites on the viral genome appear to have differential effects on viral gene expression in neurons and there is evidence that CTCF-binding can modulate H3K27me3 deposition on the latent genome (Washington et al., 2018). Given the potential for CTCF to regulate the epigenetic structure of the latent genome, more research is needed to determine how CTCF, as well as other epigenetic proteins, are recruited to viral genomes differently in neurons versus non-neuronal cells, and how this might affect the outcome of HSV neuronal infection.

### *Heterogeneity in reactivation-competent epigenetic structure.*

HSV can reactivate in response to stimuli and re-enter a lytic replication cycle. However, only a sub-population reactivate in response to a given stimuli (Cuddy et al., 2020; Sawtell & Thompson, 1992), suggesting that latency is heterogenous, and some viral genomes are more prone to reactivate. It is unclear if the marks found on the viral genome, such as H3K9me2/3 and

H3K27me3, are enriched equally, if at all, on the same or different genomes. Beyond the heterogeneity in histone modifications, there are multiple reader proteins or protein complexes that can interact even with the same histone modification, further increasing the possible forms of epigenetic silencing on latent genomes. This is also supported by heterogeneity in viral genome localization to different subnuclear domains (Catez et al., 2012; Suzich et al., 2021). Therefore, viral genomes with different epigenetic structures and localized to different nuclear subdomains may be more or less prone to reactivate. Viral genomes localized to one subnuclear domain, promyelocytic leukemia nuclear bodies (PML-NBs), are restricted for reactivation, at least in *in vitro* models of HSV latency (Suzich et al., 2021). Viral genome co-localization to PML-NBs only occurs in neurons exposed to type I interferon at the time of infection (Suzich et al., 2021). Although the downstream epigenetic changes to the HSV genomes that are associated with PML-NBs in neurons are not known, this indicates that exposure to different cytokines during initial infection can regulate the nature of latent infection and later ability to reactivate. Altered neuronal states during infection, such as neuronal stress due to NGF deprivation, impacts latency, leading to an increase in subsequent reactivation (Dochnal, Whitford, et al., 2024). It is likely that exposure to extra-cellular stimuli including cytokines, intrinsic differences in neurons themselves, and/or expression of viral factors regulate the nature of epigenetic silencing on the latent genome. Understanding whether there are subtypes of latent HSV epigenetic structures

that are more or less able to undergo reactivation may enable to development of new therapies that prevent HSV reactivation occurring.

### *The potential role of epigenetics on the clinical outcomes of HSV infections.*

Understanding how cellular epigenetic marks differ on latent HSV genomes between individuals could be important for understanding how HSV latency and reactivation can be heterogenous within a population and may result in more severe clinical phenotypes in certain individuals. Numerous studies have linked HSV infection with the development of late onset Alzheimer's disease, especially in individuals with the ApoE4 variant (Calabro et al., 2021). Recent evidence suggests that reactivation from latency occurs in waves (Cliffe et al., 2015; Kim et al., 2012), with the first wave being potentially reversible, raising the possibility of abortive reactivation events (Singh & Tscharke, 2020). Abortive reactivation and consequential leaky lytic expression in the peripheral or central nerve systems may result in transient synthesis of viral lytic proteins that could impact neuronal function and could also induce a chronic inflammation, which could have significant impacts on the health of the nervous system. It was reported that there is detectable HSV-1 DNA in the brains of ageing adults (Jamieson et al., 1991). Therefore, with upwards of 50% of the aging population having HSV infection, understanding the epigenetics surrounding HSV latency could have direct impacts on our understanding of clinical outcomes of HSV infection and potentially result in the development of new therapeutics to prevent even abortive reactivation events.

### *Herpes Simplex Virus and Alzheimer's Disease*

Numerous studies have linked HSV infection with the development of late onset AD, especially in individuals with the ApoE4 variant (Calabro et al., 2021). Alzheimer's disease is the most common form of dementia, with over 50 million patients with the disease. The accumulation of (phosphorylated) tau neurofibrillary tangles, Aβ plaques (making up senile plaques), and neuron death can lead to damage of the hippocampus, cerebral cortex, amygdala, and the basal forebrain. Synaptic loss is another major driver of AD and can be caused by mitochondrial damage, oxidative stress, and the accumulation of tau and Aβ. This damage can lead to retrograde and anterograde amnesia as well as other symptoms including, aphasia, apraxia, and agnosia. Current therapies only treat AD symptoms and so further research is needed to create therapies to prevent and cure AD (Breijyeh & Karaman, 2020).

Sporadic Alzheimer's disease does not follow a simple inheritance pattern. Instead, onset of the disease is thought to be the accumulation of many factors. These factors include age, genetics, injuries to the CNS, vascular disease, infection, and other environmental factors. There are genetic mutations associated with a higher prevalence of disease. For example, mutations to apolipoprotein E (ApoE) have been associated with AD. ApoE is a glycoprotein that acts as a receptor mediated endocytosis ligand for molecules like cholesterol. It is highly expressed in the liver and brain (astrocytes and some microglia). The ApoEε4 variant of the gene is a risk factor for AD and as

aforementioned, the presence of this allele in addition to the presence of latent HSV-1 is thought to increase risk of AD. While neither of these factors alone cause AD, when both factors are combined AD was much more likely than those with neither factor or only one (Itzhaki et al., 1997; Lovheim et al., 2019). Furthermore, a study has shown that infection of mice with HSV-1 leads to detectable spreading to the brain, the accumulation of AD factors such as amyloid plaques and tau neurofibrillary tangles, and neuroinflammation. These factors then correlated with increased cognitive defects in the mice (De Chiara et al., 2019). Future work to understand the causal link between HSV-1 and AD could lead to new treatments.

## HSV-1 Reactivation

Reactivation of HSV-1 from its latent state within host neurons is reliant upon host cell stress pathways and epigenetic factors to re-initiate viral gene transcription. Pathways that have been shown to induce reactivation include the loss of neurotrophic factor support (Cliffe et al., 2015; Kim et al., 2012; Wilcox & Johnson, 1987; Yanez et al., 2017), increased neuronal hyperexcitability (Cuddy et al., 2020), DNA damage/repair pathway activation (Hu et al., 2019), and exposure to glucocorticoids and corticosteroids (Cliffe et al., 2015). The exact mechanism downstream of these reactivation triggers and how they mediate an exit from latency and transcription of viral genes is not fully understood.

Nerve growth factor (NGF) deprivation triggers HSV-1 reactivation in a DLK and JNK-dependent manner. NGF deprivation occurs naturally during

nervous system development but also occurs later in life due to chronic stress, changes in hormones, UV irradiation, or damage to innervated tissues (resulting in the loss of cells that produce NGF) (Suzich & Cliffe, 2018). During development, NGF deprivation leads to apoptosis via Bax activation, mitochondrial outer membrane permeabilization (MOMP), and cytochrome c mediated caspase activation. In contrast, mature neurons can restrict MOMP and caspases to inhibit apoptosis (Suzich & Cliffe, 2018). Developing and mature neurons bind to NGF via the TrkA receptor which activates the MEK/ERK, PLCγ, and Pl3k/AKT pathways. Only disruption of the phosphoinositide 3 (PI3)-kinase (P13k)/AKT pathway triggers reactivation in response to NGF deprivation (Camarena et al., 2010). Inhibition of AKT, downstream of PI3K inhibition, results in dual leucine zipper kinase (DLK) activation. DLK regulates axonal stress responses, mediating a range of outcomes such as Wallerian degeneration, axon regeneration, apoptosis, and axon pruning (Tedeschi & Bradke, 2013). When activated, DLK shifts the role of the cellular stress protein, c-Jun N-terminal kinase (JNK), from its normal function in sustaining synaptic arborization in neurons to that of cellular stress (Sengupta Ghosh et al., 2011). JNK plays a significant role in the reactivation of HSV (Cliffe et al., 2015; Cuddy et al., 2020; Hu et al., 2019) and Varicella-Zoster virus (Kurapati et al., 2017), suggesting its key role in the reactivation processes of human alpha herpesviruses.

Axotomy is the well-characterized trigger of HSV-1 reactivation. In response to axon damage, calcium channels open, triggering calcium influx, increased electrical signaling, activation of adenylate cyclase, and increased

cAMP (Mahar and Cavali 2018). Rapidly following axotomy, the epigenetic regulation of the latent viral genome changes. For example, following axotomy, CTCF-mediated domain occupancy is lost (Ertel et al., 2012; Washington et al., 2018). There is also a notable increase in histone acetylation following axotomy, possibly due to the export of HDACs from the nucleus in response to calcium influx (Suzich & Cliffe, 2018). HCF-1, a transcription factor, re-localizes to the nucleus as early as 20 minutes post-axotomy (Kristie et al., 1999) and occupies lytic promoters as early as one-hour post-transplant. HCF-1 is thought to re-initiate viral gene expression because it associates with gene enhancer domains of IE proteins and correlates with RNA Polymerase II occupancy (Whitlow & Kristie, 2009). For full reactivation to occur, the chromatin structure of the viral genome must be changed so it is conducive to transcription. Histone demethylases such as LSD-1 and JMJD2 interact with HCF-1 (Liang, Vogel, et al., 2013; Liang et al., 2009) and are required for lytic gene expression. Interestingly, VP16, which interacts with HCF-1 during lytic infection, is not required for axotomy-induced reactivation (Sears et al., 1991; Steiner et al., 1990). The viral protein ICP0 was also found not to be required for axotomy-induced reactivation (Thompson & Sawtell, 2006). Since axotomy-induced reactivation occurs in the absence of the viral proteins, it highlights the role of host factors in initiating reactivation.

HSV-1 reactivates in response to fever. This stimulus can be modeled by heat shock (Dochnal et al., 2022; Halford & Schaffer, 2001) and hyperthermia (Sawtell & Thompson, 1992) but the exact mechanism that leads to reactivation

is still unclear. It is hypothesized that IL1B, IL-6, and prostaglandins are released in response to fever. These signals can in turn trigger neuronal excitation, elevation of cAMP levels, and potentially reactivation. Heat shock proteins are activated in response to heat stress but their role in reactivation is unknown. Finally, JNK is activated in response to heat stress (Suzich & Cliffe, 2018). Unlike axotomy, hyperthermic-induced reactivation is VP16-dependent (Thompson et al., 2009). Fever-induced reactivation also seems to be enhanced by ICP0 (Halford & Schaffer, 2001; Thompson & Sawtell, 2006). It is intriguing that fever, unlike axotomy, is dependent or enhanced by viral proteins, suggesting that there are differences in reactivation pathways.

Psychological stress, another trigger of HSV-1 reactivation, is associated with epinephrine, another agent responsible for an increase in cAMP levels. Catecholamines (ex., Epinephrine) and glucocorticoids are released when the sympathetic nervous system is activated. Dexamethasone, a synthetic corticosteroid, induces HSV-1 reactivation in a JNK-dependent manner (Suzich & Cliffe, 2018). IL-1B is also released under conditions of stress, fever, immune activation, and UV damage and heightens neuronal activity. When neurons are hyper-excited, they have an increased propensity to fire action potentials. IL-1B induces reactivation via neuronal excitation, cAMP elevation, and DLK (Cuddy et al., 2020). A common laboratory trigger of HSV-1 reactivation, forskolin, also activates adenylate cyclase, mimicking an increase in cAMP. DLK and JNK activation are involved in cAMP-activated HSV-1 reactivation (Cuddy et al., 2020). DLK seems to be consistently activated across studied models of HSV-1

reactivation. Further research is needed to determine the extent of its ubiquity and to identify factors that may be different downstream of various stimuli.

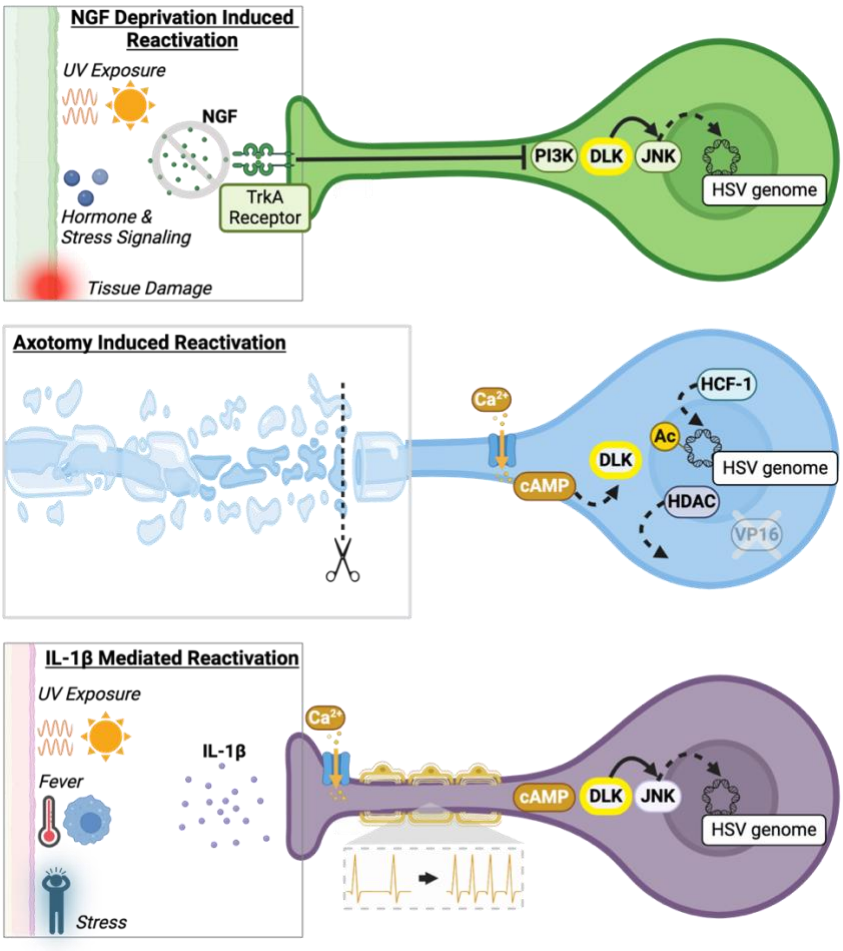


**Figure 1.1 Summary of NGF deprivation, axotomy, and IL-1β induced HSV-1 reactivation.**
Top (green) UV exposure, hormone and stress signaling, and tissue damage cause NGF deprivation. When NGF is not available, TrkA signaling to PI3K does not occur, resulting in DLK and JNK activation. JNK initiates HSV-1 reactivation. Middle (blue) axotomy results in calcium influx, cAMP upregulation, and potentially DLK activation. Transcription factor HCF-1 is recruited to the viral genome and HDACs are recruited out of the nucleus. Reactivation occurs independently of VP16.
Bottom (purple) UV exposure, fever, and stress can induce the release of IL-1β. IL-1β signaling in neurons incudes hyperexcitability, followed by DLK and JNK activation, and HSV-1 reactivation.

### *Phase I of Reactivation*

The reanimation of viral gene expression after latency is distinct from the gene expression kinetics that occur during lytic replication. In contrast to the regulated cascade of immediate early gene expression, followed by early gene expression, DNA replication, and late gene expression that occurs during lytic replication, during reactivation there is an initial burst of lytic gene expression (Phase I) that is then subsequently followed by full, robust gene expression (Phase II) (Kim et al., 2012).

Transcription during Phase I is distinct from lytic gene expression. In contrast to the lytic cycle, blocking protein synthesis before IE gene expression does not inhibit the expression of E genes during Phase I. Furthermore, the expression of L genes is unaffected even when viral DNA replication is inhibited (Kim et al., 2012). These findings suggest that the early expression of viral transcripts after reactivation differs from the initial expression patterns observed during the onset of infection in non-neuronal cells.

Phase I has largely been observed in both in the primary neuronal model of reactivation (Cliffe et al., 2015; Cuddy et al., 2020; Dochnal et al., 2022; Hu et al., 2022; Kim et al., 2012) as well as e*x vivo* and in sensory neurons (Whitford et al., 2022). In these systems, full reactivation (Phase II) requires the activities of histone demethylase enzymes, indicating that reactivation requires removal of repressive heterochromatin (Cliffe et al., 2015; Cuddy et al., 2020). However, Phase I occurs independently of lysine 9 mono- and di- methylation and lysine 27 mono-, di-, and tri- methylation removal by histone demethylases (LSD1 or

JMJD3 and UTX) (Cliffe et al., 2015; Cuddy et al., 2020; Dochnal et al., 2022; Whitford et al., 2022). Whether Phase I occurs independently of lysine 9 tri-methylation removal remains unknown.

## Lysine 9 Demethylation

Lysine methylation is a significant histone PTM that plays a crucial role in regulating chromatin structure. Among the various enzymes involved in the removal of lysine methylation, LSD1/2 is notable for its ability to demethylate H3K4me1&2 and H3K9me1&2. These demethylation events can be both repressive (H3K4 demethylation) or activating (H3K9 demethylation). The mechanism of LSD1/2 involves FAD-dependent amine oxidation (Berry & Janknecht, 2013).

LSD-1 is critical for HSV-1 viral gene expression during both lytic replication and reactivation. When viral DNA enters the cell, host chromatin is quickly deposited with H3K9me3 detectable as early as 30 minutes post-infection. For IE gene expression to initiate, repressive histone PTMs that have been deposited on the viral genome must be removed. HCF-1, a transcriptional cofactor, recruits LSD-1 to viral promotors where it then reduces the levels of H3K9 methylation. Inhibition of LSD-1 inhibited HSV-1 lytic gene expression (Liang et al., 2009).

Another group of enzymes involved in lysine demethylation is the K demethylase 4 (KDM4/JMJD2) family, including KDM4A-D. These enzymes specifically target H3K9, H3K36, and H1.4K26 residues for demethylation. Their

mechanism relies on a dioxygenase reaction that requires Fe2+, O2, and 2-oxoglutarate. Unlike LSD1/2, KDM4/JMJD2 enzymes can demethylate tri-, di-, and monomethylated lysine residues (Berry & Janknecht, 2013).

The KDM4/JMJD2 family consists of several subtypes, including KDM4A-C (also known as JMJD2A-C). These subtypes are approximately 130 kDa and possess double PHD and Tudor domains, which function as epigenome readers with different substrate specificity. Overexpression of these enzymes has been observed in cancers, potentially due to their ability to modulate transcription factors (Berry & Janknecht, 2013).

Among the KDM4 proteins, KDM4A (also known as JMJD2A or JHDM3A) is the most extensively studied. KDM4A demonstrates a preference for demethylating H3K9me3 over H3K36, a characteristic shared with KDM4B and KDM4C. It is particularly efficient in demethylating trimethylation. Moreover, the overexpression of KDM4A has been shown to decrease H3K9me3 reader (HP1γ) binding during DNA replication, indicating an antagonistic relationship between the two proteins(Berry & Janknecht, 2013).

Other subtypes of the KDM4/JMJD2 family include KDM4D-F (also known as JMJD2D-F). This subtype is approximately 65 kDa and lacks the double PHD and Tudor domains. KDM4D-F does not target H3K36 but specifically demethylates tri- and dimethylated H3K9 and can even inefficiently demethylate monomethylated lysine. It is worth noting that KDM4E and KDM4F are pseudogenes (Berry & Janknecht, 2013).

In addition to the known role of LSD-1, research has indicated that KDM4 proteins also promote HSV-1 gene expression. The viral genome has been found to contain H3K9me3, and while LSD-1 is responsible for removing di-methyl K9, KDM4 proteins are necessary for removing the trimethyl modification. The KDM4 proteins are functionally redundant in their role in promoting HSV-1 lytic gene expression and the depletion of multiple subtypes has an additive repressive effect. Similar to LSD1 (Whitlow & Kristie, 2009), the KDM4 proteins also associate with HCF-1 suggesting a mechanism by which the proteins are recruited to the viral genome. When ganglia were reactivated via axotomy, the presence of a KDM4 inhibitor restricted reactivation (Liang, Vogel, et al., 2013). The inhibitor used, ML324, is most effective against KDM4B but has also been reported to inhibit other subtypes including KDM4D and KDM4E (Kirkpatrick et al., 2018).

### The methyl/phospho switch

As mentioned above, although histone demethylases are required for full reactivation of HSV-1, Phase I is unaffected by histone demethylase inhibition. To circumvent the need for the full removal of repressive histone post translational modifications, the virus co-opts a mechanism of transcription induced by cell stress. Phase I is dependent on DLK activation followed by JNK activation (Cliffe et al., 2015). Certain host proteins including transcription and pioneer factors would be necessary to recruit JNK to the viral chromatin since JNK itself cannot bind to DNA. When JNK is activated by DLK, it phosphorylates

c-Jun, a pioneer factor involved in neuronal damage and axon loss. Yet, c-Jun was found to only affect Phase II and not Phase I (Dochnal, Whitford, et al., 2024). Therefore, more investigation is required to fully understand the mechanism downstream of JNK activation during Phase I of reactivation.

JNK activation induces histone phosphorylation of serine10 on histones that maintain the H3K9me3 modification (H3K9me3S10p) (Cliffe et al., 2015). On cellular promoters, H3K9me3S10p permits transcription even without the removal of the repressive H3K9me3 modification (Cheung, Tanner, et al., 2000). This mark is observed on lytic promoters 18 hours post reactivation, suggesting a possible mechanism by which viral transcription occurs without PTM removal.

Studies on cellular chromatin have characterized how transcription occurs after a methyl/phospho switch, although some uncertainty remains regarding the complete mechanism and whether it is consistent across all contexts. The rapid nucleosome response describes a mechanism whereby H3S10p is followed by acetylation at lysine 14 (Cheung, Tanner, et al., 2000), indicating a synergistic modification where acetylation builds up slightly after phosphorylation. Human histone acetyltransferases like PCAF and p300 also prefer phosphorylated H3 as a substrate (Lo et al., 2000). This is the first of two potential models for understanding how transcription occurs after a methyl/phospho switch. One model proposes a synergistic coupling where phosphorylation of serine 10 facilitates the recruitment of acetyltransferases, which then modify H3K9 or H3K14, while the other model suggests these are spatially linked but independent events (Clayton & Mahadevan, 2003; Sawicka & Seiser, 2012).

Finally, phosphorylation in addition to acetylation may lead to the recruitment of ATP-dependent chromatin remodeling complexes and RNA polymerase machinery (Vincent et al., 2008) (Vincent 2006). Whether these processes occur on HSV-1 chromatin is unknown but studies on cellular chromatin provide a framework with which we can understand how viral transcription potentially occurs after a methyl/phospho switch and how this switch initiates HSV-1 reactivation.

## Innate Immunity and PML-NBs in HSV-1 Infection

### The Intrinsic Immune Response and Promyelocytic Leukemia Nuclear Bodies

In response to HSV-1 infection, there are various host defenses to the virus including the intrinsic, innate, and adaptive immune responses. The intrinsic and innate responses are the first responses to infection. Intrinsic antiviral immunity refers to factors that are constitutively expressed and can act immediately at the time of infection to block viral processes and activate subsequent immune responses (Yan & Chen, 2012). These factors include innate immune regulators such as IFI16 (Orzalli et al., 2016), DNA damage response proteins such as RNF8 and RNF168 (Lilley et al., 2011), and promyelocytic leukemia nuclear bodies (PML-NBs) (Everett et al., 1998).

### *General PML-NBs*

PML-NBs (also called nuclear domains-10 [ND-10] or Kremer bodies) are membraneless nuclear organelles. Membraneless organelles allow eukaryotic cells to compartmentalize processing, regulatory signals, and specific responses. PML-NBs are liquid-liquid phase separated (LLPS) particles (Wu et al., 2023). Therefore, their formation is dependent upon physical conditions including pH, temperature, concentration, and the properties of the macromolecules that compose the bodies. Although PML-NBs can persist for hours to days, individual bodies are dynamic and have a high turnover rate. PML-NBs consist of an inner core filled with proteins (170 known) and are present in most mammalian cell nuclei (typically 5-30 per nucleus). They are a 0.1-1μm sphere (Corpet et al., 2020).

PML-NBs were initially identified in relation to the role of PML as a tumor suppressor, with PML-NB disorganization observed in acute promyelocytic leukemia (APL). In addition to acting as tumor suppressors, PML-NBs are involved in biological processes such as senescence, antiviral defense, and stemness. PML-NBs are part of the nuclear matrix and form discrete foci that are interspersed between chromatin regions (Bernardi & Pandolfi, 2007; Corpet et al., 2020). PML-NBs are indispensable for biological function as PML knockout mice do not thrive (Lallemand-Breitenbach & de The, 2010).

PML protein (also called MYL, FNF71, PP86, or TRIM19) is encoded by an interferon-stimulated gene (ISG) that can be activated by IFNα, IFNβ, and IFNγ (Chelbi-Alix & de The, 1999). The protein contains a tripartite motif (TRIM)

and an RBCC motif (R- RING finger domain, B- two cysteine-histidine-rich B-box domains, CC- alpha-helical coiled-coil domain). There are seven isoforms of PML and all isoforms (excluding PML-VII) contain an nuclear localization sequence. PML can be sumoylated, a process when the protein is covalently attached to a small-ubiquitin-like modifier (sumo) protein, at lysine 65, 160, 490, and sometimes 616. PML also contains a sumo interacting motif (SIM) which allows it to interact with sumoylated proteins, including itself. The formation of PML-NBs is controlled by the UBC9-sumo E2 conjugating enzyme which sumoylates proteins (Corpet et al., 2020). The recruitment of proteins to PML-NBs is due to sumo/SIM, the overall concentration of proteins, or post translational modifications. PML that cannot be sumoylated can no longer recruit key components of PML-NBs such as DAXX and SP100. Many proteins are targeted to nucleate at PML-NBs by a SUMO modification of SIM domain (Bernardi & Pandolfi, 2007).

The size and abundance of PML-NBs is heterogeneous and can be widely varied between cell types. Their size and abundance can also be altered in response to cellular stress, DNA damage, senescence (Bernardi & Pandolfi, 2007), and other factors such as metals (arsenic trioxide) and heat shock (Hirano & Udagawa, 2022; Lallemand-Breitenbach & de The, 2010). Cell stress leads to an increase in PML-NB formation and size. This may be due to an increase in PML transcription after interferon stimulation (Bernardi & Pandolfi, 2007), although PML transcription is not affected after interferon stimulation in neurons (Suzich et al., 2021). PML-NBs have also been shown to form in response to

oxidative stress, and the nucleation of these nuclear bodies is mediated by reactive oxygen species (ROS)-induced oxidation of PML proteins (Sahin et al., 2014). Furthermore, it has been reported that IFN signaling induces the accumulation of ROS in neurons (Alboni et al., 2013), suggesting an alternate pathway of PML nucleation in this cell type. Understanding how PML-NBs change in localization and composition in different situations and cell types may help us understand how PML-NBs act as a restriction factor against viral infection and latency.

### *PML-NBs and Heterochromatin Regulation*

One major function of PML-NBs is heterochromatin regulation. A multitude of chromatin-associated proteins are found within PML-NBs. Included in this list are histone chaperones that are responsible for depositing canonical and non-canonical histones at regions of DNA. Modified histones are displaced from DNA during replication, transcription, and DNA damage. The maintenance of chromatin states is dependent on the rapid reassembly of chromatin. Reassembled chromatin is composed of a mixture of recycled, modified histones, or newly synthesized naive histones. The synthesis of canonical histones is restricted to S phase while histone variants such as H3.3 are synthesized independently and are turned over throughout the entire cell cycle. (Voon & Wong, 2016). H3-H4 histone chaperones found at PML-NBs include the CAF-1 complex that deposits canonical H3.1 during DNA replication or HIRA, DEK, and DAXX/ATRX which deposit H3.3 in a DNA-replication-independent manner.

H3.3 can be associated with actively transcribed or repressed regions of chromatin. H3.3 only differs from the canonical H3.1 by 5 amino acids. Initially, H3.3 was identified with transcriptionally active regions of DNA. At these regions, HIRA interacts with RNA Polymerase II (or transcription factors) near nucleosome-free regions of DNA and deposits H3.3. HIRA, as well as the other proteins it associates with in complex (UBN1, CABIN-1, ASFIA), are all capable of localizing with PML-NBs. Most commonly this association occurs during senescence and viral infection and type I interferon signaling.

Later, H3.3 was identified at repressive regions of DNA. Deposition at these heterochromatic regions is carried out by DAXX, an H3.3 chaperone that associates with ATRX, a chromatin remodeler. DAXX is a constitutive component of PML-NBs and is recruited by its SIM domain (Corpet et al., 2020).

In addition to affecting the deposition of histones, PML-NBs also recruit histone writers that affect the post-translational modifications found on histones. For example, SETDB1, a histone 3 lysine 9 methyltransferase is found at PML-NBs constitutively (Corpet et al., 2020). Loss of PML alters the heterochromatic state of PML-associated domains (PADs) as associated DNA shifts from H3K9me3 to H3K27me3 enrichment. The H3K9me3/K27me3 balance is not unlike that reported in instances of PRC2 recruitment to pericentric heterochromatin to counteract deficiencies in the H3K9 methyltransferase SUV39H1. The switch in marks maintains silencing at specific locations of DNA (Delbarre et al., 2017). PML-NBs associate non-randomly with regions of heterochromatin. They can associate with actively transcribed genes (MHC Class

I and p53) as well as transcriptionally silent genes. This association my impact gene expression (Corpet et al., 2020).

### *PML-NBs in Lytic HSV-1 Infection*

During non-neuronal HSV-1 lytic infection, PML-NBs restrict viral replication by recruiting proteins (including chromatin modifiers) that counteract many viral processes. PML-NBs associate with and entrap incoming genomes as early as 90 minutes post-infection (Alandijany et al., 2018). Due to the dynamic nature of PML-NBs and their ability to rapidly associate and dissociate, upon HSV-1 infection, *de novo* PML-NBs may associate with incoming vDNA (Everett & Murray, 2005) or vDNA may associate with pre-existing PML-NBs (Alandijany et al., 2018). PML-NB recruitment to viral genomes is dependent upon ATRX (Alandijany et al., 2018). Yet, during lytic infection, the HSV-1 protein ICP0 acts to disrupt and degrade PML-NBs (Everett et al., 1998). PML-NBs therefore only associate with the viral genome (Everett et al., 2004) before they are disrupted during early infection (about 3 hours post-infection) (Chelbi-Alix & de The, 1999).

PML-NBs may facilitate heterochromatin formation on the viral genome. Because heterochromatin enrichment of H3K9me3 peaks at around 2 hours post-infection (Lee et al., 2016), it is possible that PML-NBs could promote the chromatinization of the viral genome before they are degraded at ~3 hours post-infection (Chelbi-Alix & de The, 1999). In the absence of PML-NBs, H3K9me3 enrichment of the viral genome was significantly decreased (Francois et al., 2024), suggesting a role for PML in the deposition of this mark onto viral DNA.

The removal of H3K9me3 at approximately 3 hours post-infection is ICP0 dependent (Lee et al., 2016) and could therefore be related to the ICP0-dependent degradation of PML-NBs.

ICP0 is an immediate early protein that is responsible for the degradation of many host proteins. ICP0 acts as an E3 ubiquitin ligase to ubiquitinate proteins and target them for degradation at the proteasome. ICP0 interacts with E2 ligases (UbcH5 and UbcH6) via its RING domain (Boutell et al., 2002). ICP0 preferentially targets SUMO modified PML but can also cause the degradation of PML without SUMO modification (Boutell et al., 2011).

ICP0 is required for efficient lytic infection of specific cell types at a low MOI (MOI=0.5) (Sacks & Schaffer, 1987) (Cai & Schaffer, 1992) (Yao & Schaffer, 1995). Indirectly (ICP0 does not bind to vDNA; (Everett et al., 1991)), ICP0 promotes lytic gene expression by transactivating viral genes (Cai & Schaffer, 1992) (Quinlan & Knipe, 1985). This transactivation is dependent upon the RING-finger domain of ICP0 (Boutell et al., 2002), suggesting that the ubiquitination and degradation of host restriction factors contribute to transactivation. In addition to PML, ICP0 also ubiquitinates proteins that restrict the virus such as histone deacetylases (Ferenczy & DeLuca, 2011) and histone ubiquitin ligases (Lilley et al., 2011). ICP0-mediated degradation affects the chromatin associated with the viral genome. ICP0 accumulation reduces total H3, increases histone acetylation (Cliffe & Knipe, 2008), and decreases H3K9me3 and H3K27me3 association (Ferenczy & DeLuca, 2011) (Orzalli et al., 2013) (Lee et al., 2016).

### *PML-NBs in Latent HSV-1 Infection*

PML-NBs can be found in murine and human (autopsied) neurons in the absence of infection and are also detected in the trigeminal ganglia of mice infected *in vivo*. During acute infection (6 DPI), the number of PML-NBs increases. The number of PML-NBs then decreases during latency, but *in vivo* PML-NBs are still detectable. When PML knock-out mice were infected, the number of latent genomes (28 DPI) per neuron significantly increased, suggesting a repressive role of PML-NBs during the establishment of latency. In neurons with genomes that co-localize with PML-NBs, LAT expression is not detectable, suggesting that these genomes are the most transcriptionally repressed (Catez et al., 2012).

Latency *in vivo* has been described in two patterns: single and multiple latency. In single latency, a single viral genome spot is detected in the nucleus and this genome is commonly associated with PML-NBs. In multiple latency, up to 20-30 genomes are detected in the nucleus. When multiple viral genomes are found within a single nucleus there is a heterogeneous association, with only a subset associating with PML-NBs or centromeres in the nucleoplasm. The LAT is only expressed by genomes not associated with PML-NBs or centromeres. The association of the latent viral genome with promyelocytic leukemia (PML) proteins is favored by type I IFN treatment as demonstrated in *in vitro* cultured wild type or IFNAR knockout cultured TGs (Maroui et al., 2016). The IFN response is physiologically relevant as it has been shown to build up within

infected TGs during latency establishment (via autocrine and paracrine signaling). The IFN response increases with recurrent infection. Therefore, viruses that enter in different waves will have different environments (Maroui et al., 2016).

The role of PML and ICP0 has also been studied in a quiescent model of infection where an ICP0 and VP16 null virus is transcriptionally silent and can be maintained in non-neuronal cells. In this model, quiescent genomes that are associated with PML-NBs are transcribed when ICP0 expression is induced. In an *in vitro* neuronal model or latency with wild type virus, the disruption of PML-NBs with trichostatin A (TSA) induced reactivation (Maroui et al., 2016). Similarly, observations from *in vitro* sympathetic neuron models of HSV-1 demonstrate that type I IFN signaling restricted HSV-1 reactivation in a PML-NB dependent manner (Suzich et al., 2021). These data suggest PML-NBs inhibit reactivation, but the exact mechanism is still unknown.

## PML-NB Induction of the Innate Immune Response

Although PML-NBs can act as intrinsic factors to induce rapid HSV-1 silencing, they can also trigger the innate immune response. ICP0 acts to repress ISG expression (Orzalli et al., 2012). In non-neuronal cells, ISG induction only occurs when using an ICP0 null virus at an MOI greater than 1. In these conditions, ISG transcription occurs at around 8-9 hours post-infection and is dependent upon vDNA replication, JAK, PML, and IFI16. Certain isoforms of PML are known to recruit STAT1, STAT2, HDAc1, and HDAc2 to the promoters

of ISGs during HCMV infection, suggesting a possible mechanism by which PML induces ISG expression during HSV-1 infection. The induction of ISG expression inhibits virus propagation but not plaque formation efficiency but this response was cell type specific (Alandijany et al., 2018).

## Innate Immunity and Interferon

The intrinsic immune response is followed by innate immunity that is induced during infection. Due to the speed of these responses they are often less specific than an adaptive immune response. Innate immunity is characteristic of broad pattern recognition and cytokine signaling. For example, an innate immune response that occurs in response to HSV-1 infection is the release of type I interferons (IFNα and IFNβ).

Type I IFNs are often expressed in response to the detection of pathogen-associate molecular patterns (PAMPs) by pattern recognition receptors (PRRs). There are several types of PRRs, but the most relevant to HSV-1 infection are the Toll-like receptors (TLRs). TLRs can be found on the plasma membrane, in the cytosol on endosomes and lysosomes, or the ER. Specifically, TLR2 is located on the plasma membrane and binds viral proteins gH/gL or gB. Activation of TLR2 on the plasma membrane results in signalling through MyD88 or NF-KB (a transcription factor) to stimulate the induction of pro-inflammatory cytokines such as type I IFNs (Leoni et al., 2012). In addition to TLR2, viral proteins can be sensed by herpesvirus entry mediator (HVEM). This receptor activates the NF-KB pathway in response to gD binding (Sciortino et al., 2008). It is debated

whether TLR4 (a plasma membrane receptor) is activated in response to HSV-1 infection (Danastas et al., 2020). TLR3 (Zhang et al., 2007) senses HSV RNA. Mutations to TLR3 increase the risk factor of people developing severe HSV-1 infection, indicating TLR3 as a critical restriction factor against HSV (Zhang et al., 2007). Other viral RNA sensors, MDA5 and RIG-I, are important in HSV-1 sensing and immune activation in response to viral infection (Berry et al., 2021; Chiang et al., 2018; Liu et al., 2021; Melchjorsen et al., 2010; Zhao et al., 2016). TLR9 (Lund et al., 2003), cGas (Orzalli et al., 2015), and IFI16 (Orzalli et al., 2012) sense HSV dsDNA in endosomes, the cytosol, and the nucleus respectively. IFI16 recognizes nucleosome free DNA in the nucleus in a sequence independent manner. In particular, IFI16 has a high affinity for G quadraplexes in addition to branched or cruciform DNA structures. It is hypothesized that IFI16 may be involved in the initial detection of viral DNA (the IFI16-HSV-1 DNA interaction can occur as early as 15 minutes post-infection) for chromatinization and epigenetic maintenance (Sodroski & Knipe, 2023) but it does not dictate PML recruitment (Alandijany et al., 2018). Different cell types vary in their level of sensor expression (Orzalli et al., 2015), the localization of these sensors (Orzalli et al., 2015), and the downstream effects they mediate. As a result, the immune response to viral detection is likely influenced by the specific cell type involved.

Activation of PRR sensing pathways leads to the production of interferons in many cell types. Interferons function to modulate the immune response to infection. They can mediate macrophages and NK cell activation, stimulate other

cytokines to be secreted, activate cytotoxic T lymphocytes (CTLs), induce MHC class I and II antigen presentation, and cause inflammation at localized sites. In response to microbial recognition, interferons can be released by a primary cell to activate surrounding uninfected cells via IFN binding, JAK/STAT pathway signalling, and the subsequent expression of interferon-stimulated genes. Interferon classes have distinct receptors with type I interferons binding IFN alpha receptors (IFNAR), type II binding IFN gamma receptors (IFNGR), and type III binding IFN lambda receptors (IFNLR) (Danastas et al., 2020).

Type I IFNs are expressed by most nucleated cells, in particular, keratinocytes, macrophages, and plasmocytoid dendritic cells during HSV-1 infection (Danastas et al., 2020). Type I IFNs include IFNα, IFNβ, IFNκ, IFNε, and IFNω. There are 14 subtypes for IFNα, each with varying affinities for IFNAR. All type I IFNs bind to the receptor complex made of IFNAR1 and IFNAR2 (Gibbert et al., 2013).

Type II IFN (IFNγ) is produced in response to HSV infection impact HSV lytic infection and latency. IFNγ is secreted by activated CD8+ T cells and tissue resident memory T cells ($T_{RM}$ cells). $T_{RM}$ cells are CD8+ memory T cells that can be found in both the ganglia and mucosa (Zhang et al., 2017). Finally, infiltrating CD4+ cells and NK cells will also produce IFNγ (Danastas et al., 2023). Finally, Type III Interferons (IFNλ) have been found to be produced by epithelial and non-epithelial cells (pDC) that are infected with HSV-1 (Danastas et al., 2023).

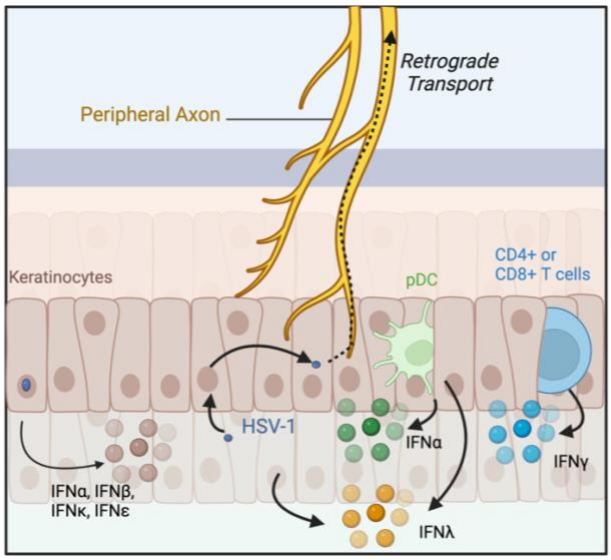


**Figure 1.2 Summary of cell-type specific interferon production**
Type I IFNs (IFNα, IFNβ, IFNκ, IFNε, and IFNω) are produced by keratinocytes, macrophages, and plasmocytoid dendritic cells (pDCs). Type II IFNs (IFNγ) are prduced by CD4 and CD8+ T cells and NK cells. Type III IFNs (IFNλ) are produced by epithelial and pDCs. Interferons impact HSV-1 lytic and latent infection.

Interferons are critical to the management of HSV-1 infection. IFNα inhibits immediate-early HSV-1 gene expression (De Stasio & Taylor, 1990). Infection of knockout IFN αβγ receptor (IFNαβγR-/-) mice with HSV-1 resulted in 100% mortality by 5 days post-infection. In contrast, but still highlighting the importance of the immune response to infection, STAT1 knockout mice infected with HSV-1 succumed to CNS infection (encephalitis) and did not survive past 10 days post-infection (Pasieka et al., 2011). To futher examine the role of IFN signaling in neuronal infection, mice expressing Cre recombinase via a nestin (neuronal specific) promoter were crossed with STAT1 floxed mice to create a new strain where STAT1 was not expressed in PNS and CNS neurons, PNS satellite glial cells, and astrocytes. Upon infection, these mice had significantly more HSV-1

replication in the trigeminal ganglia, brainstem, and brain at early time points (3-5 days) post-infection and a significantly higher mortality rate suggesting that detection of IFN by neurons is important for the management of HSV-1 pathogenesis (Rosato & Leib, 2015).

### *The effect of IFNs in neuronal infection*

After primary HSV-1 infection of epithelial cells, proximal innervating neurons are exposed to both *de novo* virus and cytokines including interferons. Interferons produced at lesion sites have the potential to modify neuronal infection. IFNβ and IFNγ stimulation of axons inhibit retrograde transport of HSV-1 in two distinct mechanisms. IFNβ and IFNγ induce local STAT1 activation (pSTAT1) which inhibits retrograde transport in a nuclear transcription-independent manner. Instead, local translation in the axon results in changes to the protein synthesis. This resulted in the downregulation of a protein (Clip2) involved in microtubule dynamics, presenting a possible mechanism by which IFN modulates retrograde transport. Beyond local translation, IFNγ has a further mechanism to inhibit HSV-1. IFNγ treatment of axons results in STAT1 nuclear localization which subsequently inhibits viral replication in the nucleus (Song et al., 2016).

Interferons have also been shown to impact the anterograde transport of HSV-1, potentially impacting the release of the virus after reactivation. All subtypes of IFN inhibit the anterograde release of HSV-1. They do so not by inhibiting anterograde transport and kinesin motor proteins. Instead it is

hypothesized the axonal IFN treatment affects exocytosis, actin mediated transport, or viral assembly (Danastas et al., 2023)

In addition to immune stimulation at the axons of neurons, stimulation at neuronal cell bodies within the ganglia has also been shown to restrict neuronal latency and reactivation (Rosato & Leib, 2015). It is unknown exactly how type I IFNs may be produced in the ganglia in order to stimulate neuronal cell bodies. Dorsal root ganglia neurons produce little type I IFN when infected with HSV-1 (Yordy et al., 2012). Yet, there is evidence that type I IFN is present in the ganglia during infection (Carr et al., 1998) suggesting that satallite glia cells (resident glia in peripheral ganglia) or other cells in ganglia produce type I IFN. Supporting this hypothesis, type I IFNs have been found to be produced by microglia in the CNS as part of the neuroinflammatory system (Roy & Cao, 2020), but more work needs to be done to understand the role of satellite glia in interferon production. Stimulation with type I IFN results in increased PML-NB formation *in vivo* and results in decreased viral transcription (Catez et al., 2012). *In vitro*, stimulation of the cell body with type I IFN is required for PML-NB formation and it must occur at the time of infection for PML-NB colocalization with the viral genome. Treatment with type I IFN at the cell body had no effect on neuronal infection rate but did result in decreased HSV-1 reactivation (Suzich et al., 2021). Furthermore, cell body stimulation with type I IFN does not prime neurons for cell death (Yordy et al., 2012), suggesting the site of type 1 IFN stimulation results in different outcomes.

Type II interferon might also be present in ganglia during HSV-1 infection. CD8+ T cells regulate HSV-1 latency by inhibiting HSV-1 replication in TG neurons and preventing neurological damage. Peak infiltration of CD8+ T cells occur in mice ganglia 12 days post-infection and persist for up to 90 days (Zhang et al., 2017). Type II interferon treatment to the cell body at the time of infection inhibited HSV-1 reactivation (Suzich et al., 2021). Whether this phenotype is PML-dependent is unknown. Yet, type II IFN did not result in the same increase in PML-NB formation as observed with type I IFN, suggesting the results of type I and II IFN stimulation of the cell body may function via distinct mechanisms.

### HSV-1 perturbation of host innate immune defenses

Just as the host response acts to limit viral infection, viral factors may antagonize the immune response to infection. Viral infection led to decreased STAT1 and STAT3 localization to the nucleus in IFN treated neurons, potentially leading to decreased ISG expression. HSV-1 has mechanisms to degrade STAT1, inhibit STAT1 activation, and inhibit STAT1 nuclear localization (Danastas et al., 2023). The viral protein ICP0 restricts many host restriction factors including PML, Sp100, and IFI16 (Chelbi-Alix & de The, 1999; Everett et al., 1998; Orzalli et al., 2012). Some host factors, such as IFI16, are able to overcome viral inhibition. IFI16 is an interferon stimulated gene (ISG) and so in cells treated with IFN, IFI16 expression is increased to a level that it is still able to repress wild type HSV-1 with functional ICP0 (Sodroski & Knipe, 2023). Just as with ICP0 degradation of PML-NBs, other viral proteins such as $\gamma_1$34.5 (Liu et al.,

2021), UL37 (Zhao et al., 2016), US11, US3, virion host shut off (vhs), VP16, and ICP27 (Danastas et al., 2020) also prevent the activation of immune pathways and/or IFN-inducible protein expression.

## ATRX restriction of HSV-1 infection

### ATRX General

ATRX is a member of the switch2/sucrose nonfermentable2 (SWI2/SNF2) family of chromatin remodeling proteins, residing exclusively within the nucleus and predominantly localizing to highly repetitive heterochromatic sequences (Noh et al., 2015). Through its various domains, ATRX interacts with a wide variety of proteins in different contexts. These proteins include but are not limited to HP1α, EZH2, MeCP2, and macroH2A (Ratnakumar & Bernstein, 2013). In addition to the large list of proteins known to associate with ATRX, ATRX has a wide variety of functions including G quadruplex resolution (Teng et al., 2021), DNA methylation (Marano et al., 2019), heterochromatin repression (Voon et al., 2015), Polycomb silencing (Sarma et al., 2014), and even transcription activation via macroH2A (Truch et al., 2022). Despite the multifunctional nature of ATRX, the most well studied role of ATRX is in association with repressive chromatin. ATRX is often found at large, tandemly repeated regions associated with heterochromatin, such as telomeres, centromeres, and ribosomal DNA (Ratnakumar & Bernstein, 2013).

The *ATRX* gene is located on the X chromosome and contains 38 exons. Expression of *ATRX* results in two isoforms: a larger ~280 KDa protein and

truncated ATRX (ATRXt) that is ~180 KDa. At the N terminal of the protein is the ATRX-DNMT3-DNMT3L (ADD) domain, consisting of a PHD zinc-finger domain, a GATA-like zinc finger domain, and an alpha-helical region. The ADD domain plays a crucial role in ATRX recruitment (Eustermann et al., 2011) and can directly target chromatin through DNA template interactions with its GATA-1–like domain (Noh et al., 2015). The ADD domain also recognizes H3 histones and is responsible for recognizing H3K4me0 and H3K9me3 (or H3K9me2) marks. At the C terminus of the ATRX protein there is a SNF2 ATPase/helicase domain (Eustermann et al., 2011; Ratnakumar & Bernstein, 2013).

Mutations to ATRX result in ATRX Syndrome, which is characterized by intellectual disability, developmental delay, distinctive facial features, and reduced alpha globin expression. Most syndrome-causing mutations are found within the ADD or ATPase domain and lead to reduced ATRX protein levels (Ratnakumar & Bernstein, 2013). Cells with loss-of-function mutations to ATRX have changes in chromatin accessibility, an increase in active chromatin marks, and H3.3 deposition at actively transcribed genes and their regulatory elements (Truch et al., 2022). Experimentally, ATRX knockdown results in altered patterns of DNA methylation, a telomere-dysfunction phenotype, aberrant chromosome segregation, premature sister chromatid separation, and changes in gene expression (Eustermann et al., 2011).

## ATRX and G quadruplexes

G quadruplexes (G4s) are DNA or RNA secondary structures that form in regions of DNA or RNA that are rich with guanine. These structures are thought to form during DNA replication and transcription when double stranded DNA is dissociated (Teng et al., 2021). The secondary structure that is formed is very stable as the four G-quartets form a hydrogen bonding network around a cation. These G-quartets then stack on top of each other to make a G4 structure. The stacking allows for even more stability as base stacking occurs and can result in multiple topologies such as anti-parallel, parallel, and hybrid (Frasson et al., 2021). G4 structures have multiple functions including inducing replicative stress or blocking transcription. G4 structures can cause replicative stress by blocking DNA replication fork progression, leading to replication fork collapse (Teng et al., 2021). They are typically found at telomeres and pericentromeric repeats but can also be found at intragenic CpGs, etc. (Dyer et al., 2017).

In HSV infection, G4 structures function to promote transcription. G4 structures are abundant on regions of the HSV-1 genome including on IE gene promoters. Parallel G4 structures are bound and unfolded by ICP4, a viral transcription factor. The specificity for parallel G4 structures, which consist of the majority of G4 structures on the viral genome, may be a way for ICP4 to specifically associate with the viral genome instead of other cellular DNA (although cellular DNA, such as telomeric DNA, has been observed to be enriched with parallel G4s (Parkinson et al., 2002)). In this way, G4 structures on

the viral genome recruit transcription factors to promoter regions (Frasson et al., 2021).

ATRX binds to GC rich regions throughout the genome. It can bind directly to G-rich tandem repeats and this binding may resolve G4 structures possibly through the deposition of H3.3 (Dyer et al., 2017). To resolve G4 structures, ATRX requires both its helicase function and H3.3 binding and chaperone capabilities (via interaction with DAXX) (Teng et al., 2021). By binding and resolving G4 structures, ATRX prevents replication stress ahead of the DNA replication fork (Teng et al., 2021). ATRX mediated G4 resolution maintains heterochromatin at these DNA regions (Teng et al., 2021). When ATRX was depleted, there was increased chromatin accessibility at G4 sites and less H3.3 and H3.3K9me3 enrichment. HIRA had no effect on H3.3 enrichment at these sites. ESET, a histone methyltransferase, was also required for maintaining the closed chromatin state at G4 structures, suggesting that heterochromatin formation ultimately was required to maintain G4 structure resolution.

This observation contrasts with other studies that suggest ATRX plays a role at multiple sites in euchromatic regions, particularly at enhancers and promoters including those located within the context of CpG islands. Many of these sequences are G-rich regions with the potential to form G4 quadruplex sequences, also known as putative G4 quadruplex forming sequences (PQS). The ATRX/DAXX/H3.3 complex binds repetitive sequences and PQS (Truch et al., 2022) and may therefore modulate G4 structure formation and subsequent transcription. ATRX can bind to G4 structures during transcriptional elongation,

resolve these structures, and therefore inhibit RNA Polymerase II stalling (Levy et al., 2015).

The cell also has a way to inhibit ATRX occupation and resolution of G4 structures. The lncRNA TERRA has been found to form G4 structures and be bound by ATRX. When ATRX is bound to TERRA its occupancy at other G4 sites on DNA such as transcriptional start sites. This leads to increased G4 abundance at these sites (Tsai et al., 2022).

It is unknown whether ATRX binds to G4 sequences on the viral genome. If it did, ATRX may function to inhibit viral transcription by blocking ICP4 recruitment to promoter regions. It is unknown how ATRX would affect chromatin formation at G4 sites on the viral genome.

### *ATRX and TERRA*

Located at the end of linear chromosomes in eukaryotes, telomeres are heterochromatin associated regions of DNA. The DNA that composes telomeres is highly repetitive and has a 3' overhang that is G-rich. Although telomeric regions of DNA are thought to be transcriptionally silent, RNA polymerase II has been found to transcribe telomeric repeat-containing RNA (TERRA). TERRAs are long non-coding RNAs that contain RNA repeats, range in lengths from 0.1-9 kb, and are exclusively located in the nucleus. The transcription of TERRA occurs in the region of genome that is adjacent to telomeres (subtelomeres) at CpG island promoters (Nergadze et al., 2009). TERRA contributes to heterochromatin via PRC2 and SUV29H1 and the deposition of H3K9me3,

H4K20me3, and H3K27me3 (Montero et al., 2018). TERRA can function in *cis* on the telomere of origin or in *trans* on neighboring telomeres. TERRA modulates telomeric accessibility in part by interacting with ATRX, a key factor in telomere stability (Tsai et al., 2022). TERRA binds to ATRX directly and decreases its occupancy at DNA sites, specifically at G4 structures. When TERRA inhibits ATRX binding it also prevents it from forming repressive heterochromatin at these locations (H3K9me3). TERRA depletion leads to elevated ATRX occupancy at cellular genes and decreased chromatin accessibility (Tsai et al., 2022).

Telomeric DNA is disrupted during HSV-1 lytic infection (Deng et al., 2014). HSV-1 remodeling of telomeric DNA promotes HSV-1 viral replication. The HSV-1 protein, ICP0, disrupts telomeres by promoting expression of telomeric DNA and the expression of telomere repeat-containing RNA (TERRA) during lytic replication of non-neuronal cells (Deng et al., 2014). Whether TERRA expression is changed during HSV-1 neuronal infection and if it mediates the association of ATRX with the viral genome is unknown.

### ATRX, MeCP2, and DNA methylation

Cytosine, a building block of DNA, can be methylated on its 5’ carbon. This methylation mark constitutes the most common covalent modification to genomic DNA. Often this mark occurs at cytosines that are followed by guanines in the 5’ to 3’ direction (denoted CpG sequences). CG sequences are very commonly methylated with 60-90% of these sites methylated on mammalian

DNA. When a cytosine is methylated, it acts to silence transcription on associated DNA (Moore et al., 2013).

DNA methyltransferases (DNMT) act as the ‘writers’ of DNA methylation, transferring a methyl group from S-adenyl methionine (SAM) onto the cytosine. There are three DNMTs. DNMT1 methylates daughter strand DNA based on a parental strand of DNA. In contrast, DNMT3A and DNMT3B are capable of methylating without a parental strand, establishing *de novo* patterns of methylation. DNA methylation is an essential process in development. In almost all cell types, DNMTs are down regulated once a cell is fully differentiated (Moore et al., 2013). The one exception to this rule exists in post-mitotic neurons.

During post-natal development, neuronal DNA continues to be methylated. This methylation differs from that found in other cell types because it is often non-CpG methylation. Non-CpG methylation can occur on cytosines neighboring adenine (mCpA), cytosine (mCpC), or thymine (mCpT). All three of these methylation patters are referred to as mCH. mCH is nearly undetectable in non-neuronal cells, is deposited mostly by DNMT3A, and increases with age in neurons. DNMT3A (but not DNMT3b) is highly expressed in neurons. Another non-canonical form of DNA methylation that is highly abundant in neurons is CG hydroxymethylation (hmCG) (Kinde et al., 2015).

MeCP2 (Methyl CpG binding protein) binds to methylated CpG sites and plays an essential role in neuronal development as mutations to this gene lead to the neurodevelopmental disease Rett’s Syndrome (RTT). Despite CpG appearing in the name of MeCP2, the protein can bind mCA just as readily

(Tillotson et al., 2021). It is debated whether MeCP2 can bind hmCG as well. MeCP2 binding of mCG and mCA is thought to be repressive. Alternatively, MeCP2 binding of hmCG may activate associated genes (Kinde et al., 2015).

MeCP2 interacts with the helicase (C-terminal) domain of ATRX and recruits it to heterochromatic foci (MeCP2 mutant resulted in no ATRX recruitment). Since MeCP2 is more abundant in neuronal cells than non-neuronal cells, it could be a more prevalent ATRX recruiter in the brain. Mutations to MeCP2 resulted in widespread delocalization of ATRX in mature neurons. This is different from other studies where the PHD domain of ATRX is required for its recruitment. Differences in requirements for ATRX recruitment may be due to post translational modifications of ATRX in mature neurons. Changes in recruitment may also be because of the abundance of MeCP2 in the mature brain outcompetes other binding partners such as HP1 (Nan et al., 2007).

MeCP2 acts to regulate gene expression by recruiting various epigenetic modulators to methylated DNA. ATRX is a major contributor to the epigenetic regulation of MeCP2 bound genes. At pericentric heterochromatin (PCH; regions of DNA surrounding the centromeres), MeCP2 and ATRX are highly enriched and contribute to higher order organization of these regions in neurons (Marano et al., 2019). MeCP2 recruitment of ATRX to PCH acts in a positive feedback loop in which ATRX also acts to recruit MeCP2 (Kernohan et al., 2010). Both ATRX and MeCP2 recruit all three subtypes of HP1 to PCH and this recruitment may also be RNA (specifically ncRNA) dependent (Marano et al., 2019).

MeCP2 also functions to regulate gene expression through higher order chromatin conformation. MeCP2 and cohesion promote chromosomal looping which leads to long-range chromatin interactions and insulation of regions of DNA. ATRX is present at sites with MeCP2 and cohesion and when ATRX was knocked out full occupancy of cohesion and CTCF was not achieved (Kernohan et al., 2010).

ATRX binds intragenic (not promoter) CpG Islands (CGIs) and differentially methylated regions (DMRs). ATRX-bound CGI sequences were more likely to be methylated and localized within gene bodies (Voon et al., 2015). Loss of ATRX lead to DNA methylation pattern changes suggesting that ATRX may also play a role in recruiting factors to promote DNA methylation (Gibbons et al., 2000)

Although there is previous evidence that HSV-1 DNA is not methylated (Kubat et al., 2004), further investigation into the role of non-canonical DNA methylation, MeCP2, and ATRX is needed.

## ATRX and Constitutive Heterochromatin

Constitutive heterochromatin silencing is thought to be a “permanent” form of repression that is highly compacted and resistant to transcription. This form of silencing occurs at repetitive DNA elements, pericentromeric and telomeric DNA. Constitutive heterochromatin is characterized by the enrichment of DNA methylation, H4K20me3, and H3K9me3. H3K9me3 is bound by the ADD domain of ATRX (Dhayalan et al., 2011). ATRX localizes to constitutive heterochromatin

and maintains silencing by depositing the histone variant H3.3 and reinforcing heterochromatin-associated marks (Voon & Wong, 2016).

ATRX maintains constitutive heterochromatin silencing is via its interaction with DAXX. ATRX and DAXX deposit H3.3 at pericentric heterochromatin (PCH), telomeres, and other heterochromatin sites throughout the genome. DAXX binds directly to H3.3 while ATRX binds DAXX and guides H3.3 incorporation (Dyer et al., 2017). During nucleosomal disruptions, ATRX/DAXX are recruited to distinct heterochromatic regions to deposit H3.3. ATRX-dependent deposition of H3.3 preferentially localizes to DNA-methylated alleles. This indicates that ATRX-dependent deposition must be driven epigenetically. ATRX binding of heterochromatin-modified regions (including a high number of DMRs) correlated with high H3.3 enrichment (Voon et al., 2015). In addition to methylated DNA binding, ATRX can be recruited to pericentric heterochromatin via H3K9me3 binding (Iwase et al., 2011).

To further propagate silencing, the ATRX/DAXX complex recruits other factors including histone lysine methyltransferases to further propagate silencing. SUV39H1/2 is recruited to telomeres and pericentromeres to deposit H3K9me3. Meanwhile, the SETDB1 and KAP1 complex deposit H3K9me3 at ERVs and DMRs (Voon et al., 2015). ATRX-mediated incorporation of H3.3 and its ensuing methylation of lysine-9 may facilitate a positive feedback loop where incorporated H3.3 then increases the recruitment of ATRX to the associated heterochromatic regions (Voon et al., 2015). ATRX/DAXX/H3.3 enrichment is essential for H3K9me3 enrichment at certain regions of the genome (Voon & Wong, 2016).

### *ATRX and heterochromatin maintenance*

ATRX maintains heterochromatic stability in CNS. In neurons, a methyl/phospho switch occurs after periods of stimulation/stress and is highly enriched at heterochromatic repeats associated with centromeres. H3K9me3S10ph-bound ATRX represses noncoding transcription of centromeric minor satellite (repetitive) sequences during instances of stress. In contrast, HP1 is a H3K9me3 reader that is not able to withstand a methyl/phospho switch. This indicates a critical role for ATRX in the maintenance of heterochromatic stability in developing neurons. Furthermore, this suggests a potentially causative mechanism underlying the severe pathologies associated with X-linked alpha thalassemia intellectual disability syndrome (Noh et al., 2015).

## ATRX and HSV-1

In human foreskin fibroblasts (HFFs), ATRX colocalizes with the viral genome as early as 10 minutes post-infection. The colocalization with ATRX begins to decrease at about 100 minutes post-infection, most likely when PML-NBs are dispersed by ICP0. ATRX colocalization in HFFs with the viral genome is IFI16 independent and DAXX dependent. ATRX restricted an ICP0 null virus lytic replication (from input and progeny virus) as early as 6 hours post-infection. The restrictive effects of ATRX were found to be cooperative with that of DAXX. When ATRX was knocked out, H3, H3.3, H3K9me3, and H3K27me3 levels on the viral genome were significantly reduced at 8 HPI and viral DNA replication was enhanced. This suggests ATRX maintains heterochromatin and inhibits viral

DNA replication during non-neuronal lytic infection. Yet, even in the absence of ATRX, H3, H3.3, H3K9me3, and H3K27me3 are still found on the viral genome, suggesting other factors are either solely responsible for their deposition or the deposition pathway can be compensated. During chromatin stress (transcription), ATRX helps to maintain the enrichment of H3K9me3 on the viral genome (Cabral et al., 2018).

When fibroblasts are infected with ICP0 null virus, ATRX and DAXX restrict viral transcription. ATRX restricts infection by reducing the accessibility of viral DNA (possibly via altering histone H3-associated chromatin) ATRX and DAXX are one of many factors that deposit H3.3. The ATRX/DAXX complex is the only nuclear H3.3 chaperone complex able to restrict ICP0 null HSV lytic infection (Cabral et al., 2021). Depletion of either DAXX or ATRX increases the efficacy of an ICP0 null virus. This phenotype is reversible with the addition of DAXX but not with DAXX mutated to lack an ATRX binding site. When DAXX is depleted, ATRX is no longer recruited to viral genomes. This suggests that DAXX and ATRX work in complex, and that ATRX recruitment and function is DAXX dependent (Lukashchuk & Everett, 2010). It remains unknown whether ATRX and DAXX deposit H3.3 onto the viral genome during neuronal infection and how they depend on each other in this cell type.

ATRX and DAXX have been found to associate with and promote the function of H3K9 methyltransferases SETDB1 and SUV39H1. Yet, in fibroblasts when these HMTs were depleted in addition to ATRX there was no significant

difference in ICP0 null virus production suggesting they do not contribute to the restrictive phenotype of ATRX in this scenario (Cabral et al., 2021). Whether ATRX and DAXX promote histone post-translation modification deposition during lytic infection or latency is unknown.

ATRX and DAXX restrict multiple DNA viruses including HSV, HCMV, AdV, and EBV. The complex has been shown to promote H3.3 deposition to the viral DNA genomes of all these viruses (Albright & Kalejta, 2016; Schreiner et al., 2013; Tsai et al., 2011). ATRX and DAXX may also be important for the maintenance of latency, as depletion of either resulted in EBV reactivation (Tsai et al., 2011). Finally, HSV, HCMV, AdV, KSHV, and EBV all degrade or displace ATRX suggesting it is a generalized restriction factor against DNA viruses (Albright & Kalejta, 2016; Full et al., 2014; Jurak et al., 2012; Lukashchuk & Everett, 2010; Schreiner et al., 2013; Tsai et al., 2011).

### *HSV mediated degradation of ATRX*

HSV has multiple mechanisms to deplete ATRX. Vhs (virion host shutoff) is an HSV-1 encoded endoribonuclease that plays a role in the depletion of ATRX mRNA in lytically infected cells. Immediately upon reactivation, (unlike lytic infection) there is no Vhs due to limited viral transcription. Whether Vhs plays a role during later stages of reactivation is unknown. ICP0 is another factor capable of degrading ATRX. ICP0 is known to degrade components of PML-NBs which results in the dispersal of PML-NB components. ATRX depletion was observed later in infection (4-8 hours) than the depletion of PML but was still found to be

proteasome dependent. During reactivation (unlike lytic infection) there is little ICP0 present to degrade ATRX (Jurak et al., 2014). Immediately upon reactivation, ICP0 is not expressed due to lack viral transcription during latency. The role of ICP0 in reactivation varies in response to reactivation trigger. Whether ICP0-dependent degradation of ATRX contributes to transcriptional activation during reactivation remains unknown.

ATRX is a target of HSV-1 miR-H1 and HSV-2 miR-H6. miR-H1 targets the 3' UTR of ATRX mRNA to downregulate ATRX expression. miR-H1 and miR-H6 share a seed sequence (nucleotides 2-8). Both miRNAs are abundant during lytic infection. miR-H1 is a late gene product, and its expression is inhibited by ACV. There is evidence for miR-H1 and miR-H6 is expression during latency. Whether these microRNAs are expressed during Phase I of reactivation to aid in ATRX depletion, and the activation of viral genes is unknown. (Jurak et al., 2014).

# Interferon Dependent Immune Memory during HSV-1 Neuronal Latency Results in Increased H3K9me3 and Restriction of Reactivation by ATRX

*This chapter has been adapted from:*

Whitford, A. L., Auguste, G., Francois, A. K., Boutell, C., Miller, C. L., Dremel, S. E., & Cliffe, A. R. (2025). Interferon Dependent Immune Memory during HSV-1 Neuronal Latency Results in Increased H3K9me3 and Restriction of Reactivation by ATRX. bioRxiv, 2025.2001.2028.633013. https://doi.org/10.1101/2025.01.28.633013

## Abstract

Herpes simplex virus-1 (HSV-1) establishes a lifelong latent infection in neurons and reactivation from this latent state is the cause of recurrent oral and ocular infections, herpes simplex keratitis, and encephalitis. Neuronal conditions during initial HSV-1 infection have a long-term impact on latency, modulating how responsive latent genomes are to reactivation and, therefore, their ability to cause disease. Type I interferon (IFNα) exposure during initial infection results in promyelocytic leukemia nuclear-body (PML-NB) formation and a more restrictive form of HSV-1 latency. Here we demonstrate that IFNα induced PML-NBs recruit histone chaperones to the viral genome and promote the deposition of the repressive heterochromatin mark, histone H3 lysine 9 tri-methylation (H3K9me3), and its reader, ATRX (alpha-thalassemia/mental retardation, X-linked). This work reveals the mechanism by which immune signaling during initial infection induces an epigenetic memory on HSV-1 genomes that is maintained during latency and inhibits reactivation. ATRX is highly abundant in neurons and is essential for maintaining cellular heterochromatin during neuronal stress. Here we find that ATRX prevents transcription, and subsequent reactivation, from H3K9me3-bound latent genomes by remaining associated with viral chromatin following stress-induced phosphorylation of histone H3. This indicates that H3K9me3-associated viral genomes are refractory to reactivation when read by ATRX. This work demonstrates that ATRX acts as a neuronal restriction factor against HSV-1 reactivation, elucidating a new potential target for inhibiting HSV-1 reactivation and subsequent human disease.

## Introduction

Herpes simplex virus 1 (HSV-1) establishes a lifelong latent infection in neurons, allowing the virus to persist in its host for extended periods and evade immune surveillance. The DNA virus genome persists in the nucleus of an infected neuron and is subjected to heterochromatin-based silencing (Cliffe et al., 2009; Kwiatkowski et al., 2009; Nicoll et al., 2016; Wang et al., 2005). It is thought that epigenetic silencing mechanisms promote and maintain latency and need to be remodeled for reactivation to occur. However, studies investigating the contribution of heterochromatin to HSV-1 latency are complicated by the heterogeneous nature of the latent viral epigenome. For example, there is evidence of heterogeneity in the subnuclear distribution of viral genomes, levels of viral gene, expression, and reactivation (Catez et al., 2012; Dochnal et al., 2022; Ma et al., 2014; Maroui et al., 2016; Sawtell & Thompson, 2004). How different epigenetic structures form and whether they differentially contribute to reactivation competencies of the viral genome is unknown. This is important to understand in the context of HSV-1, as reactivation is associated with a variety of diseases, including cold sores, herpes simplex keratitis, and encephalitis. Further, studying the epigenetics of HSV infection of neurons also informs on the function of heterochromatin-associated proteins in this specialized cell type.

As a virus that persists in a long-lived cell type, the state of the cell at the time of initial infection could impact the nature of latency and future ability to reactivate. For example, neuronal stress or immune signaling during initial

infection has been shown to modulate later reactivation (Dochnal, Whitford, et al., 2024; Suzich et al., 2021). The mechanisms underlying cell-intrinsic long-term memory during HSV-1 latency, triggered by short-term external stimuli, remain unknown. In the case of innate immune stimuli, our laboratory has previously shown that type I interferon exposure at the time of primary infection restricts later reactivation. We also showed that this was due to the formation of Promyelocytic leukemia-nuclear bodies (PML-NBs) in neurons (Suzich et al., 2021). PML-NBs are membrane-less nuclear organelles composed of the scaffolding protein PML and various stably and transiently associated proteins (Lallemand-Breitenbach & de The, 2010). PML-NBs function to compartmentalize proteins within eukaryotic cells and are known to play a role in the intrinsic repression of productive herpesvirus replication (Alandijany et al., 2018; Everett et al., 1998; Everett & Murray, 2005; Everett et al., 2004). A subpopulation of HSV genomes colocalizes with PML-NBs during latency (Catez et al., 2012). Our previous work showed that the co-localization of viral genomes with PML-NBs occurred when neurons were exposed to type I IFN solely at the time of initial infection and that PML was responsible for the IFN-dependent restriction of reactivation (Suzich et al., 2021). However, the mechanism underlying this restriction remains unclear, specifically whether it is due to changes in epigenetic silencing or the physical entrapment of viral genomes within PML-NBs.

The latent HSV-1 genome is known to be associated with repressive histone modifications. However, the intersection between extrinsic stimuli and the

latent epigenome, both in the context of latency establishment and reactivation, are unknown. Latent viral genomes are enriched with H3K9me2, H3K9me3, and H3K27me3 (Cliffe et al., 2009; Kwiatkowski et al., 2009; Nicoll et al., 2016; Wang et al., 2005). H3K9me3 is viewed as a long-term, constitutive form of heterochromatin, whereas H3K27me3 is known to mark regions of facultative heterochromatin on the host, which can potentially more readily convert to active chromatin for gene expression (Dochnal et al., 2021). However, in the context of HSV-1 infection of a terminally differentiated neuron, it is unknown whether certain types of histone post-translational modifications give rise to genomes that are more or less capable of reactivating. Furthermore, investigating heterogeneity can be a challenge as most techniques analyze a population of genomes. To investigate heterochromatin marks on a single genome, we developed a tool (NucSpotA) to quantify the labeling of an immunofluorescent stain at the viral genome that can then be standardized to the stain throughout the nucleus. This tool has enabled us to quantify subpopulations of genomes that display distinct marks (Francois et al., 2024). We hypothesized that interferon-induced PML-NBs may increase the subpopulation of latent genomes with H3K9me3 silencing. This hypothesis is based on previous studies showing that PML-NBs impact H3K9me3 deposition on cellular chromatin (Delbarre et al., 2017) and potentially on viral DNA during lytic infection (Lee et al., 2016). It remains uncertain how an increase in the percentage of viral genomes with H3K9me3 would lead to a more repressive state of latency.

H3K9me3 represses chromatin through its interaction with histone readers, including HP1 family proteins (Bannister et al., 2001; Jacobs et al., 2001; Lachner et al., 2001), ATRX (alpha-thalassemia/mental retardation, X-linked) (Dhayalan et al., 2011; Noh et al., 2015), CHD4 (Mansfield et al., 2011), TRIM66 (Jain et al., 2020), PHRF1 (Jain et al., 2020), UHRF1 (Nady et al., 2011), TNRC18 (Zhao et al., 2023), MPP8 (Chang et al., 2011), and Tip60 (Sun et al., 2009), whereas the Polycomb family of protein complexes reads H3K27me3 (Cao et al., 2002). The diversity in reader proteins and the impact on chromatin structure increases the potential complexity of viral genome silencing. The readers associated with the latent HSV-1 genome remain unidentified, but understanding their role in silencing is crucial, as reader-based silencing would need to be overcome for reactivation to occur. HSV-1 reactivation is biphasic (Cliffe et al., 2015; Cuddy et al., 2020; Dochnal et al., 2022; Kim et al., 2012; Whitford et al., 2022) and the first phase of reactivation involves the phosphorylation of the serine 10 neighboring H3K9me3 (H3K9me3pS10). This phosphorylation evicts many H3K9me3 readers allowing for transcription without the removal of repressive methylation marks. Importantly, ATRX is an H3K9me3 reader that has been shown previously to be resistant to eviction following S10-phosphorylation (Noh et al., 2015). We investigated whether ATRX restricts HSV-1 reactivation and found that ATRX inhibits reactivation from H3K9me3-enriched genomes. This inhibitory effect is further amplified by IFN treatment, which increases ATRX enrichment at the latent viral genome (Whitford et al., 2025).

## Results

### PML is required for the initiation but not the maintenance of the type I IFN-dependent restricted form of HSV-1 latency

Previously, using an *in vitro* model system of HSV-1 latent infection, we reported that PML-NBs form in peripheral sympathetic and sensory neurons following exposure to type I IFN. We also observed that the HSV-1 genome co-localizes and is maintained at PML-NBs only when initial infection occurs at the same time as exposure to type I IFN (Suzich et al., 2021). Type I IFN treatment during initial infection also resulted in repression of reactivation that could be overcome by the depletion of PML before infection. To determine the mechanism of PML-based restriction, we asked whether PML was required for both the initiation and maintenance of the repressive reactivation phenotype. Primary neurons from the superior cervical ganglia (SCG) of postnatal mice were dissected and transduced with lentivirus expressing *Pml* shRNA five days before infection with HSV-1. Infection was carried out using Stayput GFP (MOI 5 PFU/cell) (Dochnal et al., 2022), which expresses a Us11-GFP and is also defective in cell-to-cell spread, permitting the quantification of individual reactivating neurons (Figure 2.1A). Neurons were also treated with 600 IU/µl of IFNα for 18h prior to infection. Acyclovir (ACV) was added for the first 8 days post-infection to promote latency establishment and then washed out. Reactivation was triggered 10 days post-infection using the PI3K inhibitor, LY294002, as described previously (Camarena et al., 2010; Cliffe et al., 2015; Dochnal et al., 2022; Kim et al., 2012; Kobayashi et al., 2012) (Figure 2.1A). To assay the role of PML-NBs in the restriction of

reactivation, we depleted the PML protein via shRNA (Supplemental Figure 2.1) Consistent with our previous study (Suzich et al., 2021), we found PML depletion prior to infection resulted in enhanced reactivation of IFN-treated neurons to levels comparable to the untreated neurons (Figure 2.1B). However, depletion of PML after latency had already been established (5 days post-infection) did not impact reactivation in IFN-treated neurons (Figure 2.1C). These findings suggest that the presence of PML-NBs during initial infection contributes to the restrictive phenotype initiated by IFNα treatment during infection, but PML-NBs were not required to maintain IFNα-induced silencing at later time points.

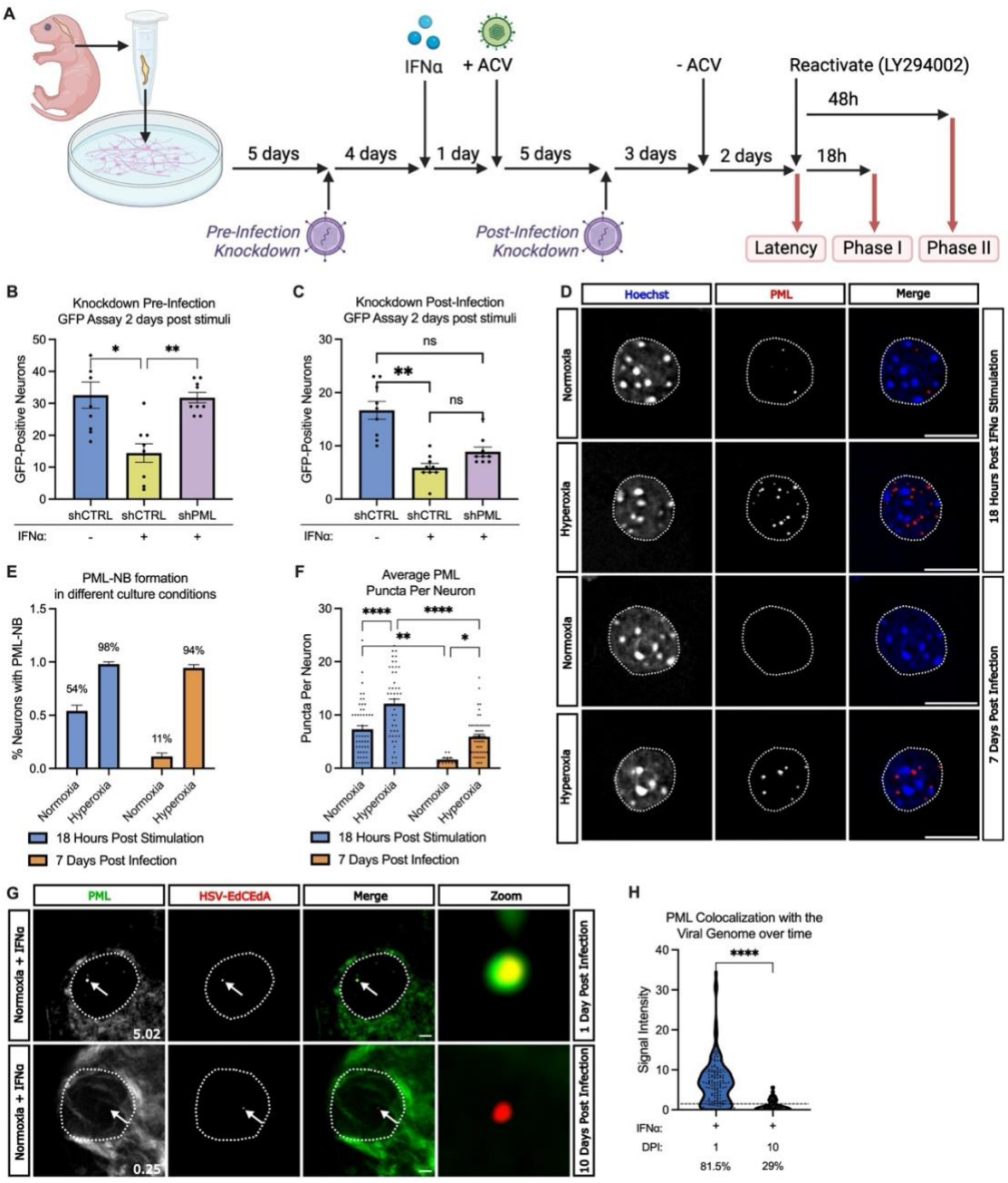
A
IFNα
+ ACV
- ACV
Reactivate (LY294002)
48h
5 days
4 days
1 day
5 days
3 days
2 days
18h
Pre-Infection Knockdown
Post-Infection Knockdown
Latency
Phase I
Phase II
B
Knockdown Pre-Infection
GFP Assay 2 days post stimuli
GFP-Positive Neurons
shCTRL shCTRL shPML
IFNα: - + +
C
Knockdown Post-Infection
GFP Assay 2 days post stimuli
ns
ns
GFP-Positive Neurons
shCTRL shCTRL shPML
IFNα: - + +
D
Hoechst
PML
Merge
Normoxia
Hyperoxia
Normoxia
Hyperoxia
18 Hours Post IFNα Stimulation
7 Days Post Infection
E
PML-NB formation
in different culture conditions
% Neurons with PML-NB
54%
98%
11%
94%
Normoxia
Hyperoxia
Normoxia
Hyperoxia
18 Hours Post Stimulation
7 Days Post Infection
F
Average PML
Puncta Per Neuron
Puncta Per Neuron
Normoxia
Hyperoxia
Normoxia
Hyperoxia
18 Hours Post Stimulation
7 Days Post Infection
G
PML
HSV-EdCEdA
Merge
Zoom
Normoxia + IFNα
5.02
1 Day Post Infection
Normoxia + IFNα
0.25
10 Days Post Infection
H
PML Colocalization with the
Viral Genome over time
Signal Intensity
IFNα: + +
DPI: 1 10
81.5% 29%

**Figure 2.1: PML-NBs initiate neuronal HSV-1 silencing but do not persist to latency to maintain silencing.**
**A)** Schematic of the primary neuronal model of HSV-1 latency and reactivation using sympathetic neurons isolated from the superior cervical ganglia (SCG) of newborn mice.
**B)** Quantification of HSV-1 reactivation based on the numbers of Us11-GFP positive neurons at 2 days post reactivation. Neurons were depleted of PML using lentivirus-mediated shRNA depletion five days prior to infection and treated with 600 IU/ml IFNα for 18h hours before infection and 24 hours post-infection. Reactivation was induced using LY294002 (20 μM). Individual repetitions (N=9; wells containing approximately 5000 neurons) from 3 independent dissections. Statistical comparisons were made using an Ordinary one-way ANOVA with Tukey's multiple comparison.
**C)** Quantification of HSV-1 reactivation based on the numbers of Us11-GFP positive neurons at 2 days post reactivation. Neurons were treated IFNα before infection as in B and depleted of PML using lentivirus-mediated shRNA depletion five days post-infection. N=9 biological replicates from 3 independent dissections. Statistical comparisons were made using an Ordinary one-way ANOVA with Tukey's multiple comparison.
**D)** Representative images of sympathetic neurons cultured in atmospheric (21% Oxygen) or physioxia (5% oxygen) conditions and fixed at either 18 hours post-treatment with IFNα (or 0h post-infection) or 7 days post-infection. Immunofluorescence was carried out for PML and cells co-stained with Hoechst. Scale bar, 10 μm.
**E & F)** Quantification of the percentage of neurons with detectable PML-NBs in their nuclei (E) and (F) detectable PML puncta per nuclei at 18 hours post-treatment with IFNα or 7 days post-infection in either atmospheric or physioxia conditions. N>50 cells from 2 biological replicates. Statistical comparisons were made using a two-way ANOVA with Tukey's multiple comparisons. In F, dots represent individual cells.
**G)** Neurons treated with IFNα at the time of infection were infected with HSV-1 EdC/EdA and fixed at 1- or 10-days post-infection. The viral genome was visualized using click chemistry, and immunofluorescence was carried out for PML. White arrows point to location of viral genome. Scale bar, 10 μm.
**H)** NucSpotA was used to quantify the signal intensity of PML at the viral genome 1- or 10-days post-infection. Each data point represents one viral genome. Percentages indicate the proportion of genomes with NucSpotA intensity ratios above the denoted co-localization threshold (dashed line). N>60 cells from 3 biological replicates. Statistical comparisons were made using a Mann-Whitney. Data represent the mean ± SEM. (ns not significant, *≤ 0.05, **≤ 0.01, ***≤ 0.001, ****≤ 0.0001).

The contribution of PML to the maintenance of the restrictive phenotype differed slightly from our previous study, where we had observed a slight increase in reactivation in neurons following PML depletion after latency was established. In our original study, neurons were cultured in atmospheric conditions. However, we have since changed the culturing conditions to more accurately mimic the oxygen concentration of peripheral neurons, which improves neuronal health, particularly in long-term cultures (Dochnal, Krakowiak, et al., 2024). We investigated whether the change in culturing conditions impacted the formation of PML-NBs at the time of infection (18 hours post IFNα stimulus) and persistence of PML-NBs during infection (Figure 1D). Here we used a latent timepoint of 7 days post infection, as compared to 10 days which is used throughout this manuscript, to compare to the previous study where PML-NBs were only cultured in hyperoxic conditions (Suzich et al., 2021). We found that IFNα treated neurons cultured in more physiological oxygen levels (5% $O_2$) were less likely to have PML-NB formation (Figure 1E) and had fewer PML-NBs per neuron and had decreased PML-NB persistence than those cultured in atmospheric oxygen (Figure 1F). These data suggest that the oxygen concentration that neurons are cultured in *in vitro* affects their response to innate immune signals. Moreover, although PML initially co-localized with HSV-1 following IFNα treatment in both atmospheric and physiological oxygen concentrations, after 10 days the co-localization was lost under physioxia (Figure 1G). We quantified this phenotype over multiple latent neurons using NucSpotA (Francois et al., 2024) (Figure 1H) and observed 81.5% of genomes co-localized

at 1 day in contrast to 29% at 10 days. The percentage of genomes co-localizing was determined by setting a signal intensity threshold based on colocalization by eye on 50 genomes. Together, our data indicate that PML associates with the viral genome during initial infection and initiates silencing, but PML-NBs do not persist during latency and are not required to maintain the restrictive phenotype of IFNα. IFNα induced restriction during initial infection is DAXX dependent.

### IFNα induced restriction during initial infection is DAXX dependent.

Our observation that PML was not required to maintain the silent state induced by IFN treatment argued against a role for the PML protein in directly contributing to genome inaccessibility in latently infected neurons. Instead, this observation argued for a PML-dependent downstream impact on latent viral genomes. We hypothesized this was due to PML-dependent altered epigenetic structures resulting from type I IFN treatment. Therefore, we focused on PML-NB components that have known roles in heterochromatin targeting. We first investigated the contribution of Death Domain Associated Protein (DAXX) to the repressive phenotype because it is a constitutive component of PML-NBs and plays a role in the deposition of histones at regions of heterochromatin. Further, previous studies have found that DAXX represses HSV-1 lytic infection (Alandijany et al., 2018; Cabral et al., 2018; Lukashchuk & Everett, 2010) via its role as an H3.3 chaperone (Cabral et al., 2021; Cohen et al., 2018; Drane et al., 2010; Lewis et al., 2010), although the function of DAXX during HSV latent infection is unknown. Using two independent shRNAs, DAXX knockdown

(Supplemental Figure 2.2) was able to recover reactivation in IFNα pre-treated neurons when it was knocked down before infection (Figure 2.2A & 2.2B). Consistent with the data on PML, the viral genome also co-localized with DAXX at early time points (1 day) following infection in neurons treated with type I IFN (Figure 2.2C) and the co-localization of viral genomes with DAXX was not maintained during latent infection arguing against a role for DAXX in maintaining the repressive nature of HSV-1 latency (Figure 2.2D & 2.2E). Additionally, we sought to determine whether the presence of PML was required for the observed enrichment of DAXX. We found that depletion of PML before infection significantly reduced the association of viral genomes with DAXX (from 80.5% of genomes co-localized with DAXX to 0.18%) (Figure 2.2F), demonstrating DAXX contributes to the repressive effects of IFNα and is recruited to viral genomes in a manner that is dependent on PML.

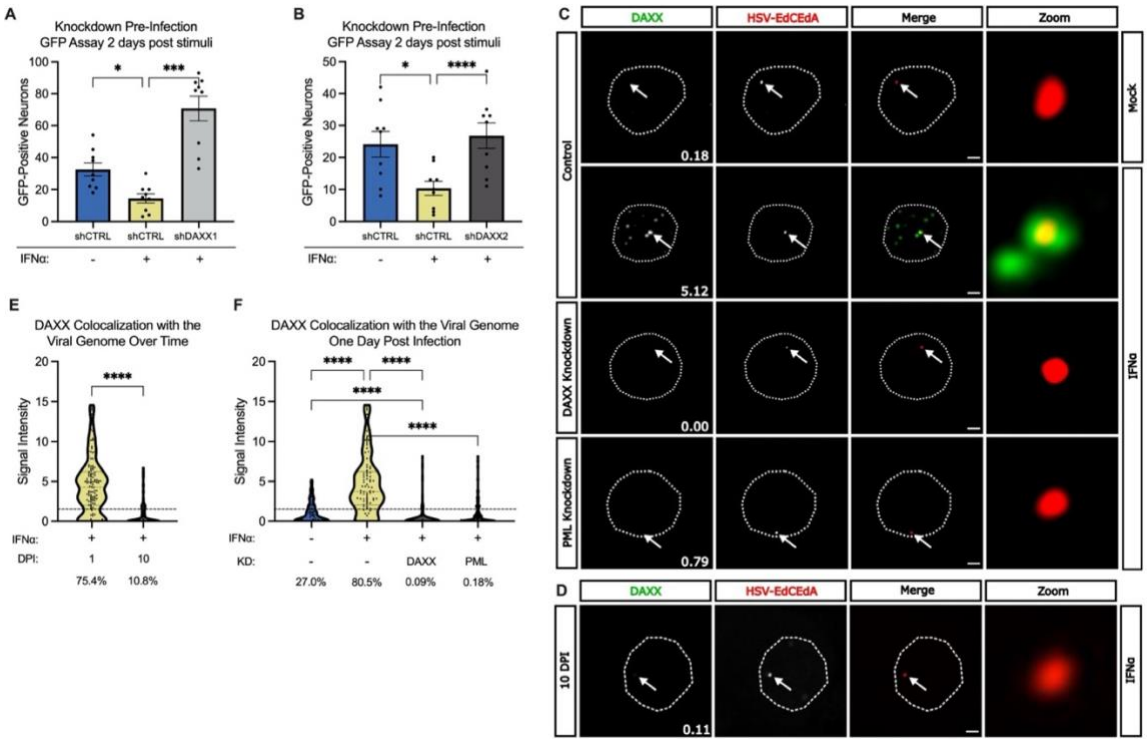


**Figure 2.2: IFNα induced restriction during initial infection is DAXX dependent.**

**A & B**) Sympathetic neurons were infected with Stayput HSV-1 in the presence or absence of IFNα and depleted of DAXX using shRNAs at 5 days pre-infection using two independent shRNAs. Reactivation was quantified based on the numbers Us11-GFP expressing neurons following addition LY294002. Data represent the mean ± SEM. N=9 biological replicates from 3 independent dissections. Statistical comparisons were made using an Ordinary one-way ANOVA with Tukey's multiple comparison.

**C & D)** Representative images of sympathetic neurons untreated or treated with 600 IU/ml of IFNα cultured in 5% oxygen. Neurons were infected with EdC/EdA labeled HSV-1 and depleted of PML or DAXX at 5 days pre-infection. Cells were fixed at 1 day (C) and 10 days (D) post-infection. The viral genome was visualized using click chemistry, and immunofluorescence was carried out for DAXX. White arrows point to location of viral genome. Scale bar, 10 μm.

**E & F)** NucSpotA was used to quantify the signal intensity of DAXX at the viral genome 1- or 10-days post-infection. Each data point represents one viral genome. Percentages indicate the proportion of genomes with NucSpotA intensity ratios above the denoted co-localization threshold (dashed line). N>60 cells from 3 biological replicates. Statistical comparisons were made using **E)** Mann-Whitney and **F)** Kruskal-Wallis test with Dunn's multiple comparison. (ns not significant, *≤ 0.05, **≤ 0.01, ***≤ 0.001, ****≤ 0.0001)

## IFNα stimulation increases H3K9me3 enrichment on the viral genome that is maintained during latency.

Previous studies have demonstrated that PML-NBs contribute to increased enrichment of H3K9me3 on cellular chromatin (Delbarre et al., 2017) and potentially on HSV-1 during lytic infection (Francois et al., 2024). Additionally, DAXX has been associated with the formation of heterochromatin characterized by H3K9me3 (Voon et al., 2015), which is known to be enriched on populations of HSV-1 genomes during quiescent infection (Cliffe et al., 2009) (Cohen et al., 2018; Roubille et al., 2024). We hypothesized that type I IFN exposure alters the epigenetic silencing of the latent HSV-1 genome via increased H3K9me3 in a DAXX and PML-dependent manner.

To test this hypothesis, we carried out immunofluorescence to determine the colocalization of H3K9me3 with the viral genome once latency was established (Figure 2.3A). To overcome problems in quantifying the co-localization of nuclear proteins with viral genomes and take into account the heterogeneity of histone enrichment at different viral genomes in a population, we used NuncSpotA; a program that quantifies the labeling of an immunofluorescent signal at the viral genome and standardizes that enrichment with the stain throughout the nucleus (Francois et al., 2024). Using this approach, we identified a subpopulation of viral genomes that co-localized with H3K9me3 in untreated neurons (49.3%), which increased significantly in the IFNα treatment to 75.3% (Figure 2.3B). Depletion of either PML or DAXX prior to infection reduced the proportion of viral genomes co-localized with H3K9me3 to levels similar to interferon treated neurons where PML and DAXX were not depleted (30.2% for PML depletion and 33.3% for DAXX depletion as compared to 75.3% in IFNα non-depletion control neurons). In comparison to interferon treated neurons where PML and DAXX

were not depleted, we did not observe a significant difference in H3K9me3 enrichment when PML or DAXX depletion occurred after latency had been established (55.9% in PML-depleted and 51.5% in DAXX-depleted neurons as compared to 75.3% in IFNα non-depletion control neurons). These data indicate that viral genomes co-localize with H3K9me3 during latent infection, and this co-localization increases when type I IFN is present during initial HSV-1 infection. Further, in the presence of type I IFN, the increased H3K9me3 co-localization was both PML and DAXX-dependent during early infection but these proteins were not required for the mark to persist at later time points.

To further validate the increased H3K9me3 association upon IFNα treatment and investigate where on viral genomes H3K9me3 was enriched, we performed Cleavage Under Targets and Tagmentation (CUT&Tag) for H3K9me3 on latently infected neurons. We first determined, in accordance with other studies (Cliffe et al., 2009), that H3K9me3 is enriched on the viral genome during latent infection. We assessed duplication rates using Picard and found that duplication was significantly higher in IgG samples as compared to H3K9me3 samples, indicating a difference in library complexities (Supplemental Figure 2.3A). For this reason, IgG duplicates were removed as recommended (Henikoff et al., 2020). Spearman correlation analysis of normalized viral read coverage across the genome revealed a strong similarity between biological replicates (Supplemental Figure 3B). Linear regression analyses of viral read distribution in both mock treated (Supplemental Figure 3C) and IFNα treated (Supplemental Figure 3D) conditions further confirmed reproducibility across datasets. We then used Integrative Genomics Viewer (E) to visualize the entire viral genome and found broad distribution of H3K9me3 is broadly distributed across the HSV-1 genome. We then sought to determine the differences in H3K9me3 enrichment in our two conditions.

Consistent with our immunofluorescence results, IFNα treatment significantly increased H3K9me3 enrichment over viral gene bodies (Fig. 3C, 3D) as well as at promoters (Fig. 3E, 3F). Viral gene bodies and promoters were quantified as H3K9me3 enrichment at both cellular promoters and cellular gene bodies has been correlated with epigenetic repression and transcriptional silencing (Lee et al., 2020). The sum of H3K9me3 enrichment over viral gene bodies (excluding promoter regions) and over promoters was quantified. Genes that had at least a twofold increase in H3K9me3 over two replicates were plotted. We concluded that there were consistent regions of the genome with increased H3K9me3 in IFNα treated. These findings suggest that IFNα promotes more H3K9me3 on the genome and that this mark persists during latency and correlates with a decrease in reactivation.

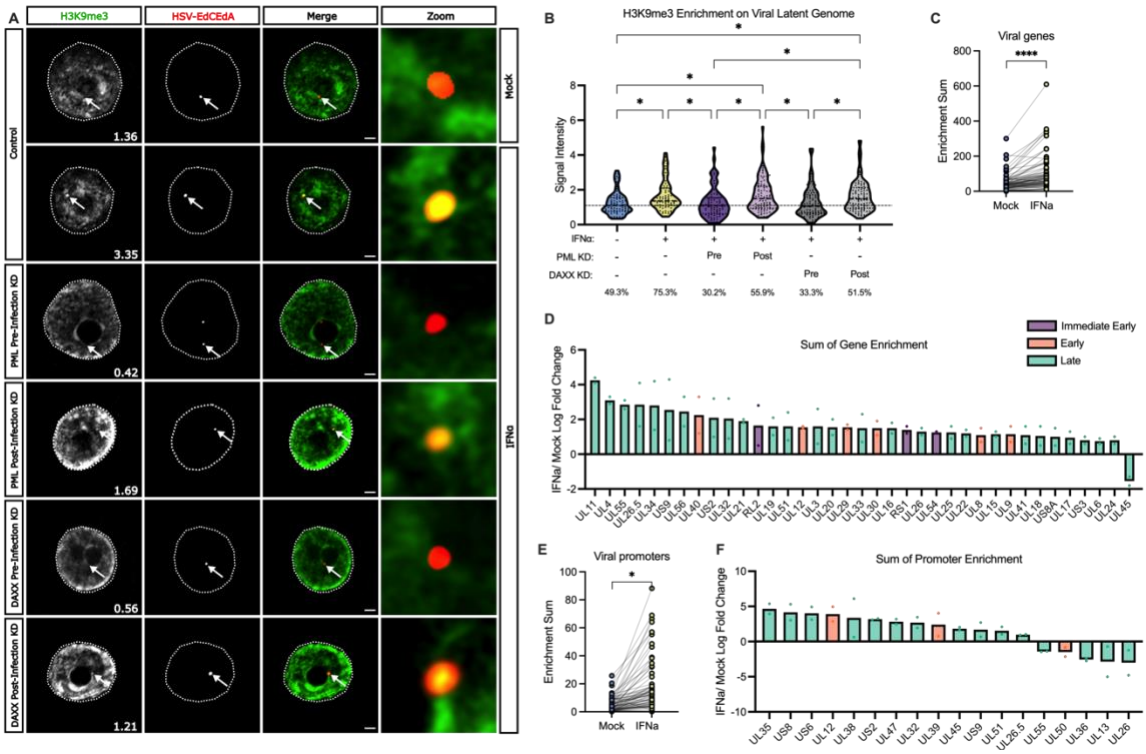

**Figure 2.3: IFNα stimulation increases H3K9me3 enrichment on the viral genome that is maintained during latency**
**A)** Representative images of sympathetic neurons untreated or treated with 600 IU/ml of IFNα cultured in 5% oxygen. Neurons were infected with EdC/EdA labeled HSV-1 and depleted of PML or DAXX at 5 days pre-infection or 5 days post-infection. Cells were fixed at 10 days post-infection. The viral genome was visualized using click chemistry, and immunofluorescence was carried out for H3K9me3. White arrows point to location of viral genome. Scale bar, 10 μm.
**B)** NucSpotA was used to quantify the signal intensity of H3K9me3 at the viral genome 10-days post-infection. Each data point represents one viral genome. Percentages indicate the proportion of genomes with NucSpotA intensity ratios above the denoted co-localization threshold (dashed line). N>60 cells from 3 biological replicates. Statistical comparisons were made using a repeated Measure One way ANOVA.
**C)** Sympathetic neurons were infected Stayput-GFP HSV-1 at an MOI of 10 PFU/cell in the presence or absence of IFNα. CUT&Tag was performed at 10 days post-infection using an antibody against H3K9me3. Fragments were sequenced and aligned to the viral genome. The sum of coverage at the defined gene body and promoter regions were used to calculate the enrichment of H3K9me3. The average enrichment sum of all viral gene bodies is plotted, with a line connecting the mock and IFNα treatments for individual viral open reading frames. Statistical analysis was made using a two-way ANOVA. N=2 biological replicates
**D)** Plot of gene bodies with a log fold change of greater than 0.5 or less than -0.5 across both replicates. Immediate early genes are colored purple, early genes are colored orange, and late genes are colored teal.
**E)** The average enrichment sums of all viral gene promoters. The line connects the same viral promoter in mock and IFNα treated cultures. Statistical analysis was made using a two-way ANOVA.
**F)** Plot of gene promoters that had a log fold change of greater than 0.5 or less than -0.5 across both replicates. Immediate early genes are colored purple, early genes are colored orange, and late genes are colored teal.
**G)** Representative integrative genome viewer images. All data was normalized to total mapped reads. Viral genes are shown in blue and viral promoters are shown in red. The y-axes were group auto-scaled between conditions.
(ns not significant, *≤ 0.05, **≤ 0.01, ***≤ 0.001, ****≤ 0.0001).

## ATRX inhibits HSV-1 reactivation, and this inhibition is enhanced by IFNα treatment.

Given our observation that PML and DAXX contributed to the initiation of IFN-mediated repression via H3K9me3, we set out to investigate ATRX, a known

interaction partner of DAXX. ATRX complexes with DAXX to deposit H3.3 and, via its interaction with DAXX, represses lytic HSV-1 infection in human fibroblasts (Lukashchuk & Everett, 2010) (Cabral et al., 2021). ATRX can also function as an H3K9me3 reader (Dhayalan et al., 2011) and has been shown to maintain the enrichment of H3K9me3 on lytically replicating viral genomes (Cabral et al., 2018). However, the role of ATRX in HSV-1 gene silencing during latency is unknown. We depleted ATRX prior to HSV infection and once latency had been established using two independent shRNAs (Supplemental Figure 2.4A, 2.4B, & 2.4C). We found ATRX depletion prior to infection resulted in enhanced reactivation of IFN-treated neurons (Figure 2.4A & 2.4B). In contrast to PML and DAXX, the depletion of ATRX after latency was established (Figure 2.4C & 2.4D), also resulted in significantly enhanced reactivation in IFN-treated neurons. This finding indicates that unlike PML and DAXX, ATRX is required for maintaining the restrictive phenotype in IFNα treated neurons.

Supporting a role for ATRX in maintaining the repressive nature of HSV-1 latency, we found that unlike DAXX and PML, ATRX co-localization with the viral genome showed detectable co-localization with ATRX at 10 days post-infection, indicating that ATRX is maintained on viral genomes once latency has been established (Figure 2.4E). This colocalization significantly increased with IFNα treatment (from 43% of genomes co-localized with ATRX to 75%) (Figure 2.4F). Notably, this association level was similar to the proportion also associated with H3K9me3, as shown in Figure 2.3B (49.3% in untreated and 75.3% type I IFN

treated). We then sought to determine whether the presence of PML was required for the observed increase in the enrichment of ATRX. We found that depletion of PML before infection significantly reduced the association of viral genomes with ATRX (from 75% of genomes co-localized to 47.1%) in IFN-pretreated neurons. However, depletion of PML after infection did not impact ATRX enrichment. Therefore, the IFN-dependent increase in ATRX association with the viral genome was dependent on PML during initial infection but did not require PML for the maintained association. These data further support that IFNα induced PML-NBs enact long-lasting epigenetic changes that are maintained independently of the bodies themselves during latency.

In contrast to PML and DAXX, we found that ATRX co-localized viral genomes even in the untreated neurons (43%), albeit to lower levels than IFN-treated neurons (Figure 2.4F). To determine whether this association occurred at levels above those obtained for random co-localization, we compared the co-localization values to those of a rotated control and found that ATRX was significantly enriched on the viral genome (Figure 2.4G). This prompted us to investigate the role of ATRX in neurons that had not been treated with IFNα. ATRX, unlike PML and DAXX, is highly abundant in neurons of the central nervous system (Berube et al., 2005) . We investigated the relative levels of ATRX in murine (SCG) and human (HD10.6 (Raymon et al., 1999)) peripheral neurons in contrast to murine (primary dermal fibroblasts) and human (human foreskin fibroblasts) fibroblasts (Supplemental Figure 2.4D) . We chose to

quantify by measuring immunofluorescence staining because of the challenges of normalizing cell numbers between vastly distinct cell types and problems carrying out Western blotting for ATRX in neurons where cell numbers are low. Consistent with previous studies, we observed higher staining intensity of ATRX in neuronal cell nuclei compared to non-neuronal cells (Supplemental Figure 2.4E). These results indicate that ATRX is highly abundant in neurons of the peripheral nervous system even without IFNα stimulation.

We investigated the impact of ATRX in repressing reactivation in untreated neurons. When ATRX was depleted after latency was established, we observed a significant increase in HSV-1 reactivation. We did not observe the same increase in reactivation following the depletion of PML or DAXX (Figure 2.4H), again consistent with ATRX playing a role in restricting HSV-1 reactivation in a manner independent of both PML and DAXX. We also observed a slight increase in the numbers of GFP-positive neurons following ATRX depletion alone in the absence of the addition of the reactivation trigger (Supplemental Figure 2.4F). This increase in GFP-positive neurons was very slight (from an average of 1.7 to 4) and was lower than the numbers observed with a reactivation trigger. We also found the increase in GFP could be blocked by an inhibitor of the DLK-dependent neuronal cell stress pathway. We hypothesized that the increase in GFP reflects an increase in spontaneous reactivation as a result of low levels of stress in the neuronal cultures as opposed to ATRX depletion directly inducing reactivation. In summary, our data indicate ATRX plays a role in limiting HSV

reactivation, and its accumulation on viral genomes increases in IFN-pretreated neurons in a manner reliant on PML-NB formation.

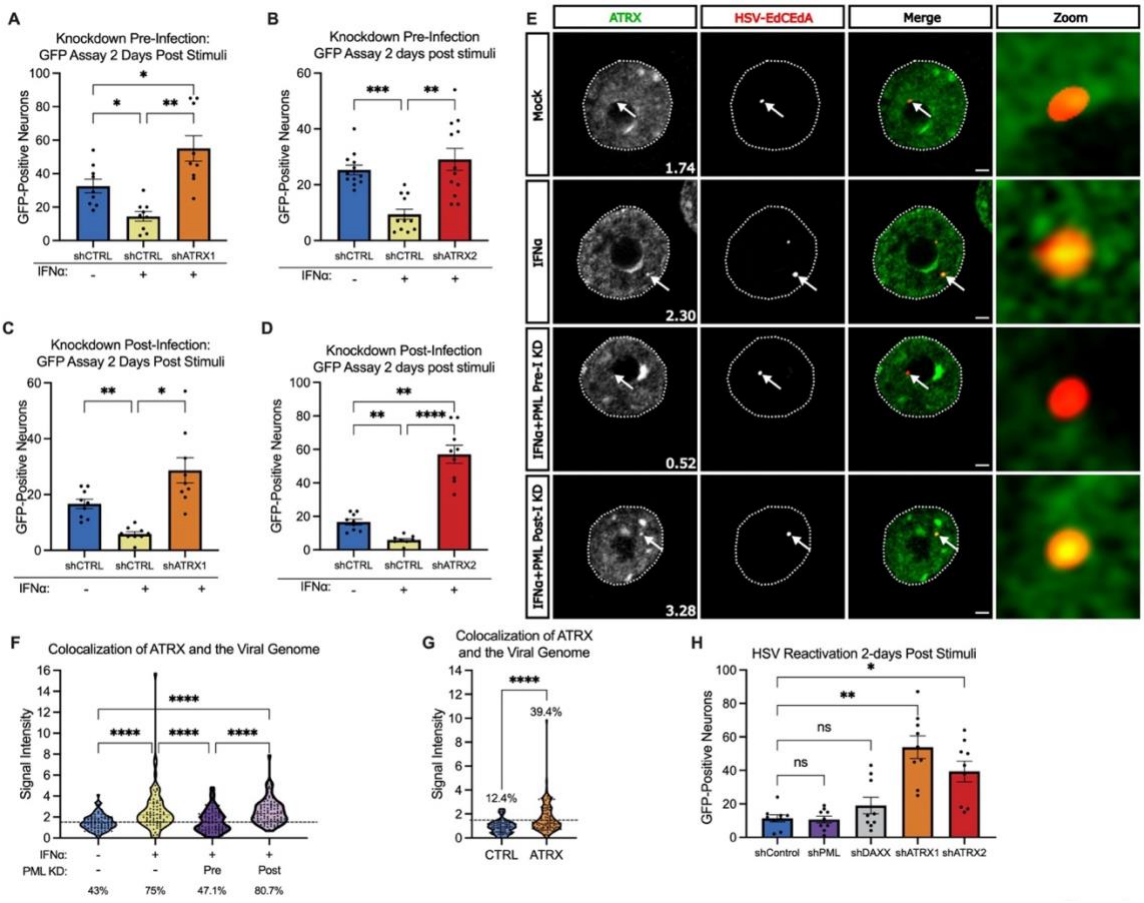

**Figure 2.4: ATRX inhibits HSV-1 reactivation, and this inhibition is enhanced by IFNα treatment.**

**A & B**) Sympathetic neurons were infected with Stayput HSV-1 in the presence or absence of IFNα and depleted of ATRX using shRNAs at 5 days pre-infection using two independent shRNAs. Reactivation was quantified based on the numbers Us11-GFP expressing neurons following addition LY294002. Data represent the mean ± SEM. N=9 biological replicates from 3 independent dissections. Statistical comparisons were made using an Ordinary one-way ANOVA with Tukey's multiple comparison.

**C & D**) Sympathetic neurons were infected with Stayput HSV-1 in the presence or absence of IFNα and depleted of ATRX using shRNAs at 5 days post-infection using two independent shRNAs. Reactivation was quantified based on the numbers Us11-GFP expressing neurons following addition LY294002. Data represent the mean ± SEM. N=9 biological replicates from 3 independent dissections. Statistical comparisons were made using an Ordinary one-way ANOVA with Tukey's multiple comparison.

**E)** Representative images of sympathetic neurons untreated or treated with 600 IU/ml of IFNα cultured in 5% oxygen. Neurons were infected with EdC/EdA labeled HSV-1 and depleted of PML at 5 days pre-infection or 5 days post-infection. Cells were fixed at 10 days post-infection. The viral genome was visualized using click chemistry, and immunofluorescence was carried out for ATRX. White arrows point to location of viral genome. Scale bar, 10 μm.

**F)** NucSpotA was used to quantify the signal intensity of ATRX at the viral genome 10 days post-infection. Each data point represents one viral genome. Percentages indicate the proportion of genomes with NucSpotA intensity ratios above the denoted co-localization threshold (dashed line). N>60 cells from 3 biological replicates. Statistical comparisons were made using Kruskal-Wallis test with Dunn's multiple comparison.

**G)** NucSpotA was used to quantify the signal intensity of ATRX at the viral genome 10 days post-infection in mock-treated neurons. CTRL denotes a randomized control where the genome-containing layer is rotated 180 degrees to provide a value for random placement. Each data point represents one viral genome. Percentages indicate the proportion of genomes with NucSpotA intensity ratios above the denoted co-localization threshold (dashed line). N>60 cells from 3 biological replicates. Statistical comparisons were made using an unpaired t-test.

**H**) Sympathetic neurons were infected with Stayput HSV-1 in the absence of IFNα and depleted of PML, DAXX, or ATRX using shRNAs at 5 days post-infection. Reactivation was quantified based on the numbers Us11-GFP expressing neurons following addition LY294002. Data represent the mean ± SEM. N=9 biological replicates from 3 independent dissections. Statistical comparisons were made using an Ordinary one-way ANOVA with Tukey's multiple comparison.

(ns not significant, *≤ 0.05, **≤ 0.01, ***≤ 0.001, ****≤ 0.0001).

## ATRX remains co-enriched with H3K9me3S10p at the viral genome during reactivation, preventing Phase 1 and protecting H3K9me3 bound genomes from undergoing full reactivation

Because we found ATRX functioned to inhibit HSV-1 reactivation in both mock and IFNα-treated conditions, and that ATRX enrichment levels mirrored those for H3K9me3, we hypothesized that ATRX restricted HSV-1 reactivation through its ability to read H3K9me3. To test this hypothesis, we performed immunofluorescence experiments to directly assess the co-enrichment of ATRX and H3K9me3 on the viral genome during latency at the single genome level (Figure 2.5A). By using NucSpotA with the previously defined cut-offs for positive co-localization, we could determine the co-enrichment values for H3K9me3 and ATRX. We found that treatment with interferon at the time of infection increased the population of neurons co-enriched with ATRX and H3K9me3 from 36% in untreated to 61% in IFNα pulsed (Figure 2.5B). Furthermore, in both mock and interferon conditions, we found only a small population of neurons with only H3K9me3 (14% in both conditions) or only ATRX (12% in mock and 16% in interferon pulsed). We determined that individual genomes that did not reach the co-localization threshold for one mark also did not reach the threshold for the second mark. Meanwhile, genomes positively co-localized with one tend to be co-localized with both. This pattern implies that the presence or absence of one factor may influence or depend on the other, reflecting interdependence or cooperative roles for ATRX and H3K9me3. These data imply ATRX functions as an H3K9me3

reader on a subset of viral genomes and with interferon treatment this subset increases.

We then investigated the enrichment of ATRX at viral genomes following a reactivation stimulus. Previous studies from our lab and others (Cliffe et al., 2015; Dochnal et al., 2022; Kim et al., 2012; Whitford et al., 2022) have established that reactivation of HSV-1 occurs in two distinct phases. Phase I is initiated when neurons are exposed to specific stressors, such as the loss of nerve growth factor signaling. During Phase I, there is JNK-dependent phosphorylation of the serine residue adjacent to lysine 9 on histone H3 (H3K9me3S10ph) (Cliffe et al., 2015; Cuddy et al., 2020). This "methyl/phospho switch" occurs on cellular chromatin during stress resulting in the eviction of some H3K9me3 readers that are unable to remain bound after serine 10 phosphorylation, allowing for transcription without the removal of post-translational modifications. However, ATRX exhibits the capability to bind to H3K9me3 even in the presence of serine 10 phosphorylation, maintaining cellular heterochromatic silencing (Noh et al., 2015). Although we have quantified reactivation following ATRX depletion based on GFP-positive neurons, this is a measure of full, Phase II reactivation. We first validated that ATRX specifically prevents entry into Phase I instead of preventing the progression from Phase I to Phase II. Depletion of ATRX after latency was established resulted in increased viral lytic gene expression in all viral gene classes (ICP27, ICP8, and gC) at the Phase I time point (18 hours post-reactivation). This ATRX-dependent increase was observed in both mock-treated (Figure 2.5C) and IFNα pre-treated

neurons (Figure 2.5D) and was independent of DAXX as depletion of DAXX after latency had been established did not impact Phase I gene expression (Supplemental Figure 2.5A). Therefore, ATRX acts independently of DAXX to specifically prevent the exit of latent genomes into Phase I gene expression following a reactivation stimulus.

Phase I of reactivation is followed by Phase II, which involves the removal of repressive PTMs, replication of viral DNA, and virus production. The removal of histone PTMs H3K27me3 and H3K9me2 is required for Phase II of reactivation (Cliffe et al., 2015; Dochnal et al., 2022; Kim et al., 2012; Whitford et al., 2022). However, we found that the removal of H3K9me3 does not contribute to reactivation, as the use of a H3K9me3 demethylase (KDM4) inhibitor (ML-324 in  had no effect on reactivation in both mock (Figure 2.5E) and IFNα (Figure 2.5F) treated neurons. Yet, when ATRX was depleted before reactivation, we found that the histone demethylase inhibitor decreased reactivation. This suggests that when ATRX is not present, H3K9me3 removal contributes to Phase II of reactivation (Figure 2.5G). This further supports the hypothesis that ATRX functions as a reader of H3K9me3 on latent genomes, preventing H3K9me3-associated genomes from reactivating.

To investigate the mechanism by which ATRX prevents H3K9me3-associated genomes from reactivation, we asked whether H3K9me3 enriched genomes were still phosphorylated during Phase I when associated with ATRX. We performed immunofluorescence on HSV-1 infected neurons, either untreated

or treated with IFNα during initial infection (Figure 2.5H). ATRX enrichment on the viral genome was not significantly different at latent and Phase I time points (Fig 2.5I). Furthermore, quantification of both ATRX and H3K9me3pS10 at viral genomes using NucSpotA revealed that ATRX and H3K9me3S10p are co-enriched on 25% of genomes in non-IFN treated neurons and 59% of IFNα treated neurons during Phase I (Fig 2.5J). These data suggest ATRX genomes are still capable of becoming phosphorylated even when bound by ATRX, but ATRX association is not lost upon following a histone phospho/methyl switch during Phase I reactivation. Together, our data indicate that ATRX functions as a restriction factor against HSV-1 reactivation by remaining bound to viral genomes even following the initial epigenetic changes known to occur during Phase I of reactivation (a phospho/methyl switch) and prevents Phase I lytic gene expression. Further, ATRX and H3K9me3 association increase when neurons are pre-treated with type I IFN to mediate the innate immune memory response in neurons that restricts HSV-1 reactivation.

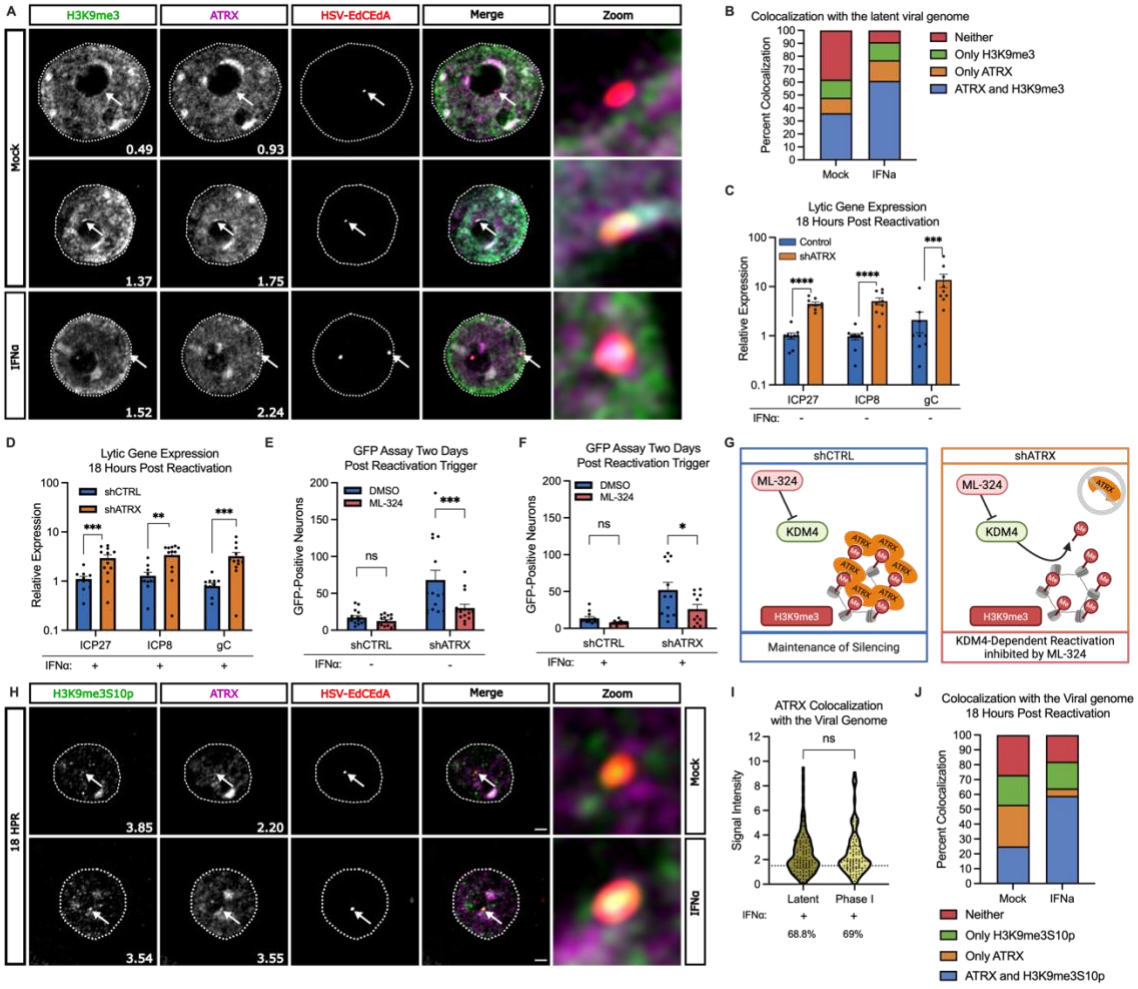
A
H3K9me3
ATRX
HSV-EdCEdA
Merge
Zoom
Mock
IFNα
0.49
0.93
1.37
1.75
1.52
2.24
B
Colocalization with the latent viral genome
Percent Colocalization
Neither
Only H3K9me3
Only ATRX
ATRX and H3K9me3
Mock
IFNa
C
Lytic Gene Expression
18 Hours Post Reactivation
Control
shATRX
Relative Expression
ICP27
ICP8
gC
IFNα:
D
Lytic Gene Expression
18 Hours Post Reactivation
shCTRL
shATRX
Relative Expression
ICP27
ICP8
gC
IFNα:
E
GFP Assay Two Days
Post Reactivation Trigger
DMSO
ML-324
GFP-Positive Neurons
ns
shCTRL
shATRX
IFNα:
F
GFP Assay Two Days
Post Reactivation Trigger
DMSO
ML-324
GFP-Positive Neurons
ns
shCTRL
shATRX
IFNα:
G
shCTRL
ML-324
KDM4
ATRX
Ub
H3K9me3
Maintenance of Silencing
shATRX
ML-324
KDM4
ATRX
Ub
H3K9me3
KDM4-Dependent Reactivation
inhibited by ML-324
H
H3K9me3S10p
ATRX
HSV-EdCEdA
Merge
Zoom
16 HPR
Mock
IFNα
3.85
2.20
3.54
3.55
I
ATRX Colocalization
with the Viral Genome
ns
Signal Intensity
Latent
Phase I
IFNα:
68.8%
69%
J
Colocalization with the Viral genome
18 Hours Post Reactivation
Percent Colocalization
Mock
IFNa
Neither
Only H3K9me3S10p
Only ATRX
ATRX and H3K9me3S10p

**Figure 5**

**Figure 2.5: ATRX remains co-enriched H3K9me3S10p at the viral genome during reactivation, preventing Phase 1 and protecting H3K9me3 bound genomes from undergoing full reactivation**

**A)** Representative images of sympathetic neurons untreated or treated with 600 IU/ml of IFNα cultured in 5% oxygen. Neurons were infected with EdC/EdA labeled HSV-1. Cells were fixed at 10 days post-infection. The viral genome was visualized using click chemistry, and immunofluorescence was carried out for H3K9me3 and ATRX. White arrows point to location of viral genome. Scale bar, 10 μm.

**B)** NucSpotA was used to quantify the signal intensity of H3K9me3 and ATRX at the viral genome 10 days post-infection. Percentage of genomes above or below the denoted co-localization threshold (H3K9me3=1.1 and ATRX=1.5) are represented as a bar graph. N>60 cells from 3 biological replicates.

**C & D**) Sympathetic neurons were infected with Stayput HSV-1 in the absence (C) or presence (D) of IFNα and depleted of ATRX using shRNAs at 5 days post-infection. RNA was collected 18 hours following the addition LY294002 (Phase I). RT-qPCR was used to quantify IE (ICP27), E (ICP8), and L (gC) viral gene expression. Statistical comparisons were made with a t test or Mann-Whitney test, Error bars: SEM) N=9 biological replicates from 3 independent dissections.

**E & F**) Sympathetic neurons were infected with Stayput HSV-1 in the absence (E) or presence (F) of IFNα and depleted of ATRX using shRNAs at 5 days post-infection. Reactivation was quantified based on the numbers Us11-GFP expressing neurons following addition LY294002 and DMSO or ML-324 (10μM; JMJD2 inhibitor). Data represent the mean ± SEM. N=9 biological replicates from 3 independent dissections. Statistical comparisons were made using a two-way ANOVA with Šídák's multiple comparisons test.

**G)** Model of proposed ML-324 mechanism.

**H)** Representative images of sympathetic neurons untreated or treated with 600 IU/ml of IFNα cultured in 5% oxygen. Neurons were infected with EdC/EdA labeled HSV-1. Cells were fixed 18 hours post-reactivation stimulus. The viral genome was visualized using click chemistry, and immunofluorescence was carried out for H3K9me3S10p and ATRX. White arrows point to location of viral genome. Scale bar, 10 μm.

**I)** NucSpotA was used to quantify the signal intensity of ATRX at the viral genome 10 days post-infection or 18 hours post-reactivation stimulus. Each data point represents one viral genome. Percentages indicate the proportion of genomes with NucSpotA intensity ratios above the denoted co-localization threshold (dashed line). N>60 cells from 3 biological replicates. Statistical comparisons were made using a Mann Whitney.

**J)** NucSpotA was used to quantify the signal intensity of H3K9me3S10p and ATRX at the viral genome 18 hours post-reactivation stimulus. The percentage of genomes above or below the denoted co-localization threshold (H3K9me3S10p=1.5 and ATRX=1.5) are represented as a bar graph. N>60 cells from 3 biological replicates.

(ns not significant, *≤ 0.05, **≤ 0.01, ***≤ 0.001, ****≤ 0.0001)

## Discussion

Based on analysis of bulk cultures of ganglia, it was known that different histone post-translation modifications including H3K9me2, H3K27me3, and H3K9me3, are enriched on the latent viral genome (Cliffe et al., 2009; Kwiatkowski et al., 2009; Nicoll et al., 2016; Wang et al., 2005). However, how histone post-translational modifications arise and whether individual viral genomes with different histone PTMs contribute to the differential abilities of viral genomes to reactivate was unknown. The restriction of latency is affected by neuronal states such as stress and immune signaling (Dochnal, Whitford, et al., 2024; Suzich et al., 2021), but whether these processes impacted the epigenetics of the viral genome was unclear. Here, we demonstrate that immune signaling at the time of infection impacts viral heterochromatin by promoting more H3K9me3-association and restricting reactivation. Furthermore, we demonstrate mechanistically how this form of heterochromatin is refractory to reactivation via the epigenetic reader ATRX (Figure 2.6). These data are important because they show that a certain type of epigenetic structure on a latent viral genome is more deeply silenced, and this deeper form of silencing can be induced via initial infection in the presence of type I IFN.

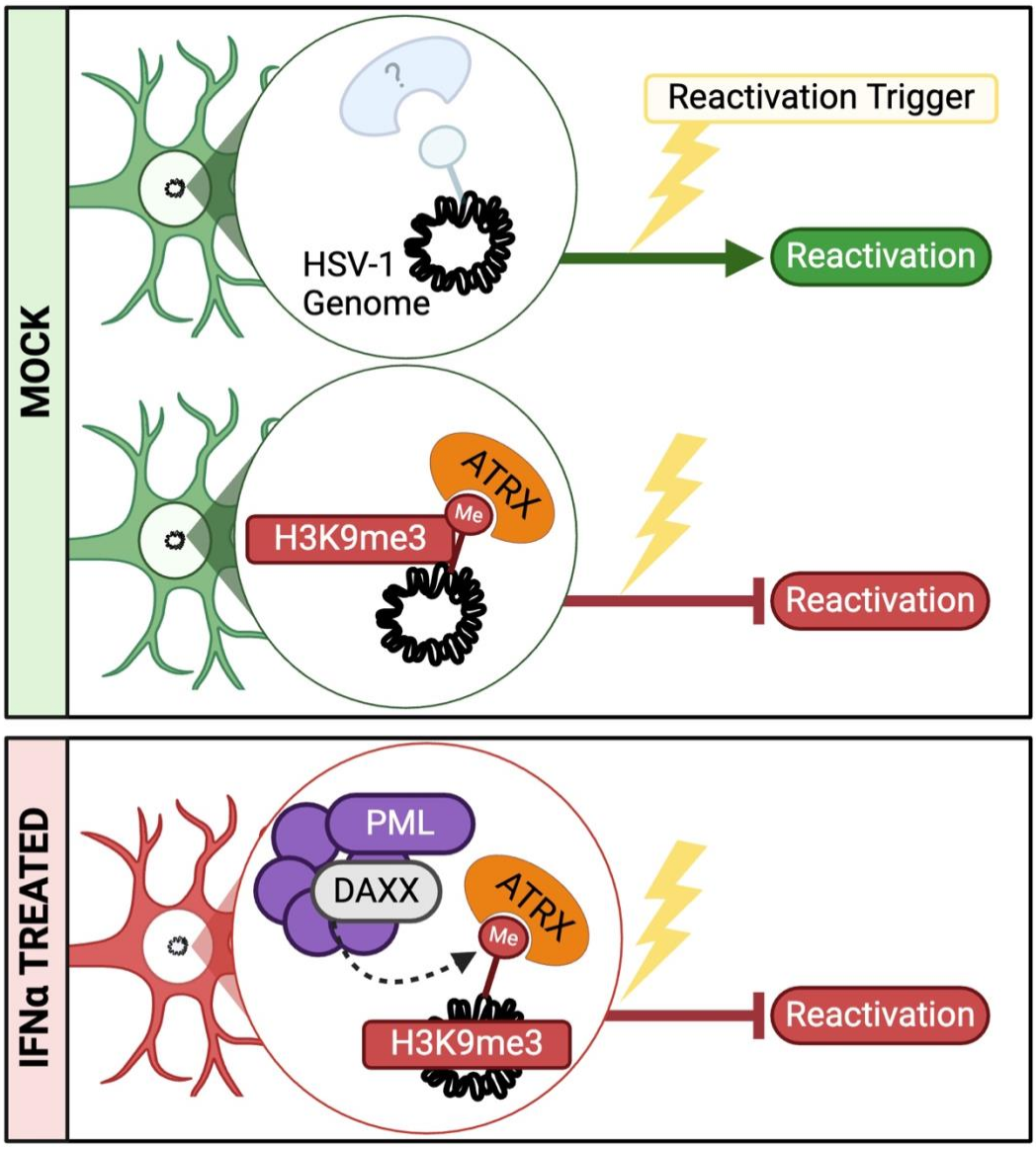


**Figure 2.6: Model for Interferon and ATRX restriction of HSV-1 in Neurons**

Model depicting latent HSV-1 infection. Under mock conditions (top panel) a population of viral genomes are enriched with H3K9me3 and ATRX, but there also exists a population (almost 40%- Figure 2.5) that have neither. When neurons are treated with type I IFN at the time of infection (bottom panel) there is an increase in the population of genomes enriched with H3K9me3 (from 50% to 75%) that is dependent on PML and DAXX. When both mock and interferon treated neurons are stimulated with a reactivation trigger, ATRX restricts H3K9me3-bound genomes from reactivating.

Prior to this study, there was little information describing the nature of histone readers that are maintained at latent HSV-1 genomes. The H3K9me3 readers include the HP1 family proteins (Bannister et al., 2001; Jacobs et al., 2001; Lachner et al., 2001), ATRX (alpha-thalassemia/mental retardation, X-linked) (Dhayalan et al., 2011; Noh et al., 2015), CHD4 (Mansfield et al., 2011), TRIM66 (Jain et al., 2020), PHRF1 (Jain et al., 2020), UHRF1 (Nady et al., 2011), TNRC18 (Zhao et al., 2023), MPP8 (Chang et al., 2011), and Tip60 (Sun et al., 2009). Our data suggest that ATRX is an important H3K9me3 reader associated with the viral genome. Further work will be required to determine the extent to which other H3K9me3 readers associate with the HSV-1 genome and their impact on latency and reactivation. As we showed, ATRX is highly abundant in neurons and displays a differential localization in comparison to non-neuronal cells. Our observations suggest ATRX remains bound to regions of heterochromatin following histone phosphorylation and confirms a previous study indicating that ATRX is essential to protect the genome of neurons in times of cell stress (Noh et al., 2015). We can now extend this role for ATRX and show that it also protects neurons from viral reactivation. We also demonstrate that ATRX maintains heterochromatin silencing on the HSV-1 genome independently of DAXX, as DAXX depletion at latent time points had no impact on reactivation. This contrasts with lytic infection of HSV-1, where ATRX and DAXX function together (Lukashchuk & Everett, 2010). Here we demonstrate that the enrichment and mechanism of ATRX during HSV-1 infection in neurons is distinct. This distinct role for ATRX may help explain why HSV-1 latency is

exclusively established in neurons. While our findings demonstrate a role for ATRX in maintaining HSV-1 latency, further research is needed to determine whether ATRX also contributes to the establishment of silencing during HSV-1 neuronal infection and, if so, whether it acts independently of DAXX and PML.

PML-NBs are typically abundant in non-neuronal cells but are much less abundant in the mouse nervous system, with *Pml* mRNA and protein levels significantly downregulated in post-mitotic neurons (Gray et al., 2004) (Regad et al., 2009). Previously, showed that PML-NBs were undetectable in post-natal and adult primary neurons cultured in vitro from the superior cervical and trigeminal ganglia (Suzich et al., 2021). These findings are consistent with reports of regional variability and subpopulations of neurons lacking PML signals (Catez et al., 2012) (Hall et al., 2016). Here, we describe that oxygen conditions also impact the formation of PML-NBs. We find that PML-NBs are only formed for a short period after IFNα stimulation and do not persist, nor colocalize, with the latent viral genome during latency when neurons are cultured *in vitro* in biologically relevant oxygen conditions. Other studies have observed at latency *in vivo* (28 days post-infection), the HSV-1 genome and PML were co-localized with DAXX (Catez et al., 2012). Differences in prior studies may reflect variable exposure to signaling molecules like interferons. Regardless, our pared-down latency model has allowed us to parse out that PML-NBs can modulate the nature of the viral epigenetic structure during latency establishment and that

ATRX can restrict HSV-1 reactivation in genomes that were once, but no longer, associated with PML-NBs.

Our findings indicate viral genomes enriched with H3K9me3 and ATRX are prevented from entering Phase I of HSV-1 reactivation. The signaling cascade that initiates Phase I of reactivation results in a JNK-dependent methyl/phospho switch (Cliffe et al., 2015). During Phase I, a burst of lytic gene expression occurs independently of histone modification removal (Cliffe et al., 2015) (Cuddy et al., 2020) (Dochnal et al., 2022) (Whitford et al., 2022). Previous work hypothesized that the H3K9me3S10p methyl/phospho switch evicted repressive readers and allowed for transcription without the removal of repressive methylation marks (Cliffe et al., 2015). In this study, we now observe that the methyl/phospho switch occurs on genomes during Phase I of reactivation but propose that ATRX remains bound and inhibits transcription. In wells treated with interferon, we demonstrate that the population of genomes associated with ATRX and H3K9me3 increases, decreasing the population of reactivation-competent genomes. Yet, even in the interferon condition, we still observe low levels of reactivation, albeit lower than in the untreated neurons. In mock conditions, we observe a limited number of genomes independently enriched with either ATRX or H3K9me3. In these independently enriched populations, it is possible that an alternative H3K9me3 reader, such as HP1, is displaced via a methyl/phospho switch, facilitating the transition to Phase I. In both the mock and interferon treatments, the subset of latent genomes lacking both ATRX and H3K9me3 may represent the reactivation-

competent population. For example, it is possible for H3K27me3, a mark observed on latent viral genomes (Cliffe et al., 2009; Kwiatkowski et al., 2009), to go through a methyl/phospho switch (H3K27me3S28p) (Gehani et al., 2010), although this mark has yet to be identified on the reactivating HSV-1 genome. Additional research is required to identify the marks and readers involved in reactivation.

Full reactivation using a PI3K inhibitor or forskolin in primary neuronal models of reactivation (Cliffe et al., 2015; Cuddy et al., 2020; Dochnal et al., 2022; Hu et al., 2022; Kim et al., 2012) as well as *ex vivo* models (Whitford et al., 2022) requires the activities of lysine 9 mono- and di- methylation, and lysine 27 mono-, di-, and tri-methylation removal by histone demethylases. KDM4 (also known as JMJD2 or JHDM3), a histone demethylase with a preference for H3K9me3, also promotes HSV-1 gene expression during reactivation induced by axotomy (Liang, Vogel, et al., 2013). Here, using a PI3K inhibitor, we found that inhibiting KDM4 did not affect Phase II of reactivation *in vitro*. Only when ATRX was depleted did inhibiting H3K9me3 removal contribute to reactivation. This further supports the hypothesis that ATRX functions as a reader of H3K9me3 on latent genomes, preventing H3K9me3-associated genomes from reactivating. The variation in KDM4 inhibition during reactivation triggered by different stimuli suggests that the kinetics of reactivation may vary depending on the type of stimulus. Previously, differential kinetics have already been observed with axotomy, with rapid recruitment of transcription factors (Kristie et al., 1999; Whitlow & Kristie, 2009), earlier occurrence of Phase I (Whitford et al., 2022), and reactivation occurring

independently of the viral transactivator, VP16 (Sears et al., 1991; Steiner et al., 1990). This implies that distinct stimuli could influence the timing, dynamics, viral and host (restriction) factors involved in reactivation. Understanding these differences could provide insights into how specific factors modulate viral latency and reactivation, potentially leading to new therapeutic strategies.

To our knowledge, this is the first report of long-lasting epigenetic changes in neurons in response to an immune stimulus. Immune memory may serve as a mechanism through which a persistent virus modulates latency and its potential to reactivate. By altering the chromatin structure of the viral genome, immune memory can suppress reactivation under certain conditions, effectively limiting viral spread. However, this same mechanism might also enable the virus to remain latent while evading immune detection, ensuring its long-term survival within the host, highlighting the balance of viral-host fitness. Memory of previous immune stimulation in a long-lived and non-replenishing cell type, could also impact the regulation of host genes, potentially modulating neural function over time. Therefore, more work is needed to determine the implications for immune memory and long-term inflammation in the nervous system. Persistent epigenetic changes driven by immune responses, such as those induced by type I interferon, could underlie the development of neuropathologies, including neurodegenerative diseases or chronic pain syndromes, highlighting the potential implications for neuronal immune memory in human health.

## Supplemental Figures

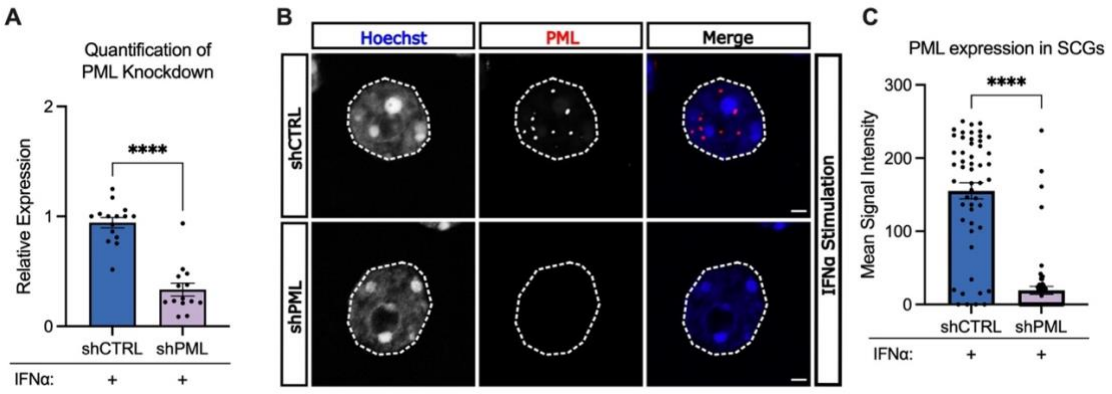


**Supplemental Figure 2.1: Depletion of PML in neurons.**
**A)** Neurons were depleted of PML using lentivirus-mediated shRNA depletion five days prior to treatment with 600 IU/ml IFNα. Five days after knockdown, RNA was collected and *Pml* transcripts were quantified via RT-qPCR. Statistical comparisons were made using a Paired t-test. N=14 biological replicates from 5 independent dissections. **B)** Representative images of sympathetic neurons treated with 600 IU/ml of IFNα cultured in 5% oxygen. Neurons were depleted of PML and fixed 5 days later. Immunofluorescence was carried out for PML. Scale bar, 10 μm. **C)** FIJI was used to quantify the signal intensity of PML in the nucleus 5 days post knockdown. Each data point represents one nucleus. Statistical comparisons were made using a Mann-Whitney test. N>50 biological replicates from 2 independent dissections. Data represent the mean ± SEM. (ns not significant, *≤ 0.05, **≤ 0.01, ***≤ 0.001, ****≤ 0.0001).

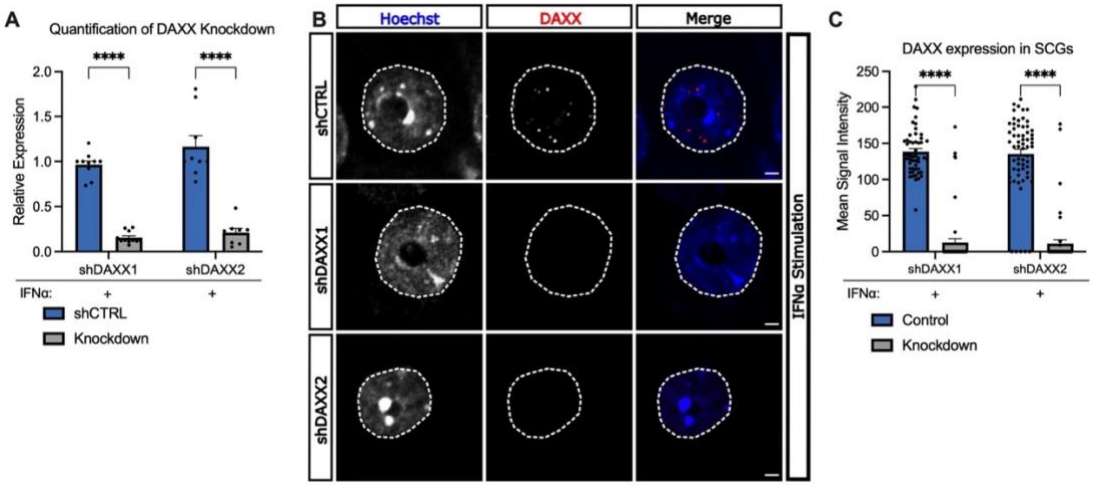


**Supplemental Figure 2.2: Depletion of DAXX in neurons.**
**A)** Neurons were depleted of DAXX using lentivirus-mediated shRNA depletion five days prior to treatment with 600 IU/ml IFNα using two independent shRNAs. Five days after knockdown, RNA was collected, and *DAXX* transcripts were quantified via RT-qPCR. Statistical comparisons were made using a Mann-Whitney test. N>9 biological replicates from 3 independent dissections. **B)** Representative images of sympathetic neurons treated with 600 IU/ml of IFNα cultured in 5% oxygen. Neurons were depleted of DAXX and fixed 5 days later. Immunofluorescence was carried out for DAXX. Scale bar, 10 μm. **C)** FIJI was used to quantify the signal intensity of DAXX in the nucleus 5 days post knockdown. Each data point represents one nucleus. Statistical comparisons were made using a Mann-Whitney test. N>50 biological replicates from 2 independent dissections. Data represent the mean ± SEM. (ns not significant, *≤ 0.05, **≤ 0.01, ***≤ 0.001, ****≤ 0.0001).

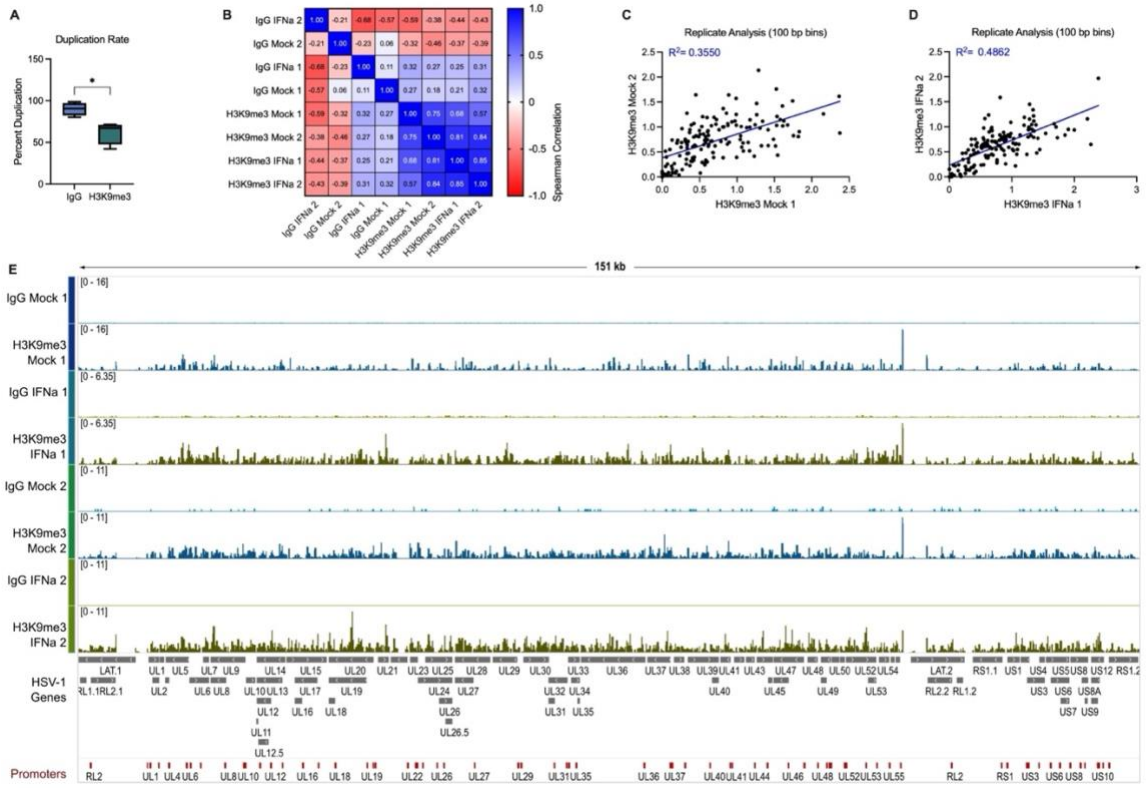


**Supplemental Figure 2.3**
**A)** Duplication rates for viral transcripts, determined using Picard, plotted for IgG and H3K9me3. **B, C, & D)** Normalized viral aligned bigwig files were assessed using MultiBigwigSummary in 1000 bp bins. Values within bins were used for Spearman correlation analysis (B) or plotted to analyze biological replicates in mock (C) or interferon-treated (D) conditions by linear regression analysis. **E)** Representative integrative genome viewer images of the complete HSV-1 genome. All data was normalized to total mapped reads. Viral genes are colored gray, and viral promoters are colored red. y-axes were scaled to be group auto-scaled between replicate and treatment.

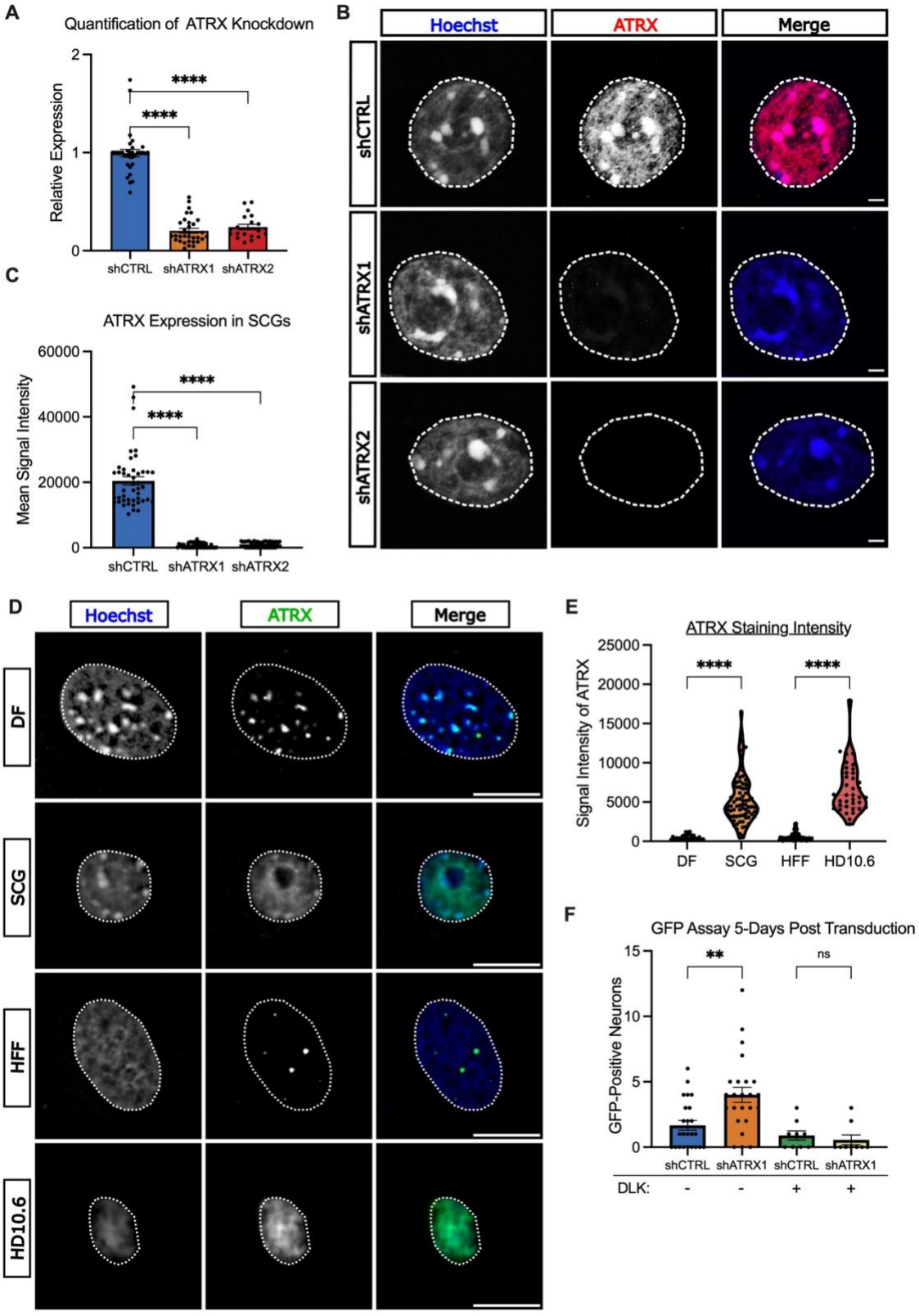
A
Quantification of ATRX Knockdown
Relative Expression
2
1
0
****
****
shCTRL
shATRX1
shATRX2
B
Hoechst
ATRX
Merge
shCTRL
shATRX1
shATRX2
C
ATRX Expression in SCGs
Mean Signal Intensity
60000
40000
20000
0
****
****
shCTRL
shATRX1
shATRX2
D
Hoechst
ATRX
Merge
DF
SCG
HFF
HD10.6
E
ATRX Staining Intensity
Signal Intensity of ATRX
25000
20000
15000
10000
5000
0
****
****
DF
SCG
HFF
HD10.6
F
GFP Assay 5-Days Post Transduction
GFP-Positive Neurons
15
10
5
0
**
ns
shCTRL
shATRX1
shCTRL
shATRX1
DLK:
-
-
+
+

**Supplemental Figure 2.4:**
**A)** Neurons were depleted of ATRX using lentivirus-mediated shRNA depletion five days prior to treatment with 600 IU/ml IFNα using two independent shRNAs. Five days after knockdown, RNA was collected, and *ATRX* transcripts were quantified via RT-qPCR. Statistical comparisons were made using an Ordinary one-way ANOVA with Tukey's multiple comparison. N>20 biological replicates from >7 independent dissections. **B)** Representative images of sympathetic neurons treated with 600 IU/ml of IFNα cultured in 5% oxygen. Neurons were depleted of ATRX and fixed 5 days later. Immunofluorescence was carried out for ATRX. Scale bar, 10 μm. **C)** FIJI was used to quantify the signal intensity of ATRX in the nucleus 5 days post knockdown. Each data point represents one nucleus. Statistical comparisons were made using a t-test. N>50 biological replicates from 2 independent dissections. **D)** Representative images of primary dermal fibroblasts (DF), primary superior cervical ganglia (SCG), human foreskin fibroblasts (HFF), and human-induced peripheral neurons (HD10.6). Immunofluorescence was carried out for ATRX. Scale bar, 10 μm. **E)** FIJI was used to quantify the signal intensity of ATRX in the nucleus of DFs, SCGs, HFFs, or HD10.6 cells. Each data point represents one nucleus. Statistical comparisons were made using a One-way ANOVA with Šídák's multiple comparisons test. N>50 biological replicates from 2 independent experiments. **F)** Sympathetic neurons were infected with Stayput HSV-1 in the absence of IFNα and depleted of ATRX using shRNAs at 5 days post-infection. Reactivation was quantified based on the numbers Us11-GFP expressing neurons following addition LY294002 and DMSO or GNE-115 (DLK inhibitor). N=9 biological replicates from 3 independent dissections. Statistical comparisons were made using a repeated Mann-Whitney.
Data represent the mean ± SEM. (ns not significant, *≤ 0.05, **≤ 0.01, ***≤ 0.001, ****≤ 0.0001).

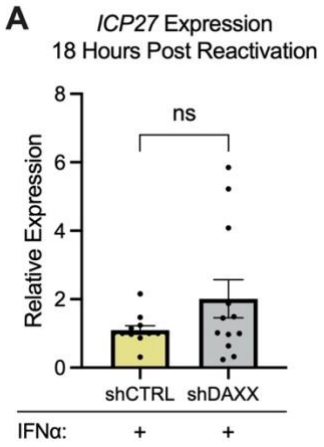


**Supplemental Figure 2.5: DAXX does not inhibit Phase I of reactivation.** **A)** Sympathetic neurons were infected with Stayput HSV-1 in the presence of IFNα and depleted of DAXX using shRNAs at 5 days post-infection. RNA was collected 18 hours following the addition LY294002 (Phase I). RT-qPCR was used to quantify IE (ICP27) viral gene expression. Statistical comparisons were made with a t-test. N=9 biological replicates from 3 independent dissections. Data represent the mean ± SEM. (ns not significant, *≤ 0.05, **≤ 0.01, ***≤ 0.001, ****≤ 0.0001)

# The role of ATRX in the establishment of HSV-1 latency

## Abstract

Herpes simplex virus-1 (HSV-1) establishes a lifelong latent infection in neurons and reactivation from this latent state is the cause of recurrent oral and ocular infections, herpes simplex keratitis, and encephalitis. Entry and maintenance of HSV latency is likely epigenetically regulated, although specific proteins that function in neurons that silence viral DNA to promote latency are not known. Alpha-thalassemia/mental retardation X-linked (ATRX) is a multi-functional heterochromatin-associated protein that is highly abundant in neurons. We have found that ATRX associates with the viral genome during initial neuronal infection, restricts lytic gene expression, and promotes entry into latent infection. We investigated the role of interacting partners of ATRX in initial neuronal infection to parse out the mechanism of ATRX restriction. Our data indicate ATRX functions independently of previously described interacting partners during initial neuronal infection. Since ATRX promotes a more silent form of latency, this work goes toward identifying new therapeutic targets to silence latent infection and prevent reactivation.

## Introduction

Herpes simplex virus type 1 (HSV-1) infects over 65% of the population of the United States (James et al., 2020). Those infected with HSV-1 maintain a lifelong latent infection in post-mitotic neurons, most commonly within the peripheral ganglia. Reactivation from latency can give rise to replication in the epithelial mucosa, which frequently causes painful cold sores and genital lesions. In immunocompromised persons and newborns, reactivation can lead to the onset of severe disease. HSV-1 reactivation is associated with herpes stromal keratitis (HSK), the most common infectious cause of blindness in the United States, and encephalitis (Tullo, 2003). A potential treatment strategy to control reactivation involves targeting the chromatin structure of the virus.

HSV-1 is a dsDNA virus. Viral DNA is non-nucleosomal in the virion and over the course of infection viral DNA chromatinized by host factors via association with histone proteins (Bloom et al., 2010). Transcription is likely modulated by epigenetic modifications to the viral genome. Epigenetics can take on many forms including DNA methylation, the addition of histones, and histone post-translational modifications (PTMs), and associated proteins such as histone PTM readers. Latent viral genomes are enriched with H3K9me2, H3K9me3, and H3K27me3 (Cliffe et al., 2009; Kwiatkowski et al., 2009; Nicoll et al., 2016; Wang et al., 2005). Yet, how different epigenetic structures form and whether they differentially contribute to transcriptional silencing of the viral genome during neuronal HSV-1 infection is unknown.

Neurons are post-mitotic, and thus, the deposition of histones onto the viral genome must be cell cycle independent. Histone variants such as H3.3 are replication-independent, so are thought to be important for chromatinization in neurons (Eustermann et al., 2011). PML-NBs are membrane-less nuclear organelles that can recruit various chromatin-associated proteins including histone chaperones (Bernardi & Pandolfi, 2007; Corpet et al., 2020). During lytic infection with HSV-1 in non-neuronal cells, PML-NBs act to restrict viral replication by recruiting proteins that counteract many viral processes. ATRX and DAXX are recruited alongside PML-NBs during initial HSV-1 non-neuronal infection (Lukashchuk & Everett, 2010). ATRX and DAXX are one of many histone H3.3 chaperones, yet they are the only nuclear H3.3 chaperone complex able to restrict HSV lytic infection where PML-NBs are not dispersed (using an ICP0 null virus) (Cabral et al., 2021). The role of ATRX, DAXX, and PML during *de novo* neuronal HSV-1 infection is unknown. Previously, using an *in vitro* model system of HSV-1 latent infection, we reported that PML-NBs only form in peripheral sympathetic and sensory neurons following exposure to type I IFN (Suzich et al., 2021). Since PML, ATRX, and DAXX have been shown to restrict HSV-1 infection of non-neuronal cells, we sought to understand whether these proteins restricted *de novo* neuronal HSV-1 infection.

ATRX is a multifunctional protein and has a wide variety of interacting partners in various contexts. In addition to PML and DAXX, the two most well studied partners in the context of HSV-1 infection, we also sought to investigate MeCP2 (methyl CpG binding protein). MeCP2 plays an essential role in neuronal

development as mutations to this gene lead to the neurodevelopmental disease Rett syndrome (RTT). MeCP2 binds to canonical DNA methylation (mCpG) as well as non-canonical DNA methylation (mCA) (Tillotson et al., 2021). There is evidence that HSV-1 DNA lacks CpG DNA methylation at the LAT and the ICP4 promoter in samples from latently infected dorsal root ganglia (Kubat et al., 2004). Intriguingly, the host genome in neurons is highly enriched with non-canonical DNA methylation (Tillotson et al., 2021). It is unknown whether the viral genome has non-canonical DNA methylation. Unlike other cell types, DNA in neurons continues to be methylated after birth and is an essential part of neuronal maturation. MeCP2 acts to regulate gene expression by recruiting various epigenetic modulators to methylated DNA (Kinde et al., 2015). MeCP2 interacts with the helicase (C-terminal) domain of ATRX and recruits it to heterochromatic foci. Since MeCP2 is more abundant in neuronal cells than non-neuronal cells, it is thought to be important for ATRX recruitment to DNA in the brain (Nan et al., 2007). As MeCP2 binds to non-canonical DNA methylation and recruits ATRX to DNA on cellular neuronal heterochromatin, we wanted to determine if MeCP2 functioned as an early restriction factor against HSV-1 neuronal infection.

## Results

### Neuronal lytic gene expression following ATRX, DAXX, MeCP2, or PML depletion.

Previous studies have demonstrated that PML-NBs, and the associated proteins DAXX and ATRX, restrict HSV-1 lytic infection in non-neuronal cells. In these studies, ATRX and DAXX function as a complex to deposit H3.3 onto viral DNA and repress lytic HSV-1 infection (Lukashchuk & Everett, 2010) (Cabral et al., 2021). We were also interested in whether MeCP2, an interacting partner of ATRX that is critical to neuronal health, impacted *de novo* neuronal infection. To determine whether ATRX and various interacting partners are involved in HSV lytic gene repression in neurons, primary neurons from the superior cervical ganglia (SCG) of postnatal mice were dissected and transduced with lentiviruses expressing either *Atrx, Daxx, Mecp2,* or *Pml* shRNAs five days before infection with HSV-1. Knockdown was quantified via RT-qPCR (Figure 3.1A). Infection was carried out using Stayput GFP (MOI 1 PFU/cell), which expresses a Us11-GFP and is also defective in cell-to-cell spread, permitting the quantification of individual neurons undergoing lytic gene expression (Dochnal et al., 2022). Depletion of ATRX using two independent shRNAs prior to infection resulted in increased expression of all viral gene classes at 24h post-infection (Figure 3.1B, 3.1C, 3.1D). ATRX depletion also resulted in a significant increase in GFP-positive neurons at 48h (Figure 3.1E). These data suggest that during early infection, ATRX restricts HSV-1 lytic infection in neurons and promotes a latent or quiescent infection. Depletion of MeCP2 or PML did not impact lytic gene

expression or the number of GFP-positive neurons. Intriguingly, lytic gene class expression [excluding early genes (ICP8; Figure 3.1C)] and GFP positive neurons were increased with one *DAXX* shRNA. This phenotype needs to be confirmed with a second shRNA but could suggest ATRX and DAXX both function during *de novo* neuronal infection of HSV-1. As there was no phenotype for PML, this might suggest that in this scenario ATRX and DAXX function independently of PML-NBs.

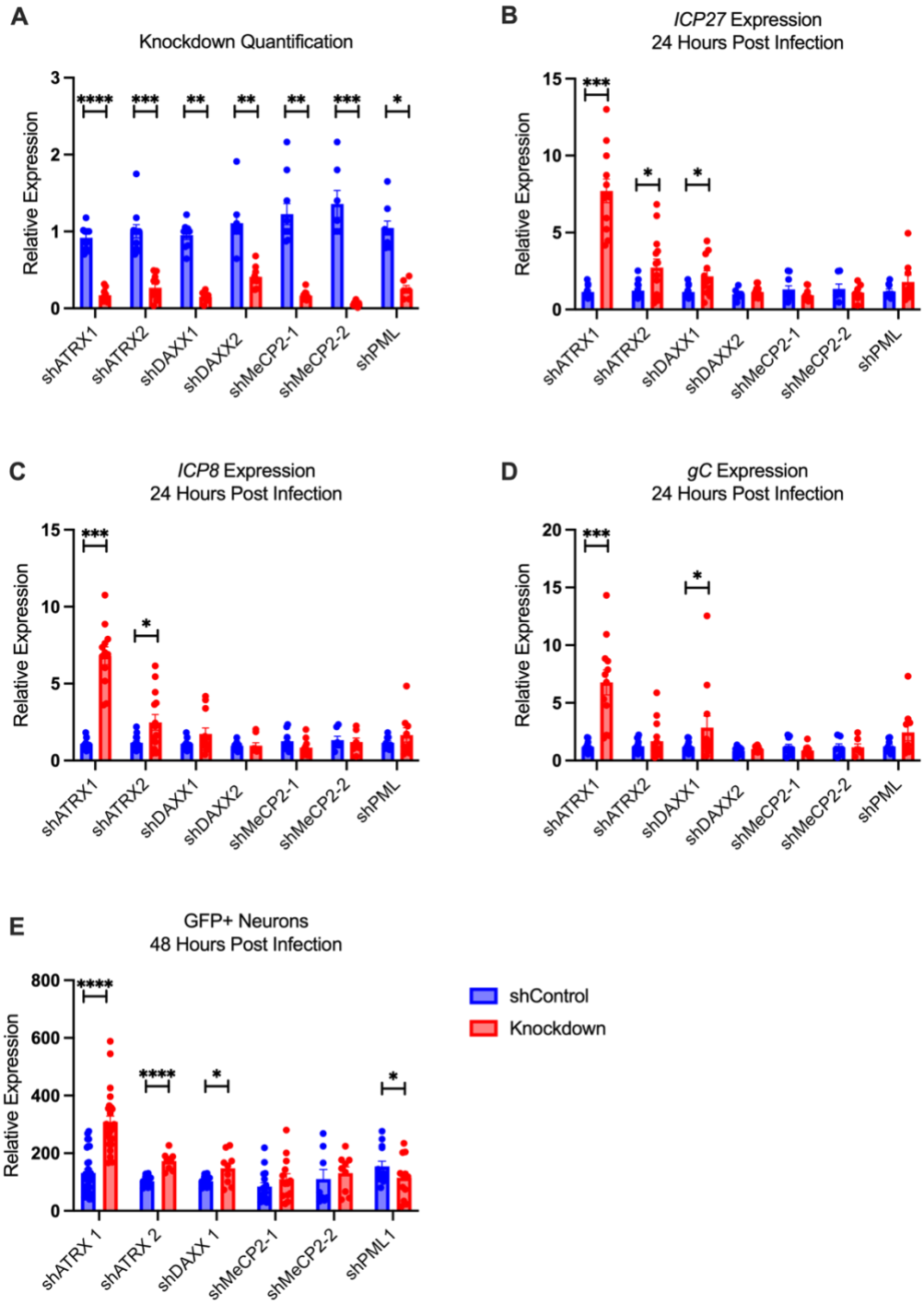
A
Knockdown Quantification
Relative Expression
shATRX1
shATRX2
shDAXX1
shDAXX2
shMeCP2-1
shMeCP2-2
shPML
B
ICP27 Expression
24 Hours Post Infection
C
ICP8 Expression
24 Hours Post Infection
D
gC Expression
24 Hours Post Infection
E
GFP+ Neurons
48 Hours Post Infection
shControl
Knockdown

**Figure 3.1: Neuronal lytic gene expression following ATRX, DAXX, MeCP2, or PML depletion.** SCG neurons were transduced with shRNA-expressing lentiviruses to deplete PML, DAXX or ATRX and 5 days later infected with HSV-1 Stayput-GFP at an MOI of 1 PFU/cell. **A)** Quantification of mRNA levels of the respective genes relative to the non-targeting control lentivirus. Viral gene expression at 24 hours post-infection was quantified by RT-qPCR for **(B)** immediate early (ICP27), **(C)** early (ICP8), and **(D)** late (gC) genes. **E)** Quantification of HSV-1 lytic infection based on the numbers of Us11-GFP positive neurons at 2 days post-infection. N≥9 biological replicates from N≥3 biological replicates (**A-E**). Statistical comparisons were made using a t test or Mann-Whitney U (**A-E**). *p<0.05, **p<0.01, ***p<0.001. ****p<0.0001. The means and SEMs are represented.

## ATRX associates with the viral genome and rapidly restricts lytic gene expression

Given our observation that ATRX restricts HSV-1 lytic infection in neurons, we set out to further characterize this phenotype. Protein depletion can impact host and cellular function, and so we first wanted to determine if ATRX associated with the viral genome during the early time point of one day post-infection (Figure 3.2A). We found that compared to a rotation control where the viral genome was rotated 180 degrees to account for random placement, ATRX was significantly enriched at the viral genome one day post-infection (Figure 3.2B). Previous studies have shown that ATRX colocalizes with the viral genome as early as 10 minutes post-infection in human foreskin fibroblasts (HFFs). Yet, this association decreases at about 100 minutes post-infection, most likely when PML-NBs are dispersed by ICP0 (Cabral et al., 2018). Our observation that ATRX colocalizes at 1-day post-infection with an ICP0 wild-type virus is, therefore, different than previous non-neuronal lytic studies, suggesting ATRX mechanisms are distinct in neurons.

In previous lytic studies, ATRX restricted an ICP0 null virus lytic replication as early as 6 hours post-infection. An ICP0 null virus was used because lytic infection of non-neuronal cells with an ICP0 null virus results in ATRX dispersal and no ATRX phenotype(Cabral et al., 2018). We observed ATRX restricted HSV-1 lytic infection at 24 hours post-infection (Figure 3.1) but sought to determine whether ATRX acted earlier, as observed in these lytic studies. Depletion of ATRX before infection resulted in increased lytic gene expression across all gene classes at 12 hours post-infection (Figure 3.2C-E). Immediate early and early genes are significantly impacted as early as four hours post-infection. These data suggest ATRX acts to silence viral gene expression of an ICP0 competent virus in neurons rapidly post-infection.

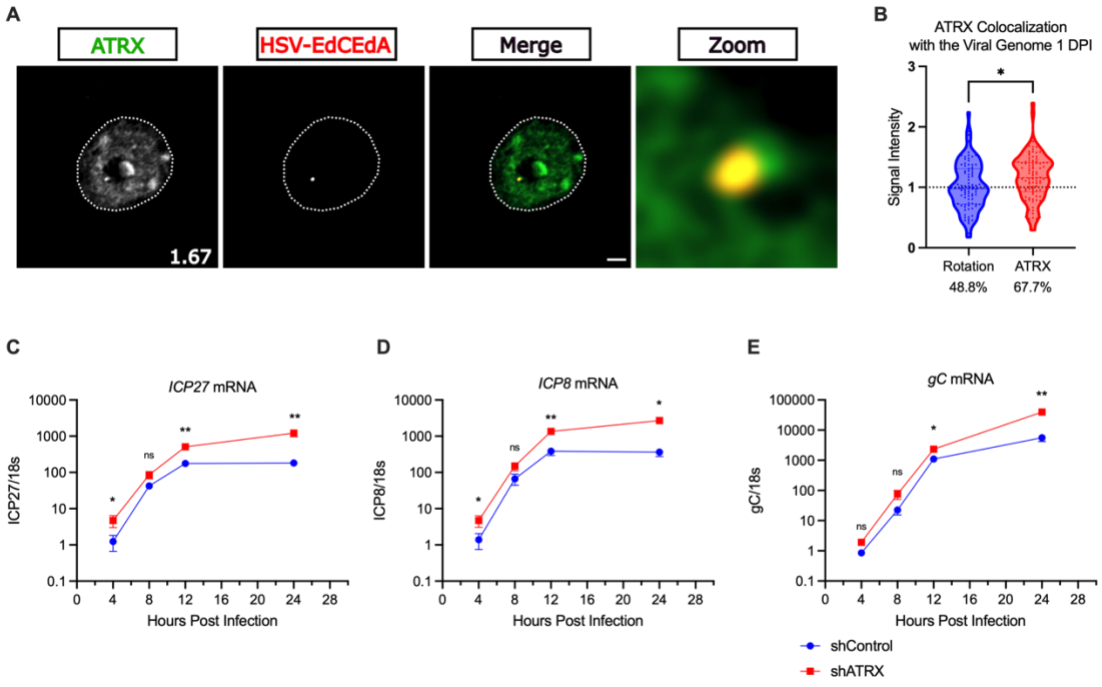

**Figure 3.2: ATRX associates with the viral genome and restricts lytic gene expression rapidly**
**A)** Representative images of sympathetic neurons infected with EdC/EdA labeled HSV-1. Cells were fixed 1-day post-infection. The viral genome was visualized using click chemistry, and immunofluorescence was carried out for ATRX. Scale bar, 10 μm. **B)** NucSpotA was used to quantify the signal intensity of ATRX at the viral genome 1-day post-infection. Rotation denotes a randomized control where the genome-containing layer is rotated 180 degrees to provide a value for random placement (Francois et al., 2024). Each data point represents one viral genome. Percentages indicate the proportion of genomes with NucSpotA intensity ratios above the denoted co-localization threshold (dashed line). N>60 cells from 3 biological replicates. **C-E)** Sympathetic neurons were transduced with shRNA-expressing lentiviruses to deplete PML, DAXX or ATRX and 5 days later infected with HSV-1 Stayput-GFP at an MOI of 1 PFU/cell. Neurons were infected for 4, 8, 12, or 24 hours. Viral gene expression also quantified by RT-qPCR for **(C)** immediate early (*ICP27*), **(D)** early (*ICP8*), and **(E)** late (*gC*) genes. N≥9 biological replicates from N≥3 biological replicates (C-E). Statistical comparisons were made using a t test or Mann-Whitney U (**A-F**). *p<0.05, **p<0.01, ***p<0.001. ****p<0.0001. The means and SEMs are represented.

## ATRX is required for the establishment of latent infection in a sub-population of neurons.

Since the depletion of ATRX resulted in increased viral transcription during early time points post-infection, we aimed to investigate whether this depletion had lasting effects on viral DNA silencing required to establish a quiescent latent infection. For these experiments, we did not use an antiviral (acyclovir) that promotes latency so that we could monitor lytic gene expression and latency establishment in the absence of viral inhibitors. ATRX was depleted prior to infection with Stayput GFP. Three different MOIs were used to determine if MOI had an impact on the ability of ATRX to silence infection. The ability of the virus to fully establish a latent infection over a 30-day period was measured by quantifying detectable GFP-positive neurons. At an MOI of 1, ATRX depletion led

to a significantly higher number of GFP-positive neurons at all measured time points through 30 days post-infection compared to the control depletion (Figure 3.3A). At a lower MOI of 0.1, both control and ATRX depletion wells had undetectable GFP at 16 days post-infection (Figure 3.3B). When cultures were infected at an MOI of 0.01, very few GFP-positive neurons were detected and there were only significantly more GFP-positive neurons in ATRX-depleted wells compared to control wells at 2- and 4-days post-infection (Figure 3.3C). In contrast, depletion of MeCP2 did not affect latency establishment at any of the MOIs used (Figure 3.3D-E). These data suggest that the establishment of latency is impaired at multiple MOIs when ATRX is depleted. This ATRX-dependent phenotype is independent of MeCP2.

Even when ATRX was depleted, latency was established in a sub-population of neurons as only 0.6% of neurons were GFP-positive at 30 days post-infection (assuming 5000 neurons/dish). At this 30-day time point, there were significantly more detectable viral genomes in ATRX depleted neurons (Figure 3.3G), possibly because there was increased viral replication during latency establishment. LAT expression in ATRX depleted neurons was much more variable compared to control and MeCP2 depleted neurons with a standard deviation of 11.15 compared to 0.4188 and 0.4776 respectively. Following reactivation of the cultures using a combined trigger of LY29002, forskolin, and heat shock [triple trigger; (Dochnal et al., 2022)], there was significantly more reactivation in ATRX depleted neurons (Figure 3.3I). Together, this indicates that a large proportion of neurons were quiescent (GFP-negative), but upon

reactivation were more susceptible reactivation in the absence of ATRX. Whether the increase in reactivation was due to reduced silencing in the absence of ATRX, the increase in latent viral genomes, or both is unknown.

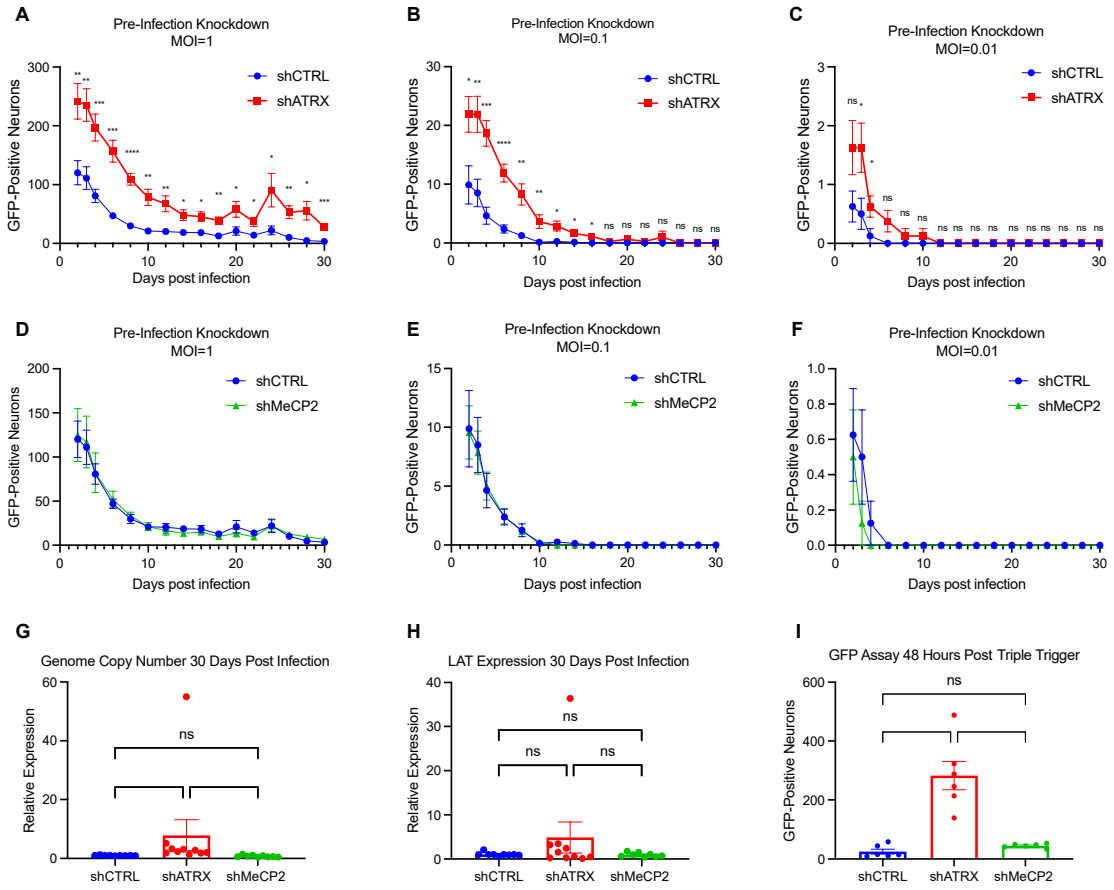

**Figure 3.3: ATRX is required for the establishment of latent infection in a sub-population of neurons.** SCG neurons were transduced with shRNA-expressing lentiviruses to deplete ATRX or MeCP2 and 5 days later infected with HSV-1 Stayput-GFP at an MOI of 1, 0.1, or 0.01 PFU/cell. **A-C)** Quantification of HSV-1 latency establishment in ATRX depleted neurons based on the numbers of Us11-GFP positive neurons over the course of 30 days post-infection. **D-F)** Quantification of HSV-1 latency establishment in MeCP2 depleted neurons based on the numbers of Us11-GFP positive neurons over the course of 30 days post-infection. **G)** Viral genome copy number at 30 days post-infection was quantified by RT-qPCR. **H)** LAT expression at 30 days post-infection was quantified by RT-qPCR. **I)** Reactivation was triggered 30 days post-infection and was quantified based on the numbers Us11-GFP expressing neurons following addition LY294002, forskolin, and heat shock. N≥9 biological replicates from N≥3 biological replicates (**A-I**). Statistical comparisons were made using a t test or Mann-Whitney U (**A-F**) or an Ordinary one-way ANOVA with Tukey's multiple comparison (**G-I**). *p<0.05, **p<0.01, ***p<0.001. ****p<0.0001. The means and SEMs are represented.

## Discussion

At latent time points, the HSV-1 viral genome is associated with cellular histones and histone post-translational modifications (PTMs) (Cliffe et al., 2009; Kwiatkowski et al., 2009; Nicoll et al., 2016; Wang et al., 2005). What controls the deposition of histones and histone PTMs is unknown. It is also not understood how different forms of chromatin contribute to lytic transcription and latency in neurons. ATRX is a multiple-faceted protein, with functions including G quadruplex resolution (Teng et al., 2021), DNA methylation (Marano et al., 2019), histone H3.3 deposition, and histone PTM reading (Voon et al., 2015). In HSV-1 lytic infection of non-neuronal cells, ATRX functions in complex with DAXX to deposit histone H3.3 (Cabral et al., 2021; Cohen et al., 2018; Drane et al., 2010; Lewis et al., 2010) and repress viral transcription HSV-1 lytic infection (Alandijany et al., 2018; Cabral et al., 2018; Lukashchuk & Everett, 2010). In this context,

ATRX and DAXX are found within PML-NBs. The function and protein interactions of ATRX in neuronal HSV-1 lytic transcription are unknown.

Our results demonstrate ATRX restricts HSV-1 lytic gene expression during *de novo* neuronal infection. ATRX acts as early as 4 hours post-infection to limit viral transcription and significantly associates with the viral genome at 24 hours post-infection. Whether ATRX associates with the viral genome at earlier time points in neurons is unknown. The mechanism by which ATRX restricts viral transcription was unknown. To gain further insight, we examined the role of previously identified ATRX-associated proteins. We predicted that PML and DAXX would not have an effect on viral transcription, as DAXX is a constitutive component of PML-NBs and PML-NBs do not form in primary sympathetic neurons in the absence of interferon stimulation (Suzich et al., 2021). We instead hypothesized MeCP2 might affect viral transcription. MeCP2 is essential for DNA silencing in the brain, is more abundant in neuronal cells than non-neuronal cells, and is thought to be important for ATRX recruitment to DNA in the brain (Nan et al., 2007). Surprisingly, MeCP2 and PML had no significant effects on viral transcription. We were surprised that DAXX depletion with one shRNA significantly increased viral transcription. This observation needs to be validated with an additional shRNA or with full DAXX knockout. If confirmed, more work needs to be done to determine whether DAXX functions independently of PML and ATRX in these circumstances. Some studies have indicated that DAXX can have functions that are SIM (the domain required for DAXX-PML interactions) and ATRX independent (Carraro et al., 2023), suggesting potential novel

mechanisms for DAXX in HSV-1 infection to be studied. Further work could also investigate whether DAXX associates with the viral genome, if it influences transcription at time points earlier that 24 hours post-infection, and whether it impacts latency establishment.

From this work we could not find a role for MeCP2 in neuronal lytic infection nor in the establishment of latency. There is limited evidence of canonical CpG methylation on the HSV-1 genome (Kubat et al., 2004). This is based on a lack of canonical CpG methylation on regions of the viral genome containing high levels of CpG such as the latency associated transcript (LAT) region and the viral lytic gene, ICP4 (Kubat et al., 2004). However, the *host* genome in neurons is subject to a high degree of non-CpG methylation, which is laid down robustly during the critical period of neuronal maturation (in humans up to 16 years, in mice up to 4 weeks) (Lister et al., 2013). We find that depletion of DNA methylation binding protein MeCP2 had no effect on neuronal lytic infection or the establishment of HSV-1 latency. Yet, this work used post-natal sympathetic neurons that would not have the same methylation patterns as mature mice. It remains to be determined whether the latent HSV-1 genome is subject to non-CpG methylation and whether the levels are altered depending on the timing of neuronal infection. More work needs to be done to investigate the role of DNA methylation and MeCP2 during HSV-1 infection of mature neurons.

Depletion of ATRX before infection has long-term effects on latency establishment and reactivation. ATRX-depleted neurons show increased lytic gene expression over time, suggesting that ATRX acts as a barrier to latency

establishment. In addition, ATRX depletion enhances reactivation. These findings suggest that ATRX contributes to viral silencing during initial infection, potentially through chromatin regulation, that supports long-term repression.

ATRX is multifaceted, and so in addition to roles as a H3K9me3 reader and H3.3 chaperone, ATRX may promote silencing of the HSV genome via higher order chromatin structure regulation and subsequent heterochromatin deposition. One known function of ATRX is the ability of the protein to bind to G quadruplets (G4), secondary DNA structures that are found on the viral genome during HSV-1 lytic infection of non-neuronal cells and control viral transcription. G4 structures are made during transcription when highly GC-rich regions of DNA bind to RNA being transcribed forming an RNA loop (Teng et al., 2021). ICP4 has been reported to bind to G4 structures located at its own promoter and the other immediate early protein promoters, positively regulating transcription during lytic infection of non-neuronal cells (Frasson et al., 2021). ICP4 is distinct in its ability to bind nascent DNA and promote transcription. This process has been investigated in non-neuronal cells where the tegument arrives in the nucleus concurrently with viral DNA. In neurons, however, this process is poorly defined and must be less reliant on tegument proteins as their axonal trafficking is significantly slower than that of the capsid. Here we describe a striking phenotype of ATRX silencing *de novo* neuronal lytic infection as early as four hours post-infection, a time point where full heterochromatin might not be fully established on viral DNA. ATRX is highly expressed in neurons can bind directly

to G quadruplets (G4s) on cellular DNA. ATRX binding to G4 structures can function to deposit heterochromatin at associated regions (Teng et al., 2021). It has not been previously reported whether ATRX binds to G4 structures on the HSV-1 genome. Although during lytic expression, G4 quadruplexes promote lytic gene expression, it is possible that in neurons, where ATRX is more highly expressed, G4 structures are more readily targeted for silencing by ATRX. Given the potential for ATRX to regulate the epigenetic structure of the latent genome, more research is needed to determine how epigenetic proteins that regulate DNA structure are recruited to viral genomes differently in neurons versus non-neuronal cells, and how this might affect the outcome of HSV neuronal infection.

# Ex Vivo Herpes Simplex Virus Reactivation Involves a Dual Leucine Zipper Kinase-Dependent Wave of Lytic Gene Expression that is Independent of Histone Demethylase Activity and Viral Genome Synthesis

*This chapter has been adapted from:*

Whitford, A. L., Clinton, C. A., Kennedy, E. B. L., Dochnal, S. A., Suzich, J. B., & Cliffe, A. R. (2022). Ex Vivo Herpes Simplex Virus Reactivation Involves a Dual Leucine Zipper Kinase-Dependent Wave of Lytic Gene Expression That Is Independent of Histone Demethylase Activity and Viral Genome Synthesis. *J Virol*, *96*(12), e0047522. https://doi.org/10.1128/jvi.00475-22

## Abstract

Herpes Simplex virus-1 (HSV-1) maintains a lifelong latent infection in neurons and periodically reactivates, resulting in the production of infectious virus. The exact cellular pathways that induce reactivation are not understood. In primary neuronal models of HSV latency, the cellular protein Dual Leucine Zipper kinase (DLK) has been found to initiate a wave of viral gene expression known as Phase I. Phase I occurs independently of both viral DNA replication and the activities of histone demethylase enzymes required to remove repressive heterochromatin modifications associated with the viral genome. Here we investigated whether Phase-I like gene expression occurs in ganglia reactivated from infected mice. Using the combined trigger of explant-induced axotomy and inhibition of PI3K signaling, we found that HSV lytic gene expression was induced rapidly from both sensory and sympathetic neurons. *Ex vivo* reactivation involved a wave of viral late gene expression that occurred independently of viral genome synthesis and histone demethylase activity and preceded the detection of infectious virus. Importantly, we found that DLK was required for the initial induction of lytic gene expression. These data confirm the essential role of DLK in inducing HSV-1 gene expression from the heterochromatin associated genome and further demonstrate that HSV-1 gene expression during reactivation occurs via mechanisms that are distinct from lytic replication.

## Importance

Reactivation of Herpes simplex Virus from a latent infection is associated with clinical disease. To develop new therapeutics that prevent reactivation it is important to understand how viral gene expression initiates following a reactivation stimulus. Dual leucine zipper kinase (DLK) is a cellular protein that has previously been found to be required for HSV reactivation from sympathetic neurons *in vitro*. Here we show that DLK is essential for reactivation from sensory ganglia isolated from infected mice. Furthermore, we show that DLK-dependent gene expression *ex vivo* occurs via mechanisms that are distinct from production replication, namely lytic gene expression that is independent of viral DNA replication and histone demethylase activity. The identification of a DLK-dependent wave of lytic gene expression from sensory ganglia will ultimately permit the development of novel therapeutics that target lytic gene expression and prevent the earliest stage of reactivation.

## Introduction

The ubiquitous human pathogen Herpes Simples Virus persists for life in the form of a latent infection in neurons. In response to a variety of different stimuli, the virus can reactivate from the latent state, resulting in the release of infectious virus and subsequent replication in the surrounding tissue. Clinically, reactivation of the virus can manifest as a variety of disease states including lesions at the body surface, keratitis, and encephalitis. In addition, there is growing evidence of a link between HSV infection and the development of late onset Alzheimer's disease, particularly in individuals with the ApoE4 variant (Baringer & Pisani, 1994; De Chiara et al., 2019; Itzhaki, 2018; Itzhaki et al., 1997; Jamieson et al., 1991; Mori et al., 2004; Piacentini et al., 2014; Readhead et al., 2018; Tzeng et al., 2018). There are potentially different stimuli that can induce HSV to reactivate from latency. These stimuli may converge on single cellular pathways or operate via distinct mechanisms to induce reactivation (Suzich & Cliffe, 2018). Identifying the cellular pathways important in reactivation is required to understand how viral gene expression initiates from the latent genome and to ultimately develop therapeutics to prevent reactivation occurring.

During a latent infection of neurons, the HSV genome is assembled into repressive heterochromatin. This has been characterized by the enrichment of post-translational modifications on histone H3; namely di- and tri-methyl lysine 9 (H3K9me2/3) and tri-methyl lysine 27 (H3K27me3) on lytic promoters (Cliffe et al., 2009; Dochnal et al., 2021; Knipe & Cliffe, 2008; Kwiatkowski et al., 2009; Liang et al., 2009; Nicoll et al., 2016; Wang et al., 2005). By assembling into

heterochromatin, viral lytic transcripts are maintained in a silent state. In addition, both host and viral miRNAs target lytic mRNAs (Jurak et al., 2014; Jurak et al., 2010; Kramer et al., 2011; Pan et al., 2014; Umbach et al., 2008). Therefore, the action of transcriptional and translational silencing results in limited synthesis of viral lytic proteins. This lack of lytic proteins suggests that HSV is reliant upon host signaling to initiate gene expression and reactivation. To understand the mechanism of HSV reactivation, it is important to determine how activation of host cell pathways ultimately converge on the repressed viral genome to induce lytic gene expression.

There is evidence that the initial induction of HSV-1 lytic gene expression following reactivation occurs in a manner that is distinct from the mechanisms of viral gene expression during lytic replication. HSV lytic genes can be divided into groups characterized by their requirements for viral protein synthesis and viral DNA replication during lytic replication (Roizman et al., 2013). Immediate early (IE) genes are expressed independently viral protein synthesis during lytic infection and instead require the viral tegument protein VP16 for maximal expression. Early (E) genes are expressed following the production of IE proteins. Certain IE proteins (including ICP4, ICP0 and ICP27) stimulate viral E protein synthesis. Late (L) genes require viral DNA synthesis and are subdivided into genes that are expressed at low levels even prior to DNA replication but increased with genome synthesis (leaky L) and those that are fully dependent on viral DNA replication (true L). The dependence on DNA replication for L gene expression is not fully understood but likely involves a shift in genome

accessibility and increased binding of host transcriptional machinery (RNA Pol II, TBP, and TAF1) (Dremel & DeLuca, 2019). In contrast to this regulated cascade, in models of HSV reactivation, an initial burst of lytic gene expression, named Phase I of reactivation, has been observed where inhibition of protein synthesis prior to the accumulation of IE transcripts does not prevent E gene expression (Kim et al., 2012). In addition, L gene expression is unaffected by inhibition of viral DNA replication (Kim et al., 2012). Together, these data indicate that initial expression of lytic transcripts during the early stages of reactivation does not resemble the early stages of *de novo* infection in non-neuronal cells.

Phase I of HSV reactivation has largely been identified in primary neuronal models of HSV latency in sympathetic neurons (Cliffe & Wilson, 2017). In these experimental models, a variety of stimuli have been found to induce HSV to reactivate from a latent infection, including loss of neurotrophic factor support (Cliffe et al., 2015; Kim et al., 2012; Wilcox & Johnson, 1987; Yanez et al., 2017), increased neuronal excitation (Cuddy et al., 2020), modulation of DNA damage/repair (Hu et al., 2019) and exposure to corticosteroids (Cliffe et al., 2015). Precisely how activation of these pathways permits expression of the viral gene transcripts for reactivation to occur is not fully understood. Previously, we have identified a role for the cell stress protein, dual leucine zipper kinase (DLK), in inducing Phase I of HSV reactivation (Cliffe et al., 2015). DLK is activated by the loss of neurotrophic factor support, which can be mimicked by inhibition of Phosphoinositide 3 (PI3)-kinase activity (Cliffe et al., 2015), and during

heightened neuronal excitation and interleukin-1 (IL-1) treatment (Cuddy et al., 2020). DLK is a master regulator of axonal responses to stress and can mediate a variety of responses including Wallerian degeneration, axon regeneration, apoptosis, and axon pruning (Tedeschi & Bradke, 2013). Upon activation, DLK is known to re-direct the cell stress protein, c-Jun N-terminal kinase (JNK), from its physiological role in neurons, maintaining synaptic arborization, to its cell stress function (Sengupta Ghosh et al., 2011). Accordingly, we and others have identified a role for JNK in reactivation of HSV from latency (Cliffe et al., 2015; Cuddy et al., 2020; Hu et al., 2019). JNK is also important in reactivation of the related Alpha herpesvirus, Varicella-Zoster virus, from a latent infection (Kurapati et al., 2017) highlighting its potential central role in reactivation of human Alpha herpesviruses.

A role for DLK and JNK in HSV reactivation has been mostly widely studied on primary neuronal models of latency in murine sympathetic neurons (Cliffe et al., 2015; Cuddy et al., 2020). In these neurons, latency is established in the presence of the HSV DNA replication inhibitor, acyclovir. After the removal of acyclovir, reactivation can be induced by PI3-kinase inhibition or forskolin (Camarena et al., 2010; Cliffe et al., 2015; Cuddy et al., 2020; Kim et al., 2012; Suzich et al., 2021). In these systems, full reactivation occurs around 48h post-stimulus, which requires the activities of histone demethylase enzymes, indicating that reactivation requires removal of repressive heterochromatin (Cliffe et al., 2015; Cuddy et al., 2020). However, the DLK-dependent Phase I peaks around 18h post-stimuli and (Cliffe et al., 2015; Cuddy et al., 2020; Hu et al.,

2022), importantly, Phase I occurs independently of lysine 9 and lysine 27 histone demethylase activity (Cliffe et al., 2015; Cuddy et al., 2020). Instead, JNK activation induces histone phosphorylation on H3Serine10 (H3S10) on histones that maintain the H3K9me3 modification (Cliffe et al., 2015); this is known as a histone methyl/phospho switch and presumably permits transcription by overriding the repressive H3K9me3 modification. However, although demonstrated *in vitro*, the possibility of a DLK/JNK-dependent wave of gene expression, characteristic of Phase I, has not been explored following *in vivo* infections.

A robust mode of HSV reactivation from infected mice is explanation of the sensory trigeminal ganglia (TG). The action of severing the axon (axotomy), is thought to be the trigger that induces HSV to reactivate. In this model, whether a Phase I-like wave of gene expression occurs has not been fully explored. Data from a previous study suggests that a H3 lysine 9 demethylase functions to promote lytic gene expression at an early time-point (6 hours post-explant) (Liang, Vogel, et al., 2013). This indicates that wave of gene expression that is independent of histone demethylase activity occurs at an earlier time-point, or that explant induced reactivation does not involve a Phase-I like wave of viral gene expression. There are multiple differences between the *in vivo* experiments and *in vitro* latency models, including the presence of host immune system *in vivo*. In addition, explant-induced reactivation has been investigated mostly in sensory neurons whereas models for *in vitro* infection often use sympathetic neurons; both neuronal types are targets of HSV latent infection in humans

(Baringer & Pisani, 1994; Baringer & Swoveland, 1973; Richter et al., 2009; Warren et al., 1978). *In vitro* models also use acyclovir to promote the establishment of latency. Finally, potential differences resulting from viral strains used cannot be ruled out. In experiments investigating the role for histone demethylases *ex vivo*, HSV strain F was used (Liang, Vogel, et al., 2013; Liang et al., 2009), whereas the in vitro models have been performed with the KOS and Patton strains (Cliffe et al., 2015; Kim et al., 2012).

To determine whether previous observations of a DLK/JNK triggered Phase I reactivation *in vitro* were recapitulated e*x vivo* and in sensory neurons*,* we dissected trigeminal ganglia from latently infected mice and determined whether we observed lytic gene expression in response to PI3-kinase inhibition. We found that after only five hours post excision, in treated ganglia, there was robust expression of IE, E, and L viral genes and this gene expression was independent of viral DNA replication. Supporting previous findings, we also found that this initial burst of lytic gene expression was not dependent upon LSD1 (H3K9-demethylase) nor JMJD3 and UTX (H3K27-demethylases). Therefore, Phase I of reactivation was observed *ex vivo* and was not reliant upon the removal of repressive heterochromatic marks. We found that this Phase 1 was dependent upon DLK, thus indicating that neuronal stress pathways can trigger bi-phasic reactivation of HSV-1 in ganglia *ex vivo*.

## Results

### Explant combined with PI3-kinase inhibition triggers robust HSV-1 lytic gene expression

We first set out to determine whether a wave of lytic gene expression occurs following reactivation of explanted sensory trigeminal ganglia (TG), similar to what has been observed in primary sympathetic neuronal cultures. Female mice were infected via the ocular route and reactivation studies were carried out at least 28 days post-infection. Previously, studies from our lab and others have shown that addition of a reactivation stimulus to sympathetic neurons infected *in vitro* yields induction of lytic viral gene expression around 15-20 hours post-stimulus (Cliffe et al., 2015; Kim et al., 2012). In addition, a previous study examining explant induced reactivation of TG combined with deprivation of nerve growth factor (NGF) also resulted in lytic gene induction around 12-15 hours post-explant (Du et al., 2011). Therefore, we initially examined the effect of PI3-K inhibition (using LY294002; 40 μM) at 20 hours post-reactivation to determine whether loss of the PI3K/AKT branch of the NGF-signaling pathway also promotes reactivation from TGs *ex vivo*. Acyclovir (ACV; 100 μM) was also introduced alongside LY294002 because late gene expression during the initial activation of viral gene expression in *in vitro* models has been reported to proceed independently of DNA replication (Kim et al., 2012).

In ganglia that were explanted and maintained in NGF to provide continued neurotrophin support, very little induction of lytic gene expression was observed at 20h post-explant, especially for representative IE and E transcripts

(Fig. 4.1B&C). A slight increase in *gC* mRNA was observed (Fig. 4.1D), although this increase was not statistically significant (P=0.1255, Mann Whitney U Test). However, the addition of the PI3-kinase inhibitor (LY294002) increased viral gene expression by 100-1000-fold. RT-qPCRs were carried out using primers against IE (ICP27, Fig. 4.1 B), E (ICP8, Fig. 4.1C) and L (gC, Fig. 4.1D) genes. All three genes were significantly induced at 20h post excision. The addition of ACV to inhibit viral DNA replication did not inhibit the induction of IE or E gene expression, as expected. However, expression of the gC mRNA was significantly reduced in the presence of ACV, indicating that its maximal expression was dependent on viral genome synthesis. However, gC mRNA levels with ACV were still significantly increased compared to the latent samples. At 20h post-reactivation, an increase in viral genomes was also observed (Fig. 4.1A). Together, these data show that at 20h post-reactivation viral gene expression does not resemble the Phase I observed in primary neuronal cultures, as genome synthesis had occurred, and full late gene expression was dependent on viral DNA replication. However, this did not rule out the possibility of a Phase I-like wave of gene expression occurring prior to 20h, especially as *gC* mRNA was still induced compared to the 0h (latent) samples.

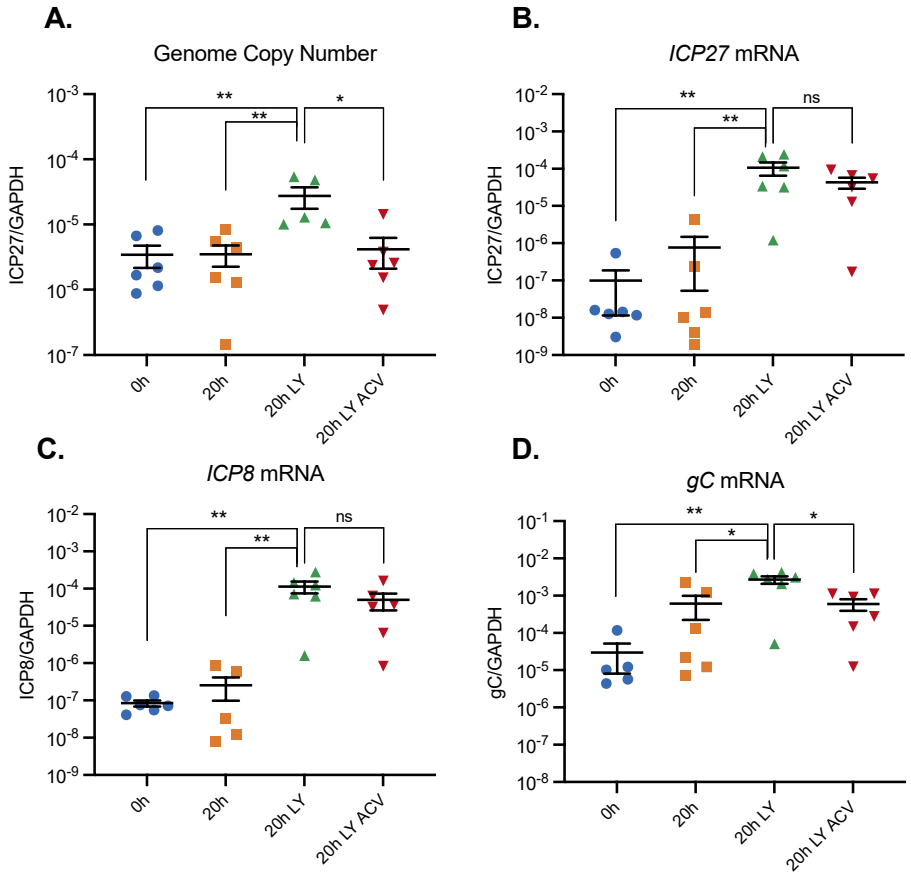


**Figure 4.1: Explant combined with PI3-kinase inhibition triggers robust HSV-1 lytic gene expression**
Mice were infected via corneal scarification and at least 28 days post-infection trigeminal ganglia were excised. Ganglia were either snap frozen at 0 hours, or reactivated for 20 hours in media alone, with LY294002 (40 μM) or LY294002 with acyclovir (ACV; 100μM). (A) Viral genome copy number was quantified by qPCR. (B) Viral gene expression was quantified by RT-qPCR for immediate early (*ICP27*), (C) early (*ICP8*) and (D) and late (*gC*) genes. Transcript copy number was normalized to cellular control (GAPDH). n=6 biological replicates. Mann-Whitney U (A-D). *p<0.05, **p<0.01. Individual biological replicates along with the means and SEMs are represented. Infections for experiments in Panels A-D were performed by Corinne Clinton or Dr. Anna Cliffe. Time point collections for experiments in Panels A-D were performed by Jon Suzich. RT-qPCRs for experiments in Panels A-D were performed by Corinne Clinton.

## PI3K inhibition/explant of trigeminal ganglia results in rapid late gene expression in the absence of detectable genome synthesis

To determine whether viral lytic gene expression occurred prior to 20h post-stimulus in explanted TG with features characteristic of Phase I gene expression, we decided to infect both male and female mice and determine changes in lytic gene expression following PI3-kinase inhibition of explanted ganglia. Because we infected both male and female mice, we assessed if sex impacted clinical manifestations of infection. Both male and female mice had minimal mortality with 92 and 88 percent survival respectively (Fig, 4.2A). To further analyze clinical symptoms, mice were evaluated by scoring lesions, neurological symptoms and eye health based on a previously described scoring metric (Riccio et al., 2019). Infection of female mouse resulted in more severe clinical manifestations at days 7 and 9 post-infection (Fig. 4.2B). Despite these differences, there was no significant differences in the percentage of weight loss following infection between male and female mice (Fig. 4.2C). Based on these criteria, we concluded there were only minor sex-dependent differences upon HSV infection.

**A.**

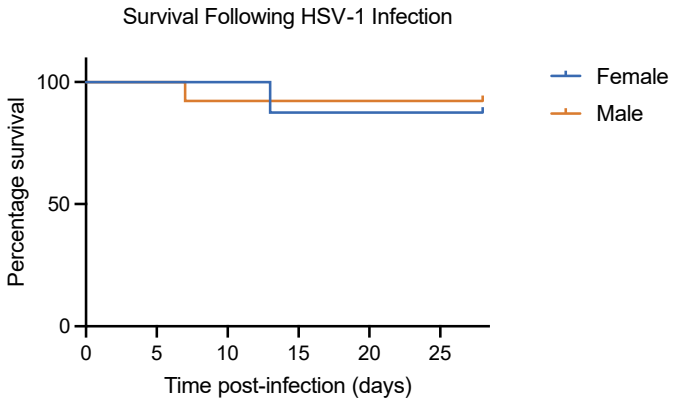
Survival Following HSV-1 Infection
Percentage survival
100
50
0
0
5
10
15
20
25
Time post-infection (days)
Female
Male

**B.**

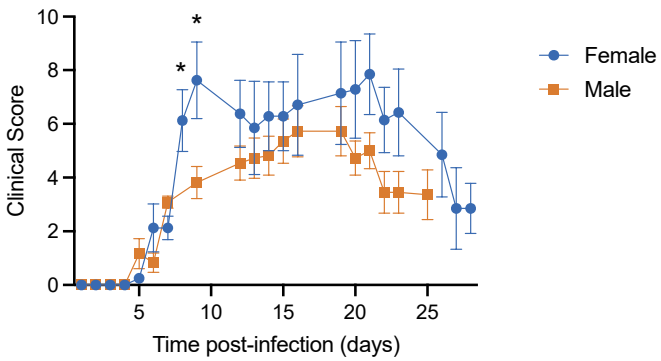
Clinical Scores Following HSV-1 Infection
Clinical Score
10
8
6
4
2
0
*
*
5
10
15
20
25
Time post-infection (days)
Female
Male

**C.**

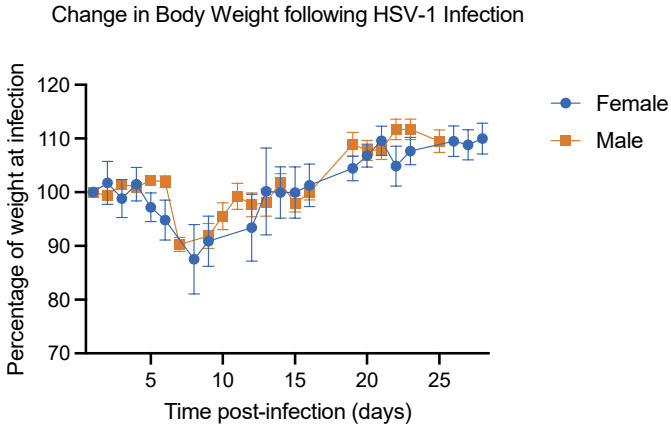
Change in Body Weight following HSV-1 Infection
Percentage of weight at infection
120
110
100
90
80
70
5
10
15
20
25
Time post-infection (days)
Female
Male

**Figure 4.2: Sex dependent phenotypes during HSV-1 *in vivo* infection.** Mice were infected via corneal scarification and monitored post-infection. (**A**) Survival over time was observed and the significance of the percentage survival between female and male mice were analyzed using Kaplan-Meier survival analysis. (**B**) Clinicals scores were calculated by scoring lesion, neurological, and eye phenotypes as outlined in table 1. (**C**) Percent weight compared to pre-infection weights. Student T test (**B-C**). *p<0.05. The mean and SEM are represented. N= 13 females, 8 males. Infections for experiments in Panels A-C were performed by Corinne Clinton or Dr. Anna Cliffe. Clinical scoring for experiments in Panels A-C were performed by Corinne Clinton.

After at least 28 days post-infection, TG were explanted and incubated in the presence of LY294002, with and without ACV. Values from both male and female mice were combined (Fig. 4.3A-D). Quantification of viral DNA loads showed that the copy number of viral genomes stayed constant up to 15 hours post-stimuli and were not affected by the presence of ACV, indicating that detectable viral genome synthesis did not occur in this time period. In contrast, a robust induction of viral lytic gene expression occurred by 5h post-stimuli, as indicated by an increase in IE (*ICP27*), E (*ICP8*) and late (*gC*) mRNA copy number. For all gene classes examined, the increase in copy number was 100-fold for IE mRNA (Fig. 4.3B), 20-fold for E mRNA (Fig. 4.3C), and 10-fold for L mRNA (Fig. 4.3D) at 5 hours post explant. The robust increase in late gene expression in the absence of detectable viral genome synthesis between 0- and 15-hours post-explant shows that late gene expression could occur even prior to DNA replication. To further support this conclusion, late gene induction occurred to equivalent levels even in the presence of ACV. The inclusion of ACV did prevent genome synthesis at 20h post-stimuli (Fig. 4.1A), indicating that the ACV

was capable of acting on the explanted ganglia. Therefore, these data indicate that the induction of lytic gene expression following PI3-kinase inhibition in explanted sensory neurons resembles at least one feature of Phase I gene expression as viral late gene expression occurred independently of viral DNA replication.

To confirm that reactivation had no sex-dependent effects we performed quantification of viral lytic gene expression in both male and female mice. We found no difference in viral genome copy number (Fig. 4.3E) or ICP27 lytic gene expression (Fig. 4.3F) at any time point. Therefore, we see no obvious differences in the efficiency of lytic gene expression following reactivation of male and female mice.

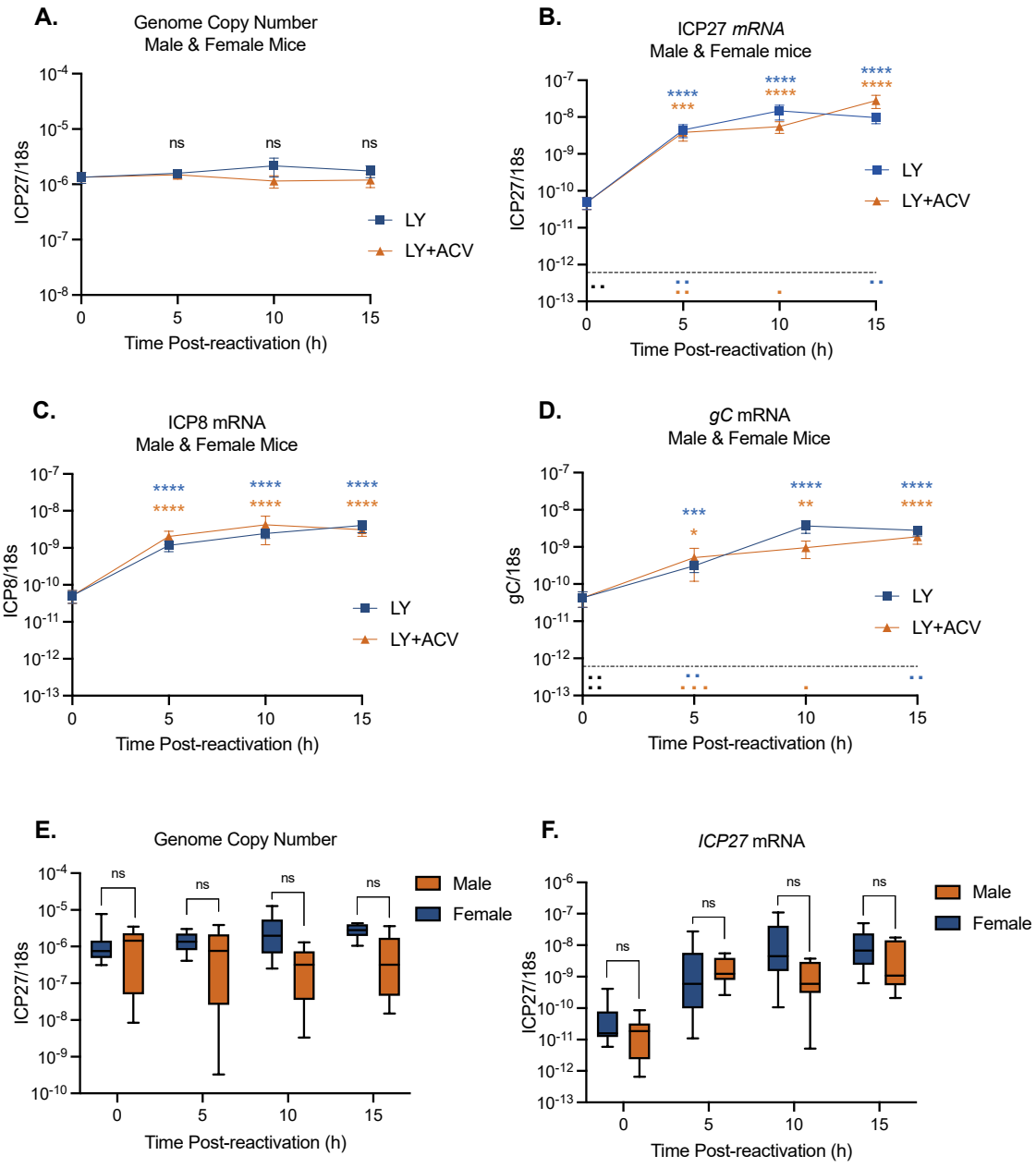
A.
Genome Copy Number
Male & Female Mice
ICP27/18s
Time Post-reactivation (h)
LY
LY+ACV
ns
B.
ICP27 mRNA
Male & Female mice
C.
ICP8 mRNA
Male & Female Mice
ICP8/18s
D.
gC mRNA
Male & Female Mice
gC/18s
E.
Genome Copy Number
Male
Female
F.
ICP27 mRNA

**Figure 4.3: PI3K inhibition of explanted trigeminal ganglia induces rapid lytic gene expression in the absence of detectable genome synthesis**
Latently infected TGs from male and female mice were reactivated for 5,10 or 15 hours with LY294002 in the presence and absence of acyclovir. (A) Viral genome copy number was quantified by PCR. Viral gene expression also was quantified by RT-qPCR for (B) immediate early (*ICP27*), (C) early (*ICP8*), and (D) late (*gC*) genes. The average genome copy number (E) and ICP27 mRNA transcripts (F) for male and female mice were calculated. Transcript copy number was normalized to cellular control (18s). Limit of detection indicated by black dashed line. N≥19 biological replicates (A-D). Mann-Whitney U (**A-F**). *p<0.05, **p<0.01, ***p<0.001. ****p<0.0001. The means and SEMs are represented. Infections for experiments in Panels A-F were performed by Corinne Clinton or Dr. Anna Cliffe. RNA/DNA isolations for 10 experimental replicates in Panels A-F were performed by Lane Kennedy. RT-qPCRs for 8 experimental replicates in Panels A-F were performed by Corinne Clinton.

## PI3-kinase Inhibition in Combination with Axotomy Triggers Rapid Lytic Gene Expression in Sympathetic Neurons *Ex Vivo*

Previous studies investigating Phase I gene expression *in vitro* have largely used sympathetic neurons, where the induction of lytic gene expression has been found to occur 15-20h post stimuli (25-27). However, we found that lytic gene expression induced *ex vivo* from sensory neurons was robustly induced by 5h post-stimulus (Fig 4.2). To determine whether the enhanced kinetics of reactivation observed *ex vivo* from sensory neurons in the TG could result from the use of different neuronal types, we investigated reactivation *ex vivo* from the sympathetic superior cervical ganglia (SCGs). Latently infected SCGs were explanted and incubated in the presence of the PI3-kinase inhibitor, LY294002. Quantification of viral DNA loads showed that the copy number of viral genomes remained constant at 5 hours after stimulation, indicating that no detectable viral genome synthesis occurred during this time (Fig. 4.4A). In concordance with our

sensory ganglia data (Fig. 4.1), there was a significant 10-fold increase in viral genome copy number at 20 hours post excision (Fig. 4.4A). By 5h post-stimuli a robust stimulation of viral lytic gene expression had occurred, as evidenced by a 10-fold increase in IE (*ICP27,* Fig 4.4B) and a 20-fold increase in late (*gC*) mRNA copy numbers (Fig. 4.4C). This indicates that the faster kinetics observed *ex vivo* in sensory neurons was not due to different neuronal subtypes and instead likely results from either the combination of triggers or as a result of *in vivo* infection.

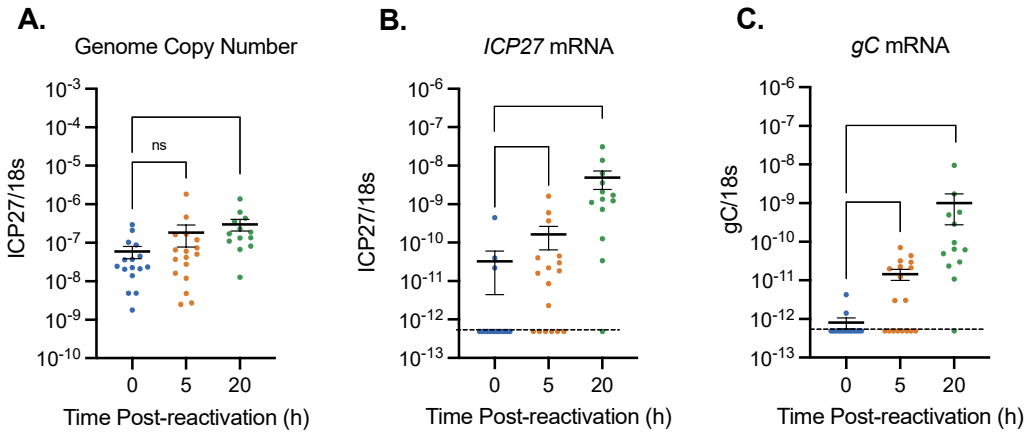


**Figure 4.4: PI3K inhibition of explanted superior cervical ganglia induces rapid lytic gene expression in the absence of detectable genome synthesis** Latently infected SCGs from female mice were reactivated for 5 or 20 hours with LY294002. (A) Viral genome copy number was quantified by PCR. Viral gene expression also was quantified by RT-qPCR for (B) immediate early (*ICP27*), and (C) late (*gC*) genes. Transcript copy number was normalized to cellular control (18s). Limit of detection indicated by black dashed line. N≥12 biological replicates (A-C). Mann-Whitney U (**A-C**). *p<0.05, **p<0.01, ***p<0.001. ****p<0.0001. The means and SEMs are represented. Infections for experiments in Panels A-C were performed by Corinne Clinton or Dr. Anna Cliffe.

## Analysis of preformed virus production in sensory neurons *ex vivo*

Based on our data that viral late gene expression was detectable by 5 hours and robustly expressed by 10 hours post-explant, we investigated when

preformed infectious virus could be detected in the explanted ganglia. The rationale for this was that Phase I lytic gene expression occurs in cultured neurons before the production of *de novo* virus (25). To ensure that we detected only preformed virus and not virus produced from remaining intact cells, the ganglia were homogenized and subjected to three rounds of sonication and two cycles of freezing and thawing. Using a viral stock of known titer, we confirmed that that this procedure did not result in a detectable loss in viral titer (data not shown). Infectious virus was robustly detected at 20h post-explant in 7 out of the 8 ganglia tested (Fig. 4.5). At 15 hours, virus was only detected in 5 out of 8 ganglia tested and at 10 hours only 2 ganglia had detectable virus. No infectious virus was detected at 7 hours post-explant. These findings suggest that a detectable increase in late gene expression occurs 10 to 15 hours before infectious virus production, observed at 20 hours, in a population of reactivating ganglia.

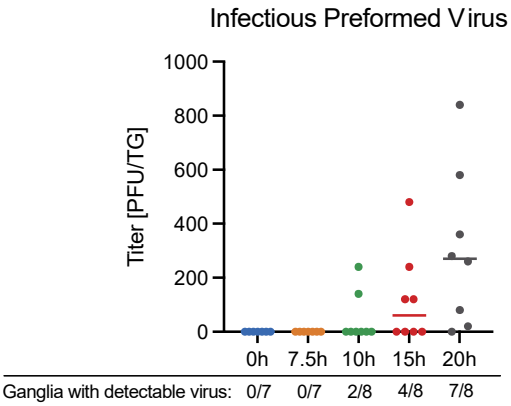

**Figure 4.5: Robust detection of pre-formed virus occurs 20 hours post excision**
Latently infected TGs from female mice were reactivated for 0, 7, 10, 15, or 20 hours with LY294002. Ganglia were homogenized and sonicated then plated on vero cells to be titrated. (A) Pre-formed virus was determined by counting plaques and calculating viral titer. Number of ganglia with detectable virus is displayed beneath the X axis. N≥7 biological replicates. The median titer is represented. Infections for experiments in Panels A-C were performed by Dr. Anna Cliffe.

## DLK activity is required for reactivation *ex vivo*

Previously, we have found that the neuronal cell stress protein dual leucine zipper kinase (DLK) is required for HSV reactivation and acts to induce Phase I lytic gene expression (27, 30). To determine whether DLK was also required for the induction of lytic gene expression in sensory neurons reactivated *ex vivo* by PI3K-inhibition/axotomy, the DLK inhibitor GNE-3551(Patel et al., 2015) was added to the explanted ganglia and viral RNA was quantified at 5h post-reactivation. Inclusion of the DLK-inhibitor resulted in *ICP27*, *ICP8*, and *gC* mRNA (Fig. 4.6 A-C) levels that were equivalent to the unreactivated samples and significantly decreased compared to the LY204002 only treated ganglia. These data indicate that DLK is required for reactivation from sensory neurons induced by the combined trigger of explant and PI3-kinase inhibition. This is the first demonstration of a role for DLK in reactivation from sensory neurons and in response to *ex vivo* axotomy.

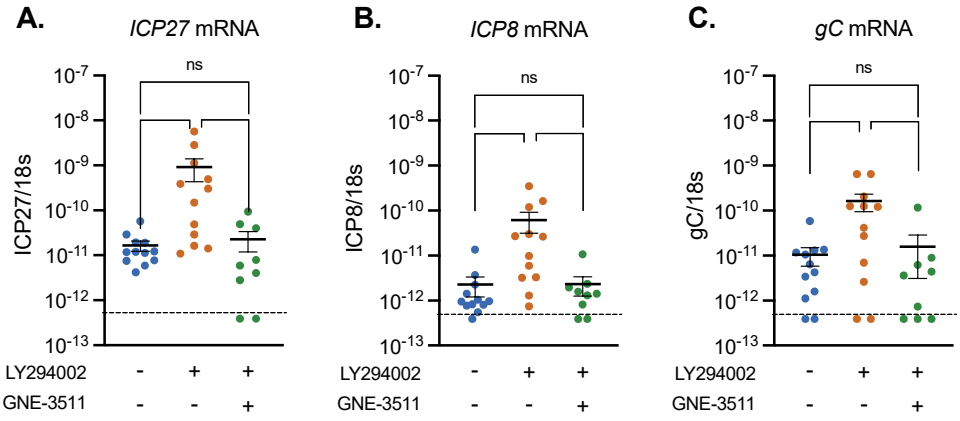


**Figure 4.6: DLK activity is required for the induction of lytic gene expression following explant/PI3-kinase inhibition of latently infected TG.** Latently infected TG were explanted and incubated with LY294002 and the DLK inhibitor GNE-3511 (8 μM) for 5 hours post excision. Viral gene expression was quantified by RT-qPCR for immediate early (*ICP27*) (**A**), early (*ICP8*) (**B**), and late (*gC*) (**C**) genes. Transcript copy number was normalized to cellular control (18s). Limit of detection indicated by black dashed line. n=12 biological replicates. Mann-Whitney U test. *p<0.05, **p<0.01. Individual biological replicates along with the means and SEMs are represented. Infections for experiments in Panels A-C were performed by Corinne Clinton or Dr. Anna Cliffe.

## Lytic gene induction upon axotomy/PI3-kinase inhibition is independent of histone H3 histone lysine 9 and lysine 27 demethylase inhibitors

HSV promoters are known to be enriched with histone H3 di- and trimethyl at lysine 9 (H3K9me2/3) and histone H3 trimethyl at lysine 27 (H3K27me3) during latency. The removal of restrictive histone modifications, specifically the aforementioned methylation marks, was previously shown to be essential for full reactivation of HSV *in vitro,* yet was not required for initial lytic gene expression during Phase I of reactivation (Cliffe et al., 2015; Cuddy et al., 2020). To determine if initial lytic gene expression was independent of histone

demethylation *ex vivo,* we used OG-L002 (60 μM), a drug that inhibits the histone lysine 9 demethylase LSD1 (Liang, Quenelle, et al., 2013), and GSK-J4 (20 μM), which inhibits the histone lysine 27 demethylases UTX and JMJD3 (Heinemann et al., 2014; Kruidenier et al., 2012). HSV reactivation has been demonstrated to be inhibited by both of these inhibitors (Cliffe et al., 2015; Cuddy et al., 2020; S. A. Dochnal et al., 2022; Liang, Quenelle, et al., 2013; Messer et al., 2015). Five hours post excision, the addition of OG-L002 and GSK-J4 had no effect on the induction of ICP27, ICP8, or gC mRNA (Fig. 4.7A-C). These results indicate that histone demethylase activity is not required for the initial induction of lytic gene expression induced by axotomy and PI3-kinase inhibition *ex vivo*.

Together, our results demonstrate that features of Phase I gene expression, namely late gene expression in the absence of viral DNA replication and lytic gene expression in the presence of histone demethylase inhibitors, can occur from ganglia isolated from infected mice. In addition, *ex vivo* reactivation was dependent on DLK activity.

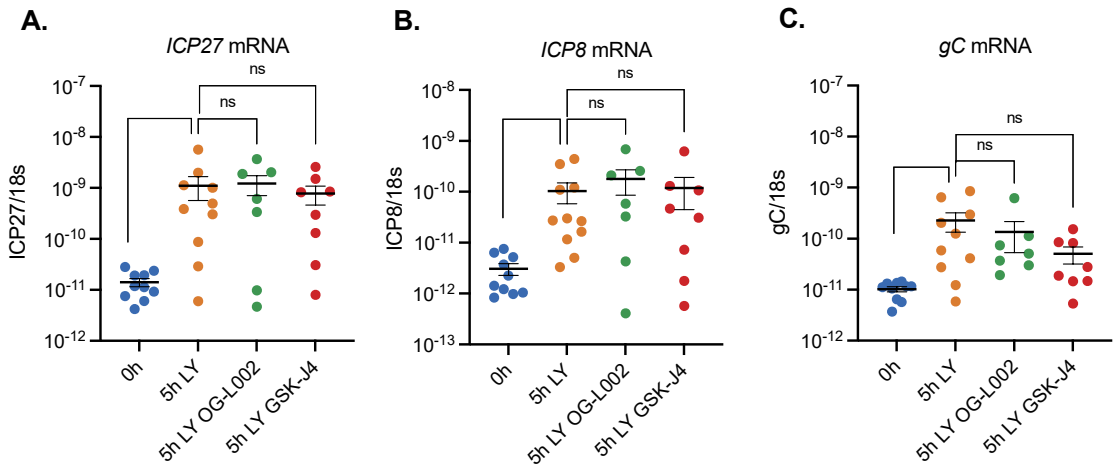

**Figure 4.7: Lytic gene induction following axotomy/PI3-kinase inhibition is unaffected by histone demethylase inhibitors.**
Latently infected TG were explanted and incubated with LY294002 along with the LSD1 inhibitor OG-L1002 (50 μM) or GSK-J4 (20 μM). Viral gene expression was quantified by RT-qPCR for immediate early (*ICP27*) (**A**), early (*ICP8*) (**B**), and late (*gC*) (**C**) genes. Transcript copy number was normalized to cellular control (18s) Mann-Whitney U (**A-C**)., **p<0.01, ***p<0.001. Individual biological replicates along with the means and SEMs are represented. Infections for experiments in Panels A-C were performed by Corinne Clinton or Dr. Anna Cliffe.

## Discussion

*In vitro* models of HSV latency are incredibly powerful for the study of molecular mechanisms HSV latency and reactivation as well as the contribution of host factors and viral factors during specific stages of infection. By including components of the host immune response, such as interferon at different stages of infection, *in vitro* models can be used to investigate how the host immune response can modulate latent infection and reactivation (Linderman et al., 2017; Suzich et al., 2021). Using these models, unique aspects regarding entry into lytic gene expression during reactivation have been uncovered, including the dependence on DLK/JNK for reactivation, the ability of late gene expression to occur in the absence of DNA replication, and transcription despite the presence of histone demethylase inhibitors. Therefore, it was highly important to validate these patterns of gene expression from ganglia infected *in vivo*. Here we have confirmed that the features of gene expression observed during Phase I reactivation *in vitro* also occur following reactivation *ex vivo* when PI3k-inhibition and axotomy is used as a trigger. These data therefore demonstrate the validity of using *in vitro* model systems to investigate the mechanisms of initiation of lytic gene expression during reactivation. We also demonstrate for the first time that Phase I gene expression occurs from sensory neurons.

There are certain caveats to our study, especially relating to the ability of inhibitors to act on intact ganglia. However, we show that the DLK inhibitor, PI3-kinase inhibitor and acyclovir can all act on intact ganglia. Therefore, we think it

unlikely that the histone demethylase inhibitors used were unable to penetrate the tissue and have an effect on viral lytic gene induction. The concentrations of histone demethylase inhibitors were higher than previously used to inhibit full HSV reactivation in primary neuronal models (Cliffe et al., 2015; Cuddy et al., 2020). We have shown that OG-L002 can inhibit forskolin mediated reactivation at 30 μM, here we used 60 μM. Similarly, we have shown that GSK-J4 can inhibit both forskolin and LY294002 induced reactivation at 3 μM; here we used it at 20 μM. Therefore, we think it unlikely that the concentrations used were too low to inhibit the histone demethylases. Experiments using higher concentrations of both GSK-J4 and OG-L002 were performed (at 60 μm and 150 μm respectively). However, these higher concentrations resulted in decreased viral genome copy number at 5h compared to latency. Because there is no detectable viral DNA replication at this time point, this indicates neuronal loss and therefore neuronal toxicity at higher concentrations.

This study demonstrates Phase I of reactivation occurs from ganglia explanted from latently infected mice. Unlike previous *in vitro* studies, we found that Phase I of reactivation in intact neurons *in vitro*, *ex vivo* had enhanced kinetics of lytic gene induction in response to axotomy and PI3-kinase stimulation. We observed this enhanced phenotype in both sensory and sympathetic ganglia. Therefore, we posit that the most likely explanation of the difference in reactivation kinetics between *in vitro* and *ex vivo* studies is the combined trigger of axotomy and PI3-kinase inhibition. It has previously been demonstrated that when nerve growth factor deprivation is paired with axotomy,

treated neurons undergo cell death more rapidly than untreated neurons. (Fletcher et al., 2000). In addition, both PI3-kinase inhibition and axotomy result in activation of DLK (Tedeschi & Bradke, 2013; Wu et al., 2015). However, there are some differences in how DLK is activated and the resulting downstream response following the two stimuli. Upon axotomy, DLK is rapidly activated at the proximal segment of the severed axon in response to loss of cytoplasmic integrity. A resulting calcium influx from cytoplasmic membrane rupture leads to DLK-dependent transcription of genes involved in axon regeneration (Asghari Adib et al., 2018). The exact mechanisms of DLK activation upon loss of NGF signaling that mediates neuronal cell death or axon pruning is not fully understood. However, it is known that in response to NGF deprivation, DLK protein levels are stabilized, DLK is phosphorylated (Huntwork-Rodriguez et al., 2013), and this phosphorylation results in the downstream activation of JNK, c-Jun, and other transcription factors. The activation of these transcription factors promotes the expression of pro-apoptotic genes (Watkins et al., 2013), although in mature neurons there are multiple brakes downstream that prevent apoptosis (Kole et al., 2013). It is therefore conceivable that these two independent pathways to DLK activation may converge following the dual trigger of axotomy/PI3-kinase inhibition to result in more rapid and robust DLK activation and HSV reactivation.

Consistent with cellular pathways converging the enhance DLK activity, we observed a robust induction of lytic gene expression at 5h post reactivation. For the IE gene ICP27 this was an approximate 100-fold induction, compared to

the 5-20-fold increase often observed in an *in vitro* mouse model with PI3-kinase inhibition (Cliffe et al., 2015). The use of an *ex vivo* model system will therefore be incredibly powerful for studying the mechanisms of gene expression that occur during Phase I. We have previously observed a histone methyl/phospho switch on lytic promoters during Phase I reactivation (Cliffe et al., 2015), which permits lytic gene expression independently of recruitment of histone demethylase enzymes. There is evidence that the methyl/phospho switch permits gene expression because repressive histone readers (for example HP1) are no longer capable of interacting with the methylated residue on histone H3K9 because phosphorylation at Serine 10 occludes binding (Fischle et al., 2005; Fischle et al., 2003). Because of the robust lytic gene induction *ex vivo*, and because we have now shown that the gene expression both *in vitro* and *ex vivo* is DLK-dependent and histone demethylase independent, the complementary models can now be used answer key questions on the mechanism of viral lytic gene induction during Phase I reactivation.

# Human Sensory Neuron Model of Herpes Simplex Virus Latency and Reactivation

## Abstract

Herpes Simplex Virus-1 (HSV-1) infection in North American has become more prevalent at genital sites where the virus latently infects neurons of the dorsal root ganglia. Reactivation from this site results in painful lesions, sexual transmission, and an enhanced risk of transmission to neonates. There are currently no therapies that target the latent or reactivation stage of HSV-1 infection. Easily scalable human sensory neuron models of HSV-1 latency and reactivation are required to develop new therapies that can prevent HSV-1 reactivation. Here we use our expertise to develop and characterize a model of HSV-1 latency in human sensory neurons differentiated from a cell line derived from the dorsal root ganglion (HD10.6). We demonstrated the ability to establish latency in this system and trigger reactivation using a combination of physiologically relevant stimuli. Next, we identified the types of sensory neurons produced in the system and determined the neurotrophins required for optimal culturing. We also confirm this model does not require antiviral drugs to promote latency establishment. Overall, this study addresses key gaps in the field of alpha herpesviruses by fully characterizing a human sensory neuron model of latency and reactivation.

## Introduction

Herpes Simplex Virus type 1 (HSV-1) is a ubiquitous human pathogen that persists for life. Currently, over 65% of the population of the United States is infected with HSV-1 (James et al., 2020). In non-neuronal cells like fibroblasts and keratinocytes, HSV-1 undergoes lytic or productive reproduction. During lytic replication, the virus expresses more than 70 lytic genes and new virus is produced that can spread to infect other cells. Following initial infection of an individual, the virus also infects neurons in peripheral ganglia where the virus establishes a persistent latent infection. Latent infection is distinguished from productive replication by restricted expression of viral lytic genes, transcription of the latency associated transcript (LAT), and no infectious virus production. In response to certain stimuli, reactivation is triggered, expression of viral genes is re-initiated, and new infectious virus is produced. Importantly, reactivation of HSV-1 from a latent infection is associated with disease and can also result in transmission (Knipe & Howley, 2013).

HSV-1 infects neurons located in peripheral ganglia. These include sensory ganglia, trigeminal ganglia (TG), dorsal root ganglia (DRG), sympathetic ganglia and superior cervical ganglia (SCG). To date, most latency and reactivation studies have been conducted in rodent neurons both *in vivo* and *in vitro*. *In vitro* models are useful to investigate the direct interaction between the virus and the infected neuron. Neurons in culture are also more readily genetically manipulated to investigate the role of host and viral proteins on the

latency and reactivation cycle. Although primary neurons isolated from animals have the advantage of being *bona fide* neurons that have undergone differentiation and maturation *in vivo*, murine neurons are not derived from the natural host species and the number of neurons that can be isolated from mice or rats is small, restricting the range of techniques that can be employed and necessitating the use of large numbers of animals for certain experiments (Suzich & Cliffe, 2018). Therefore, models using human neurons that can also easily be scaled up are required to complement primary neuronal systems.

Our lab has built upon the neuronal model of HSV-1 latency in immortalized human DRG cells (HD10.6 cells). This is the only human sensory neuron cell line available, making it the most relevant to HSV-1 infection. Most neurons are post-mitotic, limiting *in vitro* culturing. HD10.6 cells can proliferate and be passaged due to a tetracycline (off) regulated *v-myc* oncogene. Therefore, in the absence of doxycycline, the neurons remain in a neuronal progenitor state and divide. When doxycycline is added, HD10.6 cells differentiate and exhibit neuronal phenotypes (Raymon et al., 1999) (Thellman et al., 2017).

We propose that HD10.6 cells provide an effective and scalable human model for studying HSV-1 latency and reactivation. Using HD10.6 cells, we were able to establish a latent infection and induce reactivation using physiologically relevant triggers. We also propose a simplified culturing protocol that could potentially reduce costs and lead to the differentiation of distinct neuronal subtypes. Finally, we were able to establish latency and trigger reactivation

without the use of antiviral drugs. Many *in vitro* models of HSV-1 latency rely on the viral DNA replication inhibitor acyclovir (ACV) to promote a latent infection (Chen et al., 2022; Edwards & Bloom, 2019; Thellman et al., 2017). Using Stayput GFP, a virus lacking gH that prevents viral propagation and superinfection during latency establishment (Dochnal et al., 2022), we successfully established and reactivated latent infections in HD10.6 cells without the need for ACV. By combining these advances, our study provides a robust platform for investigating HSV-1 latency and offers novel insights into pathways that may be targeted to limit viral reactivation.

## Results

### HD10.6 cell latency establishment and reactivation with physiological triggers.

With the addition of doxycycline, HD10.6 cells differentiate to have characteristics of sensory neurons, consistent with previous findings (Thellman et al., 2017). To induce this maturation, HD10.6 cells were seeded onto cell culture plates with glass coverslips coated with poly-L-ornithine (PLO) and fibronectin in maturation media. After 24 hours, the *v-myc* oncogene was inhibited with the addition maturation media containing doxycycline, for a final concentration of 1 µg/ml doxycycline. HD10.6 cells were then cultured for 10 days as cells differentiated (Supplemental Figure 5.1A). Before the addition of doxycycline, HD10.6 cells were oval and did not have axon-like protrusions. By 5 days post differentiation axons are visible and by 10 days post differentiation a complex axonal network is visible (Supplemental Figure 5.1B). We used

immunofluorescence to stain HD10.6 cells at 10 days post differentiation and observed the cells stained for the neuronal markers βIII-tubulin, peripherin, and NeuN (Supplemental Figure 5.1C).

Reactivation of HSV from its latent state within host neurons is a complex process influenced by multiple triggers and cellular stress pathways. Pathways that have been shown to induce reactivation include the loss of neurotrophic factor support (Cliffe et al., 2015; Kim et al., 2012; Wilcox & Johnson, 1987; Yanez et al., 2017), increased neuronal hyperexcitability (Cuddy et al., 2020), DNA damage repair pathway activation (Hu et al., 2019), and exposure to glucocorticoids and corticosteroids (Cliffe et al., 2015). Previous studies successfully triggered HD10.6 cell reactivation by superinfection (Thellman et al., 2017) or with the histone deacetylase inhibitor TSA (Chen et al., 2022). Here, we reactivated HD10.6 cells with physiological triggers previously used in murine *in vitro* cultures. Ten days after differentiation, neurons were pre-treated with 100 μM of acyclovir (ACV) before being infected with Stayput GFP (MOI 2 PFU/cell). Stayput GFP expresses a Us11-GFP and is also defective in cell-to-cell spread, therefore permitting the quantification of individual reactivating neurons (Dochnal et al., 2022). HD10.6 cells were infected using acyclovir (ACV), as previously described (Thellman et al., 2017), to establish a latent infection. Five days after infection, once latency was established, ACV was washed out (Figure 5.1A). Before the addition of reactivation triggers, GFP positive neurons were rare, indicating a silent latent infection (Figure 5.1B). Two days after ACV was

removed, reactivation was initiated using physiological triggers such as LY294002 (PI3K inhibitor), forskolin, and heat stress. Previously, our lab demonstrated that combining physiological triggers resulted in more robust reactivation (Dochnal et al., 2022). The “triple trigger” is a combination of PI3K inhibition (mimicking neurotrophic factor support), inducing neuronal hyperexcitability (forskolin), and heat stress. This combination trigger was used to induce reactivation of latently infected HD10.6 cells. All the triggers used significantly induced reactivation (Figure 5.1C). The triple trigger resulted in the highest number of GFP positive neurons and so we chose to use this as the trigger for the remainder of our studies.

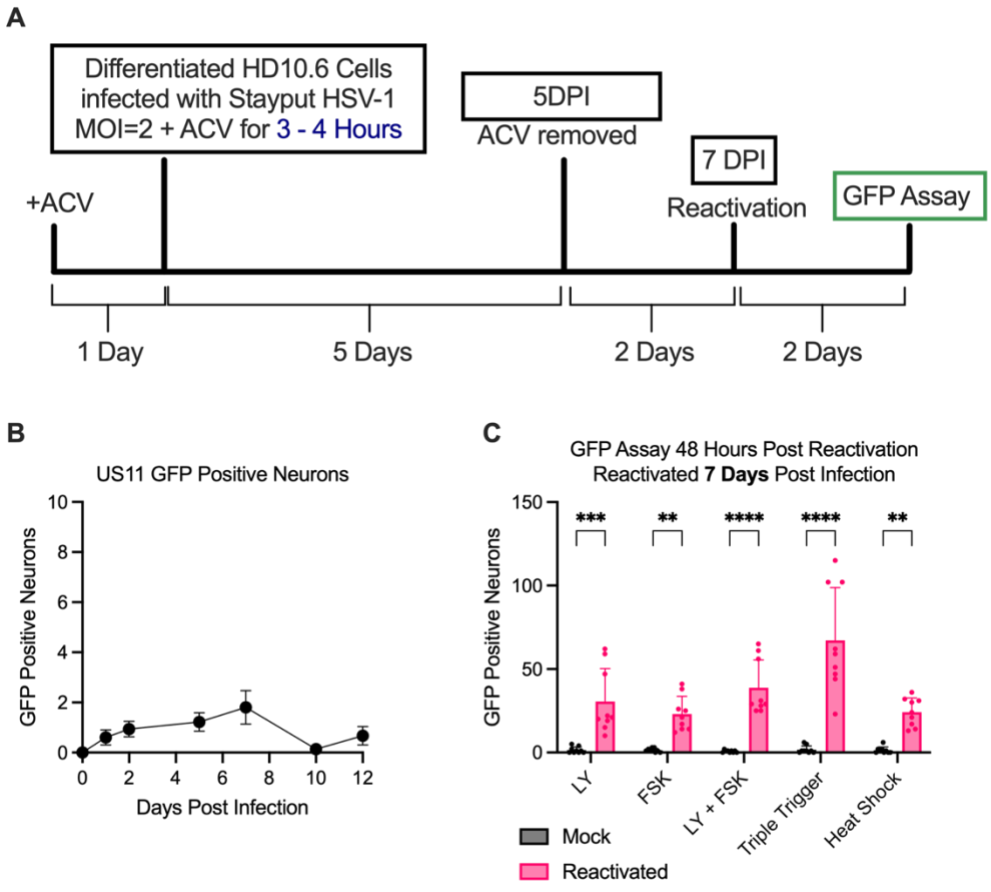

**Figure 5.1: HD10.6 cell latency establishment and reactivation with physiological triggers.**
**(A)** Timeline of HSV-1 latency and reactivation model. Acyclovir (100uM) was added to differentiated HD10.6 cells 18 hours before infection with Stayput-GFP at a MOI 2 PFU/cell. HD10.6 cells were cultured with ACV to promote latency establishment and was removed at 5 DPI. At 7DPI, cells were reactivated with LY294002 (20 μM), Forskolin (60 μM), LY294002+Forskolin, Triple trigger (LY294002, Forskolin, and heat shock), or heat shock (incubation at 43 C for 3 hours). GFP assays were conducted 48 hours post-reactivation. **(B)** Quantification of latency establishment based on GFP-positive over time after infection. **(C)** Quantification of HSV-1 reactivation based on the numbers of Us11-GFP positive neurons at 2 days post reactivation. N = 9 biological replicates from 3 experimental replicates. Significance was determined using a two way ANOVA with Šídák's multiple comparisons test. (ns not significant, *≤ 0.05, **≤ 0.01, ***≤ 0.001, ****≤ 0.0001). One replicate from experiment in Panels A-D was performed by Shrisha Poonuganti. One replicate from experiment in Panels A-D was performed by Richard Wyate Bond.

## Differentiation of HD10.6 cells in pooled neurotrophins or NGF only media results in differential neurotrophin receptor expression.

The establishment of latency and subsequent reactivation of HSV-1 is impacted by the characteristics of the neuron infected. There have been numerous studies demonstrating that certain neuronal subtypes infected with HSV-1 are more likely undergo productive lytic gene expression (Margolis,1992 Yang, 2000), express the LAT (Margolis 1992 Margolis 2006 Yang 2000) (Imai et al., 2009), or reactivate (Leib 2018). Yet the mechanism of this heterogeneity is still not well understood. Previously, HD10.6 cells were differentiated in the presence of a pool of neurotrophins, including nerve growth factor (NGF), brain-derived neurotrophic factor (BDNF), glial cell-line derived neurotrophic factor (GDNF), and neurotrophin-3 (NT-3) (Thellman et al., 2017). The neurons generated using this protocol express TrkA, TrkB, Ret, and TrkC, which are the

respective receptors for the neurotrophins listed above (Dalton et al., 2020). Aδ neurons make up the largest percentage of nociceptor neurons with high TrkA expression (Fang et al., 2005). In this study, we decided to differentiate neurons in either Pooled neurotrophins or in a simplified media with NGF-only (excluding BDNF, GDNF, and NT-3). We hypothesized that this may promote TrkA+ neurons, allowing us to study a specific subtype of neurons that have been shown to have increased LAT expression and reactivation (Leib 2018). When we differentiated neurons in NGF only media we found that there was no difference in TrkA (Figure 5.2A), TrkB (Figure 5.2B), or RET expression (Figure 5.2D). Surprisingly, we found there was a significant increase in TrkC expression in NGF only neurons (Figure 5.2C). We determined that HD10.6 cells can be maintained in simplified neurotrophin conditions, and that receptor expression varies depending on the specific neurotrophin present.

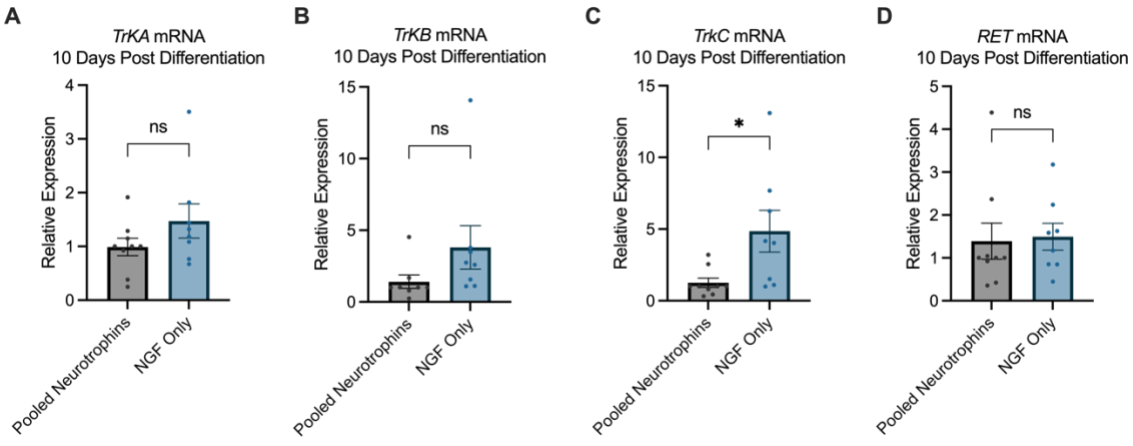

**Figure 5.2: Differentiation of HD10.6 cells in pooled neurotrophins or NGF only media results in differential neurotrophin receptor expression.** HD10.6 cells were seeded in maturation media supplemented with NGF, NT3, CNT3, and GDNF neuronal growth factors (as described in Figure 5.1) or media supplemented with only NGF. **(A-E)** RT-qPCR was used to quantify TrKA (A), TrkB (B), TrkC (C) or RET (D) mRNA 10 days post differentiation. Significance was determined using a paired t-test (B), Wilcoxon test (C), Wilcoxon test (D), and paired t-test (E). Error bars: SEM) N=9 biological replicates from 3 independent experiments. (ns not significant, *≤ 0.05, **≤ 0.01, ***≤ 0.001, ****≤ 0.0001). One replicate from experiment in Panels A-D was performed by Shrisha Poonuganti. One replicate from experiment in Panels A-D was performed by Richard Wyate Bond.

## Latency and reactivation of HSV-1 in HD10.6 cells are influenced by neurotrophin culturing conditions

Since we successfully differentiated neurons with distinct characteristics, we aimed to investigate whether these cultures exhibited differences in reactivation. HD10.6 cells cultured in pooled neurotrophins or NGF-only media were infected with HSV-1 Us11-GFP as described in Figure 5.1. GFP-positive neurons were monitored to confirm latency establishment in both conditions and we found that latency persisted even after ACV removal (Figure 5.3A). Reactivation was triggered using the triple trigger and was quantified by counting Us11-GFP+ cells. To ensure that culturing conditions did not impact initial infection efficiency, viral genome copy numbers were measured at latency. We found there was no significant difference in latent viral genomes between HD10.6 cells cultured in pooled neurotrophins or NGF-only media (Figure 5.3B). We also found there were no changes in LAT expression, as dd-qPCR on latent samples showed only a trend in decreased LAT in NGF only HD10.6 cells (Figure 5.3C).

When we reactivated these samples at 7 days post-infection, we observed robust reactivation in both pooled and NGF-only conditions. At this time point we also found no significant difference in reactivation between the conditions.

Previous reports indicate that HSV-1 latency becomes more silent and restrictive against reactivation as the length of latency increases (S. A. Dochnal et al., 2022). We find that in our HD10.6 latency model, HSV-1 reactivation significantly decreases when triggered at increasing days post-infection (Supplemental Figure 5.4). Although we found no significant difference in HSV-1 reactivation between pooled neurotrophins and NGF only conditions when we reactivated these samples at 7 days post-infection (Figure 5.3D), when we reactivated at 10 days post-infection, we observed significantly less reactivation in HD10.6 cells cultured in NGF-only media (Figure 5.3F). This indicates reactivation was restricted in NGF-only media conditions.

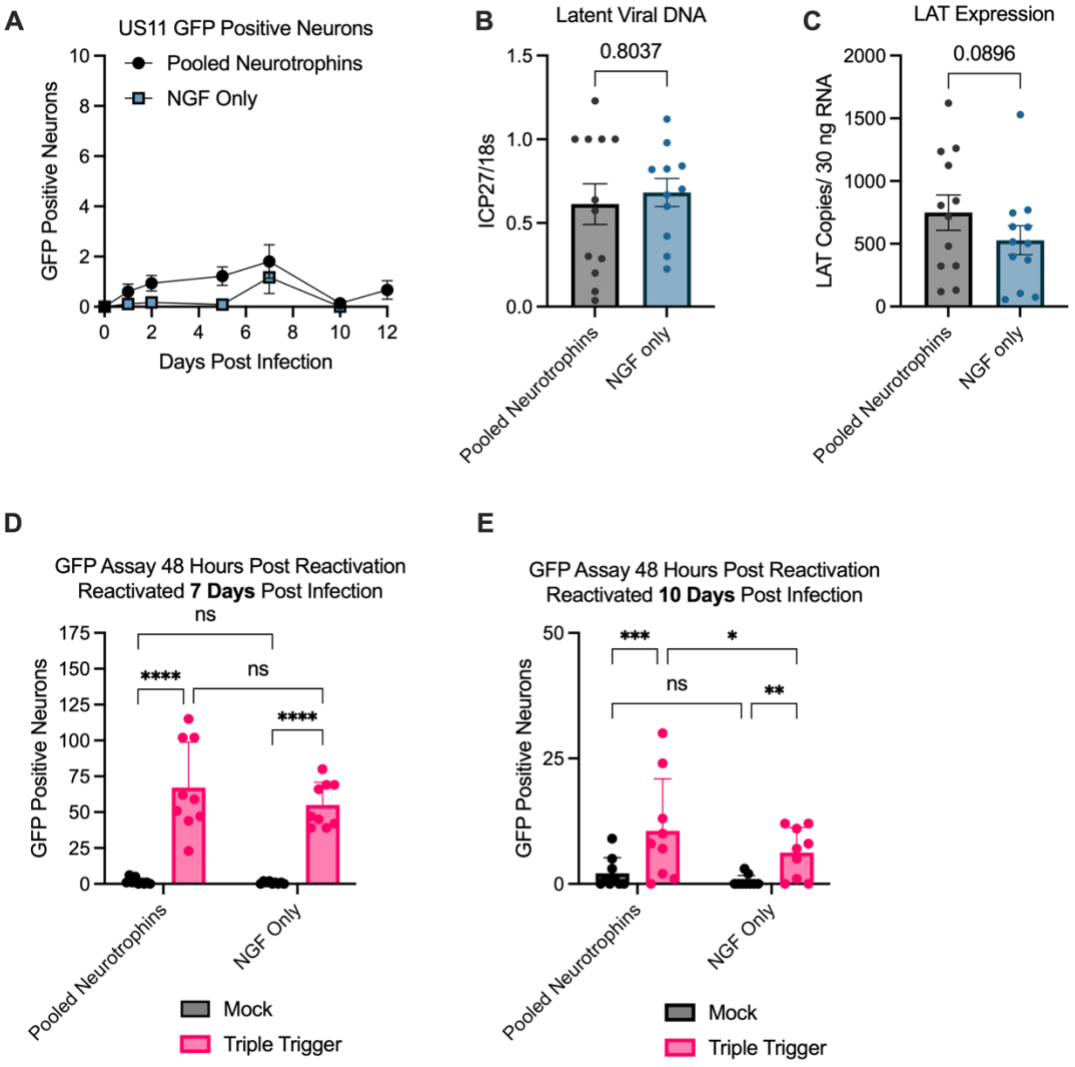
A
US11 GFP Positive Neurons
Pooled Neurotrophins
NGF Only
GFP Positive Neurons
Days Post Infection
B
Latent Viral DNA
0.8037
ICP27/18s
Pooled Neurotrophins
NGF only
C
LAT Expression
0.0896
LAT Copies/ 30 ng RNA
Pooled Neurotrophins
NGF only
D
GFP Assay 48 Hours Post Reactivation
Reactivated 7 Days Post Infection
ns
****
ns
****
GFP Positive Neurons
Pooled Neurotrophins
NGF Only
Mock
Triple Trigger
E
GFP Assay 48 Hours Post Reactivation
Reactivated 10 Days Post Infection
***
*
ns
**
GFP Positive Neurons
Pooled Neurotrophins
NGF Only
Mock
Triple Trigger

**Figure 5.3: Latency and reactivation of HSV-1 in HD10.6 cells are influenced by neurotrophin culturing conditions**
**(A)** Acyclovir (100uM) was added to HD10.6 cells cultured in pooled neurotrophins or NGF-only media 18 hours before infection. HD10.6 cells were infected with Stayput-GFP at a MOI 2 PFU/cell. HD10.6 cells were cultured with ACV to promote latency establishment and was removed at 5 DPI. Quantification of latency establishment based on GFP-positive over time after infection. N = 15 biological replicates from 5 experimental replicates. **(B)** Latently infected HD10.6 cells cultured in pooled neurotrophins or NGF-only media were collected at 10 days post-infection. RT-qPCR was used to quantify viral DNA using the immediate-early protein ICP27. N = 12 biological replicates from 4 experimental replicates. **(C)** Latently infected HD10.6 cells cultured in pooled neurotrophins or NGF-only media were collected at 10 days post-infection. dd-PCR was used to quantify LAT transcripts. N = 12 biological replicates from 4 experimental replicates.
**(D & E)** Quantification of HSV-1 reactivation in HD10.6 cells cultured in pooled neurotrophins or NGF-only media based on the numbers of Us11-GFP positive neurons at 48 hours after the addition of triple trigger, consisting of LY924002, Forskolin, and heat shock. Reactivation was triggered at 7 days post-infection (D) or 10 days post-infection (E). N = 9 biological replicates from 3 experimental replicates. Significance was determined using a paired t-test (B, C) or a 2-way ANOVA (D, E). (ns not significant, *≤ 0.05, **≤ 0.01, ***≤ 0.001, ****≤ 0.0001). One replicate from experiment in Panel A, two replicates from experiments in Panel B & C, one replicate from Panel D, and two replicates from experiment in Panel E were performed by Shrisha Poonuganti. One replicate from experiment in Panel A, two replicates from experiments in Panel B & C, two replicates from Panel D, and one replicate from experiment in Panel E were performed by Richard Wyate Bond.

## Stayput-GFP can be used to create a quiescence model in the absence of viral DNA replication inhibitors in HD10.6 cells

When neurons are infected *in vitro* with wild type virus in the absence of acyclovir, the virus undergoes lytic infection, producing new virus. The new virus produced superinfects neuronal cultures inhibiting the establishment of latent infection. This problem can be circumvented with the use of Stayput-GFP, which lacks glycoprotein gH and cannot spread from cell to cell (Dochnal et al., 2022).

Therefore, we set out to establish a model of latency establishment in HD10.6 cells without the use of DNA replication inhibitors. HD10.6 cells were infected at an MOI of 1 PFU/cell and the number of GFP-positive neurons were measured over time after infection (Figure 5.4A). The largest population of GFP positive cells was about 2,000 cells which were detectable at 2 days post-infection. There are about 100,000 neurons per well, meaning about 2% of cells became GFP-positive. This number then decreased over time until 12 days postinfection (Figure 5.4B) when no living GFP positive neurons were detectable. Over time, GFP positive neurons stain positive for cell death marker SYTOX Orange (Figure 5.4C), suggesting that lytically infected cells die. SYTOX+ neurons were not counted towards GFP assays measuring latency establishment or reactivation. A significant increase in GFP positive neurons was detected in cultures reactivated using the triple trigger. These data demonstrate that Stayput-GFP can be used to establish latency in the absence of acyclovir.

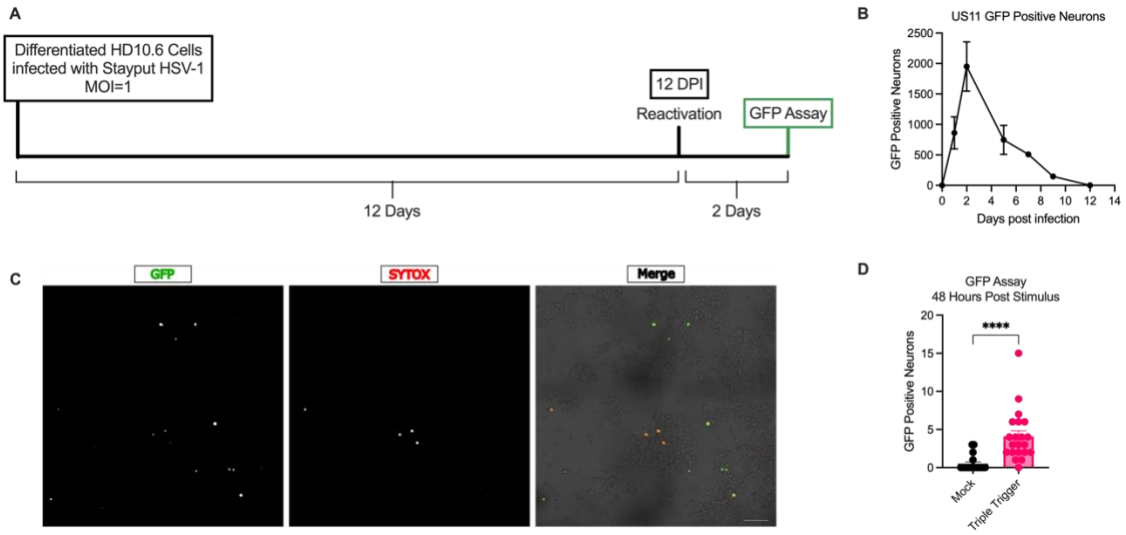

**Figure 5.4: Stayput-GFP can be used to create a quiescence model in the absence of viral DNA replication inhibitors in HD10.6 cells.**
**(A)** The latency and reactivation model scheme. HD10.6 cells cultured in NGF-only media were infected with Stayput-GFP at an MOI of 1 PFU/cell in the absence of ACV. HD10.6 cell cultures were reactivated at 12 DPI. **(B)** Quantification of latency establishment based on GFP-positive neurons over time after infection. N = 9 biological replicates from 3 experimental replicates. **(C)** Visualization of GFP- and SYTOX Orange-positive neurons using same field of view over time after infection. **(D)** Quantification of GFP-positive neurons at 48-hours after the addition of triple trigger, consisting of LY924002 (20μM), Forskolin (60μM) and Heat shock. N = 21 biological replicates from 5 experimental replicates. Significance was determined by the Mann-Whitney test. (ns not significant, *≤ 0.05, **≤ 0.01, ***≤ 0.001, ****≤ 0.0001). One replicate from experiment in Panel B and two replicates from experiment in Panel D were performed by Shrisha Poonuganti. One replicate from experiment in Panel B and two replicates from experiment in Panel D were performed by Richard Wyate Bond.

## HSV-1 reactivation in HD10.6 cells results in cell-to-cell spread

The Stayput GFP model of reactivation offers the advantage of quantifying reactivation specifically in neurons where it occurs, without the confounding effects of superinfection, and enabling the establishment of latency without the use of antivirals. However, full reactivation is defined by the production of infectious virus. Since the virus generated during reactivation in the figures above would lack gH, it cannot be assessed using a plaque assay to measure infectious virus production. Therefore, to validate our reactivation findings in the Stayput model, where reactivation is quantified by counting GFP-positive neurons, we sought to quantify infectious virus production in a model where virus generated post-reactivation would be infectious. HD10.6 cells were infected with 2 PFU/cell

with HSV-1 Patton strain US-11 GFP (Figure 5.5A). Once latency was established (Figure 5.5B), cells were reactivated using the triple trigger. Based on our data that the triple trigger can be used to robustly induce reactivation, we investigated whether reactivation resulted in the production of infectious virus, measured by cell-to-cell spread. We found that over time the number of GFP-positive neurons in culture increased (Figure 5.5C & 5.5D). These findings suggest that reactivation results in virus production that can spread to surrounding cells.

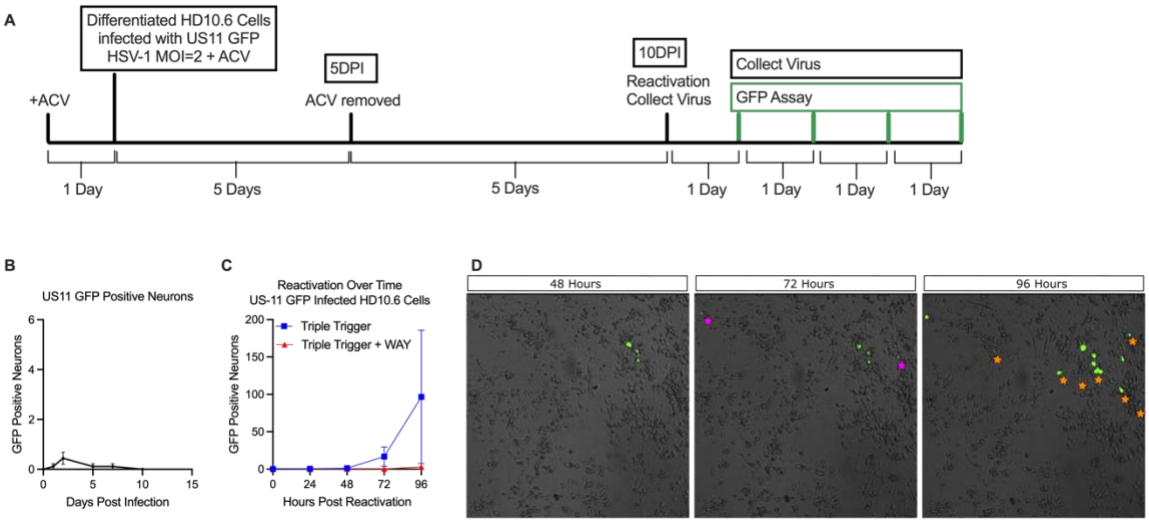

**Figure 5.5: HSV-1 reactivation in HD10.6 cells results in cell-to-cell spread.** **(A)** Acyclovir (100uM) was added to HD10.6 cells cultured in NGF-only media 18 hours before infection. HD10.6 cells were infected with wildtype Patton US-11 GFP HSV-1 at an MOI of 2 PFU/cell. HD10.6 cells were cultured with ACV to promote latency establishment and was removed at 5 DPI. GFP assays were performed at 0-, 24-, 48-, and 96-hours post-reactivation. **(B)** Quantification of latency establishment based on GFP-positive neurons over time after infection. N = 9 biological replicates from 3 experimental replicates. **(C)** Quantification of HSV-1 reactivation in HD10.6 cells based on GFP-positive neurons over time after the addition of triple trigger consisting of LY924002 (20μM), Forskolin (60μM), and Heat shock, with and without protein WAY (5μM). N = 11 biological replicates from 4 experimental replicates. **(D)** Visualization of GFP positive neurons 48, 72, and 96 hours post-infection. The same field of view over time after reactivation. Purple stars in 72-hour panel indicate new GFP positive neurons as compared to 48-hour panel. Orange stars in 96-hour panel indicate new GFP positive neurons as compared to 72-hour panel. One replicate from experiment in Panel B and two replicates from experiment in Panel C were performed by Shrisha Poonuganti. One replicate from experiment in Panel B and two replicates from experiment in Panel C were performed by Richard Wyate Bond.

## Discussion

There are currently no approved therapies that target the latent or reactivation stage of HSV-1 infection. In addition, there is increased viral resistance to current therapeutics along with toxicity associated with their use (Lv et al., 2024). Therefore, new therapies are required that can prevent HSV-1 reactivation. However, to develop new therapies, we need a better understanding of the molecular basis of HSV-1 latency and reactivation. Because HSV-1 establishes latency in neurons, developing model systems has been a challenge. Current models largely rely on murine primary neurons. Although these models are informative, they have limitations because they are not easily scalable and are not of the same host species as intended therapies (Suzich & Cliffe, 2018). Here we demonstrate that HD10.6 cells can be used to model HSV-1 latency and reactivation in a scalable, sensory human neuron cell type.

The establishment of latency and subsequent reactivation of HSV-1 is impacted by the characteristics of the neuron infected. Sensory neurons located in peripheral ganglia are diverse, with differences in morphology, responses to stimuli, surface receptors, presence of neurofilaments, glycans, etc. Distinct neuronal subtypes infected with HSV-1 are more likely undergo productive lytic gene expression (Margolis,1992 Yang, 2000), express the LAT (Margolis 1992 Margolis 2006 Yang 2000) (Imai et al., 2009), or reactivate (Leib 2018). Aδ neurons function in mechano/nociception and are found in the DRG and TG. They end with free nerve endings (FNE) to allow for detection of stimuli.

Furthermore, Aδ neurons are myelinated with neurofilaments (NefH), stain positive for calcitonin gene-related peptide α (CGRP), and possess the glycan Galβ1-4GlcNAc-R (stained by the A5 antibody) in 90% of instances (Cabrera et al., 2018). These features have been used to characterize the heterogeneous nature of HSV-1. A5+ (Yang 2000) and Aδ (NefH+ and CGRP+) neurons (Cabrera et al., 2018) have the highest expression of the LAT. Although LAT expression is often used as a marker for latency, LAT expression can be heterogeneous in latently infected cells with only 30% of latent neurons having detectable LAT expression (Mehata 1995, Chen 2002). When reactivated with axotomy and TSA, reactivation was different based on NefH and CGRP expression. Intriguingly, reactivation was highest in NefH-CGFP- (primarily stained by KH10 antibody [Galα1-3Galβ1-4NAc-R epitopes]) and NefH+CGFP+ (primarily stained by A5 antibody). This is interesting as previous studies suggest LAT expression is low in KH10+ neurons (Yang 2000), demonstrating that, in these studies, LAT expression and reactivation competency may not correlate. From these studies we can concluded that HSV-1 dynamics are heterogenous and impacted by the diversity of neurons located within the peripheral ganglia. Yet, the mechanism of this heterogeneity is still not well understood. By culturing HD10.6 cells in different neuronal subtypes we were able to modulate neuronal subtype, bringing us closer to a system where we can culture specific DRG subtypes and test what makes HSV-1 more likely to reactivate.

HD10.6 cells are classically cultured with neuronal growth factor (NGF), neurotrophin-3 (NT-3), glial cell-line derived neurotrophic factor (GDNF), and

ciliary neurotrophic factor (CNTF). Previous studies have observed that under these conditions HD10.6 cells co-express multiple neurotrophin receptors including TrkA, TrkB, TrkC, and RET (Thellman et al., 2017). During development, axonal innervation and survival are determined by secreted neurotrophins. In particular, NGF signaling binds to TrkA, resulting in survival signals and increased TrkA expression (Deppmann et al., 2008). Since Aδ neurons exhibit high TrkA expression along with elevated LAT expression and reactivation, we chose to differentiate HD10.6 cells using only NGF. We hypothesized that these culturing conditions would select for TrkA+ neurons and result in increased TrkA expression. We were surprised when there was no difference in TrkA expression. Previous studies have demonstrated that over saturating developing neurons with excessive NGF does not result in increased TrkA expression (Deppmann et al., 2008). Future research should differentiate HD10.6 cells using a lower NGF concentration and evaluate how these culture conditions impact TrkA expression.

LAT expression varies among different neuronal subtypes within latently infected ganglia (Margolis 1992 Margolis 2006 Yang 2000) (Imai et al., 2009). To quantify LAT expression in our latently infected HD10.6 cells, we used ddPCR, comparing cells cultured with either pooled neurotrophins or NGF alone. There was detectable LAT expression in both conditions. The copies of LAT per nanogram of RNA in pooled (average of 25 copies/ng) or NGF only (average of 17.6 copies/ng) were less than, but comparable in scale to experiments where we have used ddPCR to quantify LAT expression in latently infected trigeminal

ganglia (average of 148.4 copies/ng). While no significant difference was observed between the two culturing conditions, LAT expression showed a trending increase in the pooled neurotrophins group. Further investigation into this potential correlation is required as the pooled neurotrophins condition had significantly enhanced reactivation at 10 days post-infection. Since ddPCR measures bulk gene expression from pool of infected cells it does not capture heterogeneity between cells. Determining what cells have increased LAT expression by RNA FISH may be useful to determine if this correlates with the neuronal subtypes more likely to reactivate.

From this work we have shown that HSV-1 latency can be established in cells with neuronal characteristics from human dorsal root ganglia. Importantly, latency can be established in the absence of acyclovir, more similarly modeling clinical infection. The Stayput-GFP virus was essential in developing this model, which would otherwise require DNA replication inhibitors to promote latency establishment, as lytic replication during the initial infection would lead to superinfection. Additionally, the GFP tag allows us to quantify latency establishment over time and determine when our cultures our silent. Silent HD10.6 cultures retain the capacity to reactivate with physiologically relevant triggers.

Reactivation is traditionally defined by the production of infectious virus. Because Stayput-GFP is a gH-null virus, *de novo* virus is noninfectious which prevents us from quantifying virus production by plaque assay. We are still working to demonstrate that this model results in the production of infectious

virus using a virus that is not gH null. So far, we have shown that latency can be established with this virus and that latent cultures are reactivation competent. When reactivation is measured over time, GFP positive neurons appear at 48 hours. At 72 and 96 hours the number of GFP+ neurons surrounding the original GFP+ neuron increases, suggesting that new virus is made and spreading to nearby cells. We will confirm that new infectious virus is produced after reactivation by plaque assay in the future.

The HD10.6 HSV-1 latency and reactivation model provides a valuable platform for studying the cellular factors necessary for differentiating different neuronal subtypes and investigating the molecular pathways involved in HSV-1 reactivation within a human neuronal system. Identifying the key factors necessary for HSV reactivation, particularly in human neurons, will inform the development of novel therapeutics. Additionally, this system could also be used to study other neurotropic viruses including HSV-2 and varicella-zoster virus (VZV).

## Supplemental Figures

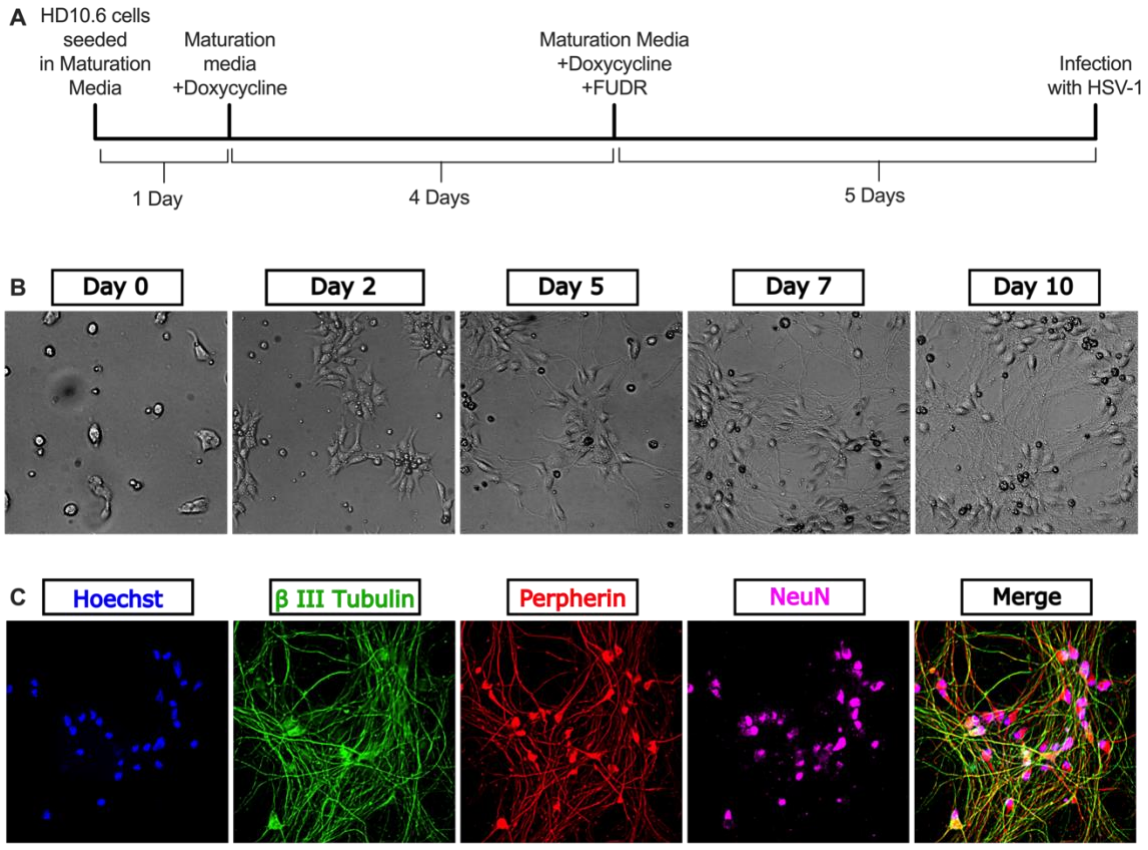


**Supplemental Figure 5.1: Differentiation timeline and immunofluorescence staining of HD10.6 cells**
**(A)** Differentiation timeline for HD10.6 cells. HD10.6 cells were seeded in maturation media supplemented with NGF, NT3, CNT3, and GDNF neuronal growth factors. Doxycycline was added to induce differentiation. To inhibit cell division and prohibit differentiation, 5-fluorodeoxyuridine (FUDR) was added at 4 days post differentiation. **(B)** Images were taken 0, 2, 5, 7, and 10 days displaying the progression of differentiation of HD10.6 cells. **(C)** Immunofluorescence staining of HD10.6 cells at ten days post differentiation. Immunofluorescence was carried out for markers of neuronal differentiation β III Tubulin (Green), Peripherin (Red), and NeuN (Magenta). Cells were co-stained with Hoechst.

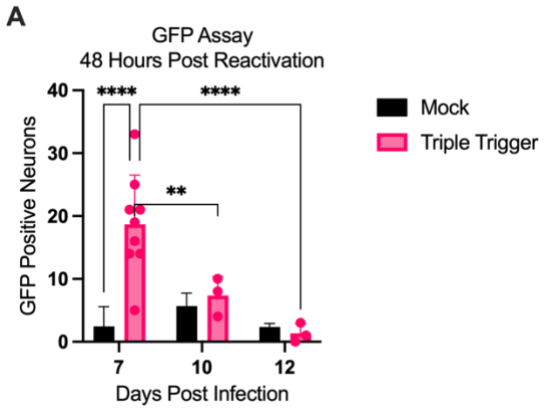


**Supplemental Figure 5.5: Strength of HSV-1 reactivation of in HD10.6 cells is influenced by the number of days post-infection when reactivation is triggered.**

**(A)** HD10.6 cells cultured in NGF-only media were infected with Stayput-GFP at an MOI of 2 PFU/cell. HD10.6 cells were cultured with ACV to promote latency establishment and was removed at 5 DPI. Reactivation triggers were added to HD10.6 cell cultures at 7 DPI, 10 DPI, or 12 DPI. Quantification of HSV-1 reactivation in HD10.6 cells based on GFP-positive neurons at 48-hours after the addition of triple trigger consisting of LY924002 (20μM), Forskolin (60μM), and Heat shock.

N = 9 biological replicates from 3 experimental replicates. Significance was determined using a 2-way ANOVA test. (ns not significant, *≤ 0.05, **≤ 0.01, ***≤ 0.001, ****≤ 0.0001). One replicate of experiments in Panel A and B were performed by Shrisha Poonuganti. One replicate of experiments in Panel A and B were performed by Richard Wyate Bond.

# Conclusions and Future Directions

Over hundreds of millions of years, herpes simplex virus 1 (HSV-1) has evolved with humans and their ancestors, resulting in a highly evolved, intertwined relationship between virus and host (Wertheim et al., 2014). HSV-1 establishes a lifelong latent infection in neurons of the peripheral nervous system (Knipe & Howley, 2013). Neurons are a long-lived cell type, providing the virus with a latent reservoir in which it can persist for extended periods while evading the immune system until reactivation, when new infectious viral particles are produced and can be spread to a new host. During latency, viral DNA is silenced and associates with host histones that can be post-translationally modified (Cliffe et al., 2009; Kwiatkowski et al., 2009; Nicoll et al., 2016; Wang et al., 2005) to likely limit transcription of viral genes. Therefore, during latency viral protein synthesis is undetectable, meaning that reactivation is initiated in the absence of viral protein. Instead, HSV-1 has evolved to co-opt host signaling pathways and transcriptional machinery to re-start viral gene expression (Cuddy & Cliffe, 2023; Krakowiak et al., 2025; Suzich & Cliffe, 2018) .

Various stressors, such as NGF deprivation and neuronal hyperexcitability, signal through the DLK- and JNK- pathway to initiate HSV-1 reactivation (Cliffe et al., 2015; Cuddy et al., 2020; Dochnal et al., 2022). Building on previous studies, the work of this dissertation found that the combined triggers of NGF deprivation and axotomy caused HSV-1 reactivation *ex vivo* via DLK and JNK activation. Although DLK and JNK are activated in response to various HSV-1 triggers, Chapter 4 demonstrates that axotomy and PI3-kinase inhibition together result in enhanced kinetics of lytic gene induction compared to

reactivation induced by PI3-kinase inhibition alone. This is consistent with a previous study showing that the kinetics of the NGF-deprivation pathway are enhanced when performed on axotomized neurons (Tedeschi & Bradke, 2013; Wu et al., 2015). These findings suggest that while DLK and JNK activation occur in response to different stimuli, the specific pathways and kinetics of reactivation vary depending on the trigger. What factors are activated downstream of JNK to lead to early reactivation events is unknown.

Transcription of viral genes immediately following HSV-1 reactivation is distinct from viral transcription during the lytic cycle. During the lytic cycle, tegument proteins such as VP16 and ICP4 promote the expression of immediate early proteins. Immediate early proteins are required for the expression of early proteins, which in turn replicate viral DNA. It is only after viral DNA replication that late genes are expressed. As such, lytic gene expression occurs in an orderly sequence and is dependent on viral proteins (Knipe & Howley, 2013). Previous *in vitro* studies have demonstrated that reactivation is biphasic, with the first phase of reactivation including a burst of transcription of all viral gene classes (Kim et al., 2012) (Cliffe et al., 2015).

Since viral proteins are likely absent during reactivation, Phase I does not rely on the viral proteins essential for the lytic cycle but instead utilizes host proteins. We propose that, unlike lytic gene expression, where DNA replication is required for late gene expression (possibly because of DNA availability), a different mechanism facilitates the transcription of viral genes, as DNA replication is not required for late gene expression during Phase I (Cliffe et al., 2015; Cuddy

et al., 2020; Dochnal et al., 2022; Kim et al., 2012; Whitford et al., 2022). This is further supported by the observation that viral transcripts are expressed independently of histone demethylases during Phase I, in contrast to the lytic cycle, where histone demethylases are required for full lytic gene expression (Francois et al., 2024; Liang et al., 2009). Thus, we hypothesize that host proteins initiate a distinct transcriptional mechanism to enable Phase I of reactivation.

The mechanisms required for the initiation of Phase I transcription are not fully understood. We do know that JNK activity is required for Phase I of reactivation. During Phase I, there is JNK-dependent phosphorylation of the serine that neighbors the lysine 9 on histone H3 (H3K9me3S10p) (Cliffe et al., 2015). This “methyl/phospho switch” occurs on cellular chromatin during stress (Cheung, Tanner, et al., 2000; Clayton & Mahadevan, 2003; Noh et al., 2015; Sawicka & Seiser, 2012). On cellular chromatin, some H3K9me3 readers are unable to bind H3K9me3 after the phosphorylation of serine 10. For example, HP1 binding to H3K9me3 is occluded upon S10 phosphorylation (Kunowska et al., 2015) . Quickly after the phosphorylation event, H3S10p is accompanied by acetylation at lysine 14. It is thought this acetylation follows phosphorylation because histone acetyltransferases preferentially bind to phosphorylated H3 peptides (Cheung, Allis, et al., 2000). The deposition of these two proteins is then thought to recruit ATP-dependent chromatin remodeling complexes and RNA Polymerase machinery (Vincent et al., 2008). However, it is important to note that transcription from viral genomes containing this methyl/phospho switch has not

been directly demonstrated. Furthermore, the accumulation of H3 serine 10 phosphorylation and lysine 14 acetylation on the same histone tail has not been observed on the viral genome during reactivation. Future studies should investigate the mechanisms that occur after the methyl/phospho switch that lead to transcription of HSV-1.

A similar mechanism is observed during HCMV reactivation. Similar to HSV-1 latency, H3K9me3 is enriched on the HCMV latent genome. After reactivation, H3S10 phosphorylation accumulates on HCMV DNA. As S10 is phosphorylated during reactivation, H3K9me3 enrichment decreases. Coinciding with an increase in H3S10p, the authors observed a stark decrease in HP1 and an increase in H3K14ac. The authors of this finding hypothesized that S10 phosphorylation is an intermediate step between H3K9 methylation and the removal of this methylation mark (Dupont et al., 2019). This then presents as a model where a methyl/phospho switch leads to eviction of HP1, acetylation, transcription, and reactivation.

This raises an intriguing hypothesis: If the methyl/phospho switch allows for reactivation, then an increase in H3K9me3 might lead to increased Phase I of reactivation. In Chapter 2 of this dissertation, we demonstrate that interferon stimulation results in an increase of H3K9me3 enrichment on the viral genome. Yet, this increase coincides with *decreased* reactivation. We find that reactivation is inhibited by ATRX, which acts as an H3K9me3 reader on the viral genome. A previous study suggested that ATRX is capable of binding to H3K9me3 even when serine 10 is phosphorylated (Noh et al., 2015) (Kunowska et al., 2015).

This resistance to eviction allows ATRX to maintain cellular heterochromatic silencing (Noh et al., 2015). Therefore, even when the methyl/phospho switch occurs on the viral genome, we demonstrate that ATRX is not evicted, and H3K9me3-mediated silencing is maintained by ATRX.

This then leads to the question: How does Phase I of reactivation occur? We do see an increase in Phase I of reactivation with ATRX depletion, suggesting that in the absence of ATRX, a methyl/phospho switch may lead to Phase I transcription. It remains unclear which proteins, if any, associate with H3K9me3 when ATRX is depleted. Additionally, it is unclear whether HP1 or other H3K9me3 readers interact with the latent HSV-1 genome and if these proteins are displaced during a methyl/phospho switch to promote reactivation. If other readers are present, this brings up the interesting question of what, if any, neuronal conditions lead to increased enrichment of alternative H3K9me3 readers instead of ATRX. We demonstrate in Chapter 2 that ATRX association with the viral genome increases with interferon treatment. It is therefore plausible to hypothesize that there are other conditions that promote other readers and result in increased reactivation. Furthermore, different neuronal subtypes may exhibit distinct distributions of ATRX and other H3K9me3 readers, ultimately affecting reactivation competency. In Chapter 5 we demonstrate that human neurons with different characteristics are more or less prone to reactivation. In the future we would like to use this human model of HSV-1 reactivation to determine if ATRX is a restriction factor in human cells, and if ATRX plays a distinct role in different subtypes of neurons.

Although ATRX inhibits transcription from H3K9me3-bound genomes, it remains unclear whether viral factors counteract ATRX during reactivation. Three known viral factors degrade or inhibit the expression of ATRX. Whether these proteins are expressed during Phase I of reactivation and could potentially remove ATRX, allowing for Phase II of reactivation is unknown.

Additionally, it is unknown whether ATRX-mediated silencing remains effective under triggers other than NGF deprivation. When ganglia were reactivated via axotomy, the presence of a KDM4 inhibitor restricted reactivation (Liang, Vogel, et al., 2013). This contrasts our findings in Chapter 2, where KDM4 inhibition only led to restriction of reactivation when ATRX was depleted. Given that axotomy-triggered reactivation occurs with significantly faster kinetics, different triggers may also influence ATRX dynamics in distinct ways. We already discerned that the kinetics of axotomy were significantly faster, suggesting that different triggers may have differential effects. These effects could extend to the regulation of ATRX. The ability of different triggers to induce reactivation from distinct populations of HSV-1 genomes, and the ability of ATRX to inhibit reactivation in different scenarios, may represent an evolutionary “bet-hedging” strategy, ensuring that only a subset of latent genomes reactivate in response to a given stimulus. This heterogeneity in reactivation potential could provide the virus with a survival advantage, allowing it to persist within the host while minimizing immune detection. Variability in ATRX levels or function across different neuronal populations or in different conditions could lead to differential regulation of latent viral genomes, further diversifying the conditions under which

reactivation occurs. By employing this strategy, HSV-1 maximizes its chances of transmission while maintaining a reservoir of latent genomes that can respond to future environmental cues.

# Materials and Methods

Cells and Viruses

HSV-1 stocks of KOS were grown and titrated on Vero cells obtained from the American Type Culture Collection (Manassas, VA) as described previously (Cliffe et al., 2009). Cells were maintained in Dulbecco's Modified Eagle's Medium (Gibco) supplemented with 10% FetalPlex (Gemini Bio-Products) and 2 mM L-Glutamine. KOS was kindly provided by Dr. David Knipe, Harvard Medical School. Stayput-GFP virus was made and titered using gH-complementing F6 cells as described previously (Dochnal et al., 2022). The Vero F6 cells were cultured in Dulbecco's modified Eagle's medium (Gibco), supplemented with 10% FetalPlex (Gemini Bio-Products) and 250 μg/mL of G418/Geneticin (Gibco).

Mouse Infections

Six-week-old male and female CD-1 mice (Charles River Laboratories) were anesthetized by intraperitoneal injection of ketamine hydrochloride (80mg/kg) and xylazine hydrochloride (10mg/kg) and inoculated with $1.5 \times 10^6$ PFU/eye of virus (in a 5μl volume) onto scarified corneas, as described previously (Cliffe et al., 2009). Mice were housed in accordance with institutional and National Institutes of Health guidelines on the care and use of animals in research, and all procedures were approved by the Institutional Animal Care and Use Committee of the University of Virginia. Criteria used for clinical scoring based on the formation of lesions, neurological and eye symptoms is shown in table 1 and based on a previously establishing scoring scale (Riccio et al., 2019). Mice were

randomly assigned to groups and all experiments included biological repetitions from independent litters.

Explant Induced Reactivation

Trigeminal ganglia (TG) and superior cervical ganglia (SCG) were removed at least 28 days post-infection. The ganglia were maintained intact and immediately placed in reactivation media containing DMEM/F12 (Gibco) supplemented with 10% Fetal Bovine Serum and Mouse NGF 2.5S (50 ng/mL). Compounds were added at the following concentrations; LY294002 40μM, GNE-3511 8μM, ACV 100μM, GSK-J4 10μM, OG-L002 50μM. For treatments with GNE-5311, ACV, GSK-J4 and OG-L002, ganglia were treated with the compounds 3-60 minutes prior to the addition of LY294002. Ganglia were placed on a shaking platform at 50rpm at 37°C.

Quantification of Viral Transcripts and Genome Copy Number from Ganglia

At the required time point, the reactivation media was removed and ganglia snap-frozen in liquid nitrogen. Lysis was carried out by addition of the excised ganglia to BeadBug™ homogenization microtubules then homogenized for 60 seconds using the BeadBug™ microtube homogenizer. DNA and RNA were isolated from the homogenized mixture using the *Quick* DNA/RNA miniprep kit. Following RNA isolation TURBO DNA-free Kit (Invitrogen) was used to remove any contaminant DNA. mRNA was reverse transcribed into cDNA using MaximaRT (ThermoFisher) using random hexamers for first strand synthesis. Equal amounts

of mRNA were used for each reverse transcriptase experiment (20-30 ng/reaction). Power SYBR Green PCR Master Mix was used for qPCR (Applied Biosystems). Standard Curves were used to calculate the relative mRNA or DNA copy number per genome and were standardized to cellular GAPDH or 18s. All RNA samples were run in triplicate and all DNA samples were run in duplicate on an Applied Biosystems™ QuantStudio™ 6 Flex Real-Time PCR System. The primers that were used are described in Table 2.

Preformed virus titration

Sterile milk was added to media containing reactivated ganglia and sample snap frozen. Ganglia were thawed at 37°C then homogenized using a BeadBug microtube homogenizer. The homogenized ganglia were then sonicated at 25% for 30 seconds three times on ice in a Fisherbrand™ Model 120 Sonic Dismembrator. After sonication, ganglia homogenates were frozen on dry ice and thawed at 37°C. Homogenates from all time points were simultaneously titrated on Vero cells.

Reagents

The reagents used in this study are described in the table below (Table 1):

Table S1: Reagents

| Compound | Supplier | Identifier | Concentration |
|---|---|---|---|
| Aphidicolin | AG Scientific | A-1026 | 3.3 µg/ml |
| Acycloguanosine | Millipore Sigma | A4669 | 10 µM, 50 µM |
| L-Glutamic Acid | Millipore Sigma | G5638 | 3.7 µg/ml |
| LY 294002 | Tocris | 1130 | 20 µM |
| IFNα | EMD Millipore | IF009 | 600 IU/ml |
| NGF 2.5S | Alomone Labs | N-100 | 50 ng/ml |
| Primocin | Invivogen | ant-pm-1 | 100 µg/ml |
| AFDye 555 Azide Plus | Click Chemistry Tools | 1479-1 | 10 µM |
| ML-324 | Axon medchem | Axon 2081 | 10 µM |
| GSK-J4 | Millipore Sigma | SML0701 | 2 µM |
| GNE-3511 | Millipore Sigma | 533168 | 4 µM |
| SP600125 | Thermo Fisher Scientific | S5567 | 20 µM |
| OG-L002 | Tocris | 6244 | 30 µM |
| GDNF | Peprotrech | 450-44 | 50 ng/mL |
| PRIME-XV IS21 Neuronal Supplement | Irvine Scientific | 91142 | 1x |
| Neurobasal Medium™, minus phenol red | Gibco | 12348017 | |

| | | | |
|---|---|---|---|
| Brain Phys | STEMCELL Technologies | 05791 | |
| Advanced DMEM/F12 | Gibco-Life Tech | 12634-010 | |
| GlutaMAX (100x) | Gibco-Lif Tech | 35050061 | 1x |
| Prostaglandin E1 | Sigma | P5515 | 10ng/ml |
| fibroblast growth factor-basic (bFGF) | Stemgent | 03-0002 | 0.5ng/ml |
| Human Fibronectin | Millipore | FC010 | 5 µg/ml |
| Poly-L-ornithine (PLO) | Sigma | P4957 | 50 µg/ml |
| CNTF | Alomone | N-100 | 25ng/ml |
| GDNF | PeproTech | 450-13 | 25ng/ml |
| NT-3 | Affymetrix eBioscience | 14-8506 | 25ng/ml |
| Doxycycline | Sigma Aldrich | D9891-1G | 1ug/mL |

Primary Neuronal Cultures

Sympathetic neurons from the Superior Cervical Ganglia (SCG) of post-natal day 0–2 (P0-P2) CD1 Mice (Charles River Laboratories) were dissected as previously described (Cliffe et al., 2015). Rodent handling and husbandry were carried out under animal protocols approved by the Animal Care and Use Committee of the University of Virginia (UVA). Ganglia were briefly kept in Leibovitz's L-15 media with 2.05 mM l-glutamine before dissociation in collagenase type IV (1 mg/ml) followed by trypsin (2.5 mg/ml) for 20 min each at

37°C. Dissociated ganglia were triturated, and approximately 10,000 neurons per well were plated onto rat tail collagen in a 24-well plate. Sympathetic neurons were maintained in CM1 (Neurobasal® Medium supplemented with PRIME-XV IS21 Neuronal Supplement (Irvine Scientific), 50 ng/ml Mouse NGF 2.5S, 2 mM l-Glutamine, and Primocin). Aphidicolin (3.3 µg/ml) was added to the CM1 for the first five days post-dissection to select against proliferating cells.

Establishment and reactivation of latent HSV-1 infection in primary neurons

Latent HSV-1 infection was established in P6-8 sympathetic neurons from the superior cervical ganglia (SCG). Neurons were cultured for at least two days without antimitotic agents prior to infection. Where indicated, neurons were pre-treated for 18 hours and then infected in the presence of IFNα (600 IU/ml) as previously described (Suzich et al., 2021). The cultures were infected with Stayput Us11-GFP at an of MOI 5 PFU/cell, (assuming 10,000 cells per well) in Dulbecco's Phosphate Buffered Saline (DPBS) + $CaCl_2$ + $MgCl_2$ supplemented with 1% fetal bovine serum, 4.5 g/L glucose, and 10 µM acyclovir (ACV) for 4 h at 37°C. The inoculum was replaced with CM1 containing 50 µM ACV. 8 days post-infection, ACV was washed out and replaced with CM1 alone. Reactivation was initiated 10 days post-infection by adding Reactivation media [BrainPhys with 10% fetal bovine serum, Mouse NGF 2.5S (50 ng/ml)] and 20 µM LY294002 (Tocris). Reactivation was quantified by counting GFP-positive neurons 48 hours after the reactivation trigger was added.

Culturing and differentiation of HD10.6 cells

The human dorsal root sensory ganglion (HD10.6) cell line was a gift from the Triezenberg Lab and cultured as previously described (Thellman et al., 2017). HD10.6 cells were incubated at 37°C and 5% $CO_2$ and passaged in proliferation media (advanced DMEM/F12 supplemented with glutaMAX, B-27 supplement, prostaglandin, and bFGF). Proliferating HD10.6 cells were grown on Nunc flasks coated with human fibronectin. HD10.6 cells destined for differentiation were plated onto German Glass coverslips (Cat. #72290, Electron Microscopy Science) coated with PLO and human fibronectin at a concentration of 50,000 cells/ well. 18 hours after plating, maturation media [Neurobasal® Medium supplemented with PRIME-XV IS21 Neuronal Supplement, NGF, l-Glutamine, Primocin, ciliary neurotrophic factor (CNTF), glial cell-derived neurotrophic factor (GDNF), and neurotrophin-3 (NT-3)] containing doxycycline was added to induce differentiation. Following the addition of doxycycline, half-volume medium changes were performed every 3 days until cells were fixed 10 days post differentiation for immunofluorescence.

Analysis of mRNA expression by reverse transcription-quantitative PCR (RT-qPCR)

To assess relative expression of HSV-1 lytic mRNA, total RNA was extracted from approximately $1.0 \times 10^4$ neurons using the Quick-RNA™ Miniprep Kit (Zymo Research) with an on-column DNase I digestion. Following extraction, mRNA underwent a reverse transcription reaction using Maxima First Strand

cDNA Synthesis Kit for RT-qPCR (Fisher Scientific) and random hexamers for first-strand synthesis to produce cDNA. Equal amounts of RNA (20–30 ng/reaction) were used per cDNA reaction. qPCR was carried out using *Power* SYBR™ Green PCR Master Mix (Applied Biosystems). The relative mRNA was determined using the comparative $C_T$ ($\Delta\Delta C_T$) method normalized to mRNA levels in control samples. Viral mRNAs were normalized to mouse reference gene 18S. All samples were run in duplicate on an Applied Biosystems™ QuantStudio™ 6 Flex Real-Time PCR System and the mean fold change compared to the reference gene calculated. Primers used are described in Table S2.

Table S2: Primers used for RT-qPCR

| **Primer** | **Sequence 5'-3'** |
|---|---|
| 18s F | CAC GGA CAG GAT TGA CAG ATT |
| 18s R | GCC AGA GTC TCG TTC GTT ATC |
| ICP27 F | GCA TCC TTC GTG TTT GTC ATT CTG |
| ICP27 R | GCA TCT TCT CTC CGA CCC CG |
| ICP8 F | GGA GGT GCA CCG CAT ACC |
| ICP8 R | GGC TAA AAT CCG GCA TGA AC |
| gC F | GAG TTT GTC TGG TTC GAG GAC |
| gC R | ACG GTA GAG ACT GTG GTG AA |
| ATRX F | AAA GGA AAG GGT GGG TCA TC |

| | |
|---|---|
| ATRX R | CTC TGT CTG CTC TGC TTC TTT |
| DAXX F | TGA CCC AGA CTC CTC GTA TTT |
| DAXX R | GTA CGG AAT TCG CTG CTC TAT G |
| PML F | GGG AAA CAG AGG AGC GAG TT |
| PML R | AAG GCC TTG AGG GAA TTG GG |

Immunofluorescence

Cells were fixed in a solution containing 1.8% methanol-free formaldehyde in CSK buffer (10 mM HEPES, 100 mM NaCl, 300 mM Sucrose, 3 mM MgCl2, 5 mM EGTA) with 0.5% Triton X-100 and 1% phenylmethylsulfonyl fluoride (PMSF) for 10 minutes. Following fixation, cells were washed three times with PBS and were then blocked for one hour using 3% bovine serum albumin. Cells were then incubated for one hour with primary antibody at room temperature with concentrations specified in Table X. Following the primary antibody treatment, the neurons were incubated with Alexa Fluor® 488-, 555-, and 647-conjugated secondary antibodies for one hour. To visualize the nuclei, cells were incubated in Hoechst stain for 30 minutes. After all incubation times, cells were washed three times with PBS.

Images were captured using a Zeiss LSM900 microscope with Airyscan capabilities at 60x. Images were processed using the ZenBlue software and then further analyzed and processed using ImageJ.

Table S3: Antibodies used and Concentrations

| **Antibody** | **Description** | **Supplier** | **RRID** | **Concentration (IF)** | **Concentration (CUT&Tag)** |
|---|---|---|---|---|---|
| Anti-ATRX | Rabbit polyclonal | Abcam | ab97508 | 1:100 | |
| Anti-ATRX | Mouse monoclonal | Santa Cruz Bio | sc-15408 | 1:250 | |
| Anti-Daxx | Mouse monoclonal | Santa Cruz Bio | sc-8043 / AB_627405 | 1:200 | |
| Anti-IFNAR1 | Mouse monoclonal | Leinco Tech | I-1188 / AB_2830518 | 1:1,000 | |
| Anti-H3K9me3S10p | Rabbit polyclonal | Abcam | ab5819 | 1:200 | |
| Anti-H3K9me3 | Mouse monoclonal | Diagenode | C15200146 | 1:500 | |
| Anti-H3K9me3 | Rabbit polyclonal | Diagenode | C15410193 | 1:500 | 1:100 |
| Anti-IgG | Rabbit polyclonal | CUTANA | 13-0042 | | 1:50 |

| | | | | | |
|---|---|---|---|---|---|
| Anti- Murine PML | Mouse monoclonal | EMD Millipore | MAB3738 / AB_2166836 | 1:100 | |
| F(ab')2 Anti-Mouse IgG Alexa Fluor® 647 | Goat polyclonal | Thermo Fisher | A21237 | 1:1,000 | |
| F(ab')2 Anti-Mouse IgG Alexa Fluor® 555 | Goat polyclonal | Thermo Fisher | A21425 / AB_2535846 | 1:1,000 | |
| F(ab')2 Anti-Rabbit IgG Alexa Fluor® 488 | Goat polyclonal | Thermo Fisher | A11070 / AB_2534114 | 1:1,000 | |
| Anti-Chicken IgY Alexa Fluor® 647 | Goat polyclonal | Abcam | ab150175 / AB_2732800 | 1:1,000 | |
| Hoechst | | Thermo Fisher | 62249 | 1:10,000 | |

Click Chemistry

SCGs were infected with EdC/EdA virus at an MOI of 7. Labeled virus was prepared using a previously described method (McFarlane et al., 2019). Click chemistry was carried out as described previously (Suzich et al., 2021). Following fixation protocol described for immunofluorescence, samples were incubated in samples from Click-iT EdU Alexa Flour 555 Imaging Kit (ThermoFisher Scientific, C10638) following the manufacturers instructions using AFDye 555 Azide Plus. Samples were incubated in this solution for thirty minutes then washed x3 in PBS. Following the click reaction, the immunofluorescence protocol was performed.

NucSpotA Analysis

NucSpotA is part of the Mitogenie suite and was used as previously described (Francois et al., 2024). Rotation control images were generated from original channel combination images using FIJI, prior to analysis with NucSpotA. The stated co-localization thresholds were blindly calibrated by eye.

Preparation of lentiviral vectors

Lentiviruses expressing shRNA against PML (TRCN0000314605-validated previously(Suzich et al., 2021)), DAXX (DAXX-1 TRCN0000218672, DAXX-2 TRCN0000225715), ATRX (ATRX-1 TRCN0000302074, ATRX-2 TRCN0000081910), or a control lentivirus shRNA (pLKO.1 vector expressing a non-targeting shRNA control) were prepared by co-transfection with psPAX2 and

pCMV-VSV-G(Stewart et al., 2003) using the 293LTV packaging cell line (Cell Biolabs). Supernatant was harvested at 40- and 64-h post-transfection and filtered using a 45 μM PES filter. Sympathetic neurons were transduced overnight in neuronal media containing 8μg/ml protamine sulfate and 50 μM ACV.

CUT&Tag

CUT&Tag was carried out on latent neuronal cultures (approximately 1.2 $x10^5$ neurons per reaction) using the Epicypher CUTANA CUT&Tag Kit and workflow (14-1102). Antibodies used for CUT&RUN are included in Table S3. Dual-indexed DNA libraries were prepared using the same kit. Pair-ended, partial lane sequencing and de-multiplexing were carried out using NovaSeq (Novogene). Data analysis was performed using Galaxy, command line and R code, and workflow, adapted from the cited tutorial. The Rivanna high-performance computing environment (UVA Research Computing) was used for the command line data processing. Data was aligned to mouse (mm39) and viral [SC16; KX946970 (Rastrojo et al., 2017)] genomes using Bowtie2. Cutadapt was used to trim i5 and i7 adapters. Bam files were converted to Bed files using samtools. Bed files were converted to Bedgraph files using bedtools. Bedgraph files were normalized to total mapped reads for host (mouse), virus (SC16), and the K Met Stat panel. Bedgraph files were visualized in integrative genome viewer (IGV) viewer, exported as SVG files, and made into figures using Inkscape. CUT&Tag experiments were repeated twice for a total of 2 biological

replicates. The sum of enrichment at viral promoters and genes was used using bedtools map. To compare mock-treated and interferon-treated samples, each interferon-treated replicate was normalized by dividing it by its corresponding mock-treated replicate. Promoters and genes showing a two-fold or greater increase or decrease in the enrichment sum were considered consistent. In Galaxy, Bam files were visualized using DeepTools bamcoverage with a bin size of 1 to generate bigwig files. Bigwig files were normalized to total mapped reads for host (mouse), virus (SC16), and the K Met Stat panel. Bigwig files were used for multiBigwigSummary to generate heatmaps. Spearman correlation analysis was performed using deeptools plotCorrelation on multiBigwigSummary.

Statistical analysis

Power analysis was used to determine the appropriate sample sizes for statistical analysis. All statistical analysis was performed using Prism V10. The normality of the data was determined with the Kolmogorov-Smirnov test. Specific analyses are included in the figure legends.

# References


1. Alandijany, T., Roberts, A. P. E., Conn, K. L., Loney, C., McFarlane, S., Orr, A., & Boutell, C. (2018). Distinct temporal roles for the promyelocytic leukaemia (PML) protein in the sequential regulation of intracellular host immunity to HSV-1 infection. *PLoS Pathog*, *14*(1), e1006769. https://doi.org/10.1371/journal.ppat.1006769
2. Alboni, S., Gibellini, L., Montanari, C., Benatti, C., Benatti, S., Tascedda, F., Brunello, N., Cossarizza, A., & Pariante, C. M. (2013). N-acetyl-cysteine prevents toxic oxidative effects induced by IFN-alpha in human neurons. *Int J Neuropsychopharmacol*, *16*(8), 1849-1865. https://doi.org/10.1017/S1461145713000266
3. Albright, E. R., & Kalejta, R. F. (2016). Canonical and Variant Forms of Histone H3 Are Deposited onto the Human Cytomegalovirus Genome during Lytic and Latent Infections. *J Virol*, *90*(22), 10309-10320. https://doi.org/10.1128/JVI.01220-16
4. Amelio, A. L., McAnany, P. K., & Bloom, D. C. (2006). A chromatin insulator-like element in the herpes simplex virus type 1 latency-associated transcript region binds CCCTC-binding factor and displays enhancer-blocking and silencing activities. *J Virol*, *80*(5), 2358-2368. https://doi.org/10.1128/JVI.80.5.2358-2368.2006
5. Antinone, S. E., & Smith, G. A. (2010). Retrograde axon transport of herpes simplex virus and pseudorabies virus: a live-cell comparative analysis. *J Virol*, *84*(3), 1504-1512. https://doi.org/10.1128/JVI.02029-09
6. Asghari Adib, E., Smithson, L. J., & Collins, C. A. (2018). An axonal stress response pathway: degenerative and regenerative signaling by DLK. *Curr Opin Neurobiol*, *53*, 110-119. https://doi.org/10.1016/j.conb.2018.07.002
7. Bacon, T. H., Levin, M. J., Leary, J. J., Sarisky, R. T., & Sutton, D. (2003). Herpes simplex virus resistance to acyclovir and penciclovir after two decades of antiviral therapy. *Clin Microbiol Rev*, *16*(1), 114-128. https://doi.org/10.1128/CMR.16.1.114-128.2003
8. Bannister, A. J., Zegerman, P., Partridge, J. F., Miska, E. A., Thomas, J. O., Allshire, R. C., & Kouzarides, T. (2001). Selective recognition of methylated lysine 9 on histone H3 by the HP1 chromo domain. *Nature*, *410*(6824), 120-124. https://doi.org/10.1038/35065138
9. Baringer, J. R., & Pisani, P. (1994). Herpes simplex virus genomes in human nervous system tissue analyzed by polymerase chain reaction. *Ann Neurol*, *36*(6), 823-829. https://doi.org/10.1002/ana.410360605
10. Baringer, J. R., & Swoveland, P. (1973). Recovery of herpes-simplex virus from human trigeminal ganglions. *N Engl J Med*, *288*(13), 648-650. https://doi.org/10.1056/NEJM197303292881303
11. Bernardi, R., & Pandolfi, P. P. (2007). Structure, dynamics and functions of promyelocytic leukaemia nuclear bodies [ReviewPaper]. *Nat Rev Mol Cell Biol*, *8*(12), 1006-1016. https://doi.org/10.1038/nrm2277

12. Berry, N., Suspene, R., Caval, V., Khalfi, P., Beauclair, G., Rigaud, S., Blanc, H., Vignuzzi, M., Wain-Hobson, S., & Vartanian, J. P. (2021). Herpes Simplex Virus Type 1 Infection Disturbs the Mitochondrial Network, Leading to Type I Interferon Production through the RNA Polymerase III/RIG-I Pathway. *mBio*, *12*(6), e0255721. https://doi.org/10.1128/mBio.02557-21
13. Berry, W. L., & Janknecht, R. (2013). KDM4/JMJD2 histone demethylases: epigenetic regulators in cancer cells. *Cancer Res*, *73*(10), 2936-2942. https://doi.org/10.1158/0008-5472.CAN-12-4300
14. Berube, N. G., Mangelsdorf, M., Jagla, M., Vanderluit, J., Garrick, D., Gibbons, R. J., Higgs, D. R., Slack, R. S., & Picketts, D. J. (2005). The chromatin-remodeling protein ATRX is critical for neuronal survival during corticogenesis. *J Clin Invest*, *115*(2), 258-267. https://doi.org/10.1172/JCI22329
15. Blackledge, N. P., & Klose, R. J. (2021). The molecular principles of gene regulation by Polycomb repressive complexes. *Nat Rev Mol Cell Biol*, *22*(12), 815-833. https://doi.org/10.1038/s41580-021-00398-y
16. Bloom, D. C., Giordani, N. V., & Kwiatkowski, D. L. (2010). Epigenetic regulation of latent HSV-1 gene expression. *Biochim Biophys Acta*, *1799*(3-4), 246-256. https://doi.org/10.1016/j.bbagrm.2009.12.001
17. Boutell, C., Cuchet-Lourenco, D., Vanni, E., Orr, A., Glass, M., McFarlane, S., & Everett, R. D. (2011). A viral ubiquitin ligase has substrate preferential SUMO targeted ubiquitin ligase activity that counteracts intrinsic antiviral defence. *PLoS Pathog*, *7*(9), e1002245. https://doi.org/10.1371/journal.ppat.1002245
18. Boutell, C., Sadis, S., & Everett, R. D. (2002). Herpes simplex virus type 1 immediate-early protein ICP0 and is isolated RING finger domain act as ubiquitin E3 ligases in vitro. *J Virol*, *76*(2), 841-850. https://doi.org/10.1128/jvi.76.2.841-850.2002
19. Breijyeh, Z., & Karaman, R. (2020). Comprehensive Review on Alzheimer's Disease: Causes and Treatment. *Molecules*, *25*(24). https://doi.org/10.3390/molecules25245789
20. Brown, J. C., & Newcomb, W. W. (2011). Herpesvirus capsid assembly: insights from structural analysis. *Curr Opin Virol*, *1*(2), 142-149. https://doi.org/10.1016/j.coviro.2011.06.003
21. Cabral, J. M., Cushman, C. H., Sodroski, C. N., & Knipe, D. M. (2021). ATRX limits the accessibility of histone H3-occupied HSV genomes during lytic infection. *PLoS Pathog*, *17*(4), e1009567. https://doi.org/10.1371/journal.ppat.1009567
22. Cabral, J. M., Oh, H. S., & Knipe, D. M. (2018). ATRX promotes maintenance of herpes simplex virus heterochromatin during chromatin stress. *Elife*, *7*. https://doi.org/10.7554/eLife.40228
23. Cabrera, J. R., Charron, A. J., & Leib, D. A. (2018). Neuronal Subtype Determines Herpes Simplex Virus 1 Latency-Associated-Transcript Promoter Activity during Latency. *J Virol*, *92*(13). https://doi.org/10.1128/JVI.00430-18

24. Cai, W., & Schaffer, P. A. (1992). Herpes simplex virus type 1 ICP0 regulates expression of immediate-early, early, and late genes in productively infected cells. *J Virol*, *66*(5), 2904-2915. https://doi.org/10.1128/JVI.66.5.2904-2915.1992
25. Calabro, M., Rinaldi, C., Santoro, G., & Crisafulli, C. (2021). The biological pathways of Alzheimer disease: a review. *AIMS Neurosci*, *8*(1), 86-132. https://doi.org/10.3934/Neuroscience.2021005
26. Camarena, V., Kobayashi, M., Kim, J. Y., Roehm, P., Perez, R., Gardner, J., Wilson, A. C., Mohr, I., & Chao, M. V. (2010). Nature and duration of growth factor signaling through receptor tyrosine kinases regulates HSV-1 latency in neurons. *Cell Host Microbe*, *8*(4), 320-330. https://doi.org/10.1016/j.chom.2010.09.007
27. Cao, R., Wang, L., Wang, H., Xia, L., Erdjument-Bromage, H., Tempst, P., Jones, R. S., & Zhang, Y. (2002). Role of histone H3 lysine 27 methylation in Polycomb-group silencing. *Science*, *298*(5595), 1039-1043. https://doi.org/10.1126/science.1076997
28. Carr, D. J., Veress, L. A., Noisakran, S., & Campbell, I. L. (1998). Astrocyte-targeted expression of IFN-alpha1 protects mice from acute ocular herpes simplex virus type 1 infection. *J Immunol*, *161*(9), 4859-4865. https://www.ncbi.nlm.nih.gov/pubmed/9794419
29. Carraro, M., Hendriks, I. A., Hammond, C. M., Solis-Mezarino, V., Volker-Albert, M., Elsborg, J. D., Weisser, M. B., Spanos, C., Montoya, G., Rappsilber, J., Imhof, A., Nielsen, M. L., & Groth, A. (2023). DAXX adds a de novo H3.3K9me3 deposition pathway to the histone chaperone network. *Mol Cell*, *83*(7), 1075-1092 e1079. https://doi.org/10.1016/j.molcel.2023.02.009
30. Catez, F., Picard, C., Held, K., Gross, S., Rousseau, A., Theil, D., Sawtell, N., Labetoulle, M., & Lomonte, P. (2012). HSV-1 genome subnuclear positioning and associations with host-cell PML-NBs and centromeres regulate LAT locus transcription during latency in neurons. *PLoS Pathog*, *8*(8), e1002852. https://doi.org/10.1371/journal.ppat.1002852
31. Chang, Y., Horton, J. R., Bedford, M. T., Zhang, X., & Cheng, X. (2011). Structural insights for MPP8 chromodomain interaction with histone H3 lysine 9: potential effect of phosphorylation on methyl-lysine binding. *J Mol Biol*, *408*(5), 807-814. https://doi.org/10.1016/j.jmb.2011.03.018
32. Chelbi-Alix, M. K., & de The, H. (1999). Herpes virus induced proteasome-dependent degradation of the nuclear bodies-associated PML and Sp100 proteins. *Oncogene*, *18*(4), 935-941. https://doi.org/10.1038/sj.onc.1202366
33. Chen, Y. C., Li, H., Martin-Caraballo, M., & Hsia, S. V. (2022). Establishing a Herpesvirus Quiescent Infection in Differentiated Human Dorsal Root Ganglion Neuronal Cell Line Mediated by Micro-RNA Overexpression. *Pathogens*, *11*(7). https://doi.org/10.3390/pathogens11070803
34. Cheung, P., Allis, C. D., & Sassone-Corsi, P. (2000). Signaling to chromatin through histone modifications. *Cell*, *103*(2), 263-271. https://doi.org/10.1016/s0092-8674(00)00118-5

35. Cheung, P., Tanner, K. G., Cheung, W. L., Sassone-Corsi, P., Denu, J. M., & Allis, C. D. (2000). Synergistic coupling of histone H3 phosphorylation and acetylation in response to epidermal growth factor stimulation. *Mol Cell*, *5*(6), 905-915. https://doi.org/10.1016/s1097-2765(00)80256-7
36. Chiang, J. J., Sparrer, K. M. J., van Gent, M., Lassig, C., Huang, T., Osterrieder, N., Hopfner, K. P., & Gack, M. U. (2018). Viral unmasking of cellular 5S rRNA pseudogene transcripts induces RIG-I-mediated immunity. *Nat Immunol*, *19*(1), 53-62. https://doi.org/10.1038/s41590-017-0005-y
37. Clayton, A. L., & Mahadevan, L. C. (2003). MAP kinase-mediated phosphoacetylation of histone H3 and inducible gene regulation. *FEBS Lett*, *546*(1), 51-58. https://doi.org/10.1016/s0014-5793(03)00451-4
38. Cliffe, A. R., Arbuckle, J. H., Vogel, J. L., Geden, M. J., Rothbart, S. B., Cusack, C. L., Strahl, B. D., Kristie, T. M., & Deshmukh, M. (2015). Neuronal Stress Pathway Mediating a Histone Methyl/Phospho Switch Is Required for Herpes Simplex Virus Reactivation. *Cell Host Microbe*, *18*(6), 649-658. https://doi.org/10.1016/j.chom.2015.11.007
39. Cliffe, A. R., Coen, D. M., & Knipe, D. M. (2013). Kinetics of facultative heterochromatin and polycomb group protein association with the herpes simplex viral genome during establishment of latent infection. *mBio*, *4*(1). https://doi.org/10.1128/mBio.00590-12
40. Cliffe, A. R., Garber, D. A., & Knipe, D. M. (2009). Transcription of the herpes simplex virus latency-associated transcript promotes the formation of facultative heterochromatin on lytic promoters. *J Virol*, *83*(16), 8182-8190. https://doi.org/10.1128/JVI.00712-09
41. Cliffe, A. R., & Knipe, D. M. (2008). Herpes simplex virus ICP0 promotes both histone removal and acetylation on viral DNA during lytic infection. *J Virol*, *82*(24), 12030-12038. https://doi.org/10.1128/JVI.01575-08
42. Cliffe, A. R., & Wilson, A. C. (2017). Restarting Lytic Gene Transcription at the Onset of Herpes Simplex Virus Reactivation [Review]. *J Virol*, *91*(2), e01419-01416-01416. https://doi.org/10.1128/JVI.01419-16
43. Cohen, C., Corpet, A., Roubille, S., Maroui, M. A., Poccardi, N., Rousseau, A., Kleijwegt, C., Binda, O., Texier, P., Sawtell, N., Labetoulle, M., & Lomonte, P. (2018). Promyelocytic leukemia (PML) nuclear bodies (NBs) induce latent/quiescent HSV-1 genomes chromatinization through a PML NB/Histone H3.3/H3.3 Chaperone Axis. *PLoS Pathog*, *14*(9), e1007313. https://doi.org/10.1371/journal.ppat.1007313
44. Corpet, A., Kleijwegt, C., Roubille, S., Juillard, F., Jacquet, K., Texier, P., & Lomonte, P. (2020). PML nuclear bodies and chromatin dynamics: catch me if you can! *Nucleic Acids Res*, *48*(21), 11890-11912. https://doi.org/10.1093/nar/gkaa828
45. Cuddy, S. R., & Cliffe, A. R. (2023). The Intersection of Innate Immune Pathways with the Latent Herpes Simplex Virus Genome. *J Virol*, *97*(5), e0135222. https://doi.org/10.1128/jvi.01352-22
46. Cuddy, S. R., Schinlever, A. R., Dochnal, S., Seegren, P. V., Suzich, J., Kundu, P., Downs, T. K., Farah, M., Desai, B. N., Boutell, C., & Cliffe, A. R.

(2020). Neuronal hyperexcitability is a DLK-dependent trigger of herpes simplex virus reactivation that can be induced by IL-1. *Elife*, *9*. https://doi.org/10.7554/eLife.58037

47. Dalton, T., Doubrovina, E., Pankov, D., Reynolds, R., Scholze, H., Selvakumar, A., Vizconde, T., Savalia, B., Dyomin, V., Weigel, C., Oakes, C. C., Alonso, A., Elemento, O., Pan, H., Phillip, J. M., O'Reilly, R. J., Gewurz, B. E., Cesarman, E., & Giulino-Roth, L. (2020). Epigenetic reprogramming sensitizes immunologically silent EBV+ lymphomas to virus-directed immunotherapy. *Blood*, *135*(21), 1870-1881. https://doi.org/10.1182/blood.2019004126
48. Danastas, K., Guo, G., Merjane, J., Hong, N., Larsen, A., Miranda-Saksena, M., & Cunningham, A. L. (2023). Interferon inhibits the release of herpes simplex virus-1 from the axons of sensory neurons. *mBio*, *14*(5), e0181823. https://doi.org/10.1128/mbio.01818-23
49. Danastas, K., Miranda-Saksena, M., & Cunningham, A. L. (2020). Herpes Simplex Virus Type 1 Interactions with the Interferon System. *Int J Mol Sci*, *21*(14). https://doi.org/10.3390/ijms21145150
50. Davison, A. J., Eberle, R., Ehlers, B., Hayward, G. S., McGeoch, D. J., Minson, A. C., Pellett, P. E., Roizman, B., Studdert, M. J., & Thiry, E. (2009). The order Herpesvirales. *Arch Virol*, *154*(1), 171-177. https://doi.org/10.1007/s00705-008-0278-4
51. De Chiara, G., Piacentini, R., Fabiani, M., Mastrodonato, A., Marcocci, M. E., Limongi, D., Napoletani, G., Protto, V., Coluccio, P., Celestino, I., Li Puma, D. D., Grassi, C., & Palamara, A. T. (2019). Recurrent herpes simplex virus-1 infection induces hallmarks of neurodegeneration and cognitive deficits in mice. *PLoS Pathog*, *15*(3), e1007617. https://doi.org/10.1371/journal.ppat.1007617
52. De Stasio, P. R., & Taylor, M. W. (1990). Specific effect of interferon on the herpes simplex virus type 1 transactivation event. *J Virol*, *64*(6), 2588-2593. https://doi.org/10.1128/JVI.64.6.2588-2593.1990
53. Delbarre, E., Ivanauskiene, K., Spirkoski, J., Shah, A., Vekterud, K., Moskaug, J. O., Boe, S. O., Wong, L. H., Kuntziger, T., & Collas, P. (2017). PML protein organizes heterochromatin domains where it regulates histone H3.3 deposition by ATRX/DAXX. *Genome Res*, *27*(6), 913-921. https://doi.org/10.1101/gr.215830.116
54. Deng, Y., Lin, Y., Chen, S., Xiang, Y., Chen, H., Qi, S., Oh, H. S., Das, B., Komazin-Meredith, G., Pesola, J. M., Knipe, D. M., Coen, D. M., & Pan, D. (2024). Neuronal miR-9 promotes HSV-1 epigenetic silencing and latency by repressing Oct-1 and Onecut family genes. *Nat Commun*, *15*(1), 1991. https://doi.org/10.1038/s41467-024-46057-6
55. Deng, Z., Kim, E. T., Vladimirova, O., Dheekollu, J., Wang, Z., Newhart, A., Liu, D., Myers, J. L., Hensley, S. E., Moffat, J., Janicki, S. M., Fraser, N. W., Knipe, D. M., Weitzman, M. D., & Lieberman, P. M. (2014). HSV-1 remodels host telomeres to facilitate viral replication. *Cell Rep*, *9*(6), 2263-2278. https://doi.org/10.1016/j.celrep.2014.11.019

56. Deppmann, C. D., Mihalas, S., Sharma, N., Lonze, B. E., Niebur, E., & Ginty, D. D. (2008). A model for neuronal competition during development. *Science*, *320*(5874), 369-373. https://doi.org/10.1126/science.1152677
57. Deshmane, S. L., & Fraser, N. W. (1989). During latency, herpes simplex virus type 1 DNA is associated with nucleosomes in a chromatin structure. *J Virol*, *63*(2), 943-947. https://doi.org/10.1128/JVI.63.2.943-947.1989
58. Dhayalan, A., Tamas, R., Bock, I., Tattermusch, A., Dimitrova, E., Kudithipudi, S., Ragozin, S., & Jeltsch, A. (2011). The ATRX-ADD domain binds to H3 tail peptides and reads the combined methylation state of K4 and K9. *Hum Mol Genet*, *20*(11), 2195-2203. https://doi.org/10.1093/hmg/ddr107
59. Dochnal, Merchant, H. Y., Schinlever, A. R., Babnis, A., Depledge, D. P., Wilson, A. C., & Cliffe, A. R. (2022). DLK-Dependent Biphasic Reactivation of Herpes Simplex Virus Latency Established in the Absence of Antivirals. *J Virol*, *96*(12), e0050822. https://doi.org/10.1128/jvi.00508-22
60. Dochnal, S. A., Francois, A. K., & Cliffe, A. R. (2021). De Novo Polycomb Recruitment: Lessons from Latent Herpesviruses. *Viruses*, *13*(8). https://doi.org/10.3390/v13081470
61. Dochnal, S. A., Krakowiak, P. A., Whitford, A. L., & Cliffe, A. R. (2024). Physiological oxygen concentration during sympathetic primary neuron culture improves neuronal health and reduces HSV-1 reactivation. *Microbiol Spectr*, *12*(12), e0203124. https://doi.org/10.1128/spectrum.02031-24
62. Dochnal, S. A., Merchant, H., Schinlever, A., Babnis, A., Depledge, D. P., Wilson, A., & Cliffe, A. R. (2022). DLK-dependent biphasic reactivation of herpes simplex virus latency established in the absence of antivirals. *bioRxiv*, 2022.2002.2025.482019. https://doi.org/10.1101/2022.02.25.482019
63. Dochnal, S. A., Whitford, A. L., Francois, A. K., Krakowiak, P. A., Cuddy, S., & Cliffe, A. R. (2024). c-Jun signaling during initial HSV-1 infection modulates latency to enhance later reactivation in addition to directly promoting the progression to full reactivation. *J Virol*, *98*(2), e0176423. https://doi.org/10.1128/jvi.01764-23
64. Drane, P., Ouararhni, K., Depaux, A., Shuaib, M., & Hamiche, A. (2010). The death-associated protein DAXX is a novel histone chaperone involved in the replication-independent deposition of H3.3. *Genes Dev*, *24*(12), 1253-1265. https://doi.org/10.1101/gad.566910
65. Dremel, S. E., & DeLuca, N. A. (2019). Genome replication affects transcription factor binding mediating the cascade of herpes simplex virus transcription. *Proc Natl Acad Sci U S A*, *116*(9), 3734-3739. https://doi.org/10.1073/pnas.1818463116
66. Du, T., Zhou, G., & Roizman, B. (2011). HSV-1 gene expression from reactivated ganglia is disordered and concurrent with suppression of latency-associated transcript and miRNAs. *Proc Natl Acad Sci U S A*, *108*(46), 18820-18824. https://doi.org/10.1073/pnas.1117203108
67. Duan, R. S., Tang, G. B., Du, H. Z., Hu, Y. W., Liu, P. P., Xu, Y. J., Zeng, Y. Q., Zhang, S. F., Wang, R. Y., Teng, Z. Q., & Liu, C. M. (2018). Polycomb protein family member CBX7 regulates intrinsic axon growth and

regeneration. *Cell Death Differ*, *25*(9), 1598-1611. https://doi.org/10.1038/s41418-018-0064-0

68. Dupont, L., Du, L., Poulter, M., Choi, S., McIntosh, M., & Reeves, M. B. (2019). Src family kinase activity drives cytomegalovirus reactivation by recruiting MOZ histone acetyltransferase activity to the viral promoter. *J Biol Chem*, *294*(35), 12901-12910. https://doi.org/10.1074/jbc.RA119.009667
69. Dyer, M. A., Qadeer, Z. A., Valle-Garcia, D., & Bernstein, E. (2017). ATRX and DAXX: Mechanisms and Mutations. *Cold Spring Harb Perspect Med*, *7*(3). https://doi.org/10.1101/cshperspect.a026567
70. Edwards, T. G., & Bloom, D. C. (2019). Lund Human Mesencephalic (LUHMES) Neuronal Cell Line Supports Herpes Simplex Virus 1 Latency In Vitro. *J Virol*, *93*(6). https://doi.org/10.1128/JVI.02210-18
71. Ertel, M. K., Cammarata, A. L., Hron, R. J., & Neumann, D. M. (2012). CTCF occupation of the herpes simplex virus 1 genome is disrupted at early times postreactivation in a transcription-dependent manner. *J Virol*, *86*(23), 12741-12759. https://doi.org/10.1128/JVI.01655-12
72. Eustermann, S., Yang, J. C., Law, M. J., Amos, R., Chapman, L. M., Jelinska, C., Garrick, D., Clynes, D., Gibbons, R. J., Rhodes, D., Higgs, D. R., & Neuhaus, D. (2011). Combinatorial readout of histone H3 modifications specifies localization of ATRX to heterochromatin. *Nat Struct Mol Biol*, *18*(7), 777-782. https://doi.org/10.1038/nsmb.2070
73. Everett, R. D., Freemont, P., Saitoh, H., Dasso, M., Orr, A., Kathoria, M., & Parkinson, J. (1998). The disruption of ND10 during herpes simplex virus infection correlates with the Vmw110- and proteasome-dependent loss of several PML isoforms. *J Virol*, *72*(8), 6581-6591. https://doi.org/10.1128/JVI.72.8.6581-6591.1998
74. Everett, R. D., & Murray, J. (2005). ND10 components relocate to sites associated with herpes simplex virus type 1 nucleoprotein complexes during virus infection. *J Virol*, *79*(8), 5078-5089. https://doi.org/10.1128/JVI.79.8.5078-5089.2005
75. Everett, R. D., Orr, A., & Elliott, M. (1991). High level expression and purification of herpes simplex virus type 1 immediate early polypeptide Vmw110. *Nucleic Acids Res*, *19*(22), 6155-6161. https://doi.org/10.1093/nar/19.22.6155
76. Everett, R. D., Sourvinos, G., Leiper, C., Clements, J. B., & Orr, A. (2004). Formation of nuclear foci of the herpes simplex virus type 1 regulatory protein ICP4 at early times of infection: localization, dynamics, recruitment of ICP27, and evidence for the de novo induction of ND10-like complexes. *J Virol*, *78*(4), 1903-1917. https://doi.org/10.1128/jvi.78.4.1903-1917.2004
77. Fang, X., Djouhri, L., McMullan, S., Berry, C., Okuse, K., Waxman, S. G., & Lawson, S. N. (2005). trkA is expressed in nociceptive neurons and influences electrophysiological properties via Nav1.8 expression in rapidly conducting nociceptors. *J Neurosci*, *25*(19), 4868-4878. https://doi.org/10.1523/JNEUROSCI.0249-05.2005

78. Ferenczy, M. W., & DeLuca, N. A. (2011). Reversal of heterochromatic silencing of quiescent herpes simplex virus type 1 by ICP0. *J Virol*, *85*(7), 3424-3435. https://doi.org/10.1128/JVI.02263-10
79. Fischle, W., Tseng, B. S., Dormann, H. L., Ueberheide, B. M., Garcia, B. A., Shabanowitz, J., Hunt, D. F., Funabiki, H., & Allis, C. D. (2005). Regulation of HP1-chromatin binding by histone H3 methylation and phosphorylation. *Nature*, *438*(7071), 1116-1122. https://doi.org/10.1038/nature04219
80. Fischle, W., Wang, Y., & Allis, C. D. (2003). Binary switches and modification cassettes in histone biology and beyond. *Nature*, *425*(6957), 475-479. https://doi.org/10.1038/nature02017
81. Fletcher, G. C., Xue, L., Passingham, S. K., & Tolkovsky, A. M. (2000). Death commitment point is advanced by axotomy in sympathetic neurons. *J Cell Biol*, *150*(4), 741-754. https://doi.org/10.1083/jcb.150.4.741
82. Francois, A. K., Rohani, A., Loftus, M., Dochnal, S., Hrit, J., McFarlane, S., Whitford, A., Lewis, A., Krakowiak, P., Boutell, C., Rothbart, S. B., Kashatus, D., & Cliffe, A. R. (2024). Single-genome analysis reveals a heterogeneous association of the herpes simplex virus genome with H3K27me2 and the reader PHF20L1 following infection of human fibroblasts. *mBio*, *15*(4), e0327823. https://doi.org/10.1128/mbio.03278-23
83. Frasson, I., Solda, P., Nadai, M., Lago, S., & Richter, S. N. (2021). Parallel G-quadruplexes recruit the HSV-1 transcription factor ICP4 to promote viral transcription in herpes virus-infected human cells [OriginalPaper]. *Commun Biol*, *4*(1), 510. https://doi.org/10.1038/s42003-021-02035-y
84. Full, F., Jungnickl, D., Reuter, N., Bogner, E., Brulois, K., Scholz, B., Sturzl, M., Myoung, J., Jung, J. U., Stamminger, T., & Ensser, A. (2014). Kaposi's sarcoma associated herpesvirus tegument protein ORF75 is essential for viral lytic replication and plays a critical role in the antagonization of ND10-instituted intrinsic immunity. *PLoS Pathog*, *10*(1), e1003863. https://doi.org/10.1371/journal.ppat.1003863
85. Gehani, S. S., Agrawal-Singh, S., Dietrich, N., Christophersen, N. S., Helin, K., & Hansen, K. (2010). Polycomb group protein displacement and gene activation through MSK-dependent H3K27me3S28 phosphorylation. *Mol Cell*, *39*(6), 886-900. https://doi.org/10.1016/j.molcel.2010.08.020
86. Gibbert, K., Schlaak, J. F., Yang, D., & Dittmer, U. (2013). IFN-alpha subtypes: distinct biological activities in anti-viral therapy. *Br J Pharmacol*, *168*(5), 1048-1058. https://doi.org/10.1111/bph.12010
87. Gibbons, R. J., McDowell, T. L., Raman, S., O'Rourke, D. M., Garrick, D., Ayyub, H., & Higgs, D. R. (2000). Mutations in ATRX, encoding a SWI/SNF-like protein, cause diverse changes in the pattern of DNA methylation. *Nat Genet*, *24*(4), 368-371. https://doi.org/10.1038/74191
88. Gray, P. A., Fu, H., Luo, P., Zhao, Q., Yu, J., Ferrari, A., Tenzen, T., Yuk, D.-i., Tsung, E. F., & Cai, Z. (2004). Mouse brain organization revealed through direct genome-scale TF expression analysis. *Science*, *306*(5705), 2255-2257.
89. Hafezi, W., Lorentzen, E. U., Eing, B. R., Muller, M., King, N. J., Klupp, B., Mettenleiter, T. C., & Kuhn, J. E. (2012). Entry of herpes simplex virus type 1

(HSV-1) into the distal axons of trigeminal neurons favors the onset of nonproductive, silent infection. *PLoS Pathog*, *8*(5), e1002679. https://doi.org/10.1371/journal.ppat.1002679

90. Halford, W. P., & Schaffer, P. A. (2001). ICP0 is required for efficient reactivation of herpes simplex virus type 1 from neuronal latency. *J Virol*, *75*(7), 3240-3249. https://doi.org/10.1128/JVI.75.7.3240-3249.2001
91. Hall, M. H., Magalska, A., Malinowska, M., Ruszczycki, B., Czaban, I., Patel, S., Ambrożek-Latecka, M., Zołocińska, E., Broszkiewicz, H., & Parobczak, K. (2016). Localization and regulation of PML bodies in the adult mouse brain. *Brain Structure and Function*, *221*, 2511-2525.
92. Heinemann, B., Nielsen, J. M., Hudlebusch, H. R., Lees, M. J., Larsen, D. V., Boesen, T., Labelle, M., Gerlach, L. O., Birk, P., & Helin, K. (2014). Inhibition of demethylases by GSK-J1/J4. *Nature*, *514*(7520), E1-2. https://doi.org/10.1038/nature13688
93. Henikoff, S., Henikoff, J. G., Kaya-Okur, H. S., & Ahmad, K. (2020). Efficient chromatin accessibility mapping in situ by nucleosome-tethered tagmentation. *Elife*, *9*, e63274. https://doi.org/10.7554/eLife.63274
94. Herrera, F. J., & Triezenberg, S. J. (2004). VP16-dependent association of chromatin-modifying coactivators and underrepresentation of histones at immediate-early gene promoters during herpes simplex virus infection. *J Virol*, *78*(18), 9689-9696. https://doi.org/10.1128/JVI.78.18.9689-9696.2004
95. Hirano, S., & Udagawa, O. (2022). Effects of arsenic on the topology and solubility of promyelocytic leukemia (PML)-nuclear bodies. *PloS one*, *17*(5), e0268835. https://doi.org/10.1371/journal.pone.0268835
96. Hu, H. L., Shiflett, L. A., Kobayashi, M., Chao, M. V., Wilson, A. C., Mohr, I., & Huang, T. T. (2019). TOP2beta-Dependent Nuclear DNA Damage Shapes Extracellular Growth Factor Responses via Dynamic AKT Phosphorylation to Control Virus Latency. *Mol Cell*, *74*(3), 466-480 e464. https://doi.org/10.1016/j.molcel.2019.02.032
97. Hu, H. L., Srinivas, K. P., Wang, S., Chao, M. V., Lionnet, T., Mohr, I., Wilson, A. C., Depledge, D. P., & Huang, T. T. (2022). Single-cell transcriptomics identifies Gadd45b as a regulator of herpesvirus-reactivating neurons. *EMBO Rep*, *23*(2), e53543. https://doi.org/10.15252/embr.202153543
98. Huntwork-Rodriguez, S., Wang, B., Watkins, T., Ghosh, A. S., Pozniak, C. D., Bustos, D., Newton, K., Kirkpatrick, D. S., & Lewcock, J. W. (2013). JNK-mediated phosphorylation of DLK suppresses its ubiquitination to promote neuronal apoptosis. *J Cell Biol*, *202*(5), 747-763. https://doi.org/10.1083/jcb.201303066
99. Imai, Y., Apakupakul, K., Krause, P. R., Halford, W. P., & Margolis, T. P. (2009). Investigation of the mechanism by which herpes simplex virus type 1 LAT sequences modulate preferential establishment of latent infection in mouse trigeminal ganglia. *J Virol*, *83*(16), 7873-7882. https://doi.org/10.1128/JVI.00043-09

100. Itzhaki, R. F. (2018). Corroboration of a Major Role for Herpes Simplex Virus Type 1 in Alzheimer's Disease. *Front Aging Neurosci*, *10*, 324. https://doi.org/10.3389/fnagi.2018.00324
101. Itzhaki, R. F., Lin, W. R., Shang, D., Wilcock, G. K., Faragher, B., & Jamieson, G. A. (1997). Herpes simplex virus type 1 in brain and risk of Alzheimer's disease. *Lancet*, *349*(9047), 241-244. https://doi.org/10.1016/S0140-6736(96)10149-5
102. Iwase, S., Xiang, B., Ghosh, S., Ren, T., Lewis, P. W., Cochrane, J. C., Allis, C. D., Picketts, D. J., Patel, D. J., Li, H., & Shi, Y. (2011). ATRX ADD domain links an atypical histone methylation recognition mechanism to human mental-retardation syndrome. *Nat Struct Mol Biol*, *18*(7), 769-776. https://doi.org/10.1038/nsmb.2062
103. Jacobs, S. A., Taverna, S. D., Zhang, Y., Briggs, S. D., Li, J., Eissenberg, J. C., Allis, C. D., & Khorasanizadeh, S. (2001). Specificity of the HP1 chromo domain for the methylated N-terminus of histone H3. *EMBO J*, *20*(18), 5232-5241. https://doi.org/10.1093/emboj/20.18.5232
104. Jain, K., Fraser, C. S., Marunde, M. R., Parker, M. M., Sagum, C., Burg, J. M., Hall, N., Popova, I. K., Rodriguez, K. L., Vaidya, A., Krajewski, K., Keogh, M. C., Bedford, M. T., & Strahl, B. D. (2020). Characterization of the plant homeodomain (PHD) reader family for their histone tail interactions. *Epigenetics Chromatin*, *13*(1), 3. https://doi.org/10.1186/s13072-020-0328-z
105. James, C., Harfouche, M., Welton, N. J., Turner, K. M., Abu-Raddad, L. J., Gottlieb, S. L., & Looker, K. J. (2020). Herpes simplex virus: global infection prevalence and incidence estimates, 2016. *Bull World Health Organ*, *98*(5), 315-329. https://doi.org/10.2471/BLT.19.237149
106. Jamieson, G. A., Maitland, N. J., Wilcock, G. K., Craske, J., & Itzhaki, R. F. (1991). Latent herpes simplex virus type 1 in normal and Alzheimer's disease brains. *J Med Virol*, *33*(4), 224-227. https://doi.org/10.1002/jmv.1890330403
107. Jurak, I., Hackenberg, M., Kim, J. Y., Pesola, J. M., Everett, R. D., Preston, C. M., Wilson, A. C., & Coen, D. M. (2014). Expression of herpes simplex virus 1 microRNAs in cell culture models of quiescent and latent infection. *J Virol*, *88*(4), 2337-2339. https://doi.org/10.1128/JVI.03486-13
108. Jurak, I., Kramer, M. F., Mellor, J. C., van Lint, A. L., Roth, F. P., Knipe, D. M., & Coen, D. M. (2010). Numerous conserved and divergent microRNAs expressed by herpes simplex viruses 1 and 2. *J Virol*, *84*(9), 4659-4672. https://doi.org/10.1128/JVI.02725-09
109. Jurak, I., Silverstein, L. B., Sharma, M., & Coen, D. M. (2012). Herpes simplex virus is equipped with RNA- and protein-based mechanisms to repress expression of ATRX, an effector of intrinsic immunity. *J Virol*, *86*(18), 10093-10102. https://doi.org/10.1128/JVI.00930-12
110. Kelly, B. J., Fraefel, C., Cunningham, A. L., & Diefenbach, R. J. (2009). Functional roles of the tegument proteins of herpes simplex virus type 1. *Virus Res*, *145*(2), 173-186. https://doi.org/10.1016/j.virusres.2009.07.007

111. Kent, J. R., Zeng, P. Y., Atanasiu, D., Gardner, J., Fraser, N. W., & Berger, S. L. (2004). During lytic infection herpes simplex virus type 1 is associated with histones bearing modifications that correlate with active transcription. *J Virol*, *78*(18), 10178-10186. https://doi.org/10.1128/JVI.78.18.10178-10186.2004
112. Kernohan, K. D., Jiang, Y., Tremblay, D. C., Bonvissuto, A. C., Eubanks, J. H., Mann, M. R., & Berube, N. G. (2010). ATRX partners with cohesin and MeCP2 and contributes to developmental silencing of imprinted genes in the brain. *Dev Cell*, *18*(2), 191-202. https://doi.org/10.1016/j.devcel.2009.12.017
113. Kim, J. Y., Mandarino, A., Chao, M. V., Mohr, I., & Wilson, A. C. (2012). Transient reversal of episome silencing precedes VP16-dependent transcription during reactivation of latent HSV-1 in neurons. *PLoS Pathog*, *8*(2), e1002540. https://doi.org/10.1371/journal.ppat.1002540
114. Kinde, B., Gabel, H. W., Gilbert, C. S., Griffith, E. C., & Greenberg, M. E. (2015). Reading the unique DNA methylation landscape of the brain: Non-CpG methylation, hydroxymethylation, and MeCP2. *Proc Natl Acad Sci U S A*, *112*(22), 6800-6806. https://doi.org/10.1073/pnas.1411269112
115. Kirkpatrick, J. E., Kirkwood, K. L., & Woster, P. M. (2018). Inhibition of the histone demethylase KDM4B leads to activation of KDM1A, attenuates bacterial-induced pro-inflammatory cytokine release, and reduces osteoclastogenesis. *Epigenetics*, *13*(5), 557-572. https://doi.org/10.1080/15592294.2018.1481703
116. Knipe, D. M., & Cliffe, A. (2008). Chromatin control of herpes simplex virus lytic and latent infection. *Nat Rev Microbiol*, *6*(3), 211-221. https://doi.org/10.1038/nrmicro1794
117. Knipe, D. M., & Howley, P. M. (2013). *Fields virology* (6th ed.). Wolters Kluwer/Lippincott Williams & Wilkins Health. Publisher description http://www.loc.gov/catdir/enhancements/fy1306/2013003842-d.html
118. Kobayashi, M., Wilson, A. C., Chao, M. V., & Mohr, I. (2012). Control of viral latency in neurons by axonal mTOR signaling and the 4E-BP translation repressor. *Genes Dev*, *26*(14), 1527-1532. https://doi.org/10.1101/gad.190157.112
119. Kolb, G., & Kristie, T. M. (2008). Association of the cellular coactivator HCF-1 with the Golgi apparatus in sensory neurons. *J Virol*, *82*(19), 9555-9563. https://doi.org/10.1128/JVI.01174-08
120. Kole, A. J., Annis, R. P., & Deshmukh, M. (2013). Mature neurons: equipped for survival [Review]. *Cell Death Dis*, *4*(6), e689. https://doi.org/10.1038/cddis.2013.220
121. Krakowiak, P. A., Flores, M. E., Cuddy, S. R., Whitford, A. L., Dochnal, S. A., Babnis, A., Miyake, T., Tigano, M., Engel, D. A., & Cliffe, A. R. (2025). Co-option of mitochondrial nucleic acid-sensing pathways by HSV-1 UL12.5 for reactivation from latent infection. *Proc Natl Acad Sci U S A*, *122*(4), e2413965122. https://doi.org/10.1073/pnas.2413965122
122. Kramer, M. F., Jurak, I., Pesola, J. M., Boissel, S., Knipe, D. M., & Coen, D. M. (2011). Herpes simplex virus 1 microRNAs expressed abundantly

during latent infection are not essential for latency in mouse trigeminal ganglia. *Virology*, *417*(2), 239-247. https://doi.org/10.1016/j.virol.2011.06.027
123. Kristie, T. M., Vogel, J. L., & Sears, A. E. (1999). Nuclear localization of the C1 factor (host cell factor) in sensory neurons correlates with reactivation of herpes simplex virus from latency. *Proc Natl Acad Sci U S A*, *96*(4), 1229-1233. https://doi.org/10.1073/pnas.96.4.1229
124. Kruidenier, L., Chung, C. W., Cheng, Z., Liddle, J., Che, K., Joberty, G., Bantscheff, M., Bountra, C., Bridges, A., Diallo, H., Eberhard, D., Hutchinson, S., Jones, E., Katso, R., Leveridge, M., Mander, P. K., Mosley, J., Ramirez-Molina, C., Rowland, P., . . . Wilson, D. M. (2012). A selective jumonji H3K27 demethylase inhibitor modulates the proinflammatory macrophage response. *Nature*, *488*(7411), 404-408. https://doi.org/10.1038/nature11262
125. Kubat, N. J., Tran, R. K., McAnany, P., & Bloom, D. C. (2004). Specific histone tail modification and not DNA methylation is a determinant of herpes simplex virus type 1 latent gene expression. *J Virol*, *78*(3), 1139-1149. https://doi.org/10.1128/jvi.78.3.1139-1149.2004
126. Kunowska, N., Rotival, M., Yu, L., Choudhary, J., & Dillon, N. (2015). Identification of protein complexes that bind to histone H3 combinatorial modifications using super-SILAC and weighted correlation network analysis. *Nucleic Acids Res*, *43*(3), 1418-1432. https://doi.org/10.1093/nar/gku1350
127. Kurapati, S., Sadaoka, T., Rajbhandari, L., Jagdish, B., Shukla, P., Ali, M. A., Kim, Y. J., Lee, G., Cohen, J. I., & Venkatesan, A. (2017). Role of the JNK Pathway in Varicella-Zoster Virus Lytic Infection and Reactivation. *J Virol*, *91*(17). https://doi.org/10.1128/jvi.00640-17
128. Kwiatkowski, D. L., Thompson, H. W., & Bloom, D. C. (2009). The polycomb group protein Bmi1 binds to the herpes simplex virus 1 latent genome and maintains repressive histone marks during latency [research-article]. *J Virol*, *83*(16), 8173-8181. https://doi.org/10.1128/JVI.00686-09
129. Lacasse, J. J., & Schang, L. M. (2010). During lytic infections, herpes simplex virus type 1 DNA is in complexes with the properties of unstable nucleosomes. *J Virol*, *84*(4), 1920-1933. https://doi.org/10.1128/JVI.01934-09
130. Lachner, M., O'Carroll, D., Rea, S., Mechtler, K., & Jenuwein, T. (2001). Methylation of histone H3 lysine 9 creates a binding site for HP1 proteins. *Nature*, *410*(6824), 116-120. https://doi.org/10.1038/35065132
131. Lallemand-Breitenbach, V., & de The, H. (2010). PML nuclear bodies. *Cold Spring Harb Perspect Biol*, *2*(5), a000661. https://doi.org/10.1101/cshperspect.a000661
132. Lee, J. S., Raja, P., & Knipe, D. M. (2016). Herpesviral ICP0 Protein Promotes Two Waves of Heterochromatin Removal on an Early Viral Promoter during Lytic Infection. *mBio*, *7*(1), e02007-02015. https://doi.org/10.1128/mBio.02007-15
133. Lee, M. Y., Lee, J., Hyeon, S. J., Cho, H., Hwang, Y. J., Shin, J. Y., McKee, A. C., Kowall, N. W., Kim, J. I., Stein, T. D., Hwang, D., & Ryu, H. (2020). Epigenome signatures landscaped by histone H3K9me3 are

associated with the synaptic dysfunction in Alzheimer's disease. *Aging Cell*, *19*(6), e13153. https://doi.org/10.1111/acel.13153
134. Leinbach, S. S., & Summers, W. C. (1980). The structure of herpes simplex virus type 1 DNA as probed by micrococcal nuclease digestion. *J Gen Virol*, *51*(Pt 1), 45-59. https://doi.org/10.1099/0022-1317-51-1-45
135. Leoni, V., Gianni, T., Salvioli, S., & Campadelli-Fiume, G. (2012). Herpes simplex virus glycoproteins gH/gL and gB bind Toll-like receptor 2, and soluble gH/gL is sufficient to activate NF-kappaB. *J Virol*, *86*(12), 6555-6562. https://doi.org/10.1128/JVI.00295-12
136. Levy, M. A., Kernohan, K. D., Jiang, Y., & Berube, N. G. (2015). ATRX promotes gene expression by facilitating transcriptional elongation through guanine-rich coding regions. *Hum Mol Genet*, *24*(7), 1824-1835. https://doi.org/10.1093/hmg/ddu596
137. Lewis, P. W., Elsaesser, S. J., Noh, K. M., Stadler, S. C., & Allis, C. D. (2010). Daxx is an H3.3-specific histone chaperone and cooperates with ATRX in replication-independent chromatin assembly at telomeres. *Proc Natl Acad Sci U S A*, *107*(32), 14075-14080. https://doi.org/10.1073/pnas.1008850107
138. Liang, Y., Quenelle, D., Vogel, J. L., Mascaro, C., Ortega, A., & Kristie, T. M. (2013). A novel selective LSD1/KDM1A inhibitor epigenetically blocks herpes simplex virus lytic replication and reactivation from latency. *mBio*, *4*(1), e00558-00512. https://doi.org/10.1128/mBio.00558-12
139. Liang, Y., Vogel, J. L., Arbuckle, J. H., Rai, G., Jadhav, A., Simeonov, A., Maloney, D. J., & Kristie, T. M. (2013). Targeting the JMJD2 histone demethylases to epigenetically control herpesvirus infection and reactivation from latency. *Sci Transl Med*, *5*(167), 167ra165. https://doi.org/10.1126/scitranslmed.3005145
140. Liang, Y., Vogel, J. L., Narayanan, A., Peng, H., & Kristie, T. M. (2009). Inhibition of the histone demethylase LSD1 blocks alpha-herpesvirus lytic replication and reactivation from latency. *Nat Med*, *15*(11), 1312-1317. https://doi.org/10.1038/nm.2051
141. Lilley, C. E., Chaurushiya, M. S., Boutell, C., Everett, R. D., & Weitzman, M. D. (2011). The intrinsic antiviral defense to incoming HSV-1 genomes includes specific DNA repair proteins and is counteracted by the viral protein ICP0. *PLoS Pathog*, *7*(6), e1002084. https://doi.org/10.1371/journal.ppat.1002084
142. Linderman, J. A., Kobayashi, M., Rayannavar, V., Fak, J. J., Darnell, R. B., Chao, M. V., Wilson, A. C., & Mohr, I. (2017). Immune Escape via a Transient Gene Expression Program Enables Productive Replication of a Latent Pathogen. *Cell Rep*, *18*(5), 1312-1323. https://doi.org/10.1016/j.celrep.2017.01.017
143. Lister, R., Mukamel, E. A., Nery, J. R., Urich, M., Puddifoot, C. A., Johnson, N. D., Lucero, J., Huang, Y., Dwork, A. J., Schultz, M. D., Yu, M., Tonti-Filippini, J., Heyn, H., Hu, S., Wu, J. C., Rao, A., Esteller, M., He, C., Haghighi, F. G., . . . Ecker, J. R. (2013). Global epigenomic reconfiguration

during mammalian brain development. *Science*, *341*(6146), 1237905. https://doi.org/10.1126/science.1237905

144. Liu, X., Ma, Y., Voss, K., van Gent, M., Chan, Y. K., Gack, M. U., Gale, M., Jr., & He, B. (2021). The herpesvirus accessory protein gamma134.5 facilitates viral replication by disabling mitochondrial translocation of RIG-I. *PLoS Pathog*, *17*(3), e1009446. https://doi.org/10.1371/journal.ppat.1009446
145. Lo, W. S., Trievel, R. C., Rojas, J. R., Duggan, L., Hsu, J. Y., Allis, C. D., Marmorstein, R., & Berger, S. L. (2000). Phosphorylation of serine 10 in histone H3 is functionally linked in vitro and in vivo to Gcn5-mediated acetylation at lysine 14. *Mol Cell*, *5*(6), 917-926. https://doi.org/10.1016/s1097-2765(00)80257-9
146. Lovheim, H., Norman, T., Weidung, B., Olsson, J., Josefsson, M., Adolfsson, R., Nyberg, L., & Elgh, F. (2019). Herpes Simplex Virus, APOEvarepsilon4, and Cognitive Decline in Old Age: Results from the Betula Cohort Study. *J Alzheimers Dis*, *67*(1), 211-220. https://doi.org/10.3233/JAD-171162
147. Lukashchuk, V., & Everett, R. D. (2010). Regulation of ICP0-null mutant herpes simplex virus type 1 infection by ND10 components ATRX and hDaxx. *J Virol*, *84*(8), 4026-4040. https://doi.org/10.1128/JVI.02597-09
148. Lund, J., Sato, A., Akira, S., Medzhitov, R., & Iwasaki, A. (2003). Toll-like receptor 9-mediated recognition of Herpes simplex virus-2 by plasmacytoid dendritic cells. *J Exp Med*, *198*(3), 513-520. https://doi.org/10.1084/jem.20030162
149. Lv, W., Zhou, L., Wu, J., Cheng, J., Duan, Y., & Qian, W. (2024). Anti-HSV-1 agents: an update. *Front Pharmacol*, *15*, 1451083. https://doi.org/10.3389/fphar.2024.1451083
150. Ma, J. Z., Russell, T. A., Spelman, T., Carbone, F. R., & Tscharke, D. C. (2014). Lytic gene expression is frequent in HSV-1 latent infection and correlates with the engagement of a cell-intrinsic transcriptional response. *PLoS Pathog*, *10*(7), e1004237. https://doi.org/10.1371/journal.ppat.1004237
151. Mansfield, R. E., Musselman, C. A., Kwan, A. H., Oliver, S. S., Garske, A. L., Davrazou, F., Denu, J. M., Kutateladze, T. G., & Mackay, J. P. (2011). Plant homeodomain (PHD) fingers of CHD4 are histone H3-binding modules with preference for unmodified H3K4 and methylated H3K9. *J Biol Chem*, *286*(13), 11779-11791. https://doi.org/10.1074/jbc.M110.208207
152. Marano, D., Fioriniello, S., Fiorillo, F., Gibbons, R. J., D'Esposito, M., & Della Ragione, F. (2019). ATRX Contributes to MeCP2-Mediated Pericentric Heterochromatin Organization during Neural Differentiation. *Int J Mol Sci*, *20*(21). https://doi.org/10.3390/ijms20215371
153. Maroui, M. A., Calle, A., Cohen, C., Streichenberger, N., Texier, P., Takissian, J., Rousseau, A., Poccardi, N., Welsch, J., Corpet, A., Schaeffer, L., Labetoulle, M., & Lomonte, P. (2016). Latency Entry of Herpes Simplex Virus 1 Is Determined by the Interaction of Its Genome with the Nuclear Environment. *PLoS Pathog*, *12*(9), e1005834. https://doi.org/10.1371/journal.ppat.1005834

154. McFarlane, S., Orr, A., Roberts, A. P. E., Conn, K. L., Iliev, V., Loney, C., da Silva Filipe, A., Smollett, K., Gu, Q., Robertson, N., Adams, P. D., Rai, T. S., & Boutell, C. (2019). The histone chaperone HIRA promotes the induction of host innate immune defences in response to HSV-1 infection. *PLoS Pathog*, *15*(3), e1007667. https://doi.org/10.1371/journal.ppat.1007667
155. McQuillan, G., Kruszon-Moran, D., Flagg, E. W., & Paulose-Ram, R. (2018). Prevalence of Herpes Simplex Virus Type 1 and Type 2 in Persons Aged 14-49: United States, 2015-2016. *NCHS Data Brief*(304), 1-8. https://www.ncbi.nlm.nih.gov/pubmed/29442994
156. Melchjorsen, J., Rintahaka, J., Soby, S., Horan, K. A., Poltajainen, A., Ostergaard, L., Paludan, S. R., & Matikainen, S. (2010). Early innate recognition of herpes simplex virus in human primary macrophages is mediated via the MDA5/MAVS-dependent and MDA5/MAVS/RNA polymerase III-independent pathways. *J Virol*, *84*(21), 11350-11358. https://doi.org/10.1128/JVI.01106-10
157. Messer, H. G., Jacobs, D., Dhummakupt, A., & Bloom, D. C. (2015). Inhibition of H3K27me3-specific histone demethylases JMJD3 and UTX blocks reactivation of herpes simplex virus 1 in trigeminal ganglion neurons. *J Virol*, *89*(6), 3417-3420. https://doi.org/10.1128/JVI.03052-14
158. Montero, J. J., Lopez-Silanes, I., Megias, D., M, F. F., Castells-Garcia, A., & Blasco, M. A. (2018). TERRA recruitment of polycomb to telomeres is essential for histone trymethylation marks at telomeric heterochromatin. *Nat Commun*, *9*(1), 1548. https://doi.org/10.1038/s41467-018-03916-3
159. Moore, L. D., Le, T., & Fan, G. (2013). DNA methylation and its basic function [ReviewPaper]. *Neuropsychopharmacology*, *38*(1), 23-38. https://doi.org/10.1038/npp.2012.112
160. Mori, I., Kimura, Y., Naiki, H., Matsubara, R., Takeuchi, T., Yokochi, T., & Nishiyama, Y. (2004). Reactivation of HSV-1 in the brain of patients with familial Alzheimer's disease. *J Med Virol*, *73*(4), 605-611. https://doi.org/10.1002/jmv.20133
161. Muggeridge, M. I., & Fraser, N. W. (1986). Chromosomal organization of the herpes simplex virus genome during acute infection of the mouse central nervous system. *J Virol*, *59*(3), 764-767. https://doi.org/10.1128/JVI.59.3.764-767.1986
162. Nady, N., Lemak, A., Walker, J. R., Avvakumov, G. V., Kareta, M. S., Achour, M., Xue, S., Duan, S., Allali-Hassani, A., Zuo, X., Wang, Y. X., Bronner, C., Chedin, F., Arrowsmith, C. H., & Dhe-Paganon, S. (2011). Recognition of multivalent histone states associated with heterochromatin by UHRF1 protein. *J Biol Chem*, *286*(27), 24300-24311. https://doi.org/10.1074/jbc.M111.234104
163. Nan, X., Hou, J., Maclean, A., Nasir, J., Lafuente, M. J., Shu, X., Kriaucionis, S., & Bird, A. (2007). Interaction between chromatin proteins MECP2 and ATRX is disrupted by mutations that cause inherited mental retardation. *Proc Natl Acad Sci U S A*, *104*(8), 2709-2714. https://doi.org/10.1073/pnas.0608056104

164. Nergadze, S. G., Farnung, B. O., Wischnewski, H., Khoriauli, L., Vitelli, V., Chawla, R., Giulotto, E., & Azzalin, C. M. (2009). CpG-island promoters drive transcription of human telomeres. *RNA*, *15*(12), 2186-2194. https://doi.org/10.1261/rna.1748309
165. Nicoll, M. P., Hann, W., Shivkumar, M., Harman, L. E., Connor, V., Coleman, H. M., Proenca, J. T., & Efstathiou, S. (2016). The HSV-1 Latency-Associated Transcript Functions to Repress Latent Phase Lytic Gene Expression and Suppress Virus Reactivation from Latently Infected Neurons. *PLoS Pathog*, *12*(4), e1005539. https://doi.org/10.1371/journal.ppat.1005539
166. Noh, K. M., Maze, I., Zhao, D., Xiang, B., Wenderski, W., Lewis, P. W., Shen, L., Li, H., & Allis, C. D. (2015). ATRX tolerates activity-dependent histone H3 methyl/phos switching to maintain repetitive element silencing in neurons. *Proc Natl Acad Sci U S A*, *112*(22), 6820-6827. https://doi.org/10.1073/pnas.1411258112
167. Oh, J., & Fraser, N. W. (2008). Temporal association of the herpes simplex virus genome with histone proteins during a lytic infection. *J Virol*, *82*(7), 3530-3537. https://doi.org/10.1128/JVI.00586-07
168. Orzalli, M. H., Broekema, N. M., Diner, B. A., Hancks, D. C., Elde, N. C., Cristea, I. M., & Knipe, D. M. (2015). cGAS-mediated stabilization of IFI16 promotes innate signaling during herpes simplex virus infection. *Proc Natl Acad Sci U S A*, *112*(14), E1773-1781. https://doi.org/10.1073/pnas.1424637112
169. Orzalli, M. H., Broekema, N. M., & Knipe, D. M. (2016). Relative Contributions of Herpes Simplex Virus 1 ICP0 and vhs to Loss of Cellular IFI16 Vary in Different Human Cell Types. *J Virol*, *90*(18), 8351-8359. https://doi.org/10.1128/JVI.00939-16
170. Orzalli, M. H., Conwell, S. E., Berrios, C., DeCaprio, J. A., & Knipe, D. M. (2013). Nuclear interferon-inducible protein 16 promotes silencing of herpesviral and transfected DNA. *Proc Natl Acad Sci U S A*, *110*(47), E4492-4501. https://doi.org/10.1073/pnas.1316194110
171. Orzalli, M. H., DeLuca, N. A., & Knipe, D. M. (2012). Nuclear IFI16 induction of IRF-3 signaling during herpesviral infection and degradation of IFI16 by the viral ICP0 protein. *Proc Natl Acad Sci U S A*, *109*(44), E3008-3017. https://doi.org/10.1073/pnas.1211302109
172. Pan, D., Flores, O., Umbach, J. L., Pesola, J. M., Bentley, P., Rosato, P. C., Leib, D. A., Cullen, B. R., & Coen, D. M. (2014). A neuron-specific host microRNA targets herpes simplex virus-1 ICP0 expression and promotes latency. *Cell Host Microbe*, *15*(4), 446-456. https://doi.org/10.1016/j.chom.2014.03.004
173. Parkinson, G. N., Lee, M. P., & Neidle, S. (2002). Crystal structure of parallel quadruplexes from human telomeric DNA. *Nature*, *417*(6891), 876-880. https://doi.org/10.1038/nature755
174. Pasieka, T. J., Collins, L., O'Connor, M. A., Chen, Y., Parker, Z. M., Berwin, B. L., Piwnica-Worms, D. R., & Leib, D. A. (2011). Bioluminescent imaging reveals divergent viral pathogenesis in two strains of Stat1-deficient

mice, and in alphassgamma interferon receptor-deficient mice. *PloS one*, *6*(9), e24018. https://doi.org/10.1371/journal.pone.0024018

175. Patel, S., Cohen, F., Dean, B. J., De La Torre, K., Deshmukh, G., Estrada, A. A., Ghosh, A. S., Gibbons, P., Gustafson, A., Huestis, M. P., Le Pichon, C. E., Lin, H., Liu, W., Liu, X., Liu, Y., Ly, C. Q., Lyssikatos, J. P., Ma, C., Scearce-Levie, K., . . . Siu, M. (2015). Discovery of dual leucine zipper kinase (DLK, MAP3K12) inhibitors with activity in neurodegeneration models. *J Med Chem*, *58*(1), 401-418. https://doi.org/10.1021/jm5013984
176. Piacentini, R., De Chiara, G., Li Puma, D. D., Ripoli, C., Marcocci, M. E., Garaci, E., Palamara, A. T., & Grassi, C. (2014). HSV-1 and Alzheimer's disease: more than a hypothesis [Review]. *Front Pharmacol*, *5*(353145), 97. https://doi.org/10.3389/fphar.2014.00097
177. Quinlan, M. P., & Knipe, D. M. (1985). Stimulation of expression of a herpes simplex virus DNA-binding protein by two viral functions. *Mol Cell Biol*, *5*(5), 957-963. https://doi.org/10.1128/mcb.5.5.957-963.1985
178. Rastrojo, A., Lopez-Munoz, A. D., & Alcami, A. (2017). Genome Sequence of Herpes Simplex Virus 1 Strain SC16. *Genome Announc*, *5*(4). https://doi.org/10.1128/genomeA.01392-16
179. Ratnakumar, K., & Bernstein, E. (2013). ATRX: the case of a peculiar chromatin remodeler. *Epigenetics*, *8*(1), 3-9. https://doi.org/10.4161/epi.23271
180. Raymon, H. K., Thode, S., Zhou, J., Friedman, G. C., Pardinas, J. R., Barrere, C., Johnson, R. M., & Sah, D. W. (1999). Immortalized human dorsal root ganglion cells differentiate into neurons with nociceptive properties. *J Neurosci*, *19*(13), 5420-5428. https://doi.org/10.1523/JNEUROSCI.19-13-05420.1999
181. Readhead, B., Haure-Mirande, J. V., Funk, C. C., Richards, M. A., Shannon, P., Haroutunian, V., Sano, M., Liang, W. S., Beckmann, N. D., Price, N. D., Reiman, E. M., Schadt, E. E., Ehrlich, M. E., Gandy, S., & Dudley, J. T. (2018). Multiscale Analysis of Independent Alzheimer's Cohorts Finds Disruption of Molecular, Genetic, and Clinical Networks by Human Herpesvirus. *Neuron*, *99*(1), 64-82 e67. https://doi.org/10.1016/j.neuron.2018.05.023
182. Regad, T., Bellodi, C., Nicotera, P., & Salomoni, P. (2009). The tumor suppressor Pml regulates cell fate in the developing neocortex. *Nature neuroscience*, *12*(2), 132-140.
183. Riccio, R. E., Park, S. J., Longnecker, R., & Kopp, S. J. (2019). Characterization of Sex Differences in Ocular Herpes Simplex Virus 1 Infection and Herpes Stromal Keratitis Pathogenesis of Wild-Type and Herpesvirus Entry Mediator Knockout Mice. *mSphere*, *4*(2). https://doi.org/10.1128/mSphere.00073-19
184. Richter, E. R., Dias, J. K., Gilbert, J. E., 2nd, & Atherton, S. S. (2009). Distribution of herpes simplex virus type 1 and varicella zoster virus in ganglia of the human head and neck. *J Infect Dis*, *200*(12), 1901-1906. https://doi.org/10.1086/648474

185. Roizman, B., Knipe, D. M., & Whitley, R. (2013). Herpes simplex viruses. In (6th ed.). Lippincott Williams & Wilkins, Philadelphia.
186. Rosato, P. C., & Leib, D. A. (2015). Neuronal Interferon Signaling Is Required for Protection against Herpes Simplex Virus Replication and Pathogenesis. *PLoS Pathog*, *11*(7), e1005028. https://doi.org/10.1371/journal.ppat.1005028
187. Roubille, S., Escure, T., Juillard, F., Corpet, A., Néplaz, R., Binda, O., Seurre, C., Gonin, M., Bloor, S., Cohen, C., Texier, P., Haigh, O., Pascual, O., Ganor, Y., Magdinier, F., Labetoulle, M., Lehner, P. J., & Lomonte, P. (2024). The HUSH epigenetic repressor complex silences PML nuclear body-associated HSV-1 quiescent genomes. *Proceedings of the National Academy of Sciences of the United States of America*, *121*(49), 2024.2006.2018.599571. https://doi.org/ARTN e2412258121
188. 10.1073/pnas.2412258121
189. Roy, E. R., & Cao, W. (2020). Antiviral Immune Response in Alzheimer's Disease: Connecting the Dots. *Front Neurosci*, *14*, 577744. https://doi.org/10.3389/fnins.2020.577744
190. Sacks, W. R., & Schaffer, P. A. (1987). Deletion mutants in the gene encoding the herpes simplex virus type 1 immediate-early protein ICP0 exhibit impaired growth in cell culture. *J Virol*, *61*(3), 829-839. https://doi.org/10.1128/JVI.61.3.829-839.1987
191. Sahin, U., Ferhi, O., Jeanne, M., Benhenda, S., Berthier, C., Jollivet, F., Niwa-Kawakita, M., Faklaris, O., Setterblad, N., de The, H., & Lallemand-Breitenbach, V. (2014). Oxidative stress-induced assembly of PML nuclear bodies controls sumoylation of partner proteins. *J Cell Biol*, *204*(6), 931-945. https://doi.org/10.1083/jcb.201305148
192. Sarma, K., Cifuentes-Rojas, C., Ergun, A., Del Rosario, A., Jeon, Y., White, F., Sadreyev, R., & Lee, J. T. (2014). ATRX directs binding of PRC2 to Xist RNA and Polycomb targets. *Cell*, *159*(4), 869-883. https://doi.org/10.1016/j.cell.2014.10.019
193. Sawicka, A., & Seiser, C. (2012). Histone H3 phosphorylation - a versatile chromatin modification for different occasions. *Biochimie*, *94*(11), 2193-2201. https://doi.org/10.1016/j.biochi.2012.04.018
194. Sawtell, N. M., & Thompson, R. L. (1992). Herpes simplex virus type 1 latency-associated transcription unit promotes anatomical site-dependent establishment and reactivation from latency. *J Virol*, *66*(4), 2157-2169. https://doi.org/10.1128/JVI.66.4.2157-2169.1992
195. Sawtell, N. M., & Thompson, R. L. (2004). Comparison of herpes simplex virus reactivation in ganglia in vivo and in explants demonstrates quantitative and qualitative differences. *J Virol*, *78*(14), 7784-7794. https://doi.org/10.1128/JVI.78.14.7784-7794.2004
196. Schreiner, S., Burck, C., Glass, M., Groitl, P., Wimmer, P., Kinkley, S., Mund, A., Everett, R. D., & Dobner, T. (2013). Control of human adenovirus type 5 gene expression by cellular Daxx/ATRX chromatin-associated

complexes. *Nucleic Acids Res*, *41*(6), 3532-3550. https://doi.org/10.1093/nar/gkt064

197. Sciortino, M. T., Medici, M. A., Marino-Merlo, F., Zaccaria, D., Giuffre-Cuculletto, M., Venuti, A., Grelli, S., & Mastino, A. (2008). Involvement of HVEM receptor in activation of nuclear factor kappaB by herpes simplex virus 1 glycoprotein D. *Cell Microbiol*, *10*(11), 2297-2311. https://doi.org/10.1111/j.1462-5822.2008.01212.x
198. Sears, A. E., Hukkanen, V., Labow, M. A., Levine, A. J., & Roizman, B. (1991). Expression of the herpes simplex virus 1 alpha transinducing factor (VP16) does not induce reactivation of latent virus or prevent the establishment of latency in mice. *J Virol*, *65*(6), 2929-2935. https://doi.org/10.1128/JVI.65.6.2929-2935.1991
199. Sengupta Ghosh, A., Wang, B., Pozniak, C. D., Chen, M., Watts, R. J., & Lewcock, J. W. (2011). DLK induces developmental neuronal degeneration via selective regulation of proapoptotic JNK activity. *The Journal of Cell Biology*, *194*(5), 751-764. https://doi.org/10.1083/jcb.201103153.dv
200. Singh, N., & Tscharke, D. C. (2020). Herpes Simplex Virus Latency Is Noisier the Closer We Look. *J Virol*, *94*(4). https://doi.org/10.1128/JVI.01701-19
201. Sodroski, C. N., & Knipe, D. M. (2023). Nuclear interferon-stimulated gene product maintains heterochromatin on the herpes simplex viral genome to limit lytic infection. *Proc Natl Acad Sci U S A*, *120*(45), e2310996120. https://doi.org/10.1073/pnas.2310996120
202. Song, R., Koyuncu, O. O., Greco, T. M., Diner, B. A., Cristea, I. M., & Enquist, L. W. (2016). Two Modes of the Axonal Interferon Response Limit Alphaherpesvirus Neuroinvasion. *mBio*, *7*(1), e02145-02115. https://doi.org/10.1128/mBio.02145-15
203. Steiner, I., Spivack, J. G., Deshmane, S. L., Ace, C. I., Preston, C. M., & Fraser, N. W. (1990). A herpes simplex virus type 1 mutant containing a nontransinducing Vmw65 protein establishes latent infection in vivo in the absence of viral replication and reactivates efficiently from explanted trigeminal ganglia. *J Virol*, *64*(4), 1630-1638. https://doi.org/10.1128/JVI.64.4.1630-1638.1990
204. Stewart, S. A., Dykxhoorn, D. M., Palliser, D., Mizuno, H., Yu, E. Y., An, D. S., Sabatini, D. M., Chen, I. S., Hahn, W. C., Sharp, P. A., Weinberg, R. A., & Novina, C. D. (2003). Lentivirus-delivered stable gene silencing by RNAi in primary cells. *RNA*, *9*(4), 493-501. https://doi.org/10.1261/rna.2192803
205. Sun, B., Yang, X., Hou, F., Yu, X., Wang, Q., Oh, H. S., Raja, P., Pesola, J. M., Vanni, E. A. H., McCarron, S., Morris-Love, J., Ng, A. H. M., Church, G. M., Knipe, D. M., Coen, D. M., & Pan, D. (2021). Regulation of host and virus genes by neuronal miR-138 favours herpes simplex virus 1 latency. *Nat Microbiol*, *6*(5), 682-696. https://doi.org/10.1038/s41564-020-00860-1
206. Sun, Y., Jiang, X., Xu, Y., Ayrapetov, M. K., Moreau, L. A., Whetstine, J. R., & Price, B. D. (2009). Histone H3 methylation links DNA damage

detection to activation of the tumour suppressor Tip60. *Nat Cell Biol*, *11*(11), 1376-1382. https://doi.org/10.1038/ncb1982
207. Suzich, J. B., & Cliffe, A. R. (2018). Strength in diversity: Understanding the pathways to herpes simplex virus reactivation. *Virology*, *522*, 81-91. https://doi.org/10.1016/j.virol.2018.07.011
208. Suzich, J. B., Cuddy, S. R., Baidas, H., Dochnal, S., Ke, E., Schinlever, A. R., Babnis, A., Boutell, C., & Cliffe, A. R. (2021). PML-NB-dependent type I interferon memory results in a restricted form of HSV latency. *EMBO Rep*, *22*(9), e52547. https://doi.org/10.15252/embr.202152547
209. Tedeschi, A., & Bradke, F. (2013). The DLK signalling pathway--a double-edged sword in neural development and regeneration [Review]. *EMBO Rep*, *14*(7), 605-614. https://doi.org/10.1038/embor.2013.64
210. Teng, Y. C., Sundaresan, A., O'Hara, R., Gant, V. U., Li, M., Martire, S., Warshaw, J. N., Basu, A., & Banaszynski, L. A. (2021). ATRX promotes heterochromatin formation to protect cells from G-quadruplex DNA-mediated stress. *Nat Commun*, *12*(1), 3887. https://doi.org/10.1038/s41467-021-24206-5
211. Thellman, N. M., Botting, C., Madaj, Z., & Triezenberg, S. J. (2017). An Immortalized Human Dorsal Root Ganglion Cell Line Provides a Novel Context To Study Herpes Simplex Virus 1 Latency and Reactivation. *J Virol*, *91*(12). https://doi.org/10.1128/JVI.00080-17
212. Thompson, R. L., Preston, C. M., & Sawtell, N. M. (2009). De novo synthesis of VP16 coordinates the exit from HSV latency in vivo. *PLoS Pathog*, *5*(3), e1000352. https://doi.org/10.1371/journal.ppat.1000352
213. Thompson, R. L., & Sawtell, N. M. (2006). Evidence that the herpes simplex virus type 1 ICP0 protein does not initiate reactivation from latency in vivo. *J Virol*, *80*(22), 10919-10930. https://doi.org/10.1128/JVI.01253-06
214. Tillotson, R., Cholewa-Waclaw, J., Chhatbar, K., Connelly, J. C., Kirschner, S. A., Webb, S., Koerner, M. V., Selfridge, J., Kelly, D. A., De Sousa, D., Brown, K., Lyst, M. J., Kriaucionis, S., & Bird, A. (2021). Neuronal non-CG methylation is an essential target for MeCP2 function. *Mol Cell*, *81*(6), 1260-1275 e1212. https://doi.org/10.1016/j.molcel.2021.01.011
215. Truch, J., Downes, D. J., Scott, C., Gur, E. R., Telenius, J. M., Repapi, E., Schwessinger, R., Gosden, M., Brown, J. M., Taylor, S., Cheong, P. L., Hughes, J. R., Higgs, D. R., & Gibbons, R. J. (2022). The chromatin remodeller ATRX facilitates diverse nuclear processes, in a stochastic manner, in both heterochromatin and euchromatin. *Nat Commun*, *13*(1), 3485. https://doi.org/10.1038/s41467-022-31194-7
216. Tsai, K., Thikmyanova, N., Wojcechowskyj, J. A., Delecluse, H. J., & Lieberman, P. M. (2011). EBV tegument protein BNRF1 disrupts DAXX-ATRX to activate viral early gene transcription. *PLoS Pathog*, *7*(11), e1002376. https://doi.org/10.1371/journal.ppat.1002376
217. Tsai, R. X., Fang, K. C., Yang, P. C., Hsieh, Y. H., Chiang, I. T., Chen, Y., Lee, H. G., Lee, J. T., & Chu, H. C. (2022). TERRA regulates DNA G-

quadruplex formation and ATRX recruitment to chromatin. *Nucleic Acids Res*, *50*(21), 12217-12234. https://doi.org/10.1093/nar/gkac1114
218. Tullo, A. (2003). Pathogenesis and management of herpes simplex virus keratitis. *Eye (Lond)*, *17*(8), 919-922. https://doi.org/10.1038/sj.eye.6700564
219. Tzeng, N. S., Chung, C. H., Lin, F. H., Chiang, C. P., Yeh, C. B., Huang, S. Y., Lu, R. B., Chang, H. A., Kao, Y. C., Yeh, H. W., Chiang, W. S., Chou, Y. C., Tsao, C. H., Wu, Y. F., & Chien, W. C. (2018). Anti-herpetic Medications and Reduced Risk of Dementia in Patients with Herpes Simplex Virus Infections-a Nationwide, Population-Based Cohort Study in Taiwan. *Neurotherapeutics*, *15*(2), 417-429. https://doi.org/10.1007/s13311-018-0611-x
220. Umbach, J. L., Kramer, M. F., Jurak, I., Karnowski, H. W., Coen, D. M., & Cullen, B. R. (2008). MicroRNAs expressed by herpes simplex virus 1 during latent infection regulate viral mRNAs. *Nature*, *454*(7205), 780-783. https://doi.org/10.1038/nature07103
221. Valenzuela, M., Amato, R., Sgura, A., Antoccia, A., & Berardinelli, F. (2021). The Multiple Facets of ATRX Protein. *Cancers (Basel)*, *13*(9). https://doi.org/10.3390/cancers13092211
222. Vincent, A., Ducourouble, M. P., & Van Seuningen, I. (2008). Epigenetic regulation of the human mucin gene MUC4 in epithelial cancer cell lines involves both DNA methylation and histone modifications mediated by DNA methyltransferases and histone deacetylases. *FASEB J*, *22*(8), 3035-3045. https://doi.org/10.1096/fj.07-103390
223. von Schimmelmann, M., Feinberg, P. A., Sullivan, J. M., Ku, S. M., Badimon, A., Duff, M. K., Wang, Z., Lachmann, A., Dewell, S., Ma'ayan, A., Han, M. H., Tarakhovsky, A., & Schaefer, A. (2016). Polycomb repressive complex 2 (PRC2) silences genes responsible for neurodegeneration. *Nat Neurosci*, *19*(10), 1321-1330. https://doi.org/10.1038/nn.4360
224. Voon, H. P., Hughes, J. R., Rode, C., De La Rosa-Velazquez, I. A., Jenuwein, T., Feil, R., Higgs, D. R., & Gibbons, R. J. (2015). ATRX Plays a Key Role in Maintaining Silencing at Interstitial Heterochromatic Loci and Imprinted Genes. *Cell Rep*, *11*(3), 405-418. https://doi.org/10.1016/j.celrep.2015.03.036
225. Voon, H. P., & Wong, L. H. (2016). New players in heterochromatin silencing: histone variant H3.3 and the ATRX/DAXX chaperone. *Nucleic Acids Res*, *44*(4), 1496-1501. https://doi.org/10.1093/nar/gkw012
226. Wang, Q. Y., Zhou, C., Johnson, K. E., Colgrove, R. C., Coen, D. M., & Knipe, D. M. (2005). Herpesviral latency-associated transcript gene promotes assembly of heterochromatin on viral lytic-gene promoters in latent infection. *Proc Natl Acad Sci U S A*, *102*(44), 16055-16059. https://doi.org/10.1073/pnas.0505850102
227. Warren, K. G., Brown, S. M., Wroblewska, Z., Gilden, D., Koprowski, H., & Subak-Sharpe, J. (1978). Isolation of latent herpes simplex virus from the superior cervical and vagus ganglions of human beings. *N Engl J Med*, *298*(19), 1068-1069. https://doi.org/10.1056/NEJM197805112981907

228. Washington, S. D., Musarrat, F., Ertel, M. K., Backes, G. L., & Neumann, D. M. (2018). CTCF Binding Sites in the Herpes Simplex Virus 1 Genome Display Site-Specific CTCF Occupation, Protein Recruitment, and Insulator Function. *J Virol*, *92*(8). https://doi.org/10.1128/JVI.00156-18
229. Watkins, T. A., Wang, B., Huntwork-Rodriguez, S., Yang, J., Jiang, Z., Eastham-Anderson, J., Modrusan, Z., Kaminker, J. S., Tessier-Lavigne, M., & Lewcock, J. W. (2013). DLK initiates a transcriptional program that couples apoptotic and regenerative responses to axonal injury. *Proc Natl Acad Sci U S A*, *110*(10), 4039-4044. https://doi.org/10.1073/pnas.1211074110
230. Weller, S. K., & Sawitzke, J. A. (2014). Recombination promoted by DNA viruses: phage lambda to herpes simplex virus. *Annu Rev Microbiol*, *68*, 237-258. https://doi.org/10.1146/annurev-micro-091313-103424
231. Wertheim, J. O., Smith, M. D., Smith, D. M., Scheffler, K., & Kosakovsky Pond, S. L. (2014). Evolutionary origins of human herpes simplex viruses 1 and 2. *Mol Biol Evol*, *31*(9), 2356-2364. https://doi.org/10.1093/molbev/msu185
232. Whitford, A. L., Auguste, G., Francois, A. K., Boutell, C., Miller, C., Dremel, S., & Cliffe, A. R. (2025). Interferon Dependent Immune Memory during HSV-1 Neuronal Latency Results in Increased H3K9me3 and Restriction of Reactivation by ATRX. *bioRxiv*, 2025.2001.2028.633013. https://doi.org/10.1101/2025.01.28.633013
233. Whitford, A. L., & Cliffe, A. R. (2022). Key questions on the epigenetics of herpes simplex virus latency. *PLoS Pathog*, *18*(6), e1010587. https://doi.org/10.1371/journal.ppat.1010587
234. Whitford, A. L., Clinton, C. A., Kennedy, E. B. L., Dochnal, S. A., Suzich, J. B., & Cliffe, A. R. (2022). Ex Vivo Herpes Simplex Virus Reactivation Involves a Dual Leucine Zipper Kinase-Dependent Wave of Lytic Gene Expression That Is Independent of Histone Demethylase Activity and Viral Genome Synthesis. *J Virol*, *96*(12), e0047522. https://doi.org/10.1128/jvi.00475-22
235. Whitley, R. J., & Roizman, B. (2001). Herpes simplex virus infections. *Lancet*, *357*(9267), 1513-1518. https://doi.org/10.1016/S0140-6736(00)04638-9
236. Whitlow, Z., & Kristie, T. M. (2009). Recruitment of the transcriptional coactivator HCF-1 to viral immediate-early promoters during initiation of reactivation from latency of herpes simplex virus type 1. *J Virol*, *83*(18), 9591-9595. https://doi.org/10.1128/JVI.01115-09
237. Wilcox, C. L., & Johnson, E. M., Jr. (1987). Nerve growth factor deprivation results in the reactivation of latent herpes simplex virus in vitro. *J Virol*, *61*(7), 2311-2315. https://doi.org/10.1128/JVI.61.7.2311-2315.1987
238. Wu, C. C., Wu, H. J., Wang, C. H., Lin, C. H., Hsu, S. C., Chen, Y. R., Hsiao, M., Schuyler, S. C., Lu, F. L., Ma, N., & Lu, J. (2015). Akt suppresses DLK for maintaining self-renewal of mouse embryonic stem cells. *Cell Cycle*, *14*(8), 1207-1217. https://doi.org/10.1080/15384101.2015.1014144
239. Wu, W., Tan, Y., Yin, H., Jiang, M., Jiang, Y., Ma, X., Yin, T., Li, Y., Zhang, H., Cai, X., & Meng, G. (2023). Phase separation is required for PML

nuclear body biogenesis and function. *FASEB J*, *37*(6), e22986. https://doi.org/10.1096/fj.202300216R

240. Xiang, J. F., & Corces, V. G. (2021). Regulation of 3D chromatin organization by CTCF. *Curr Opin Genet Dev*, *67*, 33-40. https://doi.org/10.1016/j.gde.2020.10.005
241. Xu, Y. J., Liu, P. P., Ng, S. C., Teng, Z. Q., & Liu, C. M. (2020). Regulatory networks between Polycomb complexes and non-coding RNAs in the central nervous system. *J Mol Cell Biol*, *12*(5), 327-336. https://doi.org/10.1093/jmcb/mjz058
242. Yan, N., & Chen, Z. J. (2012). Intrinsic antiviral immunity. *Nat Immunol*, *13*(3), 214-222. https://doi.org/10.1038/ni.2229
243. Yanez, A. A., Harrell, T., Sriranganathan, H. J., Ives, A. M., & Bertke, A. S. (2017). Neurotrophic Factors NGF, GDNF and NTN Selectively Modulate HSV1 and HSV2 Lytic Infection and Reactivation in Primary Adult Sensory and Autonomic Neurons [Article]. *Pathogens*, *6*(1), 5-13. https://doi.org/10.3390/pathogens6010005
244. Yao, F., & Schaffer, P. A. (1995). An activity specified by the osteosarcoma line U2OS can substitute functionally for ICP0, a major regulatory protein of herpes simplex virus type 1. *J Virol*, *69*(10), 6249-6258. https://doi.org/10.1128/JVI.69.10.6249-6258.1995
245. Yordy, B., Iijima, N., Huttner, A., Leib, D., & Iwasaki, A. (2012). A neuron-specific role for autophagy in antiviral defense against herpes simplex virus. *Cell Host Microbe*, *12*(3), 334-345. https://doi.org/10.1016/j.chom.2012.07.013
246. Zhang, J., Liu, H., & Wei, B. (2017). Immune response of T cells during herpes simplex virus type 1 (HSV-1) infection. *J Zhejiang Univ Sci B*, *18*(4), 277-288. https://doi.org/10.1631/jzus.B1600460
247. Zhang, S. Y., Jouanguy, E., Ugolini, S., Smahi, A., Elain, G., Romero, P., Segal, D., Sancho-Shimizu, V., Lorenzo, L., Puel, A., Picard, C., Chapgier, A., Plancoulaine, S., Titeux, M., Cognet, C., von Bernuth, H., Ku, C. L., Casrouge, A., Zhang, X. X., . . . Casanova, J. L. (2007). TLR3 deficiency in patients with herpes simplex encephalitis. *Science*, *317*(5844), 1522-1527. https://doi.org/10.1126/science.1139522
248. Zhao, J., Zeng, Y., Xu, S., Chen, J., Shen, G., Yu, C., Knipe, D., Yuan, W., Peng, J., Xu, W., Zhang, C., Xia, Z., & Feng, P. (2016). A Viral Deamidase Targets the Helicase Domain of RIG-I to Block RNA-Induced Activation. *Cell Host Microbe*, *20*(6), 770-784. https://doi.org/10.1016/j.chom.2016.10.011
249. Zhao, S., Lu, J., Pan, B., Fan, H., Byrum, S. D., Xu, C., Kim, A., Guo, Y., Kanchi, K. L., Gong, W., Sun, T., Storey, A. J., Burkholder, N. T., Mackintosh, S. G., Kuhlers, P. C., Edmondson, R. D., Strahl, B. D., Diao, Y., Tackett, A. J., . . . Wang, G. G. (2023). TNRC18 engages H3K9me3 to mediate silencing of endogenous retrotransposons. *Nature*, *623*(7987), 633-642. https://doi.org/10.1038/s41586-023-06688-z